WAR RESEARCH PROJECTS

A. A Study of Pro Knock Activity

B. The Dynamic Sorption of Ammonia and Butane on Charcoal

by

James Deuchars Boyd Ogilvie B. Eng. M. Sc.

Thesis submitted to the Faculty of Graduate Studies and Research of McGill University in partial fulfillment of the requirements for the degree of Doctor of Philosophy

from the

Physical Chemistry Laboratory

McGill University

under the supervision of

Dr. C.A. Winkler

April 1942.

Ph.D. Chemistry

James D.B. Ogilvie

War Research Projects

A. A Study of Pro Knock Activity

B. The Dynamic Sorption of Butane and Ammonia on Charcoal.

Part A

Various compounds were investigated to determine their pro knock activity by adding them to the air intake of, or to the gasoline used by and Ethyl 30 B Knock Testing Engine. The best compound tested was arsenic tri chloride which requires 5.8 parts per million of air by volume to cause a decrease of ten octane units in a leaded gasoline.

It was found that the best knock inducer elements were in order of effectiveness: arsenic, antimony and phosphorous. Mercury, vanadium and chromium were also found to be effective. Among the radicals the halogens were most effective, the order being bromine, chlorine, iodine and fluorine. Effectiveness of halogens appeared to be enhanced by the presence of a nitro and methyl groups.

Elements of the type

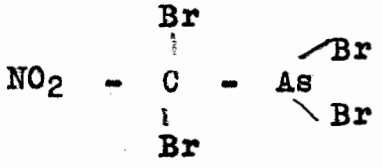

were predicted to be exceedingly effective.

PART B

Dynamic Sorption of Ammonia and Butane on Charcoal

The dynamic sorption of butane and ammonia on charcoal was studied using an apparatus which followed the sorption by weight as a function of time and permitted measurement of temperature rise and analysis of the effluent gas stream over a wide range of sorbate concentrations and flowrates. The data were applied to the theories of Danby et al and of Mecklenberg and were found to be essentially in good agreement.

ACKNOWLEDGEMENTS

The author wishes to acknowledge the co-operation of the Organic Chemistry Department of McGill University particularly Mr. B.K. Wasson and Mr. H.D. Orloff for the synthesis of many of the compounds used as pro knocks. Acknowledgement is also made to the National Research Council for a studentship and for the loan of the knock testing engine used in the pro knock investigations, and to Mr. J.A. Pearce for carrying out the experimental work on the solution investigations.

A. A Study of Pro Knock Activity

(in collaboration with S.G. Davis)

TABLE OF CONTENTS

INTRODUCTION

It has been established that many chemical substances, when introduced into the air intake of, or dissolved in the gasoline consumed by, an interal combustion engine will cause the engine to knock noticeably, decrease power output, and possibly result in damage to various engine parts (1, 2, 3). It is the purpose of these investigations to obtain quantitative data on the pro-knock activity of various substances, with a view toward examining the practicability of their use as a weapon in chemical warfare to render enemy automotive equipment inactive. If the air could be polluted with a sufficient concentration of a pro-knock compound, it is possible that aeroplanes, tanks, or other automotive equipment could be rendered inactive by passing through an area so treated, since knock of sufficient intensity will cause stoppage of the engine or mechanical failure of the engine parts.

Since engine performance depends upon the nature of the combustion of the hydrocarbon fuel in the cylinder, a brief review of the chemical and physical aspects of combustion is

essential for an understanding of the action of pro-knock compounds.

I OXIDATION OF HYDROCARBONS (4 - 10)

From a simple consideration of a reaction such as,

$$C_3H_8 + 5O_2 = 3CO_2 + 4H_2O$$

it seemed obvious that it could not occur in one step, so that several intermediate reactions were expected.

Under suitable conditions of temperature and pressure, all hydrocarbons have been found to combine slowly with oxygen without the formation of a flame and with no appreciable rise in temperature. Analysis of the products condensed at various stages of such a reaction has shown the presence of various alcohols, aldehydes, acids, oxides, peroxides, carbon monoxide, carbon dioxide, and water (4). At higher temperatures where inflammation might occur, free carbon and hydrogen and lower hydrocarbons have been isolated as well as the above.

Kinetic studies also indicated great complexity involved in the reaction. There was an induction period during which no appreciable reaction occurred, as indicated by pressure change or oxygen consumption. The reaction rate was dependent on a high power of the hydrocarbon concentration. While the oxygen concentration had little effect. This pointed very definitely to a chain mechanism, propagated by collisions of chain carriers with fuel molecules. Temperature coefficients of the reactions indicated highly complex chains; even the character of the combustion was altered at different temperatures. The chain carriers were thought to be very reactive since they were found to be short lived. Surface was noted to play a prominent part in initiating chains and had a pro-

found influence on the reaction rate. The nature and rate of the hydrocarbon oxidation have been found to be greatly influenced by catalysts;both accelerators and inhibitors being effective in very low concentrations.

Theories of Oxidation.

To account for the analytical results and the kinetic evidence, several theories of hydrocarbon oxidation have been formulated. There are two main ones, however; the hydroxylation theory and the peroxidation theory. The former was built up entirely from analytical results, while the latter took into account the kinetic evidence as well. Considerable controversy waged over the merits of the two theories, especially in so far as the initial act of the oxidation was concerned.

1. The Hydroxylation Theory (4, 10, 11) - This was first proposed by Armstrong (12) to account for the production of aldehydes in the slow oxidation of methane by Bone and Wheeler (13). In short, oxidation was assumed to occur by successive hydroxylations of the hydrocarbon molecule, an alcohol being first formed, followed by unstable di - and tri- hydroxy compounds. The di- hydroxy molecule decomposed to give water plus an aldehyde, which was then oxidized to the corresponding acid. This in turn decomposed to water and carbon monoxide or a lower aldehyde, or in the case of formaldehyde to a dihydroxy acid which decomposed to carbon dioxide and water. For methane the scheme suggested was:

(5)

$$CH_4 \longrightarrow CH_3OH' \longrightarrow \underline{CH_2(OH)_2}$$

$$H_2O + H_2{:}C{:}O \longrightarrow \underline{\begin{matrix} HO \\ H \end{matrix}\!\!>\!C{:}O} \longrightarrow \underline{\begin{matrix} HO \\ HO \end{matrix}\!\!>\!C{:}O}$$

$$CO_2 + H_2O \qquad CO_2 + H_2O$$

Secondary reactions, depending on the temperature, pressure and concentration of the reactants would give rise to lower hydrocarbons, peroxides, free carbon and hydrogen. The induction period was explained as the time necessary to form a definite amount of aldehyde which remained constant throughout the subsequent reaction period.

For slow combustion reactions the theory agreed very well with the analytical results, and at least qualitatively for explosions. However there was some doubt as to the initial act; a termolecular collision was necessary which is very improbable. Alcohols were only isolated under high pressures, while the theory predicted them first. The effect of catalysts was also hard to explain since alcohol and aldehydes affected the reaction only slightly while some peroxides had tremendously greater effect, which is the reverse of what was expected from the theory.

2. Peroxidation Theory (10, 11) - This theory was first formulated by Bach (14) and Engler and Wilde (15). A direct addition of a molecule of oxygen to the hydrocarbon to form a peroxide was postulated, followed by decomposition of the peroxide on collision with a second fuel molecule or by itself.

A chain mechanism was easy to postulate, using the decomposition products of the peroxides as carriers, which would account for all the analytical products obtained experimentally. For methane the scheme was:

$$CH_4 + O_2 \longrightarrow CH_4(O_2) \quad \text{or} \quad CH_3 \cdot O \cdot O \cdot H$$

$$CH_4(O_2) \longrightarrow HCHO + H_2O$$

followed by oxidation and decomposition of the aldehyde. Methyl alcohol was formed by:

$$CH_4(O_2) + CH_4 \longrightarrow 2CH_4(O_2) \quad CH_4 \longrightarrow 2CH_3OH$$

However the peroxides were difficult to isolate and it was hard to prove that they were formed initially. This theory required only a bimolecular collision in the initial act, which was far more likely than a termolecular collision. The induction period was explained by deactivation at the walls. Peroxides are far more effective as catalysts than alcohols or aldehydes which led to the conclusion that peroxides were more fundamentally related to the chain carrier than alcohols or aldehydes.

3. Other Theories - Several other theories, as well as modifications of the above two have been postulated:

(a) Norrish (6) - proposed a mechanism using oxygen atoms as the chain carriers. These atoms were said to be formed from formaldehyde which was formed itself by a wall reaction. The scheme for methane was:

$$CH_4 + O \longrightarrow CH_2 + H_2O$$

$$CH_2 + O_2 \longrightarrow HCHO + O$$

The formaldehyde was formed:

$$CH_4 + O_2 \xrightarrow{\text{surface}} HCHO + H_2O$$

$$HCHO + O_2 \longrightarrow (H_2CO_3) \longrightarrow HCOOH + O$$

Chains were terminated according to:

$$O + CH_4 + X \longrightarrow CH_3OH + X' \quad \text{or}$$

$$O + \text{surface} \longrightarrow \tfrac{1}{2}O_2$$

where X was an inert gas molecule. The analytical data was accounted for, but the concentration of oxygen atoms likely to be present was considered insufficient to carry the reaction (16). Methyl alcohol was said to be formed by a termolecular collision with an inert gas molecule which was unlikely as the presence of an inert gas decreased the reaction rate rather than increasing it. The induction period was explained as the time necessary to build up the formaldehyde concentration by the wall reaction. The reaction $CH_4 + O$ explained the experimentally determined fact that the ratio of hydrocarbon to oxygen concentrations of 2:1 was the most reactive.

(b) Lewis (17, 18) - assumed the primary step in paraffin oxidation to be the decomposition to the corresponding ethylene, with the liberation of hydrogen; oxygen would then add to the double bond. The scheme was thought unlikely since olefin oxidations differed greatly in character to that of the paraffins (19, 20, 21).

(c) Ubbelohde (10)- did not postulate the initial step but indicated that hydrocarbon oxidation would follow a similar mechanism to that for aldehydes since the products, rates, etc.

were similar. Here the R - C = O radical was said to be the chain carrier.

Experimental Oxidation Data (4, 10, 22, 23) -

With a knowledge of the theories of hydrocarbon combustion, the experimental results of the oxidations of particular hydrocarbons are more readily interpreted. For the slow combustion of the paraffins in either air or oxygen, the reaction products were predicted by either the hydroxylation or the peroxidation theory. All, from methane to hexane, showed induction periods during which little or no reaction occurred. The rate was found to be dependent largely on the hydrocarbon concentration, the reaction being retarded by excess oxygen or diluents. Pressure and temperature rises decreased the length of the induction period and increased the rate of reaction. For equal reaction rates a much lower temperature was required as the series was ascended. Peroxides were isolated with little difficulty from the higher members; these appeared to occur at about the same stage of the reaction as aldehydes and alcohols. The optimum concentration for maximum reaction velocity was found to be two to one of hydrocarbon to oxygen for methane and ethane, decreasing to one to one for hexane. The higher paraffins also showed considerable chemiluminescence during slow combustion. In explosive combustion all but methane yielded free carbon and hydrogen and lower hydrocarbons. This was related to the decomposition of alcohols

and aldehydes which showed the same products at similar temperatures.

Unsaturated hydrocarbons were found to act quite differently in slow oxidation. The primary step was know with a greater degree of certainty. At room temperature amylene, in the liquid state, added a molecule of oxygen to the double bond:

$$CH_3(CH_2)_2CH = CH_2 + O_2 \rightarrow CH_3(CH_2)_2CH(-O-O-)CH_2$$

It was assumed that the lower members would act similarly, since a pressure drop was observed at first in a constant volume reaction. No chemiluminescence was observed and the addition of aldehydes did not affect the rate. Acetylenes and olefins were assumed to act similarly since glyoxal was isolated. The two to one rate of hydrocarbon to oxygen was found to be the most reactive for unsaturated hydrocarbons also.

Effect of Catalysts

It has already been indicated that the addition of small amounts of reaction intermediates increases the rate of oxidation appreciably. Alcohols have been found to affect the rate only slightly, aldehydes more so, and certain organic peroxides have produced a very great increase in the reaction rate (10). Carbon dioxide, helium, argon and nitrogen all have shown a retarding effect on combustion. Roughly, their activity seemed to depend upon their thermal capacity and thermal

conductivity. Several halide compounds have also been found to retard the oxidation: carbon tetra chloride, the chlor methanes and ethanes, several bromides and iodides and phosphorous oxychloride (11). These latter have been assumed to take part in the combustion reaction itself and act by inhibiting chains. Lead tetra-ethyl and iron carbonyl have shown a similar effect, but it is doubtful whether they take part in the reaction or not. It has been attempted to justify their action on purely thermal grounds on the one hand and by participation in reaction chains on the other. Neither has been proven satisfactorily and it has appeared probable that both play a part.

II PHYSICAL ASPECTS OF COMBUSTION (24 - 28)

A great deal of the discussion of the oxidation of hydrocarbons had to do with slow combustion, but mention was made of an explosive form of cumbustion which possessed different characteristics than the slow oxidation. In fact three modes of combustion have been noted: slow oxidation, inflammation, and detonation. Slow oxidation occurred without the appearance of a flame, and the reaction took a measurable time to go to completion. At higher temperatures the oxidation auto-accelerated and reaction took plade very rapidly and with the emission of a considerable amount of light. This was called inflammation; a still more rapid oxidation was called detonation. In this case the reaction was almost instantaneous over a large portion of the charge and was extremely violent.

Inflammation has been noted to occur in two ways depending on the pressure. In the higher pressure region, a rise of temperature was found to increase the reaction rate to such an extent that the heat of reaction could no longer be dissipated. A rapid temperature rise ensued and the reaction auto-accelerated; light was emitted from fragments of molecules present in the flames. In the low pressure region limits for inflammation have been observed. In this region when the temperature was increased the equilibrium between formation and termination of reaction chains was disturbed. The result was an auto-acceleration of the reaction due to branching of the chains; the temperature rose and light was emitted. The lower pressure limit resulted from deactivation of chain carriers at the walls; the upper limit from deactivation of the chain

carriers in the gas phase.

There have been found, also, upper and lower limits of composition of the mixture, for each hydrocarbon, only within which ignition would occur under given conditions of temperature and pressure. This range of composition narrowed in passing up the paraffin homologous series, e.g. for methane in air the limits are 5 - 15%, for hexane 1 - 4% (24). Endothermic compounds like acetylene have been found to have very wide inflammation limits (3 - 52%). The presence of diluents was found to narrow the upper limit considerably. An increase of temperature also caused widening of the limits. The effect of pressure was found to depend on the mode of ignition (whether spark or hot surface). Generally an increase of pressure widened the limits although optimum pressures have been reported. The ignition limits (pressure), inflammation limits (composition) and the ignition temperature have all been found to depend on: the mode of ignition, the shape and size of the vessel, and the degree of turbulence. The latter raised the ignition temperature but widened the composition limits.

With the higher hydrocarbons, a chemiluminescence occurred for some time before the actual ignition point was reached. These were called "cool flames", and aldehydes were present when this occurred.

The actual speed of propagation of flames was found to depend mainly on the experimental conditions. Here again the

nature and concentration of the mixture, the shape and size of the vessel and the degree of turbulence were the most important factors influencing the speed. Pressure and temperature had little effect. For all the hydrocarbons the flame temperatures were in the vicinity of 1900°C. The unsaturates showed slightly higher temperatures than the paraffins but were within 50°C of them. With air mixtures the flame speeds were from 60 -260 cms. per sec. and with oxygen mixtures from 1000 - 4000 cms. per sec., unsaturates having slightly greater speeds.

Due to compression waves before the flame and other pressure differences in the vessel the flame was sometimes noticed to take up a vibratory form of motion, with a resulting increase in the average rate of burning. Both the uniform and vibratory forms of flames were far below the velocity of sound, so that the compression wave corresponded to a low pressure gradient. The flame speeds and temperature depended, in general, on the freedom offered for the expansion of the burnt products.

Detonation , the most violent form of combustion was said to occur when an accelerating flame catches up with the crest of the compression wave being propagated ahead of it. A sudden increase of rate and pressure was noted. The sudden energy release in the reaction activated a large portion of the charge to sudden reaction. Another possibility for the occurrence of a detonation was said to be the reflection of a compression wave from the walls into the path of the flame or vice versa. The change from ordinary inflammation to detonation

has been reported as occurring at once, or by a series of increases in flame velocity. Detonation waves are reported to travel much faster than sound, the reason being that the wave is propagated by a much greater pressure gradient between successive layers. They have been said to be propagated uniformly at a rate of about 12000 feet per second. In ordinary flames burning occurs by conduction of heat from layer to layer whereas in a detonation it is mainly by adiabatic compression, the flame becoming a compression wave. As is the case with inflammations, limits of composition have been found within which, but not outside of which, detonation would occur. Similarly factors which influenced inflammations have also been found to have a similar effect on the propagation of detonation waves.

In a detonation the reaction has been found to be practically complete and instantaneous in the flame front, while in normal inflammations the reaction has been noted to occur behind the flame front for a short time. Many detonations were noted not to travel linearly, but helically near the walls of the reaction tube. These are called spin detonation waves. Doubt has been expressed whether it was the head of the detonation wave only that was propagated helically or whether it was the whole body of the gas.

III KNOCK

Combustion in Internal Combustion Engines (27)

The combustion phenomena observed in internal combustion engines is similar to that in laboratory equipment when the conditions of operation are considered. The mixture is spark ignited, although it is also heated by the walls of the cylinder. The combustion occurs at fairly high pressure, with a considerable degree of turbulence in the mixture. Near the end of the compression stroke the fuel-air mixture is spark ignited. A flame travels through the compressed gas, as in normal inflammation. The reaction is fairly complete in a narrow flame front. The pressure is increased greatly due to formation and heating of the products and the energy is utilized on the expansion, or power stroke. For maximum power it is desirable to have a high compression ratio so the pressure at the time of ignition will be high. The flame speeds are of the order of 25 - 250 feet per second. In normal combustion very little reaction occurs before the flame. As in simple explosions the pressure increases to its maximum value of about 1000 lbs. per square inch in 0.001 sec. without pulsation or vibration, when the engine is operating normally.

Knock in Internal Combustion Engines (27,29)

Under certain circumstances the character of combustion in an I.C. engine may change accompanied by a knocking sound. It results in loss of power and efficiency and may result in damage to the engine through mechanical failure of some of the

parts. This is especially so in high duty aircraft engines where gumming, pitting and seizure occur.

Examination of the nature of this type of combustion has shown that it is an abnormally rapid explosion of a certain portion of the charge which is the last to burn, resulting in the formation of pressure waves in the gas. The portion of the charge undergoing knocking combustion may be as high as three quarters of the whole charge. The flame and other characteristics of the combustion preceding knock has been found to be quite regular and identical with that in the entire absence of knock. However the flame begins to vibrate and suddenly accelerates. The ignition of the unburnt mixture ahead of the flame sometimes precedes or is synchronous with this acceleration. A re-illumination or after-glow flashes back and forth from the flame front with the speed of sound through the burnt products and the pressure pulse or shock wave accompanies this after-glow (24). The velocity of the pressure wave is about 900 metres per second, the pressure rise is about 10000 pounds per square inch in 0.001 of a second. It is these pressure waves which on reflection from the cylinder walls set up a state of resonant vibration which gives the audible sound associated with knock. The knocking part of the charge, immediately before the onset of knock is in a highly sensitized state due to partial combustion at the temperatures caused by compression and conduction from the walls. Knock would thus be increased by any factors which tend to increase the tem-

perature of the charge or the length of the time of heating prior to ignition. These are called the temperature and time factors. Knocking fuels have a thin flame front and pronounced re-illumination when the shock wave is reflected from the walls. With a non knocking fuel there is a continuous zone of combustion extending back from the flame front. Multiple knock may occur when the shock wave or reflection from the walls separates the unburnt mixture into two regions which may not knock at the same instant.

Theories of Knock (11, 27, 29)

From what has been said previously, knock and detonation might appear to be identical or at least very similar. The evidence seems to indicate that knock is not a true detonation, but is a type of combustion intermediate between inflammation and detonation. It is similar in that it is a violent and almost instantaneous reaction of a presensitized fuel-air mixture. However it is neither as violent nor as rapid as a true detonation. The flame velocity in knocking combustion is about 1000 feet per second, and the pressure developed is only about 10,000 pounds per square inch in 0.001 of a second, while the velocity of a true detonation is as high as 10,000 feet per second and the pressure developed is much higher than for a knocking explosion. It is also unlikely, from conditions of the mixture, temperature, pressure and vessel shape and size, that a true detonation could occur in an engine cylinder.

Explanations of the knocking sound and its relation to flame conditions were offered by a number of investigators. Midgely and Boyd (30) attributed the knocking sound to impact between the piston and the cylinder walls, and later (31) to the impact of a high velocity, high pressure wave against the cylinder walls. The pressure and velocity of the explosion wave in knocking combustion are far greater than in normal combustion due to the exceedingly high pressure differential between successive layers. A long cylinder would thus have greater tendency to knock, which is found to be true. Egerton and Gates (32,33) account for the knocking sound by compression waves set up by enhanced vibratory combustion near the cylinder walls. Maxwell and Wheeler (34) reported a vibratory combustion during knocking which started a shock wave through the fuel causing it to detonate.

This did not explain the origin of knock, that is the chemical reactions which precede and accompany a knocking explosion and how thy differ from those in normal combustion. Several theories have been advanced to explain the origin of knock, and much controversy arose because of the variety of conditions under which the various investigators operated. Ricardo (35) attributed the knock to the spontaneous ignition of the last part of the charge to burn. Expansion of the normal burning charge compressed the unburned protion before it, heating it, until, when this heat could no longer be dissipated, the remainder of the charge ignited spontaneously before the flame reached it. From this, the knocking tendency

of a fuel should be a function of its ignition temperature, which is certainly not always true. For example, Tizard and Pye (36) pointed out that carbon disulfide has a lower ignition temperature than heptane but has less tendency to knock. Withrow and Boyd (37) however showed by pictures of the explosion that spontaneous ignition did occur in many cases before the flame reached the part of the charge involved in the knock. In spite of this controversy there appears to be, in many cases, a sort of parallelism between ignition temperatures and knock tendency of fuels. It has been suggested, also, that the initial temperature of slow oxidation was related to knock tendency. Callendar (38) proposed a nuclear theory which differs radically from any other theory of knock. He suggested that when a fuel was atomized in the air the drops, as they evaporated, left a residue or liquid nucleus consisting largely of the less volatile constituents such as the higher paraffins. These drops would serve as foci of ignition since they have a lower ignition temperature than the vaporized mixture. When peroxides were shown to have considerable knocking effect, Callendar (39) suggested that the peroxides were formed and accumulated in the nuclear drops, and acted as a primer, causing simultaneous ignition of the whole drop. Egerton and Gates (40,41) however showed that knocking could and did take place in the gas phase. They believed that peroxides catalyse the knocking reaction but would not act as primers. In support of the liquid phase origin of the knock Moreau, Dufraisse and

Chaux (42) showed that the higher boiling hydrocarbons form peroxides much more readily than the lower members. However it is unlikely that liquid nuclei play a part in oxidation.

The formation and accumulation of peroxides is believed by many authorities to be the origin of knock. Egerton & Gates (40, 41) Salmoni (43) Dumanois (44) Roberti (45) and Prettre (46) support the idea in some form. Unsaturated hydrocarbons form peroxides more easily than saturates yet their knocking tendency is much less. Mondain, Monvall and Quanquin (47) did not believe that the peroxides themselves caused knock but rather highly oxygenated fragments of molecules. Peroxides which are readily split do promote knocking, while those similar to the ones formed by ethylenes do not appreciably (48, 49). This is in agreement with the suggestion that peroxide fragments are active, and is similar to results obtained in reaction between hydrogen and oxygen (50).

Rice (51) noted the relation between knock ratings of heptane isomers and the number of molecules of lower hydrocarbons produced during their thermal decomposition. This, he argued, showed that knock was due to thermal decomposition before oxidation. Steele (52) attributed the knock to free hydrogen liberated during thermal decomposition before combustion. Free hydrogen and lower hydrocarbons react very rapidly with oxygen and their rates of flame propagation are about ten times that of gasoline-air mixtures. The thermal decomposition has been suggested to occur by absorption of radiation (53). Ionization and emission of electrons in the burning charge which

sensitize the unburned portion has also been suggested as a possible cause of knock (54).

Most observers however agree that knock is caused by some sort of presensitization of the last part of the charge, explainable by a chain reaction mechanism. Beatty and Edgar (55) point out that under the conditions necessary for a knocking combustion the mixture is in a critical state of composition. The end gas is undergoing slow oxidation, in which the number of chains formed equals the number deactivated. When the temperature and time factors (p.24) are such that knocking can take place chain branching occurs, increasing the number of active products in the end gas, so that when the flame reaches this region there is almost instantaneous reaction throughout. In a detonation the probability of chain branching is unity so that the chains multiply in a geometric progression. Here it is supposed that every collision leads to activation of a reactant molecule, so that the rate of reaction is proportional to the speed of moving of chain carriers and the flame and pressure wave sweep through simultaneously. In knocking combustion the collision efficiency is less than for a detonation.

Out of all this no really satisfactory explanation of the origin of knock has yet been advanced. The knocking sound is likely due to pressure wave impacts arising from sudden reaction of the last part of the charge which has been presensitized. This presensitization probably is the accumulation of active chain carriers, highly oxygenated molecular fragments, or extensive branching of reaction chains. Whether the sudden

reaction occurs before or after the flame reaches the presensitized gases is still a little doubtful. Radiation, ionization, and thermal decomposition of the fuel may be contributory factors to the knock although this too is doubtful.

Measurement of Knock

The higher the compression ratio in an I.C. engine the greater is the power developed from a given amount of fuel. It is thus highly desirable that such an engine should operate at as high a compression ratio as possible. But, however, the tendency for knock to set in increases with the compression ratio which more than offsets the power gain from the increased compression ratio. Also under similar conditions the intensity of knock of various fuels differs, but the relative audibility of knock is not sufficiently sensitive for comparision of fuels.

Ricardo (56) determined the highest compression ratio at which an engine could be operated without audible knock. This was called the highest useful compression ratio. Several other methods using the audibility of knock have been suggested: (a) the spark advance determined at various knock intensities,(57); (b) determination of I.H.P. at various rates of fuel flow at the throttle setting for incipient knock (58); (c) power developed at throttle opening for incipient knock, at constant mixture ratio, speed and spark (59). In some cases an audiometer was used to measure the audibility of the knock (60, 61). Temperatures of the cylinders have also been measured directly (62) and compared with standard reference fuels of known knock rating. Rate of pressure rise in bombs (63), ignition tem-

peratures (64), and the time to rupture a diaphiagm of known thickness (65) have all been suggested.

In 1928 the Cooperative Fuel Research Committee standardized the methods, using a bouncing pin indicator (66). A steel pin rests on a thin steel diaghragm in direct contact with the compustion chamber. When knock occurs the pin is driven upwards, closing a pair of contacts, thus causing current to flow in an electric circuit containing a hot wire element. A thermocouple placed near the hot wire element is connected to a millivoltmeter, the reading of which varies with the temperature of the element and hence with the knock intensity. The millivoltmeter is known as a knockmeter. This merely gives a comparison of the knock of a given fuel with that of reference fuels of standard knock rating.

A scale for measuring relative knock rating of fuels has been established. The primary standard fuels, upon which this scale is based are iso octane, a hydrocarbon of high anti knock value and normal heptane, a hydrocarbon of low anti knock value. Iso octane is assigned an "octane rating" of 100 and normal heptane 0. The octane rating of any fuel is the percentage of iso octane in a mixture of N. heptane and iso octane (67) which matches the knocking characteristics of that fuel. Secondary standards are generally used comprised of a mixture of two straight run hydrocarbons, one of high the other of low octane rating, which have been carefully calibrated against iso octane and normal heptane.

The Ethyl 30 - B Knock testing engine is a one cylinder

valve in head, variable compression engine, fitted with a bouncing pin indicator and thermal element knockmeter. A constant speed synchronous motor is used for starting the engine and for absorbing the power at constant speed when the engine is running. The engine is operated at 900 rpm, engine temperature 345°F, spark advance 15 degrees, shim thickness 0.375 inches and at a compression pressure of 130-133 pounds per square inch at full throttle. The compression ratio is maintained constant and the throttle set to give almost full knockmeter scale deflection for any desired difference of octane numbers. The air to fuel ratio which gives maximum knock is used. Knockmeter readings are determined for the fuel being tested and are bracketed by those of reference fuels of slightly lower and slightly higher octane rating. The octane rating of the test fuel is then determined by linear interpolation.

The 30B Engine is now considered obsolete and has been replaced by a variable compression engine designed by the Cooperative Fuel Research Committee. The principle upon which it operates is essentially the same as for the 30B type. The specifications called for by the American Society for Testing Materials (68) are as follows: speed 900 rpm; spark advance is automatically controlled by the compression ratio; the compression pressure, at 5.3:1 compression ratio, is set at 114 ± 2 psi; the compression ratio is determined by the test fuel, being adjusted to give a knockmeter scale reading between 55-60 divisions. Reference fuels are used within two octane numbers

on either side.

The accurate determination of octane rating varies considerably with changes in conditions. Hence the specifications for testing are always rigidly fixed. The outstanding factors are: compression ratio (69), throttle opening (70), engine speed (71), spark timing (72), mixture temperature (71), Jacket temperature (71) and intake air temperature (71). Knockmeter readings must be taken at the air fuel ratio for maximum knock (72).

In road tests (73, 74) different makes of automobiles have different speeds, spark timing, mixture ratios and temperature so that laboratory data do not always correlate with road tests in any particular car. On the average, the present standard laboratory conditions agree quite closely with road tests.

Knocking Characteristics of Various Fuels (75)

Considerable work has been done in an attempt to relate molecular structure of fuels to their knock tendency. The fact that different isomers have radically different qualities as fuels show that structure is important. For example, 1 hexane and cyclohexane, and normal heptane and 2, 2, 3 trimethyl butane; the latter two are extremes in knock tendency. For normal or straight chain paraffin hydrocarbons there appears to be a steady increase in knock tendency with increase in length of the hydrocarbon chain. This effect of increase in length also occurs in the case of branched hydrocarbons where the longest

straight chain is considered. Successive additions of methyl groups to a carbon atom chain results in a regularly decreased tendency to knock. Among paraffin isomers the more compact the molecular structure, the less is the tendency to knock. The actual number of carbon atoms in a paraffin hydrocarbon has no significance due to these effects of chain lengthening and chain branching. Olefines in general show better anti knock qualities than the corresponding paraffins. The same effects of chain lengthening and branching are obvious here. The position of the double bond is important, the nearer it is to the centre of the molecule the less the tendency to knock. The length of the unbroken chain has the same effect as chain length in paraffins. Cyclic hydrocarbons are superior in anti knock qualities to the corresponding normal paraffins. The presence of an unbranched side chain causes an increase in knocking tendency, the effect being proportioned to the length of the side chain. Branching of the side chain on cyclohexane causes a great decrease in knocking tendency; some branched side chain compounds being superior in this regard to cyclohexane itself. The relative positions of two or more side chains has apparently little effect. A double bond in the ring as in cyclohexenes has the same properities relative to cyclohexane as in ethylenic double bond has to straight chain hydrocarbons. Aromatic hydrocarbons are superior in knock tendency to the aliphatic compounds. The presence of a straight side chain on a benzene ring decreases the knock tendency up to a length of 3 carbon atoms and increases it thereafter. Methyl groups added to the ring improve

the anti knock value. Para positioned side chains are superior to meta and ortho.

The greater part of the work on molecular structure and knock tendency has been done in dilute solution of a standard hydrocarbon, due to the difficulty in obtaining sufficient of the pure hydrocarbons for engine tests. However work that has been done on pure hydrocarbons agrees well with the dilute solution effects.

IV ANTI KNOCK COMPOUNDS

Midgely and Boyd (76, 77, 78) seeking to improve quality of gasolines discovered a large number of compounds which, when added to motor fuels in small quantities resulted in a large increase in their knock rating. These are called anti knock compounds. Since then a great deal of work has been done in an effort to find more effective anti knocks. Often included under this class of compounds are the so called "non knock fuels." These are fuels in themselves of high knock rating. When added to poorer quality fuels, the knock rating of the blend is increased. Large quantities of these (from 10 - 60%) have to be added to a low quality gasoline to raise its knock rating. Among these non knocking fuels are: benzene, terpenes (79), alcohol, iso - octane, and cracked gasolines. It is difficult to decide whether the effect obtained in a blend of a non knocking fuel with a knocking fuel is merely the sum of the partial effects of the two, or whether the non-knocking fuel also acts as an inhibitor of the knock caused by the other fuel. There are some indications that non knocking fuels do exert a slight anti knock effect (80).

The true anti knock compounds suppress or greatly decrease the knocking, far out of proportion to the amount added. A large number of organo-metallic compounds and many nitrogen compounds are particularly effective. There follows a list of the more important compounds classified according to their chemical structures.

1. Nitrogen Compounds.

These are true anti knock compounds, the better of these

shows measurable effect at a concentration as low as 0.1%, an amount which can hardly be considered to modify the bulk concentration of the fuel. The anti-knock effect is not due to the presence of nitrogen alone, since some nitrogen compounds (nitro, nitrites, and nitrates) actually promote knocking. The effectiveness apparently depends upon a special type of linkage between the nitrogen and the organic radicals (81). In this class, amines show the greatest effect. Table I shows the relative effectiveness of several amines. Values are the reciprocal of the number of moles giving the same anti-knock effect as one mole of aniline.

The presence of an aromatic linkage to the nitrogen greatly increases the anti-knock effect. Side chains on the aromatic ring also increases the effectiveness. Secondary amines are in general better than primary or tertiary.

TABLE I (81)

Comparison of Anti-Knock Activity of Several Amines
(Numbers are reciprocals of the moles giving the same effect as one mol of aniline.)

Ammonia	0.9	Toluidene	1.22
Ethyl amine	0.20	m-Xylidene	1.4
Diethyl amine ..	0.50		
Triethyl amine .	0.14	Monomethyl aniline..	1.4
Triphenyl amine.	0.09	Monoethyl aniline .	1.02
Aniline	1.0	Dimethyl aniline ..	0.21
Diphenyl amine ..	1.5	Diethyl aniline ...	0.24

Amides (82), imines (83), carbamides (84) and cyanogen compounds (85, 86) have been shown to have anti-knock properties, but to a much lesser extent than the amines.

2. Other Group Five Elements.

(a) Phosphorous and arsenic (84). Some of these compounds

are known to be oxidation inhibitors, but there is very little mention of anti-knock properties.

(b) Antimony ((84, 87). Trivalent antimony acts as an anti-knock compound, while pentavalent antimony is a pro-knock. Antimony triphenyl and trichloride are effective anti-knocks.

(c) Bismuth (84, 88, 89, 90). Some bismuth compounds are rather good anti-knocks, e.g. bismuth trimethyl, triethyl and triphenyl.

3. Halogens.

Although halogens, particularly the lighter ones, are generally considered to possess pro-knock tendencies, several halogen compounds are anti-knocks. Carbon tetra-chloride (91), ammonium halides (91), alkyl halides, particularly iodides (81, 84, 92), chloro, bromo and iodo naphthalene (91), iodine (84, 93) and phenyl halides have all been reported as being anti-knock compounds. Iodine compounds are stated to be the best, bromine next, and chlorine the least effective (82).

4. Sulphur, Selenium, Tellurium.

Several sulphur compounds such as inorganic sulfides (84), organic sulphur compounds and sulphur itself are anti-knocks. Selenium compounds have a much greater anti-knock tendency than sulphur and tellurium more than selenium. Selenium diethyl (84, 88, 90) is quite a good anti-knock and selenium diphenyl (84, 88) is fair. Tellurium diethyl (88) is a strong knock inhibitor and the diphenyl (88) slightly less so.

5. Other Non-metals.

(a) Boron (84). Has slight anti-knock effect.

(b) Silicon (84, 91). Silicon tetraethyl is a fair anti-knock.

6. Metals.

A great many metal compounds, both their salts and organo-metallic compounds, have anti-knock properties. Here the action is identified more closely with the element itself rather than with the type of linkages (88). There has been much discussion as to whether uncombined metals have or have not anti-knock effect, without a definite conclusion having been reached. The most effective anti-knock compounds known belong to this type.

The lighter metals have been found not to have very great effect. Among the potassium compounds, the gallate (92), oxalate (84), citrate (84), ethylate (94), and iodide (95) are effective. However potassium vapor acting in the oxide form is more effective than tetra ethyl lead. Barium carbide (96) has also been reported as having anti-knock properties.

However, it is mainly the heavy metallic elements that possess greatest anti-knock activity. Lead compounds have received the greatest attention and it appears that tetravalent lead almost always has anti-knock power, while bivalent lead compounds are ineffective (84). Lead tetramethyl (90) is quite good, lead tetraethyl (84, 88, 90) is the best anti-knock known and has found wide practical application, lead tetrapropyl (84), dimethyl diethyl (97, 98) and many others have all been studied and found effective in varying degrees.

Iron, cobalt and nickel are also very effective. The

carbonyls are next to tetraethyl lead in activity (84, 88, 90, 99, 100, 101). Iron acetyl acetone (90) is also effective.

Chromium phenyl (100) has a slight effect, as has molybdenum carbonyl (99).

Tin tetramethyl, tetraethyl and tetraphenyl (84) are fairly good, and some of the stannic halides have also been reported as anti-knock (84, 88, 90, 98, 102).

Compounds of zinc (91), cadmium (88), mercury (103, 104), cerium (83, 84), thallium (105), vanadium (84) and titanium (88) have also been used as anti-knock agents.

The following tables show the relative effectiveness of a number of anti-knock compounds:

TABLE 2 (81, 106, 107)

Relative Effectiveness of

Different Compounds of the Same Element

(Number is reciprocal of the number of mols giving the same effect as one mole of aniline)

Elements	Ethyl Compound	Phenyl Compound
Iodine	1.09	0.88
Selenium	6.9	5.2
Tellurium	26.8	22.0

TABLE 3 (108)

Relative Anti-Knock Effestiveness

(Reciprocal of the number of mols giving the same effect as one mol of aniline)

Lead tetraethyl	118	Bismuth trimethyl	23.8
Lead tetraphenyl	70	Bismuth triethyl	23.8
Lead diphenyl dimethyl	115	Bismuth triphenyl	21.4
Lead diphenyl diethyl	109	Stannic chloride	4.1
Lead diethyl chloride	79	Stannic iodide	15.1

Lead thioacetate	10	Monophenyl arsine	1.6
Cadmium dimethyl	1.24	Triphenyl arsine	1.6
Titanium tetrachloride	3.2		

In all cases where the element is the determining factor rather than the linkage, the change from ethyl to phenyl causes at most a 20% decrease in activity (88). The effectiveness varies with position in the periodic table, increasing down the groups.

7. Aromatic Compounds.

In general aromatic compounds possess anti-knock activity; this activity decreases with hydrocarbon side chains but increases with hydroxyl or amine groups (109). Phenyl chloride (91), iodide (84, 93), sulphide (84) nitrite (80), monophenyl and triphenyl arsines (88), diphenyl oxide (84), dihydroxy benzene (84, 90), phenol (100), cresol (84) and quinone (110, 84) have been reported to possess anti-knock properties.

8. Ketones and Esters.

In general these do not show very great pro- or anti-knock activity. Some ketones (109) particularly higher ones are effective. Methyl and ethyl esters, and salts of boric, silicic and acetic acids (91) show some effect. Some of the naphthenic acid esters (111), ferrocyanic acidsesters (112), the esters of palmitic, oleic, myristic, and lauric acids (84), and potassium gallate, oxalate and citrate (84) are anti-knocks.

9. Inorganic Salts.

Carbonates of lead, copper, calcium and sodium; nitrates

of lead and copper (113), hydroxy compounds (109) and water (84) decrease knocking.

Another type of anti-knock action has been suggested, that of coating the inside of the explosion chamber of the cylinder with substances which would suppress knocking. Carbonates of lead, copper, calcium, magnesium, sodium or patassium, mixed with an inert material such as silica have been patented (113). The oxides of vanadium, cobalt and rare earth metals especially cerium have also been suggested (114). The efficiency of such compounds is low and give rise to many mechanical difficulties such as fouling.

Some compounds, actually not anti-knocks, are added to gasoline in small amounts to preserve the anti-detonant properties of the cracked stock. Aniline, hydroquinone, napthalene and anthracene (115) have all been found to prevent loss of anti-knock properties of a fuel in storage. Any antioxidant is effective in this regard.

V PRO-KNOCK COMPOUNDS

Little was known of the action of pro-knock compounds on fuels until the last two years. Previously these compounds were discovered in the search for anti-knock compounds, or were suspected of being intermediate compounds in the combustion of fuels. As in the case of anti-knock compounds knocking fuels may be considered in this classification. They are merely fuels of a low octane rating. Ethers and aldehydes (84) belong to this class and the addition of a relatively large quantity of these to a fuel will increase its knock tendency.

It has been known for some time that organic peroxides (83) were very powerful knock-inducers. These are, of course, believed to be intermediates in certain modes of combustion of hydrocarbons. Ozone (116) has a pro-knock effect comparable in magnitude with the anti-knock effect of lead tetraethyl. Hydrogen peroxide (83) dimethyl, diethyl, and ethylhydrogen peroxides (83, 29) are among the most powerful; ethylidene, acetyl, benzoyl, cetyl and diaceto peroxides (84, 117, 118) only slightly less so. Methyl and ethyl ketone peroxides and olefine peroxides are not effective (83, 84, 118, 119). Several organic nitrogen compounds, especially the highly oxidized ones, are quite powerful pro-knocks. The aliphatic nitrites (84, 110, 119, 120) are among the best of the nitrogen compounds, while the corresponding nitrates (93) nitro compounds and the oxides of nitrogen (80, 83, 84, 119, 120) are much less effective although several have a pro-

nounced effect. The halogens too, have in many cases pronounced knock inducing characteristics. Bromine and chlorine (83, 84, 104) and several organic hallides have been reported as pro-knocks. Chlorine and chlorine compounds have been stated to have greater activity than bromine and the corresponding bromine compounds. Iodine compounds are considered to have more anti-knock than pro-knock tendency.

In recent years a concentrated study of pro-knock activity as a war weapon has veen made. A preliminary study of some 197 compounds by the author (1) was made using a 1933 chevrolet engine. Both qualitative and semi quantitative determination of pro-knock activity were made, using audibility of knock as the criteria of effectiveness. Chloropicrin was found to cause slight knock at a concentration of 3 parts per million of air and serious knock at 21 parts per million of air. Iso amyl nitrite, t-butyl nitrite, n butyl nitrite, bromopicrin, ethyl nitrate, t butyl nitrate, aceto acetic ester, and thionyl chloride were effective in concentration ranging from 4 parts per million for n butyl nitrite to 400 parts per million for thionyl chloride. Other compounds which showed knocking at higher concentration were methylene chloride, butyraldehyde, isopropyl ether, ethyl tert. amyl ether, diethyl ether, nitro methane and nitro propane. The effectiveness of nitrites, nitrates, nitro compounds and halogens was noted.

Sugden (2) in a report on pro-knock activity lists carbon disulfide and chlorine as causing considerable knocking.

Stacey and Wasson (121) in an extended study of anti-

and pro-knock compounds, found the following to be powerful knock inducers: Nitrites (ethyl, isopropyl and amyl), aldehydes (benzaldehyde, and heptaldehyde), methyl nonyl ketone, cetyl alcohol, stearic acid, cobalt oleate, petrolatum, thio carbanilide, nitro iso-siopropyl-p-toluidine, allyl iso cyanate and the chlocyanate, amyl ether, methyl sulphate, several organic metallic compounds (mercury diphenyl, tin tetraphenyl, silicon tetraphenyl, zinc diethyl, lead triphenyl iodide, amyl mercuric iodide, and phenyl mercuric iodide, cobalt oleate), cadmium bromide and ammonia gas. They concluded that nigrogen when present as an organic nitrate or nitrite showed pro-knock properties, but when present in the amine form show either anti-knock properties or an effect. Iodine is found to exhibit both pro and anti-knock activity.

Lapeyrouse and Lebo (122) list the octane blending improvement (O. B. I.) of some 300 compounds. Here O. B. I. equals $\frac{C - A}{X}$ where C is the octane member of a blend of X in the base stock, A is the octane member of the base stock, and X is the proportion (fractional part) of the blending agent. Compounds showing a high negative O. B. I. are:

o - p - ditolyl - p phenylene diamine - 300

Allyl isocyanate - 200

Aliphatic hydroxy amines - 1000

Zinc salt of the diketone $C_5H_7O_2$. -9 940

Ferric salt of the diketone $C_5H_7O_2$ - 940

The octane blending improvement of chloropicrin would be -16700.

Midgely and Henne (34) have reported pro-knock investi-

gations by the National Defence Research Committee, done on C. F. R. knock testing engines. The effect of pro knock on both leaded and unleaded fuels was tested. Among the more effective were (on the basis of a twelve octane drop):

Sulphur trioxide

Nitrogen chloride

Butyl dichlorophosphine

Sulphur chloride

1 chloro 1 nitro propane

1, 1, dichloro 1 nitro ethane

Phosphorous sulphochloride

Phosphorous tri bromide

Phosphorous tri chloride

Phosphorous oxychloride

Chloropicrin

Chromyl chloride

Sulfuryl chloride

Sulphur tri oxide causes the 12 octane drop, on a leaded fuel (5.36 ml tetra ethyl lead per gallon), at 41 parts per million of the air consumed by the engine; in unleaded fuels much higher concentrations of pro knock are required. It appeared that some compounds acted by neutralizing the lead such as phosphorous oxychloride while others such as isoamyl nitrite had approximately equal effect in leaded and unleaded fuels. Sulphur tri-oxide counteracts lead, but in unleaded fuel also has pro knock value. The pro knock activity also varied with the base stock of the gasoline. A number

of these compounds duplicate investigations reported herein; mention will be made of these in the discussion.

While not in the class of pro-knocks, several compounds in minute quantities have other detrimental effects on the operation of automotive equipment. Sugden's report (2) states that phosphorous tri chloride, phosphorous oxychloride, and carbon tetra chloride caused an engine to stop by gummed pistons, or fouled spark plugs. At the Thomas and Hochwalt laboratories (123) several resins were found to render gasoline unuseable in Delco Lite engines. Para dura 10 P, a commercial oil soluble phenolic resin at 10 grams per gallon will effectively gum the piston of an engine after about one gallon of doped fuel has passed through each cylinder. Paradura 367, super bechacite 1001, santo resin, chinawood oil, phosphorous tri chloride, $PNCl_2$ and metal napthenates are somewhat less effective.

VI THEORIES OF ANTI AND PRO-KNOCK ACTION

The facts to be accounted for by any anti-knock theory are that (a) anti and pro-knock compounds show considerable effect in very minute quantities. (b) Compounds having similar anti-knock properties have widely different chemical composition and structure. (c) The change from normal to knocking combustion is abrupt rather than continuous. (d) Anti-knock effect of large quantities of non knock fuels.

Naturally the theories accounting for anti-knock action will be closely related to one or another of the theories for the cause of knock.

Where the walls were assumed to initiate knocking combustion the action of anti-knocks was to deposit on the sharp edges and points in the cylinder increasing their radius of curvature and thus making them less capable of initiating combustion ahead of the flame (124). This however fails to take account of either the action of the organic amines as anti-knocks or of pro-knocks. In addition, knocking is found to recommence as soon as gasoline free from lead is used. This should not be so since lead and its oxides should continue to cling to the walls. Sokal (125) reduced knocking by coating the walls of the chamber with carbonates or oxides of lead, cerium and other elements.

Corresponding to the radiation and ionization theories of knock, anti-knock action was explained, by absorption of radiation or electrons (126, 127)thus reducing the rate at which combustion accelerated. The heavier elements in the lower right hand corner of the periodic table would be the most

effective, and hence would be the best anti-knock materials. Wendt and Grimm found that ion recombination above a pool of benzene was facilitated by tetra ethyl lead, but others (128) have found differently. However ionization or absorption of radiation is not generally accepted as causing knock so this explanation of the action of anti-knocks is unlikely. Furthermore pro-knocks should thus increase ionization which has not been observed. No explanation of action of amines is advanced.

The action of anti-knocks has been explained by their destruction of peroxides or highly oxygenated fragments in a variety of ways. Many assume the decomposition of lead tetra ethyl to metallic lead, the lead forming an oxide or peroxide by reaction with organic peroxides present. (129, 130). Some however believe (131, 132) that the lead must first be oxidized, the oxide then reacting with the organic peroxide, itself forming a peroxide. The properties of a good anti-knock would thus be a metal which is oxidized, yet capable of oxidation to a higher oxide and which is dispersed throughout the charge so as to be almost vapor. The metal peroxide subsequently regenerates the metal itself. Organic amines act similarly, but are not nearly so effective since, once oxidized, they are less readily regenerated. Pro-knocks would facilitate the formation of peroxides. Most effective anti-knocks would be metals which readily form peroxides, potassium, sodium, manganese and lead.

Callendar proposed a theory of anti-knock action based on his liquid droplet theory of knock (133). Anti-knocks, if

concentrated in the liquid droplets, either in their original form or as a colloidal metal deposit on the surface would prevent these foci from igniting spontaneously ahead of the flame, by arresting peroxide formation. This would explain the action of anti-knocks in such small quantities. However the droplet theory of knock is considered very doubtful.

A number of theories have been advanced in which the anti-knock actually accelerates combustion. Multiple spark plugs are known to decrease knock, so that fine incandescent lead particles in the cylinder would act as multiple miniature spark plugs, which would cause evener and more uniform reaction (134, 135). Charch, Mack and Boord (136) and Lewis (137) however attributed the multiple ignition centres, not to incandescent lead particles, but to the heat of reaction liberated where a lead particle oxidized, which initiated slow combustion uniformly throughout the cylinder. The action of organic amines would be that their heat of oxidation acted similarly. Clark Brugman and Thee (135) suggested that anti-knock compounds catalysed an alternative mode of combustion which did not lead to the formation of substances which cause knocking.

A great many attempts have been made to relate anti-knock action to the effect of the anti-knock on the spontaneous ignition temperature of the fuel. Egerton and Gates (129) and others found that several anti-knocks raised the ignition temperature of the fuel. Still others (126, 138, 139) concluded that no relation was possible between anti-knock action and its effect on ignition temperatures. It is worth noting that the effect of catalysts on spontaneous ignition tempera-

tures depends to a great extent on the mode of ignition. The effect being much more marked when a hot wire was used rather than a spark. The hot wire would permit slow combustion to occur before actual ignition. Schaad and Boord (138) attributed anti-knock action to the inhibition of pre flame combustion.

Many experiments have been carried out to determine whether it is the anti-knock compound itself, or the finely divided metal particles which cause the anti-knock action. Finely divided metal sols of lead and nickel in the gasoline were found to have little if any anti-knock effect (140, 141), but fine lead particles in the vapor were found to have an effect equal to that of lead tetra ethyl (142).

From all this no definite anti-knock mechanism may be formulated. These compounds appear to decrease the pre-sensitization of the knocking portion of the charge, probably by decreasing the number of the active chain carriers formed, by an oxidation, reduction mechanism. However it is possible that the different classes of anti-knock compounds, i.e. organo metallics and organic amines may act by entirely different mechanisms. The action of pro-knocks appears to be by an increase in number of active chain carriers, causing excessive chain branching.

EXPERIMENTAL

The investigation consisted essentially of determining the octane drop caused by various concentrations of a compound added to the air intake of, or dissolved in the gasoline used in a knock testing engine. The octane number of the gasoline itself was first determined and then the rating of the fuel with the pro-knock added. The octane drop was determined by the difference of the above two readings. Several concentrations of pro-knock were used for each compound.

For this, an Ethyl Knock Testing Engine Type 30B was available. Although this engine is considered obsolete for accurate fuel testing, it was found to be quite satisfactory for these investigations where absolute octane ratings were not required. Perhaps not as convenient for routine laboratory tests, this machine is still quite satisfactory. Results obtained in checking the octane numbers of gasolines agreed closely with those determined by the company which supplied the gasoline. Also data on pro-knock activity as determined on this engine agreed closely with that from other laboratories using the more modern Cooperative Fuel Research Engine under American Society for Testing Materials specifications.

The gasoline used for these determinations was an 80

octane leaded aviation fuel of 72.6 octane cracked base stock, as supplied to the R.C.A.F. by Shell Oil Company. It was used chiefly because it was the gasoline of the highest octane number that could conveniently be used without modification of the 30B Engines. A leaded gasoline was used since these would be met in field applications. Reference fuels were those specified and supplied by Standard Oil Development Company.

The chemicals used as pro-knocks came from a variety of sources. Many were synthesised in these laboratories: in particular the nitrites, nitro and brom methanes, and chloropicrin. Others were supplied by various manufacturers of fine chemicals, the chemically pure compounds being used.

Since it was desired to express the concentrations of pro-knocks as parts by volume per million of air consumed by the engine, the air consumption of the engine was determined. For this a 200 cubic foot per minute gas meter was attached in series with a 45 gallon drum as ballast tank, to the air inlet of the engine. One inch diameter rubber tubing and iron piping connections were used. The resistance of the calibration apparatus was always less than four inches of water, as measured by a simple U type water gauge. Measurement of the rates of air consumption at various throttle openings were made. The graph of air consumption in cubic feet per minute against throttle opening is given in figure 2.

The conditions of operation of the engine were as follows: At full throttle sufficient shims were inserted to give a compression pressure of 136 pounds per square inch; the throttle

was set at 18 degrees, this particular setting giving a conveniently wide linear range of knockmeter readings for a ten octane range. This setting was determined by taking knockmeter readings over a ten octane range at various settings of the throttle and knockmeter rheostat. Engine speed was maintained constant at 900 rpm and a spark advance of 15 degrees was used. Spark plugs were those prescribed, the spark gap being 0.025 inches. The bouncing pin contacts were maintained approximately .007 inches apart, but were adjusted from time to time to maintain the wide knockmeter range at the 18 degrees throttle setting.

The standard method of determining the octane rating of a gasoline requires about two hours per determination and ratings are expressed to 0.1 of an octane number. However in this case absolute octane ratings were not required, and accuracy to ±0.5 of an octane number was sufficient. Hence a more rapid method was determined which was quite satisfactory for these investigations. The average time for a determination was reduced to less than ten minutes.

The method consisted essentially in calibrating the knockmeter scale. However a simple calibration of octane number against knockmeter reading was not satisfactory since, under constant engine conditions, the knockmeter reading is not always consistent for a single octane rating. However for two fuels of different octane ratings, the difference in the knockmeter deflections for the fuels was constant to within one scale division. For example for two fuels of

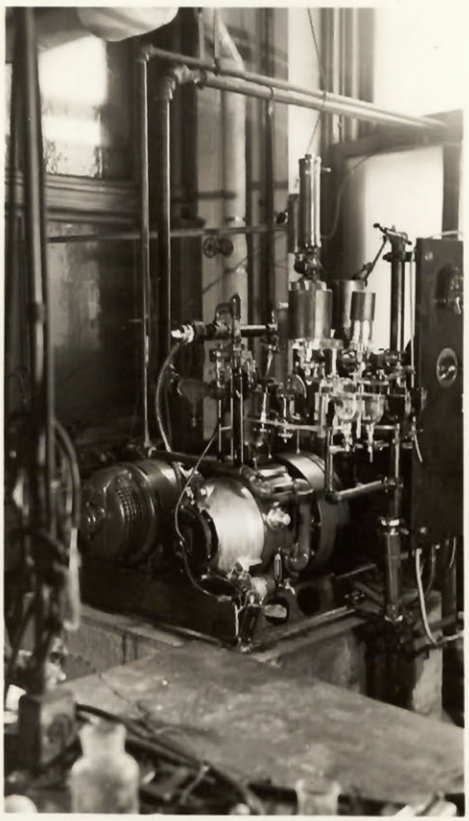

KNOCK TESTING ENGINE.

octane numbers 70 and 80 respectively the knockmeter readings, taken alternately might be 80, 50; 78, 48; 82, 53. The difference in knockmeter reading is 30 1 for the ten octane range. A range such as this was readily obtained by suitable adjustment of bouncing pin contacts, throttle and knockmeter rheostat as stated previously. A typical calibration is shown figure (1). The detailed procedure of a determination was:

(1) The 80 octane fuel used in these tests was standardized by the usual A.S.T.M. method using standard reference fuels (only for new orders of gasoline).

(2) The knockmeter reading for this fuel was then determined.

(3) A knockmeter calibration graph was established using standard reference fuels over the desired range.

(4) The knockmeter readings for several tests using an adulterant were taken. Before and after each of these the knockmeter reading for the 80 octane fuel was checked. The octane change for each of these was then readily determined from the graph.

(5) From time to time the calibration graph was checked using a standard reference fuel. The position of the curve might have changed very slightly over a period of time. The newly determined position would then be used as the calibration graph for the next few determinations.

All readings were taken at the air-fuel ratio which resulted in maximum knock.

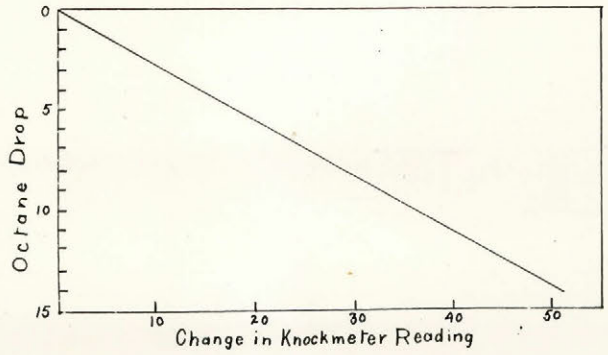

Fig. 1. Typical Calibration Curve

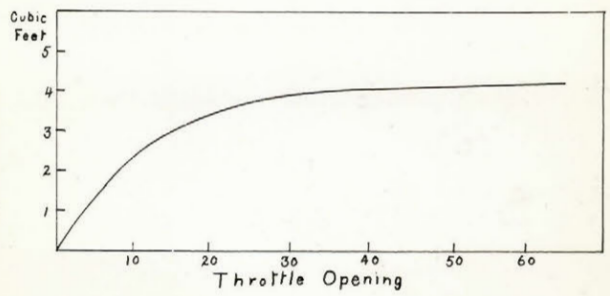

Fig. 2, Air Consumption

Since gaseous, liquid and solid compounds were used, various techniques were required to admit their vapours into the air inlet of the engine.

The liquid compounds were generally handled by bubbling a small air stream through the compounds. This air stream then joined the air taken into the engine. In some cases the liquid had to be heated or cooled, and in all cases the small air stream had to be perfectly dry.

About five cc. of the liquid was placed in a pycnometer E (figure 3) which was then closed with ground glass caps and weighed. The pycnometer was then placed in the set up as shown. Air was taken from a compressed air line and passed into a 45 gallon drum to smooth out minor pressure changes in the line. Part of the air from this drum, the amount controlled by adjusting outlet K, was then passed through a long calcium chloride tube and over phosphorous pentoxide C to dry it well. The air flow was measured on a dibutyl phthalate flowmeter D. The air was bubbled through the liquid in the pycnometer E and then into the air inlet of the engine, carrying the vapor of the liquid with it. If the compound was too volatile, an ice or ice-salt bath was placed around the pycnometer. If it were a high boiling point compound, the pycnometer was heated electrically. In this latter case, the inlet tube G was also electrically heated throughout its length to prevent condensation of the vapour there. The concentration of the vapour in the air entering the engine

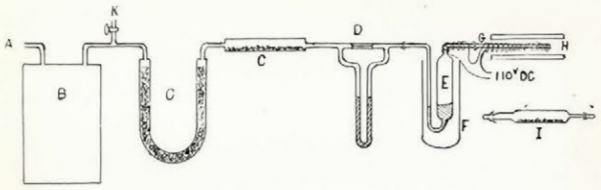

Fig 3, Apparatus for Adding Liquids to Air Intake.

A: Compressed air line.
B: Large drum.
C: $CaCl_2$ and P_2O_5 drying tubes.
D: Butyl phthallate flowmeter.
E: Pycnometer containing liquid.
F: Heating or cooling bath.
G: Inlet tube; heated if required.
H: Air inlet to engine.
I: Pycnometer for solids.
K: Excess air outlet.

was controlled by varying the air flow as measured on the flowmeter.

The air was blown through for ten minutes, and the knock-meter reading at maximum knock air-fuel ratio was found during this time. A stop-watch was used to time this interval. The pycnometer was then removed, caps put on, and reweighed. From the loss in weight of the pycnometer and the air consumption the concentration in number of parts of compound as vapour per million of air was determined.

At least five such determinations were made for each compound and the data thus obtained was plotted, octane drop vs. Concentration, on a semilog graph paper. The concentration necessary to give a ten octane drop was determined from this curve.

A similar technique was used for handling solids with an appreciable vapour pressure. For these, a horizontal type of pycnometer was used (figure 3). The dried air was passed above the compound and into the engine. If heating was required to increase the vapour pressure over the compound, the tube was placed in a heating coil.

Compounds which were gases at room temperature were handled in a different manner. They were added by their direct displacement by an inert compound from a suitable burette attached to the inlet tube (figure 4). In most cases mercury was used as the displacing medium, but in cases where the mercury reacted with the gas, e.g. for chlorine, concentrated sulphuric acid was used; with still other gases, a high

boiling saturated paraffin hydrocarbon was used.

The vessel containing the gas was attached to A (figure 4), and the apparatus evacuated through E. Then the gas was admitted into the burette until the pressure was about atmospheric, and stopcock A was closed. Final adjustment of the pressure to atmospheric was done by moving the levelling bulb D. Stopcock F was then opened and varying flows of the displacing liquid were admitted into burette, the rate being controlled by the stopcock C. The rate was measured by noting with a stop-watch the time for 5 or more cc. to be displaced.

For gases that were better than about thirty parts per million for a drop of ten octane, it was necessary to previously dilute them with dry air, and the mixture was displaced from the burette.

In solution work, five cc. of the liquid was diluted to 500 cc. with gasoline. A quantity of this stock solution was then taken and diluted to 200 cc. This fuel was then tested in the engine and the knockmeter reading recorded. Increased quantities of the stock solution were diluted to 200 cc. and knockmeter readings taken until a ten or more octane drop was noted.

When solids were used in solution work, a weighed quantity was dissolved in 500cc. of gasoline and this was used as a stock solution from which other dilutions were made.

The gasoline used in all this work was 80 octane aviation fuel. This fuel was made from a base stock of 73 octane plus lead tetraethyl.

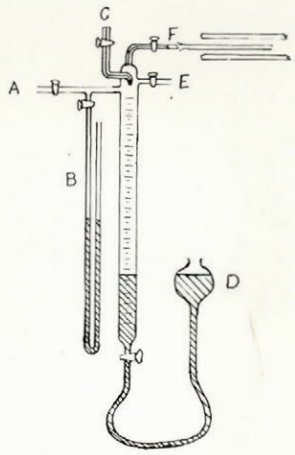

Fig. 4, Gas Displacement Apparatus.

A: Gas Inlet. D: Leveling Bulb.
B: Mercury Manometer. E: To Vacuum Pump.
C: To Mercury Reservoir F: To Engine Air Intake.

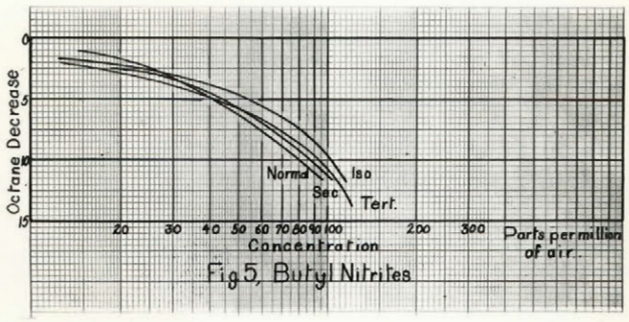

Fig 5, Butyl Nitrites

RESULTS

The concentration necessary for ten octane drop was the point used to compare the relative effectiveness of the compounds tested. Those compounds that were tested in solution were calculated as parts per million of air by using the relationship that 1000 cc. of gasoline, which was consumed in two hours, was equivalent to 3960 cubic feet of air which was consumed in the same time. The results are arranged as near as possible into groups of related compounds. The graph of octane drop vs. concentration in parts of compound as vapour per million of air is also given in the accompanying figures.

1. Butyl Nitrites.

TABLE 4

	P. p.m. for 10 octane drop
m Butyl nitrite	82.5
Isobutyl nitrite	107.0
Sec. butyl nitrite	88.0
Tert. butyl nitrite	95.5

The complete graphs for these compounds are shown in figure 5. Normal butyl nitrite has the lowest required concentration. Branching of the chain seems to increase the required amount. The isobutyl nitrite curve seems to be displaced more than the slight difference in configuration

of the chain could account for. Compactness of the molecule decreases knocking tendency, similar to that discussed under knocking characteristics of fuels, and properties of anti-knock cpds.

2. Amyl Nitrites.

TABLE 5	P. p.m.
N Amyl nitrite	62.0
Isoamyl nitrite	63.0
Tert. amyl nitrite	92.0
Nitrite of sec. butyl carbinol	92.0
Nitrite of diethyl carbinol	93.0

Figure 6 shows these curves. Again the normal is the best. Branching at the end of the chain as in isoamyl nitrite does not appear to have much effect. Branching near the nitrite group has the greatest effect. There would appear to be an optimum branching effect above which increased branching has little or no effect.

3. Normal Paraffin Nitrites.

TABLE 6	P. p.m.
n Propyl nitrite	125.0
n Butyl nitrite	82.5
n Amyl nitrite	62.0
n Octyl nitrite	45.0

From table 6 and Figure 7, it is apparent that pro-knock quality improves with increased length of carbon chain, at least to the eight membered carbon chain. Figure 8 is the plot of number of carbon atoms in the chain vs. the concentration for ten octane drop. This curve seems to become asymptotic to the 20 p.p.m. line and does so around the 16 membered chain.

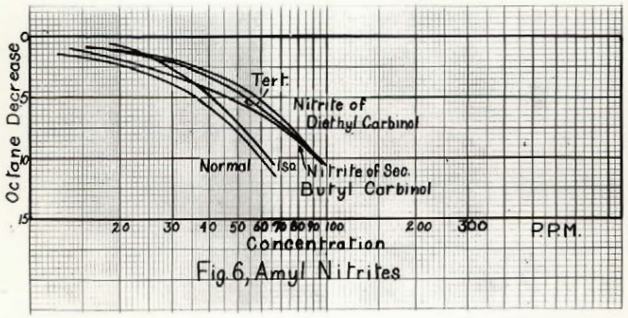

Fig. 6, Amyl Nitrites

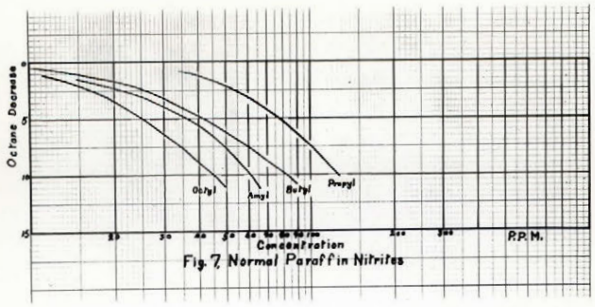

Fig. 7 Normal Paraffin Nitrites

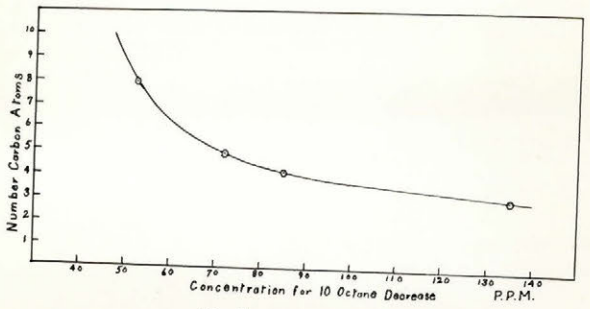

Fig. 8, Normal Paraffin Nitrites

4. Bromine and Nitro Substituted Methanes.

TABLE 7	P.p.m.
Tetra nitro methane	88.0
Bromonitro methane	21.5
Monobromo trinitro methane	15.7
Dibromodinitro methane	11.4
Tribromonitro methane (Bromopicrin)	8.2

The curves for these are shown in figure 9. Tetra-nitro methane is much better than nitro methane (a value for this obtained by extrapolating the curve of figure14, would be above 300 p.p.m.). Also monobromotrinitro methane is better than monobromomononitro methane, giving some indication as to the effectiveness of the nitro radical. But the bromine radical has considerably more pro-knock effect than the nitro group; the pro-knock effect of the nitro groups can almost be neglected compared with the bromine. Figure 10 shows the concentration in parts per million for ten octane drop vs. number of bromine radicals. This curve would have a greater slope if the nitro groups were not present on the molecule.

5. Chloro-nitro Substituted Paraffins.

TABLE 8	P.p.m.
2 Chloro-2 nitro propane	91.4
1 Chloro-1 nitro ethane	28.9
Trichloro nitro methane (Chloropicrin)	15.6
1,1 Dichloro-1 nitro ethane	12.4

These are shown in figure 11. It appears that the radicals are most effective when on the end carbon atoms, for in table 6, increased length of carbon atom chain caused

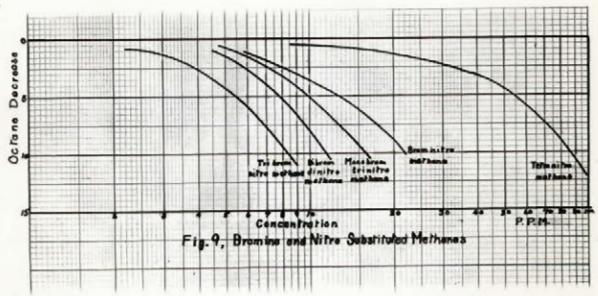

Fig. 9, Bromine and Nitro Substituted Methanes

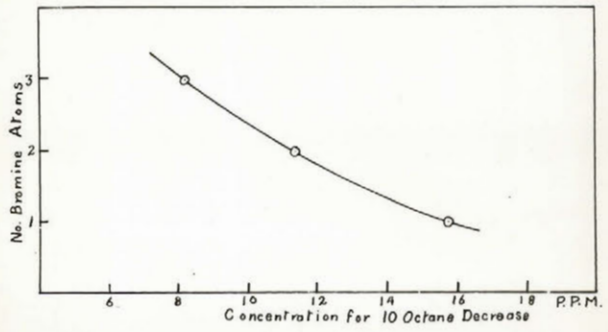

Fig. 10 Brom Nitro Substituted Methanes

increased pro-knock activity, whereas here the 1 chloro-1 nitro ethane is far better than 2 chloro-2 nitro propane. 1,1 dichloro-1 nitro ethane is better than trichloro nitro methane which is rather surprising. Evidently the increased length of chain has a greater pro-knock effect than the third chlorine radical.

Bromine compounds appear better than the corresponding chlorine compounds, bromopicrin is nearly twice as powerful a pro-knock as chloropicrin.

6. Halogens and Halides.

TABLE 9 P.P.M.

Iodine	56 (approx)
Chlorine	40.0
Bromine	16.2
Hydrogen chloride	30.0
Iodine trichloride	10.8

In the table 9 and figure 12, bromine again appears to be the best pro-knock among the halogens tested. The value for iodine is only approximate due to condensation of the iodine in the intake pipe. Halogen halides seem to be a good group to investigate further.

7. Halogen Substituted Methanes.

TABLE 10 P.p.m.

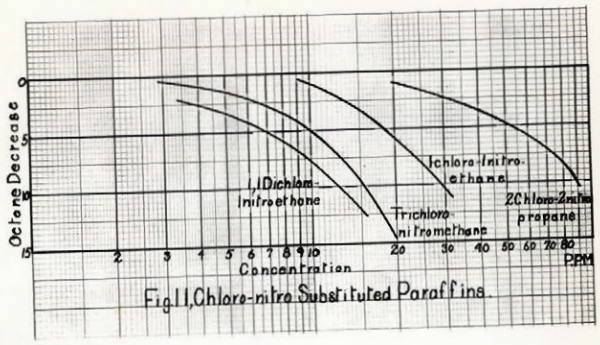

Fig 11 Chloro-nitro Substituted Paraffins.

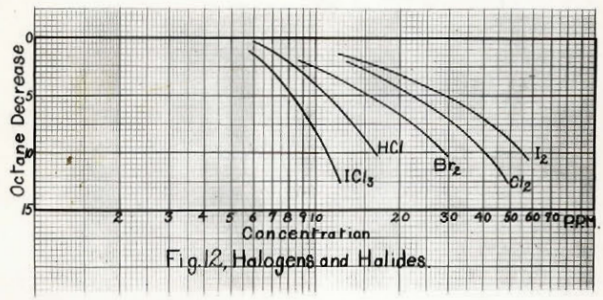

Fig.12, Halogens and Halides.

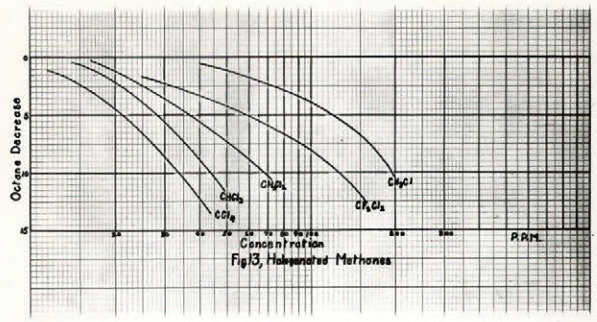

Fig 13, Halogenated Methanes

Methyl chloride	195
Methylene chloride	68.0
Chloroform	44.0
Carbon tetrachloride	33.0
Difluoro-dichloro methane (freon)	125

Table 10 and figure 13 shows the effect of increased substitution of the hydrogens of methane with chlorine. This is further shown in figure 14 where the relationship of number of chlorine atoms on the methane base is plotted against the concentration required for ten octane drop.

Fluorine here has less pro-knock effect than chlorine. The two fluorine radicals on difluoro dichloro methane increase its stability which may explain the fact that it is not as effective as dichloro methane alone.

8. Chlorethanes.

TABLE 11 P.p.m.

Ethyl chloride	156
Ethylene dichloride	78.0
1,1,2-Trichloroethane	55.0
1,1,2,2-Tetrachloroethane	40.0
Pentachloroethane	27.0
Hexachloroethane	16.4

Figure 15, and figure 16, the curve of number of chlorine atoms on an ethane stem vs. concentration in parts per million for ten octane decrease, again show the effect of substitution of the hydrogen of a paraffin with a chlorine radical.

9. Oxychlorides (figure 17)

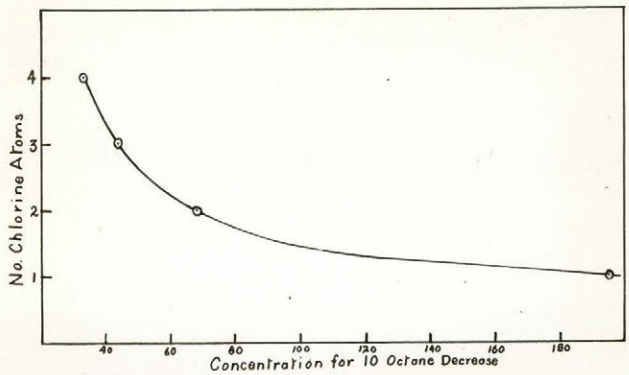

Fig. 14, Chloromethanes

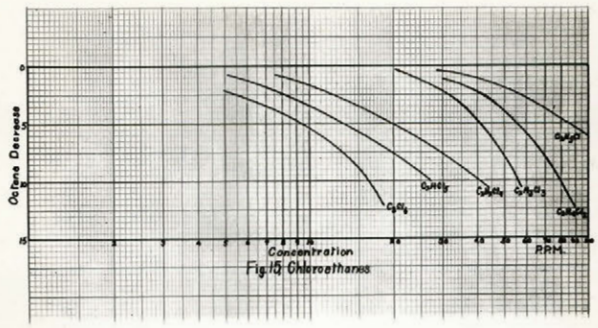

Fig. 15 Chloroethanes

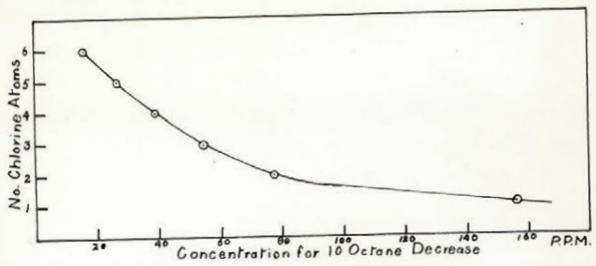

Fig. 16, Chloroethanes

TABLE 12	P.p.m.
Thionyl chloride	15.1
Selenium oxychloride	8.3
Phosphorous oxychloride	7.7

The oxychloride group appears to have a very great pro-knock effect.

10. Arsenic, Antimony and Phosphorous Halides.

TABLE 13	P.p.m.
Phosphorous trifluoride	3.5
Phosphorous trichloride	8.6
Phosphorous pentachloride	6.5
Arsenic trifluoride	11.0
Arsenic trichloride	5.8
Antimony pentachloride	6.1

The octane drop-concentration curves for these are shown in figure 18.

The chlorine radical is again better than the fluorine radical, probably due partly to the increased stability of the fluoride. Arsenic trichloride is the best pro-knock yet investigated. Increased halogen substitution again increases the pro-knock activity, c.f. phosphorous trichloride and phosphorous pentachloride.

11. Miscellaneous (Good Pro-Knock Activity) (Figure 19).

TABLE 14	P.p.m.

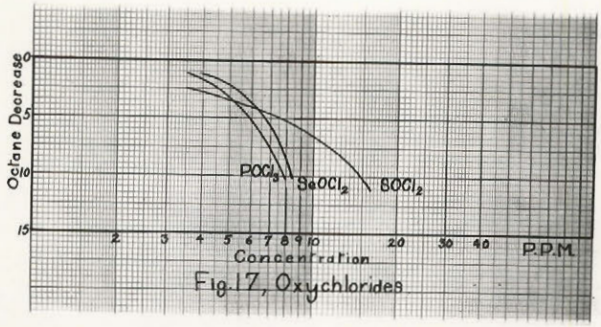

Fig. 17, Oxychlorides

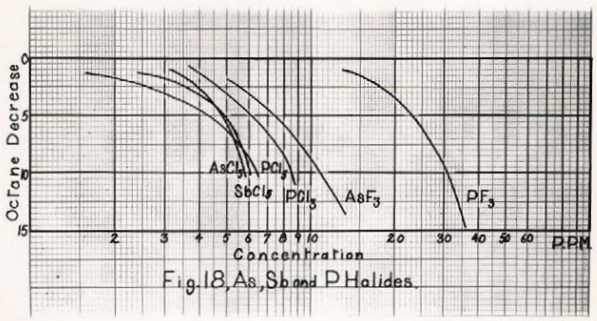

Fig. 18, As, Sb and P Halides.

Methylene bromide	48.3
Oxalyl chloride	45.1
Silicon tetrachloride	23.0
Sulphur chloride	10.6

The bromine radical is here shown to be better than the chlorine radical since methylene chloride required 68.0 p.p.m.

Silicon tetrachloride is better than carbon tetrachloride which required 33.0 p.p.m. Here again this may be due to the decreased stability and ease of hydrolysis of silicon tetrachloride, or it may be that silicon is a better pro-knock than carbon.

12. Miscellaneous (Poor pro-knock Activity) (Figure 20).

TABLE 15	P.p.m.
Sulphur hexafluoride	195
n Butyl thionitrite	130
Boron trifluoride	115
Cyanogen bromide	113
Ethyl sulphite	100
Trichlorethyl nitrite	76.0

n Butyl thionitrite is not as good as n butyl nitrite (82.5 p.p.m.). Trichlorethyl nitrite is better than ethyl nitrite. A value for ethyl nitrite obtained by extrapolation of figure 4 is about 220 p.p.m. Ethyl sulfite is better than the nitrite or the chloride and so a longer chained sulfite might be quite an effective compound.

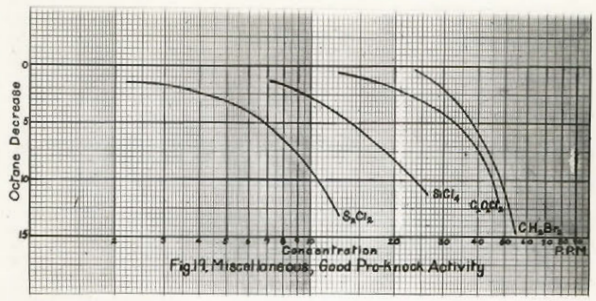

Fig. 19. Miscellaneous, Good Pro-knock Activity

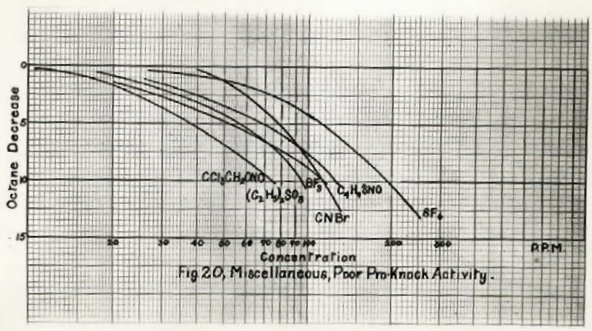

Fig. 20, Miscellaneous, Poor Pro-Knock Activity.

13. Compounds with No Pro-Knock effect.

TABLE 16

Nitrous Oxide	no effect
Cyanogen	no effect at 600 p.p.m.
n Butyl borate	no effect
Ascaridol	no effect
Nitrous oxide	no effect
Triphenylchlormethane (only slightly soluble)	no effect at 0.075%
Butyraldehyde	no effect

Table 17 presents the result of work done in solution. The results are presented in parts per thousand by volume of gasoline and in terms of parts of vapour per million of air consumed, using the relation stated in the first paragraph of this section.

In this solution work a gasoline leaded to 80.5 octane from a 73 octane base stock was used. This leaded gasoline reacted in many cases with the compound added before the "doped" gasoline had entered the engine. This was particularly noticeable with the chlorides which caused a precipitation of the lead. As the lead does not precipitate out immediately in most cases but may require as long as twelve hours, the octane decrease would depend on the time between preparing the stock solution and using it. The results are of use in determining the effect of sabotaging gasolines, when sufficient time has been allowed, but if any reaction occurs between the gasoline and the adultrant outside the engine, they are not of value in determining the effect of use in an air barrage. It

would appear that the effect of adding the compound in the air stream and in the gasoline is about the same if no reaction occurs.

Some metal naphthanates of unknown molecular weight

TABLE 17

Results of Solution Work

Adultrant	P.p.t. of fuel by volume	Remarks	P.p.m. calculated	P.p.m when added to air stream
Chloropicrin	0.6	Causes faint cloudiness	12.0	15.6
Bromopicrin	0.7	Faint cloudiness	13.0	8.2
Dibromo dinitro methane	0.7	No visible change	15.0	11.4
1,1 dichloro-1, nitro ethane	0.7	No visible change	12.0	12.4
Trinitro bromo methane	0.9	No visible change	17.0	15.7
Silicon tetrachloride	0.9	Slight colorless ppt.	16.0	2300
Phosphorous oxychloride	1.2	Brownish ppt.	26.5	7.7
Selenium oxychloride	1.5	Brownish-yellow ppt.	43.5	8.3
1-chloro-1-nitro ethane	1.6	No visible effect	36.0	28.8
Pentachlorethane	1.6	No visible effect	27.0	
Carbon tetrachloride	1.9	No visible effect	40.0	33.0
Tetrachloroethylene	2.1	No visible effect	41.5	
Tetrachloroethane	2.1	No visible effect	40.5	
2-Chloro-2-nitro propane	2.3	No visible effect	41.0	91.4
1,2 Dichloroethylene	2.4	No visible effect	63.0	
Chloroform	2.5	No visible effect	62.5	40.0
Tert-butyl chloride	2.5	No visible effect	45.5	
Dichloromethane	2.9	No visible effect	68.5	
1,1,2-trichloroethane	3.1	No visible effect	67.0	55.0
Tetranitro methane	3.5	Greenish colour	58.5	88.0
n-Butyl nitrite	3.8	Greenish colour	67.0	82.6
Nitroform	4.8	Greenish colour; part did not dissolve	101.	
Isoamyl nitrite	5.0	Greenish colour	74.5	63.0
n Octyl nitrite	5.8	No visible effect	62.5	45.0
Monochloroethane	5.8	No visible effect	156	
Ethyl sulphite	9.2	No visible effect	143	100.

Calculated using an approximate density.

were investigated in solution. The results are shown in

table 18. They were found to gum up the piston rings and valves very badly and to cause a heavy formation of carbon in the cylinder, necessitating frequent overhauling of the engine.

TABLE 18

Metal Naphthenates Investigated in Solution

Metal Naphthenate	Octane decrease caused by adding 0.3 gram per 100 c.c.	Octane decrease adding 0.03 gram per 100 c.c.	Octane decrease adding 0.003 gram per 100cc.
Cobalt	1.5	1.5	1.0
Zinc	0.8	0.0	0.0
Copper	2.3	0.8	0.4
Manganese	1.8	1.2	0.8
Chromium	412	1.1	0.8
Iron	3.0	0.0	0.0
Mercury	16.0	2.5	0.0
Lead	0.8	0.3	0.0
Magnesium	1.2	0.0	0.0
Potassium	insoluble in gasoline		
Vanadium	10.0	1.8	1.1
Nickel	3.3	2.0	0.3

DISCUSSION

THe best compounds for inducing knock, on the basis of a ten octane drop from an 80.5 octane leaded aviation gasoline have been found to be:

Compound	Parts per million of air for 10 octane drop.	Structural formula
Dichloro methyl arsine	3.8	$Cl_2As\text{-}CH_3$ (143)
Cacodyl chloride	4.2	$(CH_3)_2As\text{-}Cl$ (143)
Lewisite	4.6	$CHCl{=}CH - AsCl_2$ (143)
Arsenic tri-bromide	4.6	$Br - AsBr_2$ (143)
Arsenic tri chloride	5.8	
Antimony penta chloride	6.1	
Phosphorous penta chloride	6.5	
Phosphorous oxy chloride	7.8	$O = PCl_3$

Phosphorous tri chloride 8.5

Inspection of the chemical formulae of these compounds indicates that compounds of arsenic, antimony and phosphorous are highly effective as pro-knocks, especially if halogens are also present in the molecule. It is possible that a consideration of the elements constituting, and the properties of, the effective pro-knock compound would lead to a prediction of types of chemical compounds which would be the most effective for inducing knock. The most effective elements appear to be in groups V, VI, and VII of Mendeleef's periodic table. The members of group V, when present in the molecule as an electro positive element appear to cause greatest pro-knock effect. Arsenic is particularly effective in this respect. The halogens also exert a powerful pro-knock action, bromine being the most effective. Group VI elements such as oxygen and sulphur are somewhat less effective than the group V elements as are also the group IV elements. Other groups have little or no pro-knock activity.

In considering the groups themselves, in many cases the pro-knock activity shows an optimum molecular weight in going down the group. With the halogens bromine is the most effective, chlorine and fluorine decreasingly so. Iodine is also less effective than bromine. This is true not only for the elements themselves but is obvious in most of their compounds: bromopicrin is more effective than chloro and fluoro picrins, arsenic tri bromide is more effective than the tri-

chloride or the tri fluoride. In group V the activity increases, as indicated by their halides, from nitrogen to arsenic and decreases with antimony and still more with bismuth. In group IV silicon tetra chloride is more effective than carbon tetra chloride. From the study of the napthenates it is possible that mercury and vanadium might be rather effective. Among other radicals which are effective the nitrites which are much less effective than the corresponding halides but are more effective than nitrates or nitro compounds. Ethyl sulfite appears to be more effective than ethyl nitrite from extrapolation of the graph in figure 8. Thie nitrites are much less effective than the corresponding nitrites. The thiocyanate radical has much greater effect than the isothiocyanate although neither are very effective. Butyl borate had no effect. Oxychlorides are also very effective and are the same order as the chloride itself.

The successive substitution of a halogen for a hydrogen as in methane and ethane causes increase in the pro-knock activity. The substitution of a nitro group for one of the halogens increases its effectiveness considerably as in chloro and bromo picrins although tetra nitro methane itself is much less effective than carbon tetra chloride. Substitution of a methyl group for one of the halogens as in the choro arsines result in increased pro-knock astivity.

Among the chlorides and nitrites, increased length of the hydrocarbon chain increases the effectiveness of the compound. However this effect is more pronounced with the

nitrites than with the chlorides as shown below.

Concentration for 10 octane drop (P.p.m

	Nitrite	Chloride
Methyl	300 x	195
Ethyl	200 x	156
Heptyl	49 x	88

(x) extrapolated or interpolated values.

Branching the hydrocarbon chain decreases the effectiveness of the butyl and amyl nitrites. This corresponds to the observations of the knocking characteristics of fuels which also increase with chain length and decrease with chain branching and the increased compactness of the molecule. Aromatic compounds are not very effective pro-knocks which corresponds also with the knock tendency of aromatic fuels.

On the basis of this evidence it seems that a compound of the form?

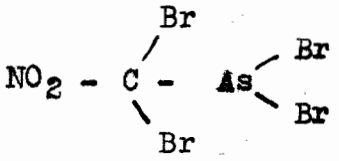

might be exceedingly effective as a pro-knock. A compound such as this combines the pro-knock effectiveness of several of the best compounds studied. It contains arsenic, several bromine atoms, a methyl group and a nitro group. It would probably be a solid (if at all stable) and might have to be

modified unless it is possible to use solids dispersed as a smoke. Synthesis of, and tests with compounds of this type are projected for the near future.

Although sufficient data are not available to postulate a mechanism of pro-knock activity some generalizations may be made in addition to the discussion of the effectiveness of elements as related to their position in the periodic table. Work on both leaded and unleaded fuels has indicated that some compounds such as phosphorous oxychloride appear to act entirely by counteracting the tetra-ethyl lead (3). With others such as iso-amyl nitrite similar effects are observed in both leaded and unleaded gasolines. Many however appear to act both by counteracting the tetra-ethyl lead and on the fuel itself. For most of the compounds studied here some effect was shown on the fuel itself since the base stock was only eight octane lower than the leaded fuel. The effect on the fuel itself appears to depend to a large extent on the nature of the base stock i.e. whether cracked or straight run etc.

Attempts to relate the relative pro-knock effectiveness of various compounds to other properties of the molecules, such as heats of formation and combustion, were limited by insufficient data of this nature. However a relation has been found between the concentration required for a ten octane drop and that required to give optimum reduction in the half-time value in the rate of oxidation of butane (144).

The results obtained in these investigations are in accord with those of others (3, 121, 122) both in the general variation with chemical structure and in the actual values of the results obtained where comparisons are possible.

Whether the use of pro-knocks as a weapon in chemical warfare is practical, cannot be stated. Estimates of the octane drop required to render an aeroplane engine inactive vary, and no quantitative data is available. It is essential that this should be determined before any real estimate of the value of pro-knocks in military tactics can be made. If field trials demonstrate that the action of a pro-knock can in fact, hinder the operation of military motorized equipment, at least of certain types, it would seem perfectly justifiable to seek still further for compounds of increased pro-knock activity.

REFERENCES

(1) Ogilvie, J.D.B. - Master's Thesis - McGill University 1940

(2) Sudgen, S. - Memorandum on Attack of I.C. Engines by Chemical Agents p.t.n. 1271 (P 21455) (1940)

(3) Midgely, T. and Henne - United States National Defence Research Council Report.

(4) Bone, W.S. - Bakerian Lecture J.C.S., 1599 (1933)

(5) Bone, W.S. and Townend, D.T.A., - Flame and Combustion in Gases (1927)

(6) Norrish, R.G.W. - PRSL 150A, 36 (1935)

(7) Bodenstein, M. - Chem. Rev. 7, 220 (1930)

(8) Egloff, G. and Schaad, C.E. - Chem. Rev. 6, 91 (1929)

(9) Milas, N.A. - Chem.Rev. 10, 295 (1932)

(10) Ubbelohde, A.R. - Science of Petroleum p 2937 (1938)

(11) Bailey, K.C. - The Retardation of Chemical Reactions.

(12) Armstrong, H.E. - JCS 1088 (1903)

(13) Bone, W.A. and Wheeler, R.V. - JCS 1074 (1903)

(14) Bach - Compte Rend. 124, 951 (1897)

(15) Engler and Wilde - Ber 30, 1699 (1897)

(16) Johnson, H.M. and Walker, L.K. - JACS 55, 187 (1933)

(17) Lewis, B. - JCS 1555 (1927)

(18) Berl, E. and Winnacker, K. - Z Phys. Chim. 139A, 453 (1928)
145A, 161 (1929)
148A, 36, 261
(1930)

(19) Steacie, E.W.R. and Plewes - PRSL 146A, 72 (1934)

(20) Egerton, A.C. and Pidgeon - PRSL 142A, 26 (1933)

(21) Prettre, M. - Ann. Comb. liq. 6, 7, 269, 533 (1931)
7, 699 (1932)

(22) Newitt, D.M. and Townend, D.T.A. - Science of Petroleum
p 2860 (1938)

(23) Nweitt, D.M. and Townend, D.T.A. - Science of Petroleum
p 2884 (1938)

(24) Wheeler, R.V. - JCS 113 (45) 1918.

(25) Maxwell, G.B., and Wheeler, R.V. - Science of Petroleum
P 2976 (1938)

(26) Fraser, R.P. - Science of Petroleum p 2983 (1938)

(27) Egerton, A.C. - Science of Petroleum p 2914 (1938)

(28) Lafitte, P.F. - Science of Petroleum p 2995 (1938)

(29) Beatty, H.A. and Edgar, G. - Science of Petroleum
p 2927 (1938)

(30) Midgely, T. and Boyd, T.A. - Ind. Eng. Chem. 14, p894
(1922)

(31) Midgely, T. and Boyd, T.A. - JSAE 15, 659 (1920)

(32) Egerton, A.C. and Gates, S.F. - PRSL 114A, p402 (1927)

(33) Egerton, A.C. and Gates, S.F. - PRSL 116A,p516 (1927)

(34) Maxwell, G.B. and Wheeler, R.V. - Ind. Eng. Chem 20,
p 1041 (1928)

(35) Ricardo, H.R. - JSAE 10, p308 (1922)

(36) Tizard H.T. and Pye, D.R. - Phil Mag. (1922), p 79;
(1926) p 1049.

(37) Withrow, L. and Boyd, T.A. - Ind. Eng. Chem 23, p 539
(1931)

(38) Callendar, H.L., King, A., and Sims, C.J. - Engineering
121, p 475 (1926)

(39) Callendar, H.L. - Engineering 123, p 132, 147, 210 (1927)

(40) Egerton, A.C. and Gates, S.F. - JIPT 13, p 281 (1927)

(41) Egerton, A.C. and Gates S.F. - Nature 119, p 427 (1927)

(42) Moreau, Duffraise, and Chaux, R. - Compte Rend, 184 p413
(1927)
Chim et Ind 17, p 99 (1927)
Chim et Ind 18, p 3 (1927)

(43) Salmoni - Giorn. chim. ind. appl. 13, p.12 (1931).

(44) Dumanois, P. - Compte rend 186, p. 292 (1928)

(46) Prettre, M. - Bull. Soc. chim. 51, p. 1132 (1932)

(47) Mondain Monvall, and Quinquinn, - Ann Chim 15, p309 (1931)

(48) Ubbelohde, A.R. and Egerton, A.C. - Nature 135, 67 (1935)

(49) Egerton, A.C., Smith, F.D., and Ubbelohde, A.R. - Phil.
Trans. Roy. Soc. 234, p 433 (1935)

(50) Hinshelwood, C.N., Williamson, A. and Wolfenden, G. -
PRSL 147A, p 48 (1934)

(51) Rice, F.O. - Ind. Eng. Chem. 26 p 259 (1934)

(52) Steele, S. - Nature 131, p 725 (1933)

(53) Clarke and Henne, - JSAE 20, p264 (1927)

(54) Wendt, G.L. and Grimm, F.V. - Ind. Eng. Chem. 23, p 539 (1931)

(55) Beatty, H.A. and Edgar. G. - Science of Petroleum p 2927 (1938)

(56) Ricardo, H.R. - Auto Eng. 11, pp 51, 92 (1921)

(57) Roesch, Daniel - JSAE 19, p 17 (1926)

(58) Cummings, H.K. - JSAE 20, p 605 (1927)

(59) Wilson, R.E. - Bull. A.P.I. 8, p 192 (1927)

(60) Huf, H.F., Sabina, T.R., and Hill, J.B. - JSAE 29, p 134 (1931)

(61) Stansfield, R. and Carpenter, R.E.H. - JIPT 18, p 513 (1932)

(62) Heron, S.D. - ASME Trans 52 (i) p 233 (1934)

(63) Leslie, E.H., Brown, G.G. and Hunn, J.U. - Ind. Eng. Chem. 17, p 397 (1925)

(64) Campbell, J.M. and Boyd, T.A. - Science of Petroleum p3057 (1938)

(65) Lee, S.M. and Sparrow, S.W. - JSAE 12, p 11 (1923)

(66) Midgley, T., Thomas, L. and Boyd, T.A. - JSAE 10, p 7 (1922)

(67) Edgar, G. - Ind. Eng. Chem. - 19, p 145 (1927)

(68) A.S.T.M. Standards - Bulletin D357-41T

(69) Ricardo, H.R. - Auto Eng. 11, 130 (1921)

(70) Mac Coull, N. - JSAE 22, 457 (1928)

(71) Stansfield R. and Thole, F.B. - Ind. Eng. Chem. (anal. ed.) 1, p 98 (1929)

(72) Campbell, J.M., Lovell, W.E., and Boyd, T.A. - JSAE 29 p129 (1931)

(73) Veal, C.B., Best, H.W., Campbell, J.M. and Holaday, W.M. - Bull. A.P.I. 15 (iii) p 139 (1932)

(74) Veal, C.B., Best, H.W., Campbell, J.M. and Holaday, W.M. - JSAE 32, p 105 (1933)

(75) Lovell, W.G. and Campbell, J.M. - Science of Petroleum p 3005 (1938)

(76) Midgely, T. and Boyd, T.A. - Ind. Eng. Chem 14, p 589 (1922)

(77) Midgely, T. and Boyd, T.A. - Ind. Eng. Chem. 14, p 849 (1922)

(78) Midgely, T. and Boyd, T.A. - Ind. Eng. Chem. 15, p 421 (1923)

(79) Graetz, A. - Ann. comb. liq. 3, p 69 (1928)

(80) Callingaert, G. - Science of Petroleum p 3024 (1938)

(81) Boyd, T.A. - Ind. Eng. Chem. 16, p894 (1924)

(82) Ormandy, W.R. - J.I.P.T. 10, p 235 (1924)

(83) Egerton, A.C. - Science of Petroleum p 2914 (1938)

(84) Marek, L.F. and Hahn, B.A. - The Catalytic Oxidation of Organic Compounds in the Vapor Phase - Chap. 11, Chemical Catalog Company (1932)

(85) Cross, R. - U.S. Patent 1, 883, 393 Oct. 18.

(86) Rosenstein, L. - British Patent 349, 475, Nov. 18, 1929.

(87) John, R. - U.S. Patent 1, 733, 394, April 8.

(88) Calingaert, G. - Science of Petroleum p 3024 (1938)

(89) Cross, R. - U.S. Patent 1, 883, 393 Oct. 18.

(90) Kalichevsky, V.A. and Stagner, B.A. - Chemical Refining of Petroleum Chap. 8, Chemical Catalog Company (1933)

(91) I.G. Farbenind A.G. - British Patent 334, 181, April 5, (1928)

(92) Midgely, T. and Boyd, T.A. - ISAE 15, p 659 (1929)

(93) Kettering, C.F. and Midgely,T. - U.S. Patent 1, 635, 216 July 12.

(94) Layng, W.E. and Youker, M.A. - Ind. Eng. Chem. 29, p 1048 (1928)

(95) Kettering, C.F. and Midgely, T. Jr. - U.S. Patent 1, 635, 816 July 12.

(96) Bone, C.A. - French Patent 733, 497, Mar. 15, 1937.

(97) Ethyl Gasoline Corp. - French Patent 825, 921, Mar. 18, 1938.

(98) Standard Oil Development Company - French Patent 825, 525 Mar. 4, 1938.

(99) Denner, P.S. - Can. Patent 332, 361, May 9, 1933.

(100) Callendar, H.L., King and Sims, R.C. - Engineering 121, p 475 (1926)

(101) Longinus, Asphalt Tenrind, E. - 26, p 519 (1926)

(102) Stevens, D.R., Morley, S.P. and Grüse, W.A. - U.S. Patent 1, 593, 040, July 20.

(103) Dunamp, A.J. - British Patent 335, 828, Dec. 4, 1928.

(104) Hormer, F.E. - British Patent 309, 191, April 5, 1928.

(105) Egerton, A.C. - U.S. Patent 1, 771, 169, July 22.

(106) Midgely, T. and Boyd, T.A. - Ind. Eng. Chem. 14, p 589, 849, 894 (1922)

(107) Midgely, T. and Boyd. T.A. - Ind. Eng. Chem. 15, p 421 (1923)

(108) Charch, W.H., Mack, E,, and Boord, C.E. - Ind. Eng. Chem. (anal ed.) 1, p 26 (1929)

(109) Endo, E. - J. Fuel Soc. Japan 11, 584, (1938)

(110) Charch, W.H., Mack, E., and Boord, C.E. - Ind. Eng. Chem. 18, p 334 (1926)

(111) Rosenstein, L. and Hund, W.T. - U.S. Patent 1, 920, 766, Aug. 1.

(112) Rosenstein, L. - British Patent 349, 475, Nov. 18 (1929)

(113) Sokal, E. - British Patent 285, 145, Nov. 11, 1926.

(114) Sokal, E. - JSCI 43, p 283-4T (1924)

(115) Egloff, G. Farragher, W.F. and Morell, J.C. - Refiner and Nat. Gas Mfr. 9-No. 1, p80 (1930)

(116) Beatty, H,A. and Edgar, G. - Science of Petroleum p 2927 (1938)

(117) Schmidt, A.W., Generach, H. Scholz, G., and Mehry, F. - Braunkohle 35, p 535 (1936)

(118) Hersted, O. - Oil, Kohle, Edoel, Teer, 14, p 579 (1938)

(119) Gilman, H., Sweeney, O.R. and Kerby, J.E. - Iowa State College, J. Sci. 3, p 1 (1928)

(120) Mardles, E.W.J. - JCS p 872 (1928)

(121) Stacey, H.R. and Wasson, J.I. - Anti Knock Characteristics of Various Chemical Compounds - Standard Oil Development Research Laboratories.

(122) Lapeyrouse, M. and Lebo, R.B. - Anti Knock Characteristics of Various Chemical Compounds - Mar. 25, (1937)

(123) Thomas and Hochwalt Laboratories - "Chemical Treatment of Oils" - (1941)

(124) Jolibois, P. and Normand, G. - Compte rend 179, p 27 (1924)

(125) Sokal, E. - J.S.C.I. 43, p 283 (1924)

(126) Midgely, T. - JSAE 7, p 489 (1920)

(127) Wendt, G.L. and Grimm, F.V. - Ind. Eng. Chem. 23, p 539 (1931)

(128) Clark, G.L., Brugmann, E.W., and Thee, W.C. - Ind. Eng. Chem. 17, p 1226 (1925)

(129) Egerton, A.C. and Gates, S.F. - J.I.P.T. 13, p 244 (1927)

(130) Egerton, A.C. and Gates, S.F. - Nature 119, p 227, (1927)

(131) Emeleus, H.J. - JCS p 1336, (1926)

(132) Backstrom, H.L.J. - Trans. Farad.Soc. 24, p 501, (1928)

(133) Callendar, H.L. - Engineering 123, p 147, 182, 210 (1927)

(134) Dickinson, H.C. - JSAE, 8, p 558 (1921)

(135) Clark, G.L. and Thee, W.C. - Ind. Eng. Chem. 17, p 1219 (1925)

(136) Charch, W.H., Mack, E. and Boord, C.E. - Ind. Eng. Chem. 18, p 334 (1926)

(137) Lewis, J.S. - JCS p 2241 (1930)

(138) Schaad, R.W. and Boord, E.E. - Ind. Eng. Chem. 21, p 756 (1929)

(139) Ormandy, W.R., and Craven, E.C. - J.I.P.T. 10, p 335 (1924)

(140) Olin, H.L., and Jebens, W.J. - Ind. Eng. Chem. 21 p 43 (1929)

(141) Olin, H.L., Read, G.D., and Goos, A.W. - Ind. Eng. Chem. 18, p 1316 (1926)

(142) Berl, E., Heise, K., and Winnacker, K. - Z. Phys. Chem. 39A, p 453 (1928)

(143) Davis, S.G. - War Research Report CE39, Mc Gill University (1942)

(144) Gillies, A. - Private Communication.

B. The Dynamic Sorption of Ammonia and Butane on Charcoal

(in collaboration with S.G. Davis)

TABLE OF CONTENTS

INTRODUCTION

The introduction of the service respirator as a defence against toxic gases, stimulated the study of the dynamic sorption of gases by charcoal. Early work was done empirically to estimate the protective power of the respirator. More recently the attempts have been made to predict the protective power from the physical constants of the gas and charcoal and the experimental conditions. From these previous investigations a number of theories of dynamic sorption have been postulated.

An apparatus has been designed in this laboratory (1) to follow continuously the amount of sorption, the temperature rise at various points in the charcoal bed, and to collect samples of the sorbate passing out of the charcoal beds. This apparatus permits a correlation of temperature rise and other sorption data at various rates of air flow, moisture contents of air and charcoal, concentrations of the sorbate to be studied, and at various depths of the charcoal bed.

It is the purpose of this investigation to obtain data using this apparatus on the sorption of butane and ammonia on charcoal, which has been found difficult by other methods (2), and to correlate this data with that of other investigators in the light of the various theories of dynamic sorption which have been proposed.

I Static Sorption in Gaseous Systems

At any gas-solid interface the concentration of gas has been found to be highest in the immediate vicinity of the solid surface. The gas is said to be adsorbed by the solid. Many workers prefer to use the word sorption rather than adsorption and use the term adsorption to refer to a particular type of sorption. This phenomenon has been noticed and investigated for a long time and a considerable amount of data is available for various sorbents and sorbates (3,4). The first quantitative relation between the amount of gas taken up by the solid and the experimental conditions was that with the pressure of the gas in equilibrium with the solid. The classical isotherm was a modified Henry's law expression for solid solution, for sorption, of the form:

$$x = k P^{1/n} \qquad (1)$$

where x is the amount sorbed, P is the pressure of sorbate, k and n are constants. This relation was found to agree with experimental values at lower pressures, but not at higher pressures. The best relation yet postulated was that derived by Langmuir (3), considering a unimolecular layer of sorbate on the solid:

$$x = \frac{aP}{1 + bP} \qquad (ii)$$

where a and b are constants of the sorbate and sorbent. The amount of adsorption was also found to vary with temperature. Sorption has been investigated from temperatures a few degrees above absolute zero to very high temperatures. At lower temperatures the amount of gas taken up by any sorbent was greater

than at higher temperature. Titoff (6) and Miss Homfray (7) found a linear relation between the logarithm of the amount sorbed and the temperature. The temperature coefficient is quite high; a few degrees difference in temperature makes a large difference in the amount of sorption. In fact it is thought that for some sorbates a different mechanism of sorption predominates over different temperature ranges. Different gases under similar conditions have been found to sorb in greatly different amounts on the same solid (8). The amount of sorption has been found to be in the order of the condensibilities or boiling points of the sorbates. It has also been related to the van der Waals constant "a" of the sorbate. The order of sorbability of various gases remains much the same from one sorbent to another (9), but the magnitudes of the sorption vary from almost infinitesimal amounts to quite large amounts. Activated charcoal has been found to be one of the better sorbents for most materials. The nature of the surface of the sorbent is important in determining its sorption capacity. Charcoal, for example, may be activated by heating to a high temperature or by soaking in a solution such as zinc chloride. Studies of the rate of sorption have indicated that it occurs very rapidly at first, then decreases rather sharply to approach the equilibrium value which may take months or years to reach (3,4). Heat is always evolved on sorption. The heat of sorption for additional increments in the pressure of the sorbate decreases steadily. Lamb and Coolidge (10) have given a relation:

$$q = ax^b$$

Attempts have been made to relate the heat of sorption to the latent heat of vaporization of the sorbate, and to the relative reactivities of the sorbates (10,11). The heat of sorption is nearly always greater than the latent heat of vaporization, and for any particular family of compounds, i.e. the paraffins there is a relation between the reactivity and the heat of sorption. In mixtures of gases one or other has, in general, been found to be sorbed preferentially to a greater or less extent, and the presence of one gas sorbed on charcoal lowers the sorption of a second (4).

II Mechanisms of Sorption

The manner in which a solid such as charcoal takes up a sorbate is probably by one or more of several mechanisms. A few of the more common mechanisms are:

1. Adsorption (proper) (3,4) - The sorbate is held at the surface of the sorbent by residual valence bonds. There appears to be two different types of adsorption: van der Waal's adsorption in which gas molecules are held by the electrostatic forces of attraction between molecules of the sorbate and the sorbent; and chemisorption where there are actual chemical bonds formed between the surface atoms of the sorbent and the sorbate molecules. Two main theories of adsorption have been postulated. Polanyi suggested an adsorption potential exerted by the sorbent which decreased with the distance from the sorbent. However, agreement with the experimental results is not good and even Polanyi himself has abandoned the theory. Langmuir postulated a unimolecular layer of sorbate on the surface of the sorbent. From this he derived his isotherm, which agrees with experimentally determined values very well.
2. Capillary Condensation (3 ch. 16) - The vapor pressure of a liquid in a capillary is much less than on a flat surface. Hence it has been postulated that sorbed vapors held by the charcoal are condensed to liquid drops in the capillary pores and other surface irregularities of the sorbent. This undoubtedly does occur and in some cases may be the governing mechanism but in most cases it is merely an additional phenomenon.

3. Solution in Adsorbed Water - Actually this is not sorption but in many cases charcoals have been known to remove gases from their surroundings, by solution of the gas in water adsorbed on the surface of the charcoal.
4. Decomposition by Water - Some gases like phosgene are decomposed by hydrolysis in the water adsorbed on the surface of a sorbent.
5. Decomposition of the sorbate may be catalysed by impregnants in the sorbent. The products of the decomposition might then be sorbed by one of the other mechanisms.

A study of the experimental results has indicated that two or more of these mechanisms may be operating simultaneously, one or other predominating depending upon the conditions. This is certainly indicated by extremely large temperature coefficients of sorption and by the nature of the rate of sorption curves for many substances.

III Dynamic Sorption

In dynamic sorption studies a mixture of the sorbate in an inert carrier, such as air, is passed over a charcoal bed. The rate at which the gas is taken up depends upon the rate at which it is supplied. The governing rate factor may be either the actual process of sorption or the diffusion from the air stream to the charcoal surface. Thus the presence of the carrier gas may interfere with the true adsorption velocity. However dynamic studies enable efficiency as well as capacity data to be studied. The sorption should increase linearly with time (the rate of supply) and should reach a point when the charcoal ceases to be 100% efficient in removing the gas. The weight-time curve will then slope off gradually to a horizontal straight line, at which time the charcoal is in equilibrium with the gas stream being passed over it.

Most dynamic studies to date have been carried out with charcoal to estimate its protective power in removing toxic gases from air in service respirators. The time at which a given charcoal ceases to be 100% efficient in removing the toxic gas from an air stream is used as an estimate of the protective power of that charcoal under the given experimental conditions. This time is called the breakdown or service time.

Theories of Dynamic Sorption

Out of all the work done on dynamic sorption, there are only two main treatments of the data and mechanism. Danby, Davoud, Everett, Hinshelwood and Lodge (12) in England, starting

from purely theoretical considerations developed a theory from which equations could be derived for the various measurable quantities. Mecklenberg (13,14) assumed that the sorption took place by capillary condensation and derived formulae on this basis for the quantities desired.

1. The Theory of Danby et al

This theory was first developed in a simple form for rough comparisons and was followed by a more rigorous mathematical solution of a partial differential equation.

In the simple theory, the concentration of the gas over the charcoal was assumed to decrease exponentially with length and to increase exponentially with time, viz:

$$C = C_o e^{-\frac{k\,l}{L}} \cdot e^{\frac{kbT}{L}} \qquad \text{(iii)}$$

where k is a measure of the rate of sorption, L the linear flow rate, b the rate of exhaustion of the charcoal, C_o the initial concentration of the sorbate in the gas stream and C the concentration of the gas after passing through a length l of the charcoal, and for a time T. From this is obtained an equation for the service time T':

$$T' = \frac{N_o}{C_o L}\left[\lambda - \lambda_c\right] \qquad \text{(iv)}$$

where N_o is the number of active centres per cc. of charcoal, λ the total length of the charcoal bed, and λ_c the "critical length". The critical length was defined as the distance that a detectable amount of gas travelled through the bed before being removed from the air. Above this length there would be a linear relation between the service time and the bed length.

In the more detailed theory the fundamental equation

for the removal of a gas in an absorbing column:

$$\frac{\partial c}{\partial l} = \frac{1}{L}\left[\frac{\partial x}{\partial t} + \frac{\partial c}{\partial t}\right] \qquad (v)$$

was used, where L is the linear flow rate, $\partial c/\partial l$ the rate of concentration change of gas in the air stream, with length, $\partial c/\partial t$ the rate of concentration change with time, and $\partial x/\partial t$, the rate of sorption of the gas by the charcoal with time. It was assumed that the rate of removal of the gas was proportional to the concentration of gas in the air stream, c, and to the number of active centres per cc. of charcoal, N_o. This gave:

$$\frac{\partial x}{\partial t} = k\, c\, N_o = \frac{N_o}{t} \qquad (vi)$$

It is also assumed that each active centre was made up of N active centres of unit activity, N_o'. One centre of unit activity was assumed to be destroyed each time a molecule of gas was sorbed by the charcoal. Substituting equation (v) in equation (vi), and solving, yielded equations for critical length and service time:

$$c = \frac{L}{N_o k}\left(\ln c_o/c' - 1\right) \qquad (vii)$$

$$T' = \frac{1}{kC_o} \ln\left(e^{kN_o/L} - 1\right) - \ln\left(c_o/c' - 1\right) \qquad (viii)$$

Rearranging these equations to the forms:

$$T' = \frac{N_o}{C_o L} \left[\lambda - \lambda c \right] \qquad \text{(ix)}$$

$$T' = \frac{N_o}{C_o} \left[\frac{1}{L} - \frac{1}{Lc} \right] \qquad \text{(x)}$$

$$T' = \frac{1}{kC_o} \left[\frac{kN_o}{L} - \ln \frac{C_o}{C'} \right] \qquad \text{(xi)}$$

it was predicted that the service time would vary:

(a) with the specific properties of the charcoal as with k and N_o

(b) linearly with the column length

(c) with the reciprocal of the flow rate L

(d) with the reciprocal of the initial concentration C_o when C_o is very small.

The critical length λc should vary with the log of the initial concentration C_o. For carbon tetra chloride, nitrous fumes, arsine and hydrogen sulfide the service time relations agreed with those predicted.

From the simple theory the concentration of the sorbing gas should fall off exponentially with the length of the charcoal bed.

$$C = C_o \, e^{-kl/L} \, e^{KbT/L} \qquad \text{(iii)}$$

At various times t_1, t_2, etc. the gradients would be as those shown in figure 1., where concentration is plotted against column length. A similar figure would be obtained for the amount of sorption along the bed. From the more detailed theory the concentration of the gas in the gas phase falls off according to the relation:

FIGURE 1.

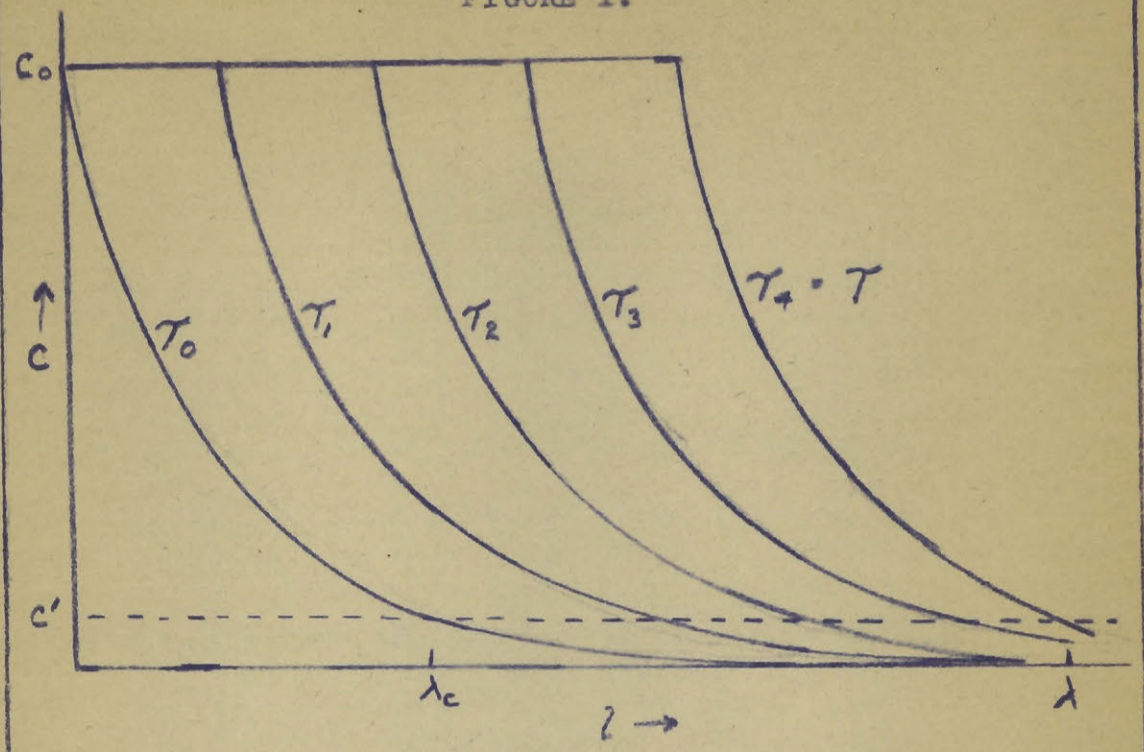

FIGURE 2.

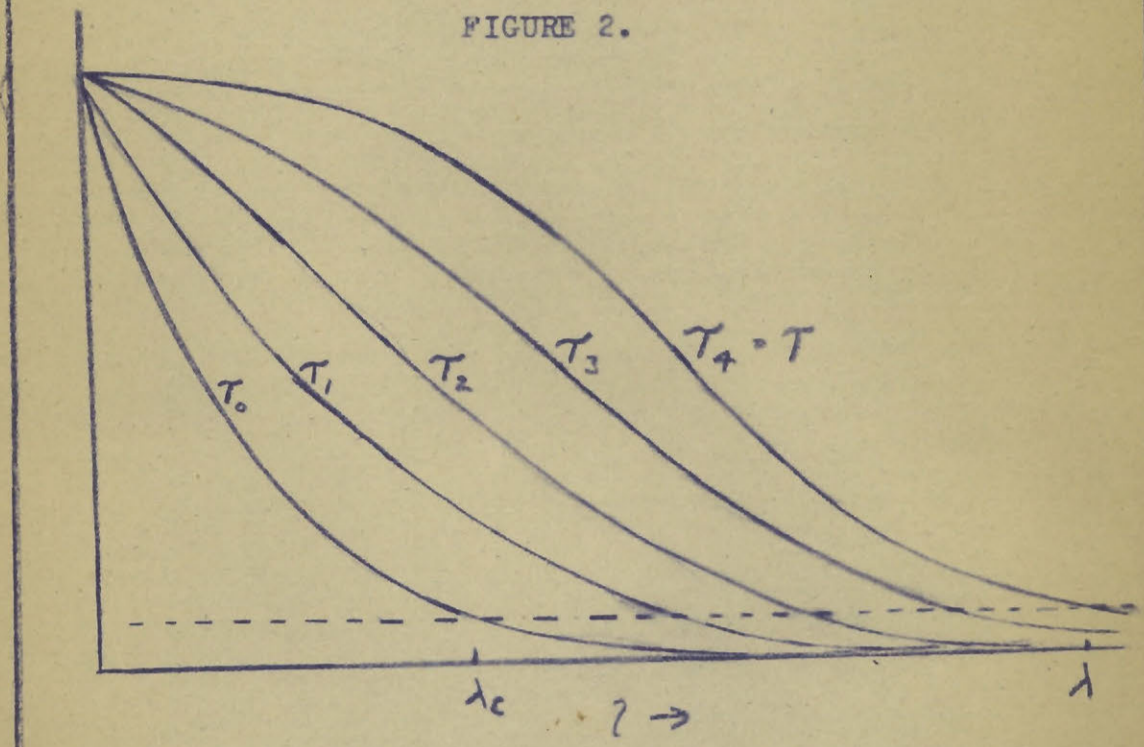

CONCENTRATION OF TOXIC GAS AT DIFFERENT DISTANCES ALONG THE COLUMN.
(a) Simple Theory
(b) More Detailed Theory

$$C = \frac{C_o}{e^{-kC_oT\left(e^{kN_o/L}-1\right)}+1} \qquad (xii)$$

and the gradients are shown in figure 2 for times t_o, t_1, t_2, t_3, etc. It may be seen that the gradient changes shape from t_o to t_4 and moves along the bed at constant rate and shape thereafter. The existence of the service time may be seen from these curves. If c' is the concentration of gas required to give a test, when the first trace of gases extending beyond the column length is detected, the time corresponding to that gradient is the service time T'.

2. The Mecklenberg Theory

Mecklenberg visualized a charcoal bed after a gas stream had been passing for some time as being divided into three parts:

(a) A length next the front surface saturated with gas.

(b) A "working" length in which the gas was being taken up, and

(c) A length not yet reached by the gas.

Mecklenberg concerned himself with the investigation of the working length.

He assumed that the gas was being taken up by the charcoal by condensation in the capillaries of the charcoal. He further assumed that he was dealing with a "mathematical" charcoal whose capillaries were of uniform and constant cross section, and that the gas diffused out of the air stream and

into the capillaries with a velocity similar to that given by Nernst for a heterogeneous reaction:

$$-\frac{\partial c}{\partial t} = \frac{DF}{\delta}(c - c') \qquad \text{(xiii)}$$

in which c is the partial pressure of the gas in the air outside the charcoal capillaries, c' is the vapor pressure of the toxic gas inside the capillaries, D is the diffusion coefficient of the gas in air, F is the outer surface of the charcoal grains per cc. exposed for the diffusion, δ is the thickness of the gas layer sorbed on the charcoal grains, and t is the time.

Using this and the above assumptions he derived equations for the service time T' and the dead length h:

$$T' = \frac{k' Q}{V C_o}(L - h) \qquad \text{(xiv)}$$

$$h = \frac{\delta_r}{DF}\left(\frac{kQ}{V}\right)^{n-1}\left[\ln \frac{C_o - C'}{C_x - C'} - \frac{C_o}{C_o - C'}\right] \qquad \text{(xv)}$$

where k' is the maximum amount of gas sorbed per cc. of charcoal under the experimental conditions, Q is the cross section of the charcoal bed and L its length, V is the linear velocity of the air stream over the charcoal, δ_r is a constant relating to the thickness of the layer of gas adhering to the surface of the charcoal kQ is that portion of the cross section of cell not actually filled with charcoal, C_x is the minimum detectable concentration of the gas, and n is a constant.

From equation (xv), Mecklenberg was able to predict that the dead length h was:

(a) inversely proportional to the square root of the cross section, Q,

(b) directly proportional to the diameter of a single charcoal grain a,

(c) directly proportional to the square root of the rate of flow of the air stream, V, and

(d) directly proportional to the logarithm of the initial concentration, C_o.

These were all confirmed by experiment by Mecklenberg himself and Engel (15).

Shilow, Lepin, and Wosnessensky (10) determined the amount of chlorine sorbed by different sections of a charcoal bed under different experimental conditions. They found that:

$$C_o \times T' = \text{constant} \qquad \text{(xvi)}$$

where C_o is the initial concentration, and T' the service time, for chlorine concentrations from 0.66 to 1.36%. Mecklenberg (14) applied their data to his equations for the service time as a function of

(a) the diameter and length of the charcoal bed

(b) the velocity and initial concentration of the gas stream

(c) the capacity and specific surface of the charcoal, and,

(d) the vapor pressure of the sorbate in the capillaries of the charcoal.

In each case good agreement was obtained between the predicted and experimental values.

Dubinin, Pairshin, and Pupuirev (17) investigated the service time of short charcoal bed lengths, using chlorine and found that there was some protective action with bed lengths shorter than the "dead length". They concluded that the "dead length" was purely a mathematical fiction and that it had no physical significance.

Mecklenberg explained that, at the beginning, of a run there would be no liquid in the capillaries of the charcoal and in consequence the term C' in his equation would be zero. This would change the concentration term in his equation to:

$$\ln \frac{C_o}{C_x} - 1 \qquad \text{(xvii)}$$

As the gas is sorbed, C' would increase gradually to its maximum value C_o. In the service time - bed length plot, this would cause the service time to decrease linearly as the bed length decreased until at some point it would curve in toward the origin and cut the bed length axis at a much shorter distance than the extrapolation of the linear portion of the curve. Mecklenberg checked this behavior using chloropicrin.

Shilow, et al (16) constructed a series of gradients, at different times, along the charcoal bed, from their data on the sorption of chlorine. A reproduction of their diagram is shown in figure (3). They found that those representing the early penetration of the charcoal bed by the gas such as OP, OQ, and OR different in shape to those at later times as represented by OA, OB, OC etc., and were gradually built up to

this shape which remained constant as the gas penetrated further into the charcoal bed. They further noted that during this building up period the gradients decreased from the point O which represented the initial concentration of the gas stream as it came into contact with the surface of the charcoal bed. When the gradient was completely formed it moved at constant velocity through the bed. They also pointed out that the areas OPQ, OQR, etc. increased up to the area OAB and thereafter remained constant.

From equation (xv), Mecklenberg derived an expression for the falling off of the concentration of the gas in the air stream along the charcoal bed:

$$C = C_o e^{-\frac{DF}{\delta_r}\left(\frac{V}{kQ}\right)^{n-1} .S} + C' \qquad \text{(xviii)}$$

where S is the distance along the bed. This is shown graphically in figure (4) by the curve CDB. This equation predicted that the "falling off" curve would be of the shape of that at the beginning of the bed, i.e. OP, or as shown in figure (4), CDB. The charcoal bed from the front surface up to CC' would thus be completely saturated.

Mecklenberg considered the process of the sorption of a gas by a charcoal bed as divided into two parts:

(a) The building up of the sorption gradient or working length to its constant shape. This, he said, was the length of bed necessary to reduce the concentration of the gas in the air stream from its initial value to the "threshold" concentration. He defined the threshold concentration as that required to give the chemical test used in determination of service time.

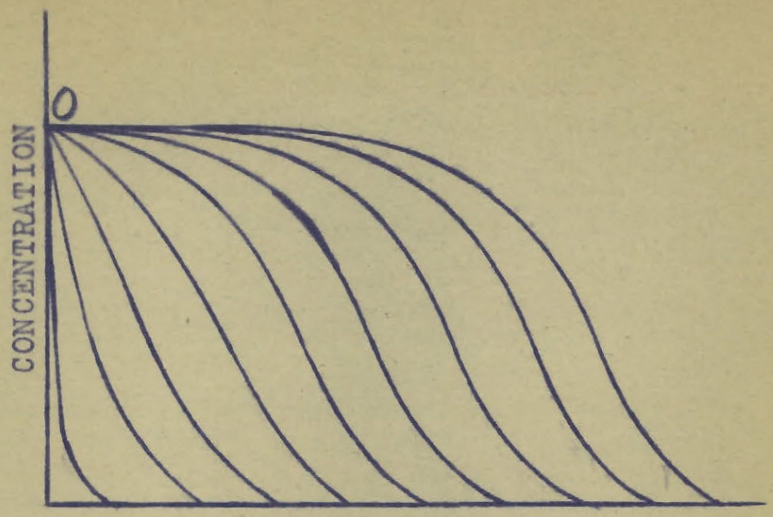

GAS PHASE GRADIENTS (SHILOW)

FIGURE 3.

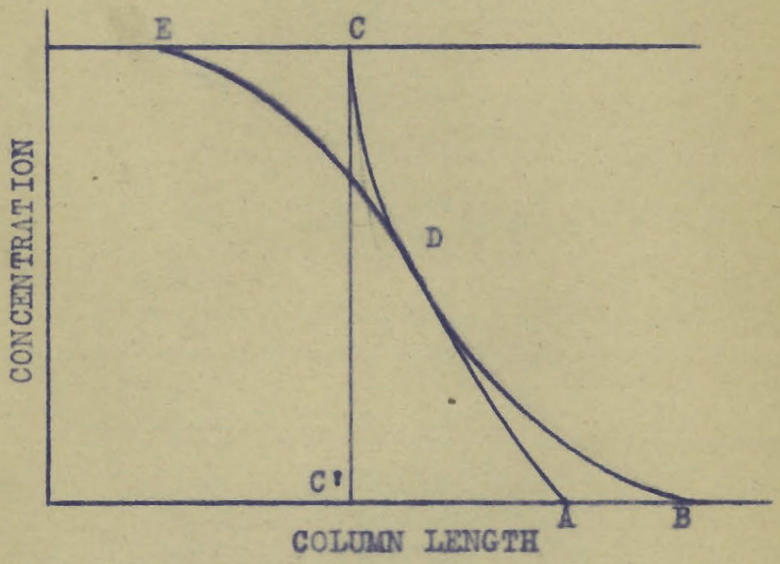

"MATHEMATICAL" (CDF) AND ACTUAL (EDA)
CONCENTRATION GRADIENTS (MECKLENBERG)

FIGURE 4.

(b) The movement of this gradient, once it is built up, through the charcoal bed with a constant linear velocity.

He then considered the process in detail. Suppose the air stream entering the bed is divided into differential amounts, 1, 2, 3, etc., and the charcoal bed divided into differential layers a, b, c, etc. If the differential amount of air, 1, is considered: This amount of air enters the layer, a, of the charcoal bed and an instantaneous equilibrium is set up between the gas and the charcoal, as predicted by the sorption isotherm. This will remove a large part of the gas from the air stream. The air then moves on to layer b and the remaining gas comes to equilibrium between the air and charcoal, and some more gas is removed from the air. This process continues until at some layer S_1, the concentration of the gas has fallen below the threshold value. When the differential amount of air, 2, enters layer a, only a small amount of gas is taken up by the charcoal to set up a new equilibrium since layer, a, has a large amount of gas sorbed from the passage of 1. The second threshold value is reached at layer S_2. As the process continues each particular layer of charcoal will take less and less gas from each successive differential amount of air that passes over it. Finally, at some time, t_x, when a differential amount of air, x, enters the bed, layer, a, becomes saturated and the sorption gradient has reached its full length and extends through the bed to some layer S_x. The next differential amount of air will saturate layer b and the gradient for this will extend one

layer past S_x. The gradient then moves through the bed with constant velocity.

For the first differential amount of air the front trace of gas has moved through the charcoal bed from the front surface to a point S, during the differential time interval. When the second differential amount of air enters the front trace of gas moves a distance $S_2 - S_1$, in an equal time interval. By the time this gas reached S_1, its concentration has been considerably lowered in passing over the partially saturated charcoal in that section, so that the distance $S_2 - S_1$ must be shorter than the length S_1. Similarly the distance travelled by the front trace of gas for the third amount of air, $S_3 - S_2$ is less than $S_2 - S_1$. Thus the front trace of gas moves through the charcoal with a constantly decreasing velocity, reaching a constant minimum velocity when layer a becomes saturated. Shilow et al confirmed this behavior with chlorine at concentrations of 2.13%.

Until the sorption gradient is completely built up, the concentration of the gas at the front surface of the charcoal is the initial concentration, C_o, of the gas in the air stream. This concentration falls off along the charcoal bed as indicated. Thus the gradients in this region must extend from the point 0 in Shilow's diagram (figure 3).

To explain the change in shape along the bed to the form EDA (figure 4) Mecklenberg pointed out that:

(a) a "mathematical" charcoal had been assumed which

possessed capillaries of uniform and constant cross section, and

(b) Nernst's diffusion law had been assumed to hold for the diffusion of the gas from the air stream to the capillaries.

In actual fact the charcoal capillaries are neither of uniform nor constant cross section, but that there are some which are much smaller than the average and some which are larger. The smaller capillaries result in the shortening of the bottom part of the gradient from DB to DA. The larger ones, which were assumed not to fill as rapidly as the remainder, are not saturated as they should be if equation (xviii) were to hold. The result is that the curve is distorted toward the form EDA. In addition he assumed that chlorine would be displaced from the outer layers by the air stream, being resorbed further along the bed. This acts in the same direction as the effect of the larger capillaries and further distorts the curves so that when constant conditions are reached the gradient would have the form EDA rather than CDB.

Effect of Experimental Conditions on Sorption Data

From these theories of sorption the variation of sorption data such as service time, dead length, and sorption capacity with experimental conditions has been predicted. It is interesting to summarize these predictions and to see how they have been verified by experiment.

1. The service time - This has been defined as the time, from admission of the gas stream to the charcoal, until a sensitive chemical test indicates that the sorbate is present in the gas stream which has passed through the bed. Its dependence on the experimental conditions, has been predicted, from the theories of Mecklenberg and Danby et al as follows:

(a) Variation with bed length - A linear relation has been predicted by both theories. Mecklenberg further predicted that as the bed length was decreased the graph would curve in toward the origin and cut the bed length axis at a shorter distance than the extrapolation of the linear portion. Many investigators have found this to be true: Shilow et al (16) and Dubinin et al (17) for chlorine; Danby et al (12) for hydrogen sulfide, carbon tetra chloride, nitrous fumes and arsine; Mecklenberg for chloropicrin (14); Syrkin and Kondraschow (18) for vapors of carbon disulfide; pyridine, isobutyl alcohol and dimethyl ethyl carbinol; Izmailov and Sigalovskaya (19) for the vapors of benzine, n heptane, phenol, napthalene and carbon disulfide; and Ruff (20) for solutions of acetic acid and phenol in water.

Dubinin (21) expressed the relation in a different form:

$$T = \phi L - \tau \qquad \text{(xix)}$$

where ϕ is the coefficient of protective action and τ the protective time loss due to the very rapid penetration of the gas at the start of a run.

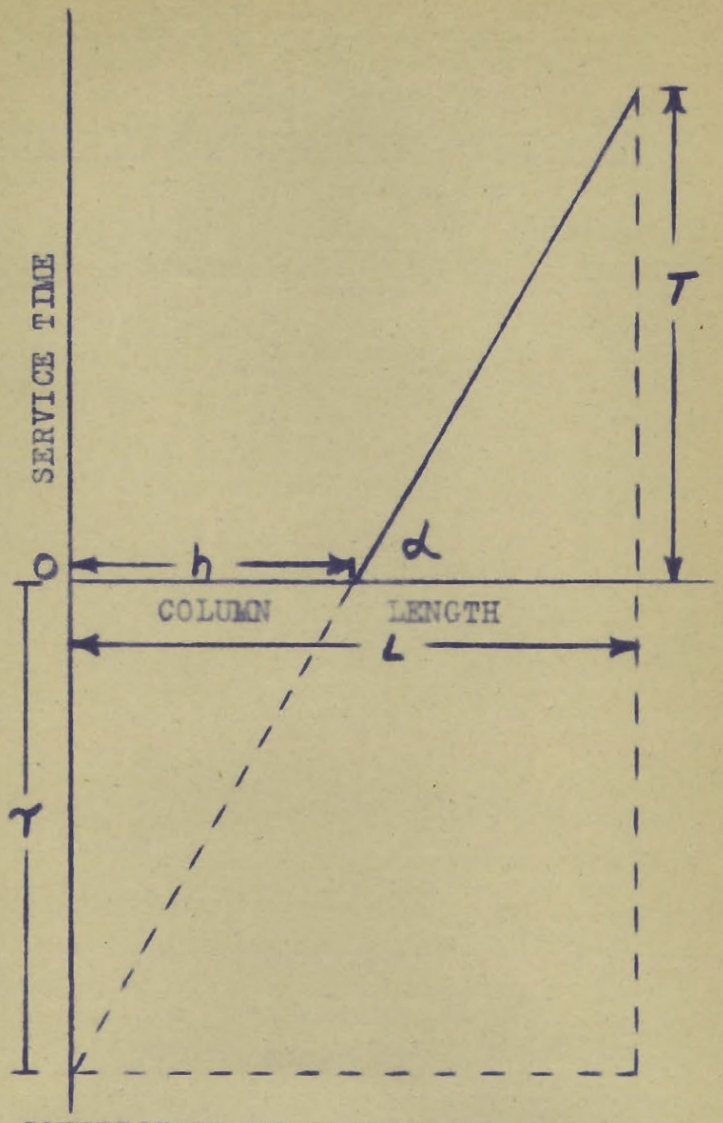
SERVICE TIME
T
O
h
α
COLUMN
LENGTH
L
γ
COEFFICIENT OF PROTECTIVE ACTION

FIGURE 5.

Shilow et al (16) deduced the relation:

$$h = \frac{\tau}{\delta} \qquad \text{(xx)}$$

where h is the dead length, τ the initial loss of time of protective action and δ the coefficient of protective action.

These latter two equations may be related with the help of figure (5). The coefficient of protective action is the slope of the linear portion of the service time - bed length relation and the protective time loss is the intercept of the extrapolated linear relation on the negative service time axis.

(b) Variation with flow rate - Both theories predict a linear relation between the service time and the reciprocal of the flow rate. Danby et al postulate a critical flow rate above which there is an immediate breakdown of the charcoal bed. This latter however has not been verified experimentally, although good agreement has been found with the predicted linear relation.

(c) Variation with the cross-section of the bed - The Mecklenberg equation (xiv) indicates a direct linear relation which has been verified by his experiments.

(d) Variation with the physical constants of the charcoal - Danby et al predict linear variation of the service time with the diameter of the charcoal grains and confirmed this, by experiments with arsine and carbon tetra chloride. Mecklenberg predicted and found similar results.

(e) Variation with initial concentration - Danby et al noted the difficulty of predicting the variation of service time with initial concentration from their theory, but stated that at low initial concentrations the service time should vary as the reciprocal of the initial concentration. They found this to be true for arsine, carbon tetra chloride and hydrogen sulfide. Shilow et al also predicted this and confirmed their prediction by experiment using chlorine in concentrations from 0.66 - 1.36%

2. The dead length

This, as has been previously mentioned, is a means of measuring the residual activity of the charcoal at the service time. Some investigators (12, 16) have attempted to give it a physical significance as previously mentioned while others (14, 21) have claimed that it is merely a mathematical fiction which enables the prediction of the service time - bed length plot over the linear portion. Mecklenberg has, however, shown that there is a dead length, which is,however, different from its original interpretation as a length below which there is an immediate breakdown. Several relations are obvious from the theories, as well as from an equation developed by Allmand (22):

$$h = \frac{Q - \ln \gamma_B}{K_o} \left(\frac{V}{A}\right)^{\frac{1}{2}} d \qquad \text{(xxi)}$$

where Q is a coefficient peculiar to charcoal and vapor γ_B the fraction of the entering concentration of the vapor trans-

mitted at the service time, V the volume of air flow per unit time, A the cross sectional area of the charcoal bed, d the average diameter of a charcoal granule, and K_o a constant equal to $(1/T)^{\frac{1}{2}}$.

(a) Cell and charcoal constants - The dead length has been predicted to vary with the reciprocal of the cross-sectional area of the charcoal bed and directly with the diameter of the charcoal granules. Mecklenberg and Engel have confirmed these relations using chloropicrin.

(b) Flow rate - Mecklenberg from equation (xv) predicted that:

$$h = \text{const.} \times V^{1-n} \qquad \text{(xxii)}$$

where n is a constant which is usually about 0.5 so that the dead length would vary with the square root of the linear velocity. From equation (vii) of the Danby treatment the dead length should vary linearly with the flow rate. Engel has confirmed its dependence on the square root of the flow rate.

(c) Initial Concentration - Both theories from equations (vii) and (xv) predict a linear relation between the dead length and the logarithm of the initial concentration. This was confirmed by experiments on chloropicrin by Mecklenberg and on chlorine by Shilow et al.

3. Sorption Capacity

In static systems the sorption capacity of a given charcoal depends on the molecular weight and boiling points of

the sorbing gas. Engel noted that this was true also for dynamic systems.

Not much attention has been devoted to the actual sorption capacity of charcoals in comparison to that given to the service time and the dead length. The volume activity of a charcoal has been used however as an indication of its protective power. It is measured by sorbing carbon tetra chloride under the given experimental conditions until it is detected in the effluent stream.

$$\text{The Volume Activity} = \frac{\text{Increase in weight of the charcoal}}{\text{volume of charcoal}} \times 100 \qquad \text{(xxiii)}$$

In the Danby et al treatment of the dynamic sorption of gases, the sorptive capacity of the charcoal is expressed in terms of a capacity constant N_o, the number of active centres each of which is capable of removing one molecule of sorbate, and a rate constant k which determines the rate of removal of the sorbate from the gas stream. These are assumed by the theory to be independent of factors such as initial concentration, flow rate, etc.

In Mecklenberg's service time equation:

$$T' = \frac{k}{VC_o}\left(V - Qh\right) \qquad \text{(xiv)}$$

k is the maximum amount of sorbate which the charcoal is capable of taking up under the experimental conditions. He

investigated its dependence on the initial concentration, and found that it followed, for chlorine, the Freundlich isotherm:

$$k = aC_o^{\,b} \qquad \text{(i)}$$

where a and b are constants a = 8.38 and b = 0.164.

Ruff (20), for liquids in aqueous solution also found that the adsorption isotherm expressed the relation between the sorption capacity and the initial concentration.

Syrkin and Kondraschow (18), from purely kinetic considerations deduced a formula for the amount sorbed, c_1 by the entire charcoal bed at any time T :

$$\log \frac{A}{A - c} = 0.434\ KT \qquad \text{(xxiv)}$$

where A is the maximum amount of gas capable of being sorbed by the charcoal under the given conditions, and K is a constant which was found to vary with temperature according to the relation:

$$\tau = \frac{K_{T_1}}{K_{T_2}}^{\frac{10}{T_2\ T_1}} \qquad \text{(xxv)}$$

where τ is the temperature coefficient. They found that their formulae held for the vapors of carbon disulfide, pyridine, isobutyl alcohol, dimethyl ethyl carbinol over the temperature range 10 - 100°c.

The experiments discussed in this thesis were done to obtain numerical data for the sorption of butane and ammonia under various conditions, and thus to test further the relations given by the theories of Danby and of Mechlenberg.

EXPERIMENTAL

Apparatus

The apparatus used in these investigations consisted essentially of a charcoal cell mounted on one arm of an analytical balance, to permit the sorption to be followed by weight as a function of time. Provision was made for measuring the mixture of air and sorbate admitted to the, and for sampling and analysis of the effluent gas stream from the cell. This type of apparatus was first described by Pearce (1) and was used here with minor modifications.

A detailed discription of the apparatus may be simplified by considering separately the following systems: air, sorbate, charcoal, the cell itself, the effluent gas stream and the analysis. Figure 6 shows the apparatus diagrammatically. A detailed sketch of the cell is shown in figure 7 and the analytical apparatus is shown in figure 8.

Air was introduced from a compressor to a 45 litre ballast volume V_1 (figure 6). The ballast volume eliminated the small pressure variations which occurred in the line. Since carbon dioxide is appreciably sorbed by charcoal, it was removed from the air stream with three soda lime tubes A connected in series. Water vapor was also removed, in four calcium chloride drying tubes B, and three sulfuric acid bubblers C in series. This system could be used to obtain air of any desired humidity by adjusting the concentration of the acid in

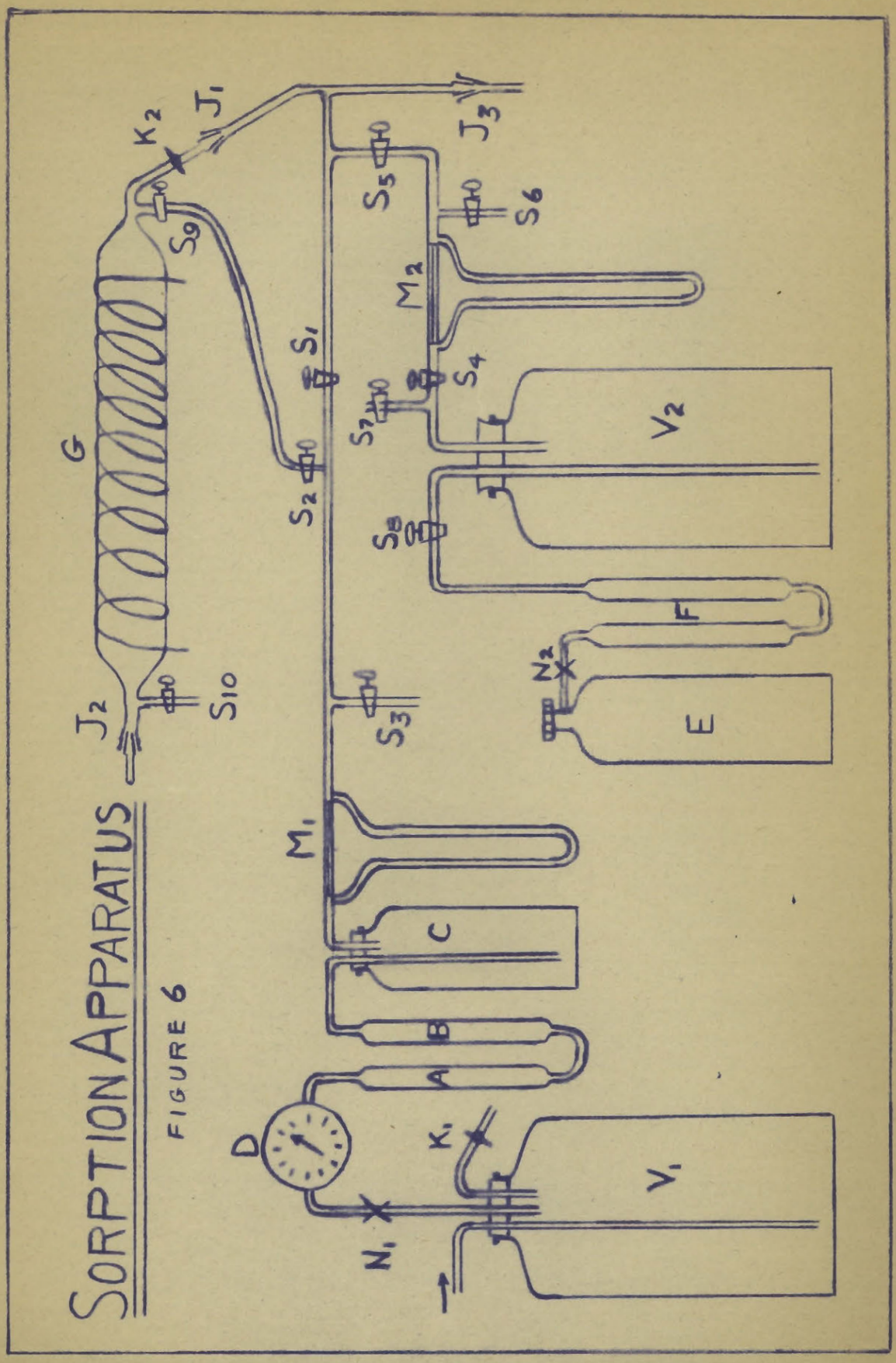
SORPTION APPARATUS
FIGURE 6
G
J1
J2
J3
K2
S1
S2
S3
S4
S5
S6
S7
S8
S9
S10
M1
M2
A
B
C
D
E
F
K1
N1
N2
V1
V2

the bubblers. The present study was confined to the use of dry air, hence concentrated sulfuric acid was used. The rate of air flow was measured with a rotary wet test meter D, filled with butyl phthallate, inserted in the line between the ballast volume and the soda lime tubes. Setting of the flow rate was facilitated by a calibrated capillary flowmeter M_1 of the usual type. Butyl phthallate was used as the manometer fluid. Regulation of flow was accomplished by a blow off valve K_1, which consisted of a screw clamp on a short length of rubber tubing, for rough adjustment, and a metal needle valve N_1 for finer control. The air could be admitted to the cell, to the conditioner or to a fume hood as desired, by stopcocks S_1 and S_2 and S_3.

The sorbate was admitted directly from the storage cylinder E. It was dried over four calcium chloride drying tubes, F, in series. After passing through the 50 litre ballast volume V_2, the sorbate entered the air stream through the stopcock S_4. Rough regulation of the flow was obtained by a scratch on the stopcock while finer control was accomplished by adjusting the needle valve N_2 on the cylinder. The flow rate was measured by the calibrated capillary flowmeter M_2 containing butyl phthallate as the manometer fluid. Stopcocks S_5 and S_6 allowed the sorbate stream to be admitted to the air stream or diverted to a fume hood. The whole sorbate system could be evacuated through the stopcock S_7.

The charcoal was conditioned in a stream of dry, carbon-dioxide-free air in the conditioner G, which was constructed from a pyrex tube about a foot long and two inches in

diameter. It was heated electrically, and insulated with asbestos. A slide wire rheostat, regulating the current, permitted the temperature to be controlled. The conditioner was mounted above the cell and at a slope of about thirty degrees with the horizontal. The ground joint J_1 allowed the conditioner to be removed for refilling, which was done through the ground joint J_2. at the upper end. The air stream for conditioning entered through the stopcock S_9, and was released through the stopcock S_{10}, on the upper end. The conditioner was connected to the ground joint J_1, by a short length of rubber tubing provided with a screw clamp K_2.

The charcoal was allowed to fall into the cell from the conditioner, by opening the screw clamp K_2 and gently tapping the conditioner. Since the charcoal always dropped from a constant height, the packing of the granules in the cell was constant, as shown by the fact that reproducibility of the results was readily obtained. No moisture or carbon dioxide could contaminate the conditioned charcoal, since it only came into contact with dry, carbon-dioxide-free air, after being conditioned.

The charcoal cell itself (figure 7) consisted of a piece of glass tubing 4 cm. inside diameter and 21 cm. long. A brass cap was fitted over the top and sealed to the glass with de Khotinsky cement. A section of thin brass tubing 1.5 cm. in diameter and 7 cm. long was soldered through the centre of the cap and extended down into the cell. A brass ring about a quarter of an inch wide, with small projections on each side was sealed around the outside of the cell at the

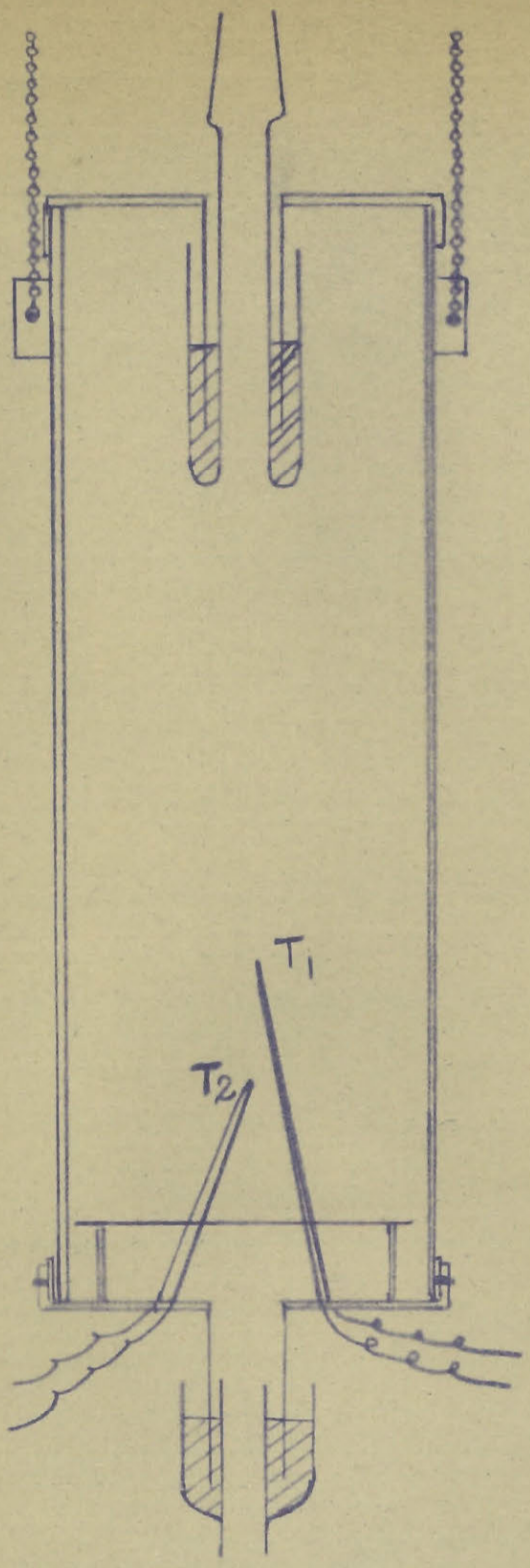

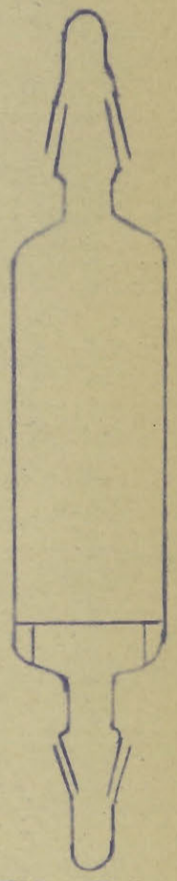

FIG. 7 A

FIGURE 7
CHARCOAL CELLS

bottom. A detachable brass cap, similar to the one at the top was machined to fit snugly around the brass ring, and could be drawn against the bottom of the ring to form an air tight seat, by oblique slots operating over the projections on the ring. A length of brass tubing extended downward from the centre of the brass cap.

The charcoal was supported on a circular disc of metal gauze of the type generally used in respirators. To allow the air to flow freely out of the cell this gauze disc rested on a ring of glass tubing about half an inch in height. The cell was marked off in centimeters so that the depth of charcoal in the cell could be varied from one to five centimeters. Two thermocouples T_1 and T_2, were inserted into the cell, through the bottom, the positions of the junctions being altered as desired. The thermocouple wires were copper and constantan B and S gauge number 28. They were coiled loosely outside the cell and connected to fixed binding posts, so as not to interfere with the weighing. Temperatures were measured on a Cambridge unipivot millivoltmeter with a thermal scale.

The cell was suspended by a light chain from one arm of an analytical balance adapted for this purpose. To allow the cell to move freely and to prevent escape of any gases from the cell, the brass tubes dipped into cups containing butyl phthallate. These cups were attached to the inlet line at the top by a ground joint J_3 and to the outlet line at the bottom. The weight of the empty cell assembly was about 200 grams.

Where greater accuracy was desired, and where equilibrium weights were sufficient, a modified cell was used

(figure 7b). This was made from a piece of pyrex tubing fitted with ground joints at either end. The charcoal rested on a piece of gauze as in the previous cell. This cell could replace the former, being connected to the air line by the ground joint J_3. Weight could not be followed as a function of time with this, but it had the advantage that it could be readily removed, when sufficient time had been allowed for equilibrium, sealed with ground joint caps, and weighed accurately on an analytical balance.

The gas stream leaving the bottom of the cell (hereafter called the effluent stream) passed through one arm of a T tube to the fume hood. A short length of glass tubing to contain test papers could be inserted in the exit line if desired. To sample the effluent stream, evacuated pipettes were connected to the other arm of the T tube, to which a capillary tube was attached, the bore of the capillary being such that the bulbs filled at a rate less than the rate of gas exit from the cell. In this way only the effluent stream was drawn into the pipettes.

The analysis of the effluent stream was carried out in the apparatus shown diagrammatically in figure 8. The sample pipette H was supported at an angle of about 30 degrees and the gases were displaced from the bulb with mercury from the reservoir L.

For butane analysis, the gases from the bulb, after mixing with dry carbon-dioxide-free air, were passed through a quartz tube Q about three feet long and one-quarter inch in

diameter. This quartz tube was heated for about one foot of its length in an electric furnace P, to a temperature of 1000°C. A rheostat and an ammeter were used to maintain the temperature. The carbon dioxide formed during the combustion was absorbed in standard sodium hydroxide solution in the absorption tube R. For efficient absorption a sintered disc bubbler V, of the type shown in the figure was used, and a few drops of butyl alcohol added to reduce the surface tension of the solution so that a fine foam was obtained. The oxygen stream purified by passing through soda-lime tube W, was regulated to give about three inches of foam. Standard acid was used to titrate the excess sodium hydioxide, using phenolphthalein as indicator.

For ammonia, the apparatus used was slightly different. The ammonia displaced from the bulb was absorbed directly in standard acid after mixing with a dry carbon-dioxide-free air stream to obtain the necessary degree of foaming in the absorbing liquid. Standard sodium hydroxide was used to titrate the excess acid, using a solution of methyl red and brom cresol green as indicator.

Procedure

Details of the experimental procedure will be much clearer if the procedure of a typical experiment is described and the results recorded.

The charcoal was dried in the conditioner (figure 6) for twelve hours at 150°C in a stream of dry carbon-dioxide-free

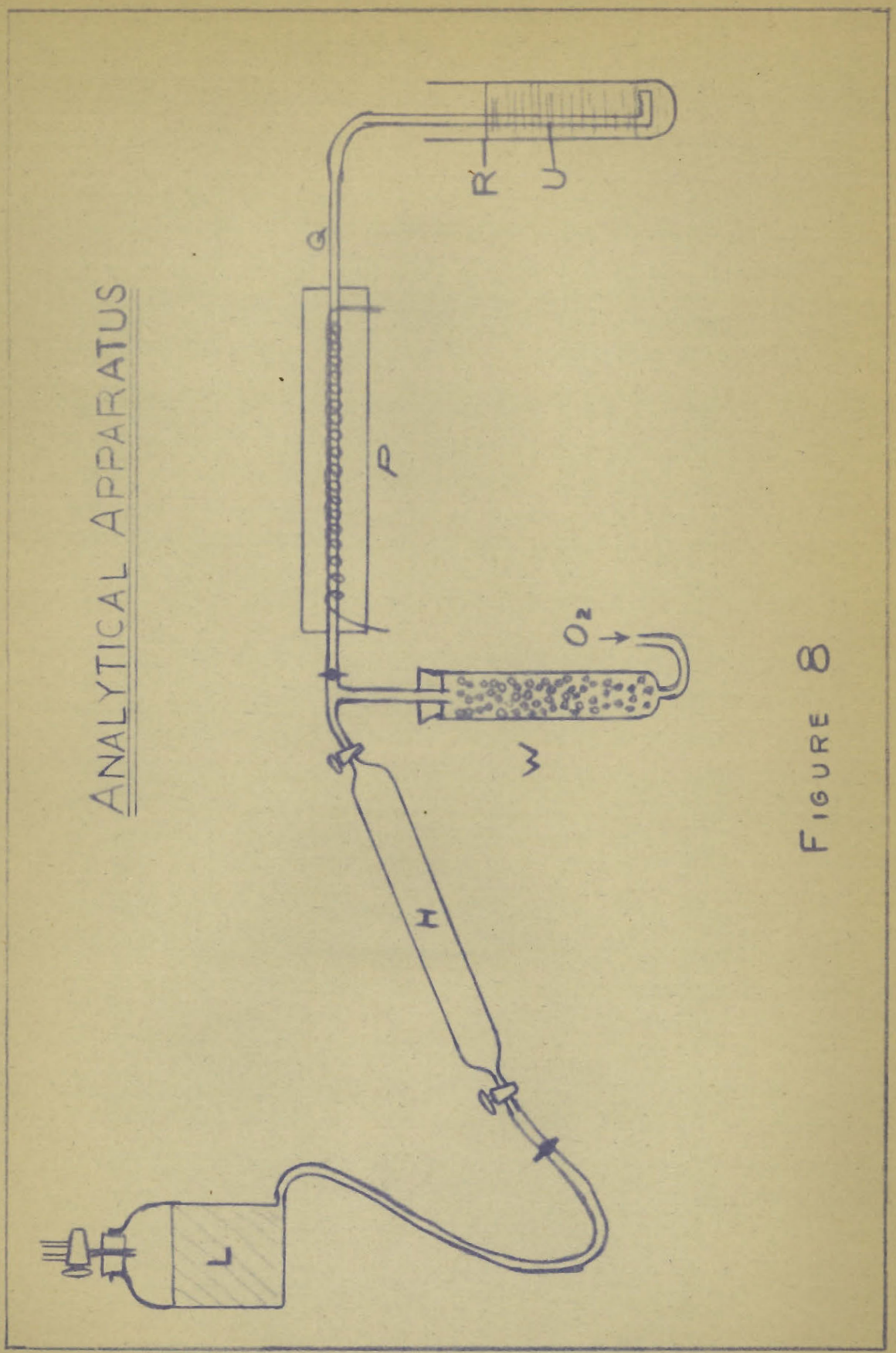

FIGURE 8

air, and allowed to come to equilibrium with air of the desired moisture content at room temperature for a further twelve hours.

Since the sorption is dependent on the temperature of the charcoal, it was important that room temperature be kept reasonably constant throughout any one experiment and for all comparable experiments. Atmospheric pressure appeared to have little effect on the amount of sorption.

The cell was thoroughly flushed out using the dry carbon-dioxide-free air. The air stream was then diverted through the stopcock S_3, while the weight of the empty cell was determined. Care must be taken to have the cell swinging freely in the liquid seals. Charcoal was then admitted to the cell to the desired depth and its weight determined without air passing through the cell. Dry air was passed through the cell, and regulated to the desired flow rate, the blow off valve K_1 and the needle valve N_1. With the stream being diverted through S_3, the sorbate stream was then regulated to the desired value, using the scratched stopcock S_4 and the needle valve N_2. At the beginning of the experiment the flow was set by adjustment of the scratched stopcock and regulated thereafter by the needle valve, which was found to give finer control. The zero weight of the charcoal cell was next found with the air stream passing through the bed. The zero thermocouple readings were also taken. When conditions were steady the sorbate was directed into the air stream, a stop watch

started, and the initial reading on the rotary air meter taken. Thereafter, weight and temperature readings were taken at two minute intervals. Samples of the effluent stream were drawn at appropriate intervals (the first being taken shortly after the beginning of the run, the second immediately after the bottom thermocouple reading had reached its maximum value, and others at regular intervals until the end of the experiment. The time between samples was determined by the sorbate and air flow rates and the depth of the charcoal bed). Care was taken throughout to prevent, as far as possible, any variations in air or sorbate flow rate. Room temperature and atmospheric pressure were read when convenient, as were the temperature and pressure of the air stream on the wet test meter. When the charcoal was no longer adsorbing, as indicated by constant weight readings for a period of at least fifteen minutes, and the thermocouple readings having returned to their original values, a final analysis sample was taken on the effluent stream. The final air meter reading and time were determined. Both the air and sorbate streams were diverted and the final static weight of the cell, charcoal and sorbate determined. The net weight of gas sorbed as indicated by the difference between the initial and final static weights and the zero and final weights with the air stream passing through the cell should check. This was nearly always found to be so. Occasionally a sample of the effluent gases was taken before the maximum temperature was reached to see if any sorbate was passing through the charcoal before it was expected.

For analysis, the bulbs were connected in the analy-

tical apparatus (figure 8) and the gases displaced as described previously. About five minutes was allowed for the displacement to ensure complete combustion and absorption. The percent sorbate in the effluent gases was determined by titration of the excess absorption solution.

The method of analysis outlined above was used in preference to ignition by a hot wire. In this method, as used by Pearce (1), a measured quantity of sample was burned, the carbon dioxide formed, frozen out by liquid air, and the remainder of the gas pumped off. The amount of carbon dioxide formed from the combustion was determined by its pressure in a calibrated volume. Combustions by this method were found to be incomplete, however, and reproducible results could not be obtained despite the considerable time spent in attempting to improve the technique. It seems likely that the accuracy and reproducibility of the slow combustion method have been exaggerated. The method used in these investigations, however, resulted in complete combustion and readily reproducible results (within 1% of each other in duplicates). One part of carbon dioxide in 10,000 parts of air was detectable. Several blanks were analysed to confirm this accuracy.

In the desorption experiments, the charcoal was allowed to come to equilibrium with a saturating stream of air and sorbate of the desired proportions in the usual manner. When the desired desorption conditions were steady, the desorbing stream was admitted to the cell. Weight

and temperature were followed as a function of time as in the sorption studies and sample bulbs were taken of the effluent gas at appropriate intervals.

The accuracy attained using this apparatus was about 5%, as it is very difficult to obtain greater accuracy in studying colloidal systems. Weight readings were accurate to about 0.005 of a gram. Variations in sorbate and air flow rate accounted for the greater part of the experimental error. Moisture and carbon dioxide determinations on the air stream showed that it contained undetectable amounts of carbon dioxide (less than 1:10,000) and less than 0.004% water.

The materials used in these investigations were:

(a) charcoal - Canadian SBT 95-96, silver impregnated

(b) ammonia - anhydrous ammonia obtained from Canadian Industries Limited

(c) butane - C.P. (99.5%) obtained from the Ohio Chemical and Manufacturing Company.

Both the ammonia and butane were used without purification except for drying with calcium chloride.

Typical Data Sheet

Run No. 84 6/2/42

Air: 2.6 (3.0 litres/min.) Butane: 30.0(24.0 cc/Min.)

Room Temperature: 23°C Atmospheric Pressure:759 mm.Hg.

Height of charcoal bed	4 cm.
Weight of charcoal plus cell	31.38 gm.
Weight of cell	3.59
Weight of charcoal	27.79
Final weight	35.34
Butane sorbed	3.96 gm.

Air - Temperature: 23°C Pressure: 3.70 in. Hg.

Initial meter reading 48.556

Final meter reading 60.427

11.871 cu. ft. Time: 114 min.

$$\text{Air rate} = \frac{11.871}{114} \times 28.3 \times \frac{273}{296} \times \frac{853}{760} = 3.045 \text{ litres/minute}$$

* Time	Weight	T_1	T_2	W
0	32.02	24.0	24.0	
2	32.11	27.0	24.0	0.09
6	32.32	31.0	28.0	0.30
10	32.53	32.0	29.5	0.51
18	32.99	33.5	31.5	0.97
34	33.93	30.5	34.0	1.91
50	34.87	26.5	31.0	2.85
70	35.71	23.5	26.0	3.69
90	35.96	23.0	23.5	3.94
110	35.98	23.0	23.0	3.96

Analysis *

Bulb	Time of Sampling	CC. H_2SO_4	CC. N_aOH	CC. base neutralized by CO_2	K	% C_4H_{10} in air stream
4	25	10.20	9.93	0.03	0.1045	0.003
1	110	3.13	2.92	7.08	0.0935	0.660

$$K = \frac{\text{normality}}{1000} \times 22.4 \times \frac{100}{V} \times \frac{T}{273} \times \frac{760}{P}$$

V = volume of sample bulb T = room temperature

P = atmospheric pressure % = K x (CC. N_aOH used)

* These tables have been considerably condensed.

$$x/m = \frac{3.96}{27.79} \times \frac{22400}{58} = 54.9 \text{ CC./gm.}$$

$$\text{Partial pressure} = \frac{24.0}{3069} \times 760 = 5.70 \text{ mm. Hg.}$$

$$\text{Corrected height} = \frac{27.79}{6.57} = 4.23 \text{ cm. of charcoal.}$$

Note - At the slow flowrates for ammonia, sample bulbs required approximately six minutes to fill completely. In calculations, the sample was considered as having been taken three minutes after the bulb was opened to the effluent stream. For butane, much larger flow rates were possible, and a larger capillary allowed the bulbs to fill completely in two minutes. The sample was then considered to have been taken one minute after sampling was started.

RESULTS

A. Ammonia

The weight increase of the charcoal bed with time, the temperature rise with time and the analysis of the escaping gases were carried out using ammonia concentrations of 0.05 - 100% and flowrates of 0.16 - 3.2 cm. per second, and at column lengths of 3,4 and 5 cm. of charcoal as previously described. The service times, dead length, amount of sorption, and escaping concentration were calculated.

1. Amount of Sorption

The increase in weight of the charcoal bed as the ammonia-air mixture is passed over it is shown as a function of time for various concentrations, flowrates and column lengths, in figures 9 and 10. It is seen that the weight increases linearly with time until the service time is reached. This rate depends on the ammonia flowrate (as figure 10 shows) and is independent of the air flowrate (figure 9). After the service time is reached, the weight falls off gradually with time until a constant weight is reached, at which time the charcoal is in equilibrium with the ammonia-air stream being

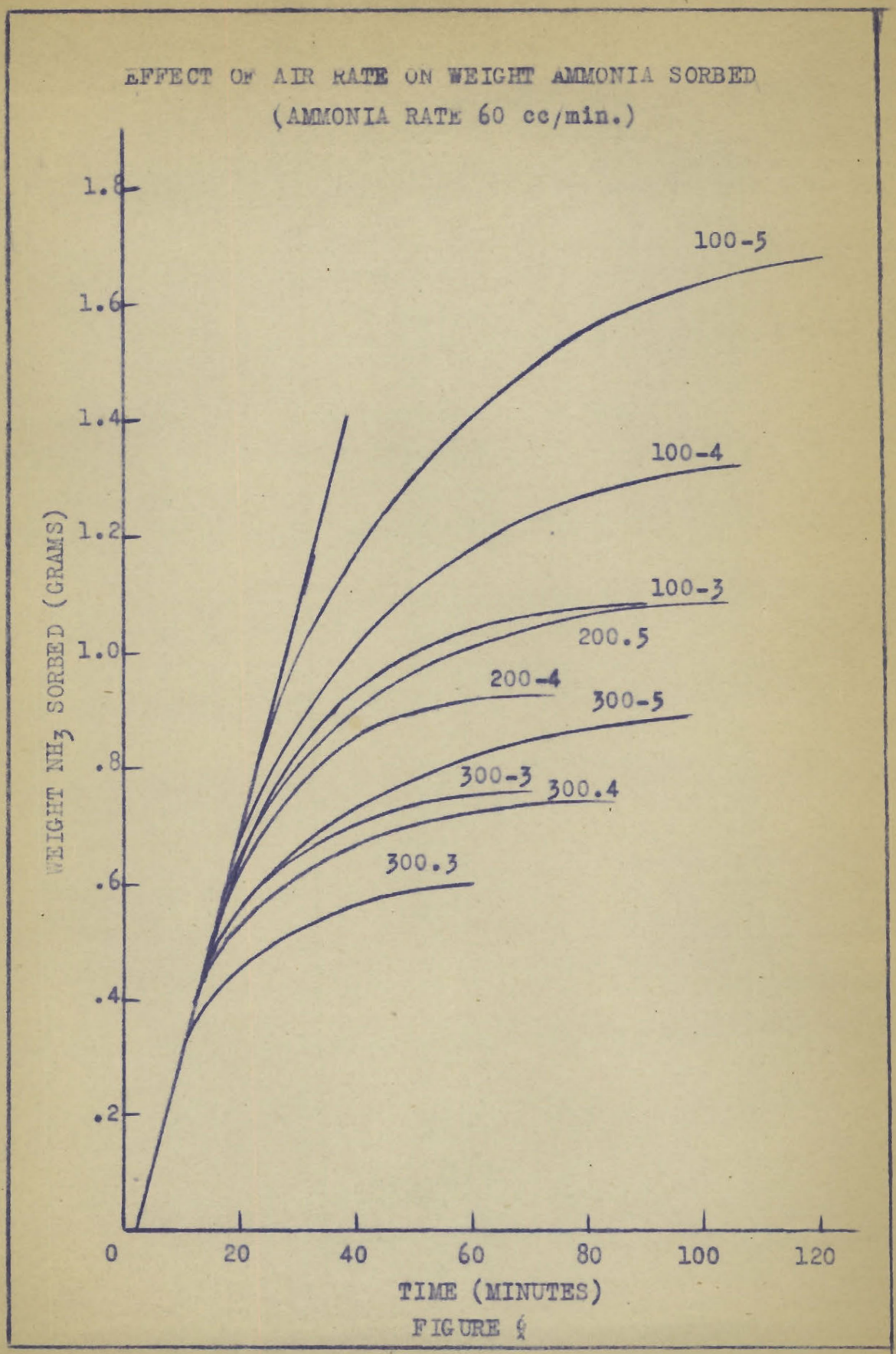
EFFECT OF AIR RATE ON WEIGHT AMMONIA SORBED
(AMMONIA RATE 60 cc/min.)
WEIGHT NH_3 SORBED (GRAMS)
1.8
1.6
1.4
1.2
1.0
.8
.6
.4
.2
0
20
40
60
80
100
120
TIME (MINUTES)
100-5
100-4
100-3
200.5
200-4
300-5
300-3
300.4
300.3

FIGURE 4

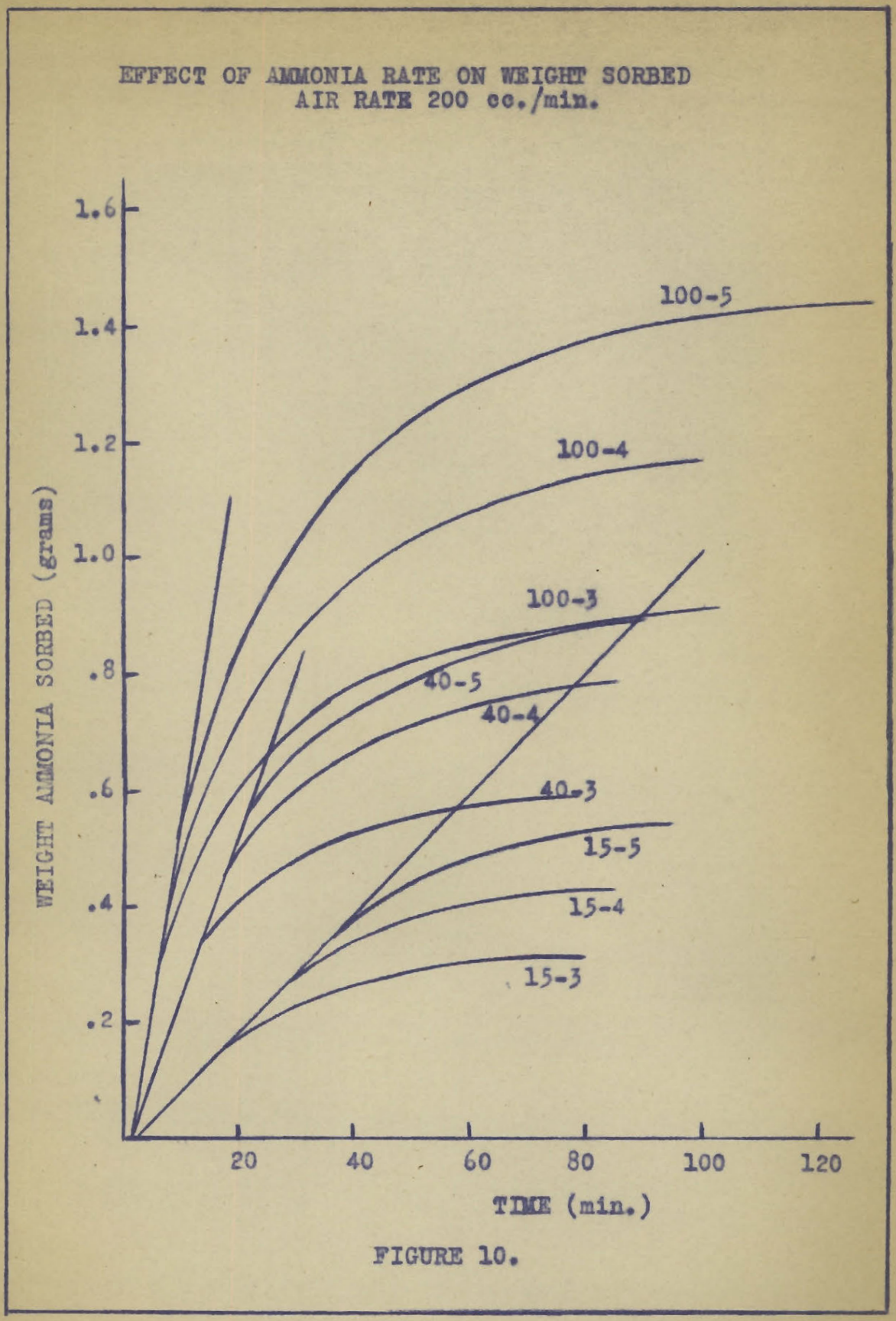
EFFECT OF AMMONIA RATE ON WEIGHT SORBED
AIR RATE 200 cc./min.
WEIGHT AMMONIA SORBED (grams)
1.6
1.4
1.2
1.0
.8
.6
.4
.2
100-5
100-4
100-3
40-5
40-4
40-3
15-5
15-4
15-3
20
40
60
80
100
120
TIME (min.)

FIGURE 10.

passed over it.

The equilibrium sorption weights are given in tables I and II for various concentrations, flowrates and column lengths. The column length was determined using an average centimetre bed, which weighed 6.57 gm. This was the average weight of a centimetre bed length determined from the weights of all the beds used throughout the work. The column lengths given in tables I and II are approximate. The correct bed lengths, calculated from the weight of charcoal have been used however in plotting graphs of the column length. Figures 11 and 12 show that the equilibrium weight sorbed is a linear function of column length at constant concentration.

The variation of the equilibrium sorption, expressed as the volume sorbed per gram of charcoal, with the rates of flow of the ammonia and air streams is shown in tables III and IV and in figures 13 and 14. It is seen that at constant ammonia flow, the effect of increasing the air flowrate from zero is quite marked at first but the effect diminishes until the amount sorbed becomes almost independent of the rate of the air flow. When plotted as the logarithm of the volume sorbed per gram of charcoal against the logarithm of the air rate a straight line is obtained (figure 15). The effect of increased ammonia flow is to increase the amount of sorption. A linear relation is obtained between the logarithm of the volume sorbed and the logarithm of the ammonia flowrate (figure 16).

Variation of the equilibrium sorption with partial

TABLE I

Weight Sorbed (Grams) at Various Air Rates and Column Lengths

(ammonia rate = 60 cc/min.)

Air Rate (cc/min.)	Column Length (cm.) 5	4	3
0	3.65	-	2.16
100	1.67	1.34	1.00
200	1.08	0.89	0.67
300	0.92	0.76	0.59
550	0.34	-	-
2000	-	-	0.10

TABLE II

Weight Sorbed (Grams) at Various Ammonia Rates and Column Lengths

(air rate = 200 cc/min.)

Ammonia Rate (cc/min.)	Column Length (cm.) 5	4	3
15	0.55	0.43	0.32
42	0.92	0.79	0.59
60	1.08	0.89	0.67
100	1.45	1.18	0.87

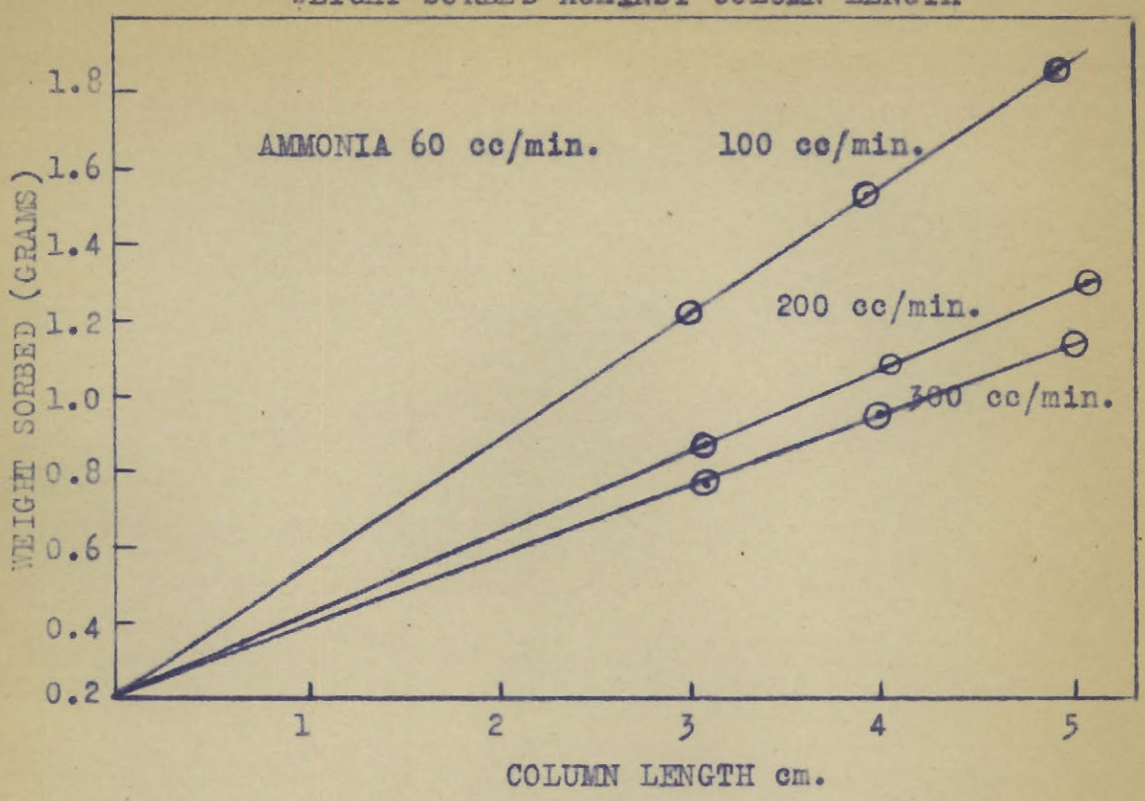

(VARIABLE AIR FLOW)
FIGURE 11.

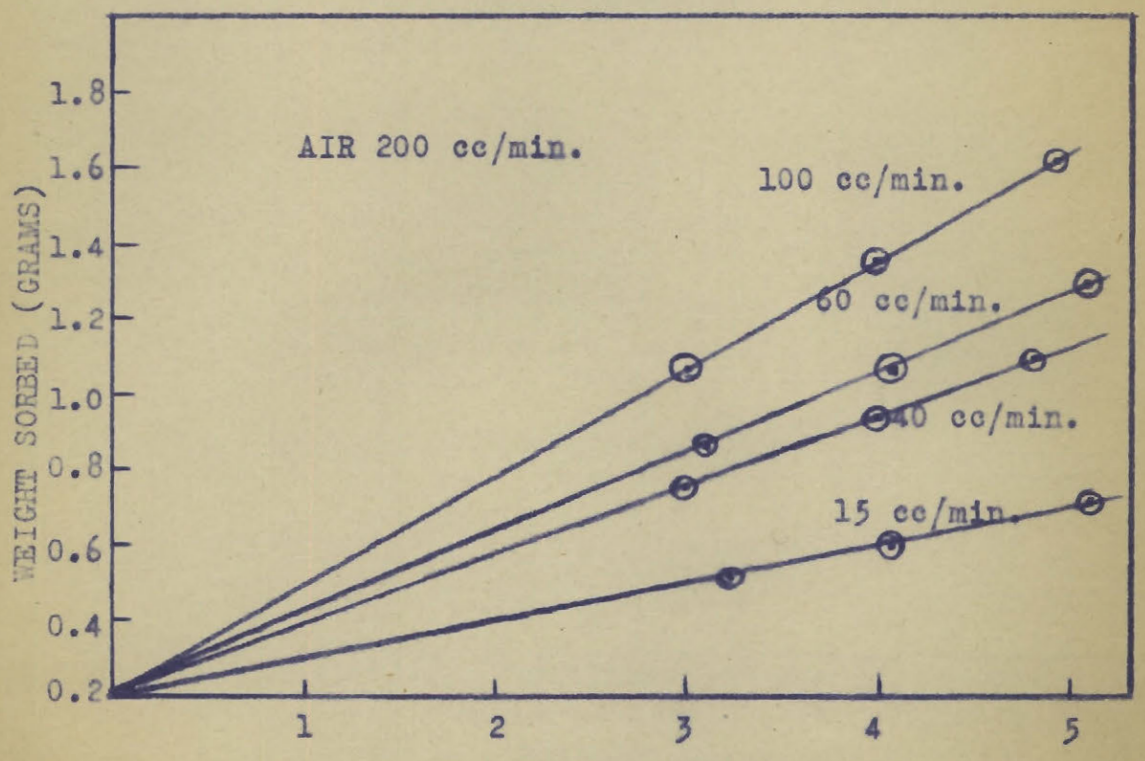

(VARIABLE AMMONIA FLOW)
FIGURE 12

TABLE III

Volume Sorbed Per Gram at Various Air Rates and Column Lengths

(ammonia rate = 60 cc/min.)

Air Rate (cc/min.)	Column Length (cm.) 5	4	3
0	145.	-	146.
100	69.0	68.8	69.2
200	44.0	44.0	45.5
300	38.2	38.2	38.2
550	25.4	-	-
2000	-	-	12.5

TABLE IV

Volume Sorbed Per Gram at Various Ammonia Rates and Column Lengths

(air rate = 200 cc/min.)

Ammonia Rate (cc/min.)	Column Length (cm.) 5	4	3
13.2	19.8	-	-
15	21.2	21.2	21.7
42	38.9	39.4	38.6
60	44.0	44.0	45.5
100	59.4	59.4	58.2

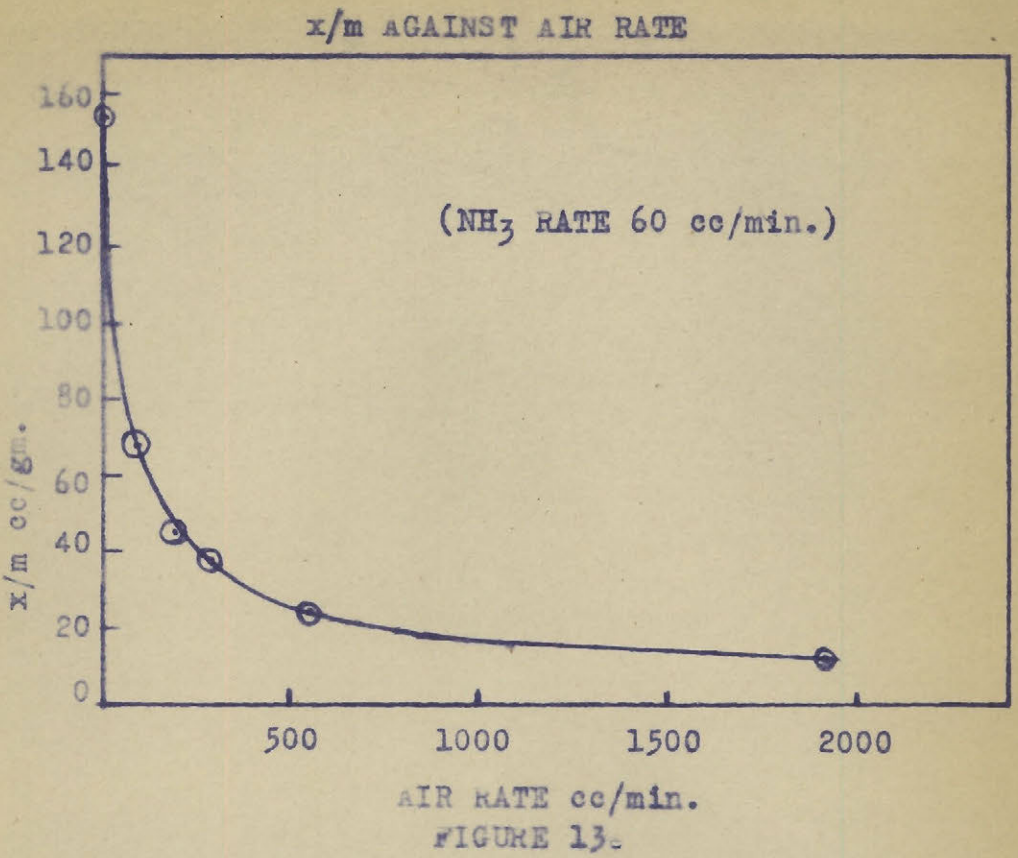

FIGURE 13.

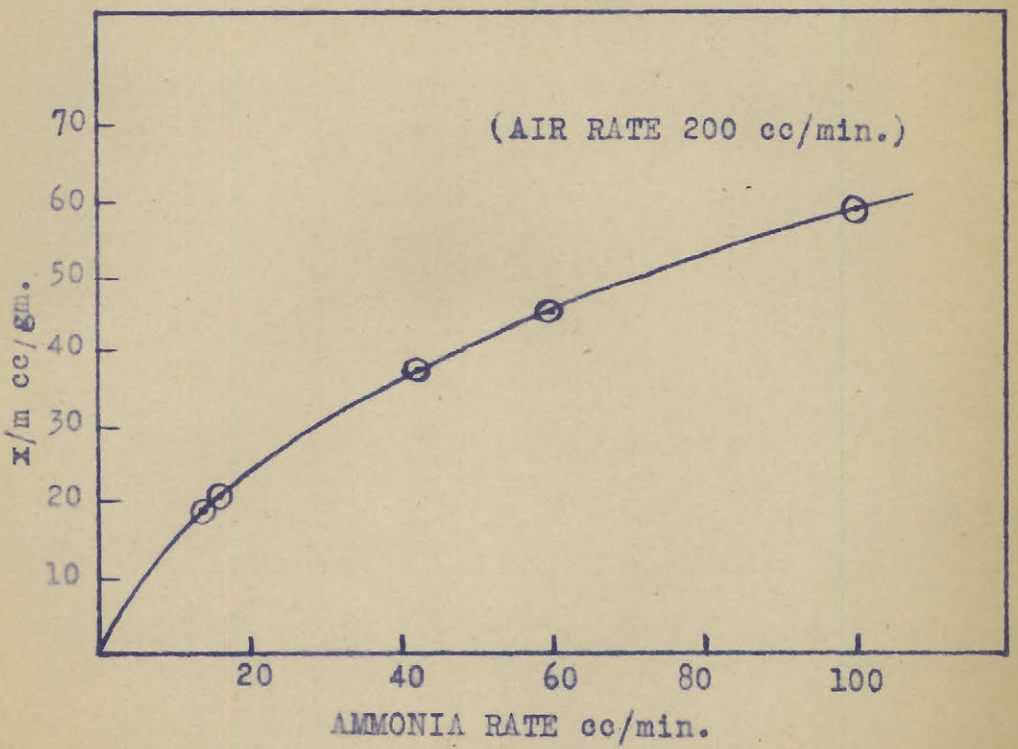

FIGURE 14.
x/m AGAINST AMMONIA RATE

LOG x/m AGAINST LOG AIR RATE

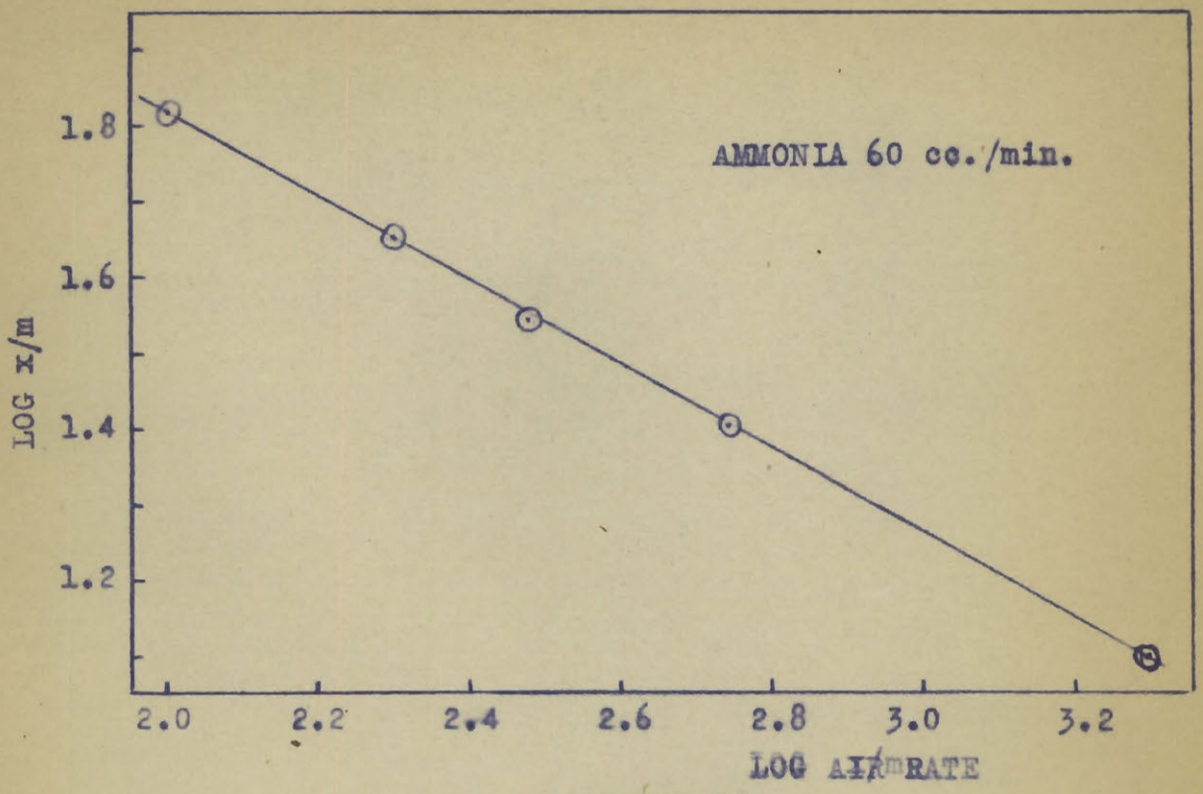

FIGURE 15.

LOG x/m AGAINST LOG AMMONIA RATE

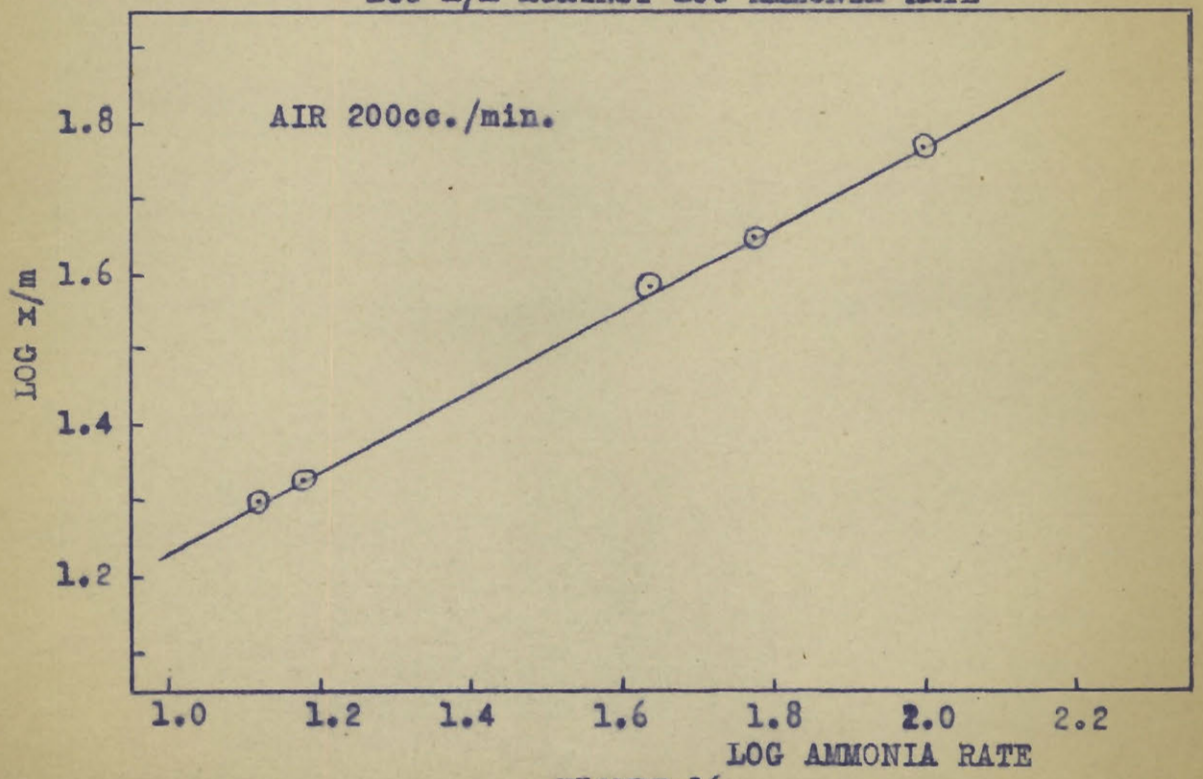

FIGURE 16.

pressure is given by the usual isotherm used in describing the amount of sorption of a gas. In figure 17 the graph of the volume sorbed per gram (x/m) is plotted against the partial pressure. The data are given in table V. Over the range from 50 mm. partial pressure of ammonia to 760 mm. the relation is approximately linear with no indication of attaining a constant value of x/m at higher partial pressures. Below 50 mm. partial pressure the graph curves downward toward the origin as the partial pressure is further decreased. (see enlarged graph 17a). The logarithm of the equilibrium sorption plotted against the logarithm of the partial pressure gives a straight line (figure 18) for partial pressures between 50 and 760 mm. and a second straight line of lower slope for partial pressures below this. Above 50 mm. the Langmuir or Freundlich isotherms may be applied, the equations being:

$$x/m = \frac{0.278P}{1 + 0.000555P}$$

$$x/m = 1.06P^{1/1.31}$$

where x/m is in cc. per gram and P in mm. of mercury. Others have found these isotherms to hold for dynamic systems of: chlorine (16) aqueous solutions (20) and chloropicrin (14).

The linear velocity of the ammonia-air stream, at constant ammonia concentration was found to have no effect on the equilibrium amount of ammonia sorbed. Table VI shows the data for four runs of this nature at total flowrates from 0.16 to 0.79 cm. per second.

TABLE V

Effect of Partial Pressure on Volume of Ammonia Sorbed per Gram

Air Rate (cc/min.)	NH_3 Rate (cc/min.)	Part.Press.NH_3 (mm. Hg)	Volume Sorbed (cc/gm.)
0	60	760	145.
54	200	465	103.
150	97	300	67.2
100	60	285	69.0
200	100	254	59.4
200	60	175	44.8
200	42	134	38.9
100	20	132	38.2
500	100	132	38.2
300	60	127	38.0
550	60	75	27.5
200	15	53	21.2
2,000	60	22.1	12.5
3,270	60	13.7	11.2
3,270	17	3.9	4.1
3,270	14.7	3.4	5.7
3,270	13.2	3.1	5.6
3,270	3.4	0.79	2.3
3,270	1.6	0.37	1.1

x/m AGAINST PARTIAL PRESSURE OF AMMONIA

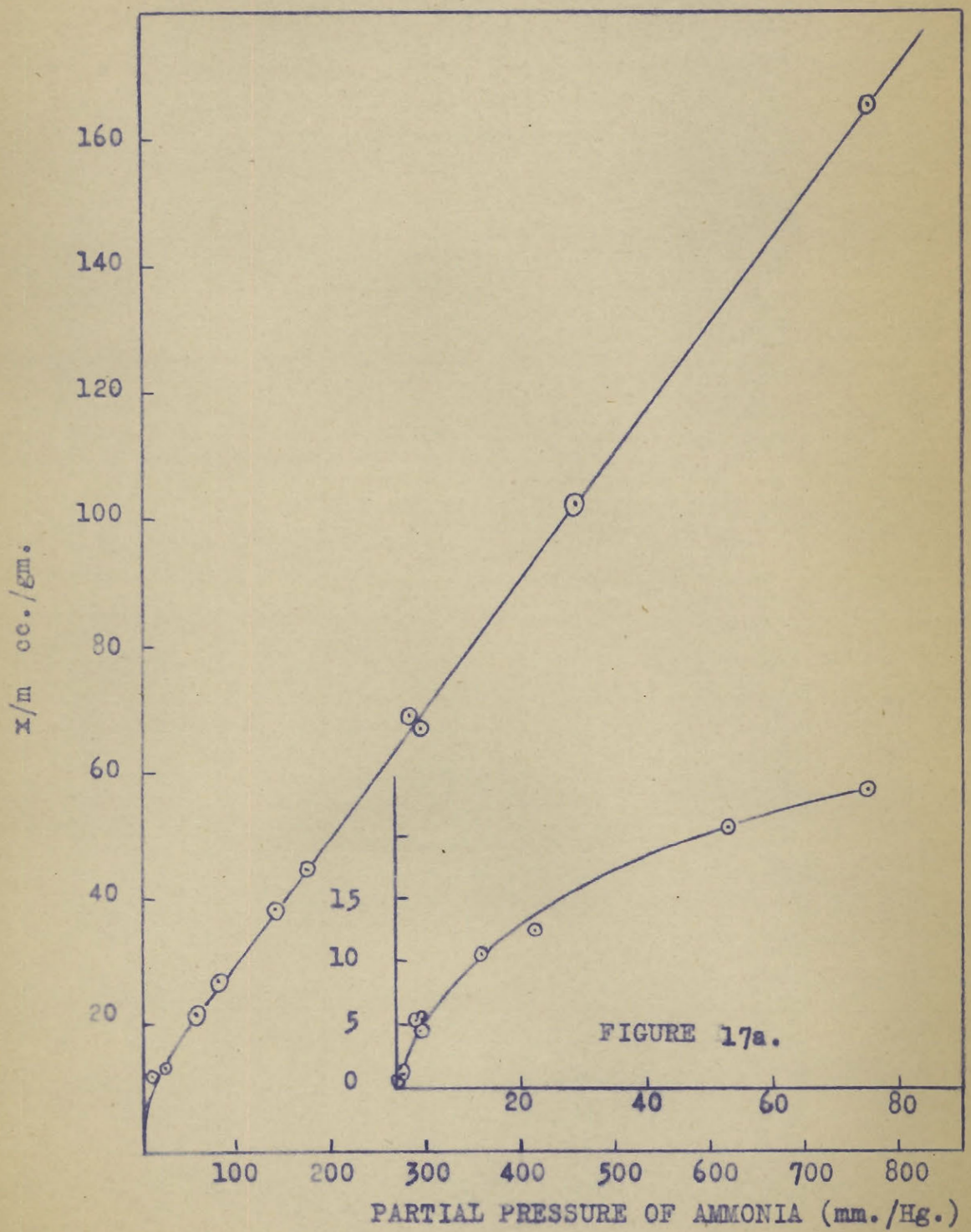

FIGURE 17a.

FIGURE 17

LOG x/m AGAINST LOG PARTIAL PRESSURE

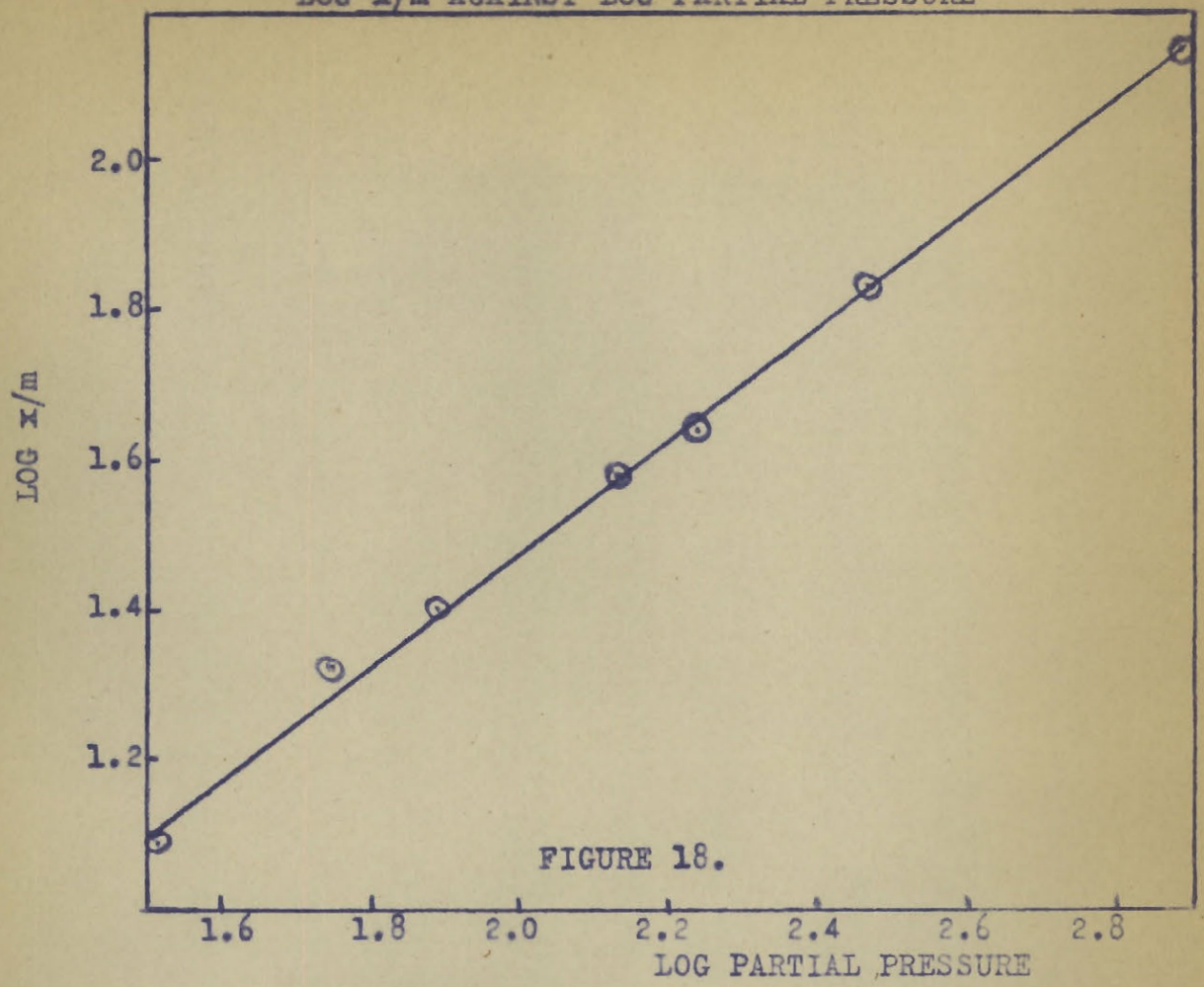

FIGURE 18.

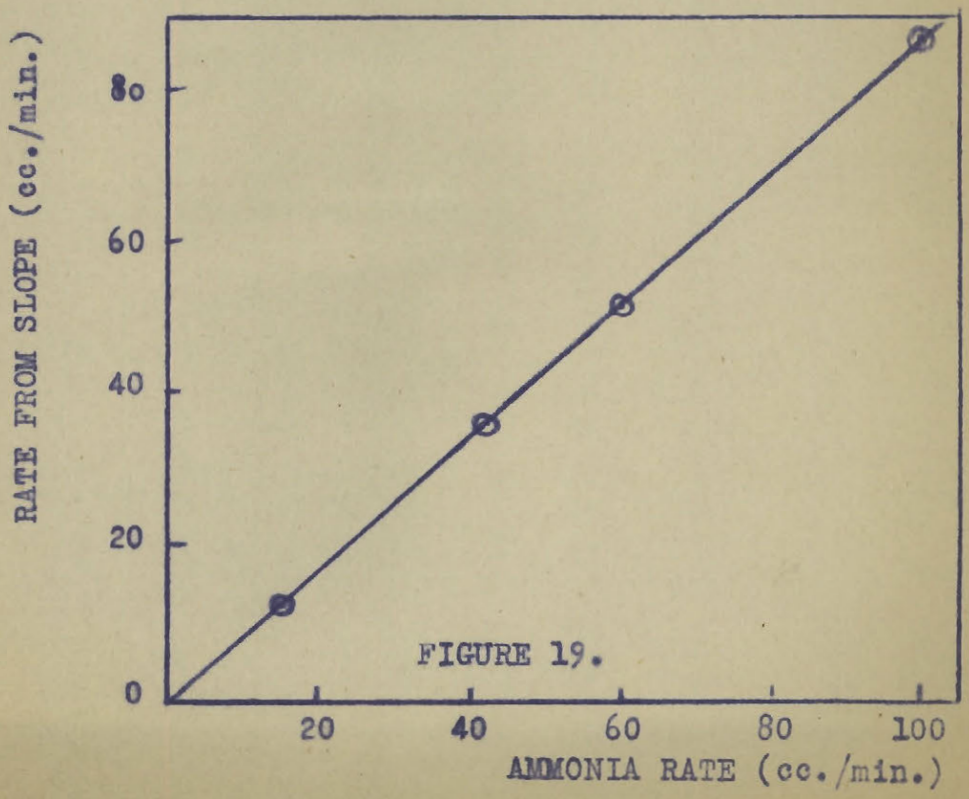

FIGURE 19.

The slopes of the linear portion of the weight-time curves should give a measure of the rate of sorption during this time. If all of the ammonia supplied is being sorbed (as should be the case) the slope would be equal to the ammonia flowrate if expressed in appropriate units. It was found, however, that the rate of sorption in cc. per minute was lower than the ammonia flowrate (see table 7). A graph of this slope against the ammonia flowrate is shown in figure 19. Further discussion of this is postponed until the analytical results and desorption studies.

TABLE VI

Effect of Total Velocity on Equilibrium Sorption (at Constant Composition)

Conc. Ammonia %	Flow rate of Air/Ammonia (cc/min.)	Total Flow rate (cm/sec.)	Amount Ammonia Sorbed gms.	cc/gm.
16.7	120	0.16	0.92	11.2
16.7	242	0.32	0.92	11.4
16.5	360	0.48	0.92	11.2
16.7	600	0.79	0.95	11.2

TABLE VII

Calculated Slopes at Various Ammonia Rates

NH_3 Rate (cc/min.)	Slope (cc/min.)
13	10.6
15.7	13.8
42	36.5
60	51.5
100	87.5

2. Analytical data

The concentration of ammonia in the escaping gases is shown as a function of time in figures 20 - 23 for various conditions. Figures 20, 21, 22 and 23 show the variation with column length, air flowrate, ammonia flowrate and total linear velocity respectively. It is seen that no ammonia appears in the effluent gases until the service time is reached, indicating complete sorption of the ammonia supplied in the entering air stream. After the service time, the concentration of ammonia in the escaping gases increases rapidly at first, but approaches a constant value when the charcoal bed is saturated. In these graphs the concentration is expressed as a percent of the total flowrate of the ammonia-air stream entering the charcoal bed.

On the same graphs is plotted the differential amount sorbed as a function of time. This was obtained by graphical differentiation of the weight-time curves plotted in figures 9 and 10. When expressed in the same units as the concentration of the ammonia in the escaping gases, it is a complementary curve to that of the analysis of the effluent stream, representing the percent of the total entering stream which is being removed by the charcoal at any time. It therefore is constant until the service time, and thereafter decreases, approaching zero when the charcoal bed is saturated.

If the escaping concentration of ammonia in the

effluent stream is related to time by plotting the logarithm of $1/c$ against time as in figure 24 a curve is obtained in contrast to the predictions of Danby et al who find a linear relation from their equation:

$$c = \frac{c_o}{e^{-kc_o T}(e^{kN_o 2/L} - 1) + 1} \qquad (xii)$$

A linear relation is obtained, however, between the logarithm of $1/c$ and the reciprocal of the time (figure 25) if the time is measured from the service time. The data for figures 24 and 25 are given in table VIII.

It may be noted that the sorption as indicated by the constant differential amount sorbed does not correspond to the ammonia flowrate as measured by the analysis of the escaping gases when the charcoal is saturated (figures 20 -23). This was found to be due to air displaced from the charcoal by the ammonia, and will be discussed later under the desorption studies which confirmed this behavior.

The escaping concentrations calculated from the differential sorption curves would not, then, represent the true concentration of ammonia in the effluent stream. However, the deviation is not appreciable since curves of escaping concentration against time practically coincide. The apparent weight of ammonia on the charcoal is less than that actually sorbed by the weight of the air displaced.

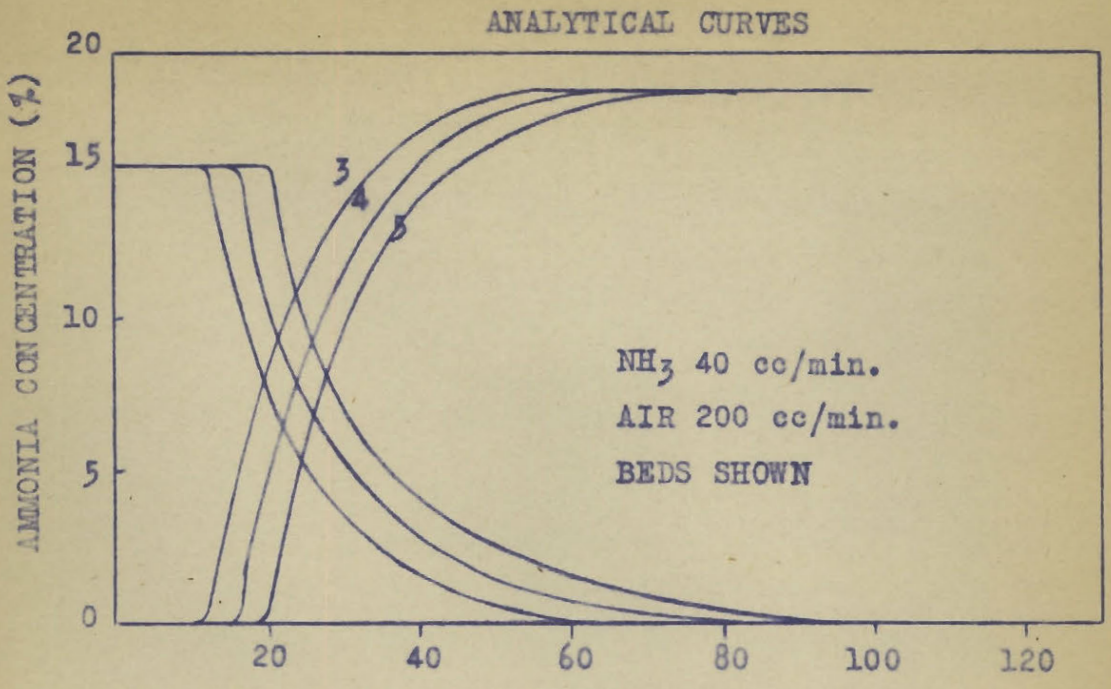

EFFECT OF BED LENGTH

FIGURE 20

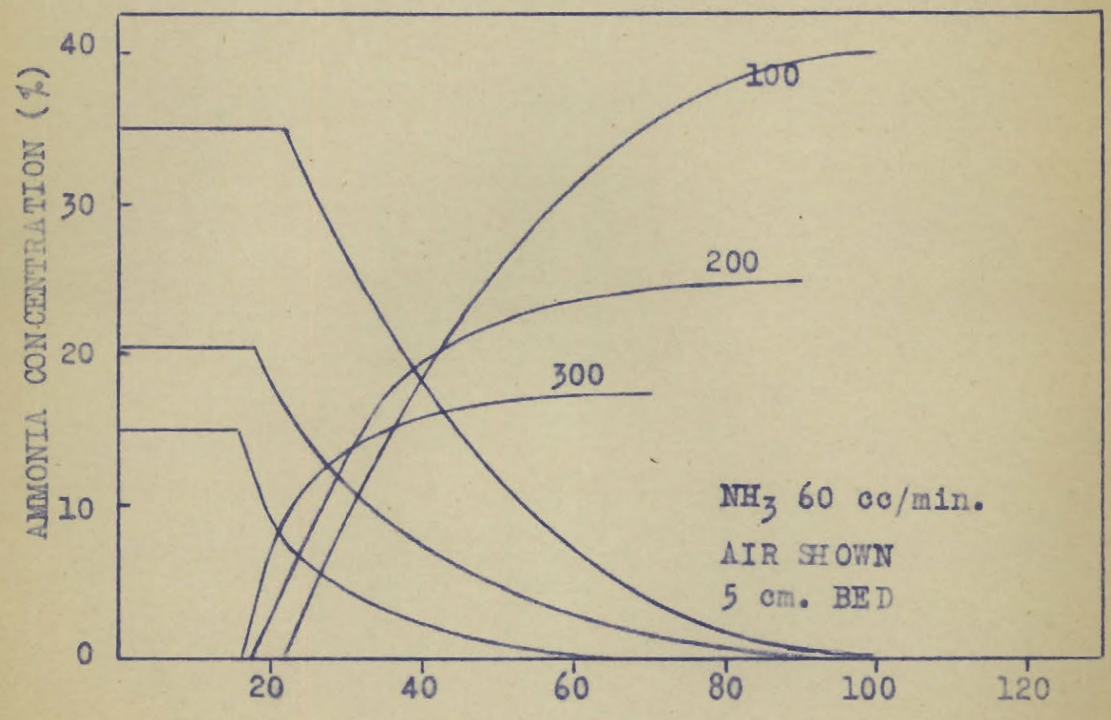

EFFECT OF AIR RATE

FIGURE 21.

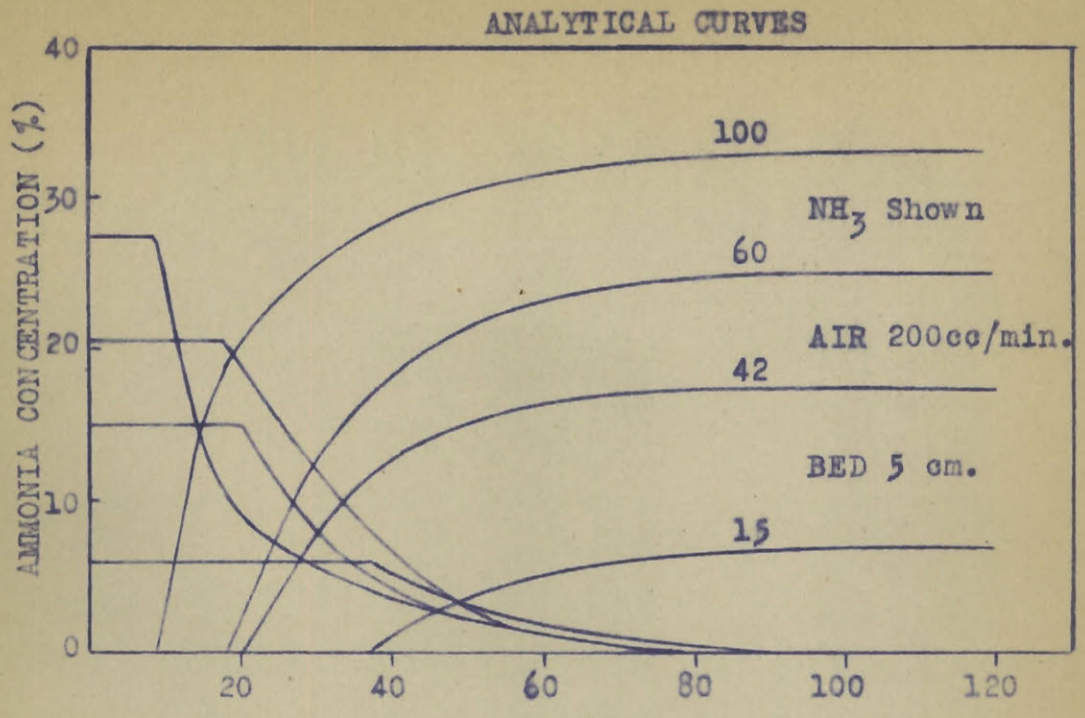

EFFECT OF AMMONIA RATE

FIGURE 22.

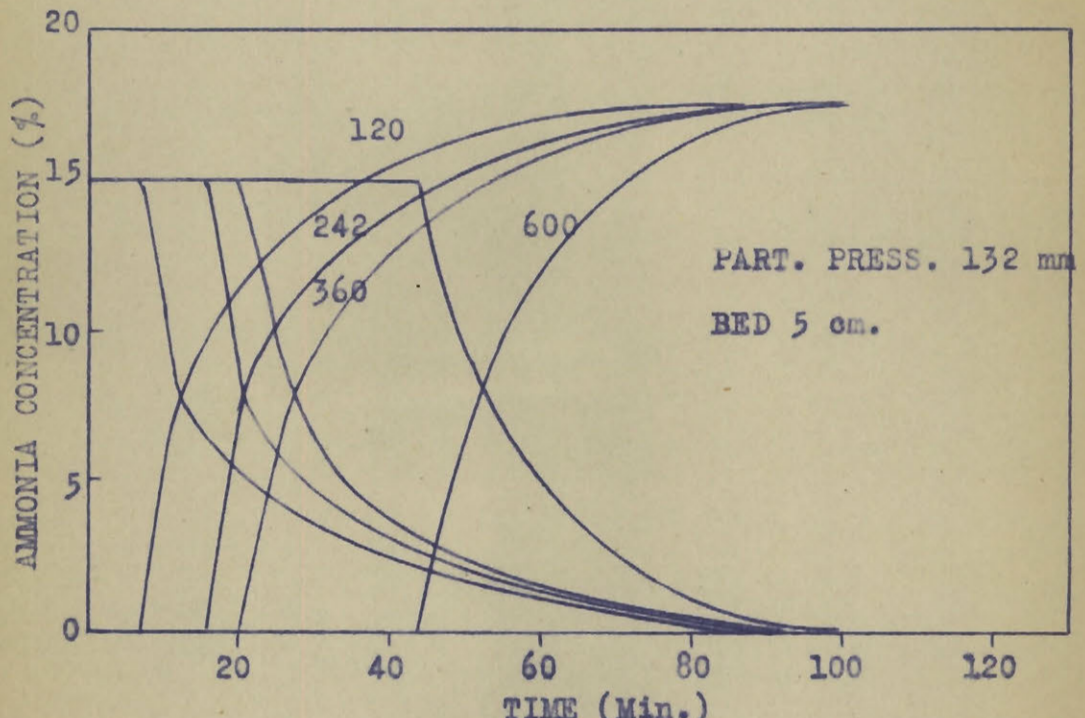

EFFECT OF FLOWRATE

FIGURE 23.

TABLE VIII

Escaping Concentration as a Function of Time

Time after S.T. Min.	1/T	Concentration C%	log 1/C
4	.250	4.3	$\bar{1}$.366
10	.100	10.2	$\bar{2}$.992
14	.0712	12.0	$\bar{2}$.921
19	.0526	13.5	$\bar{2}$.870
25	.0400	15	$\bar{2}$.824
30	.0333	15.6	$\bar{2}$.807
40	.0250	16.3	$\bar{2}$.788
50	.0200	16.8	$\bar{2}$.775
60	.0167	17.0	$\bar{2}$.770
80	.0125	17.4	$\bar{2}$.760

ESCAPING CONCENTRATION

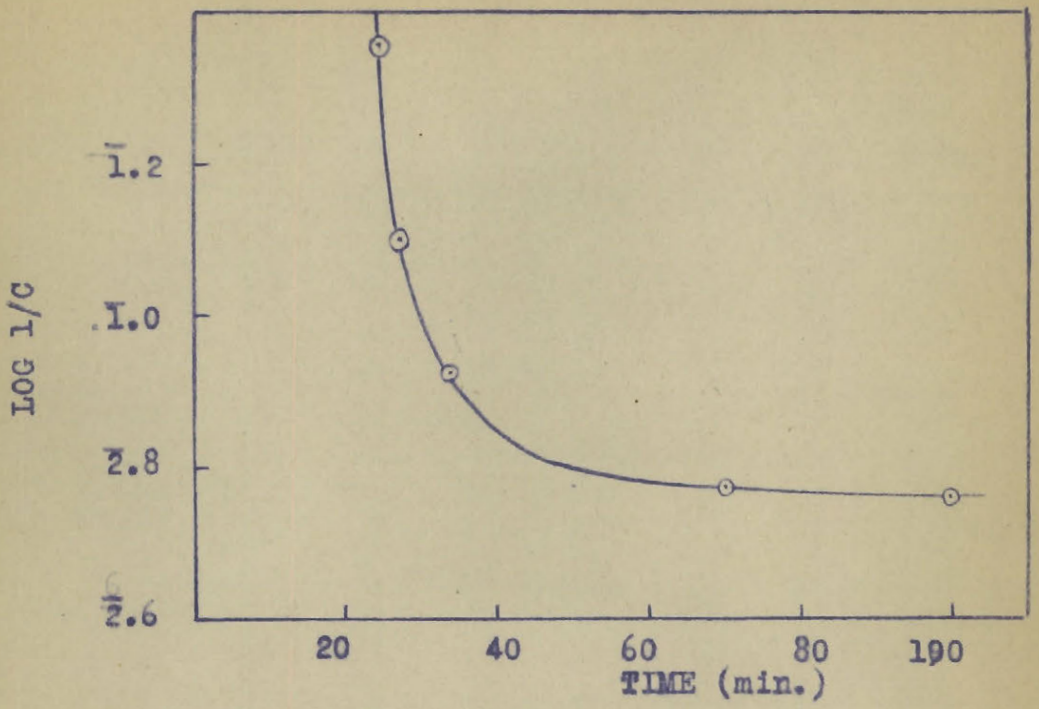

FIGURE 24.

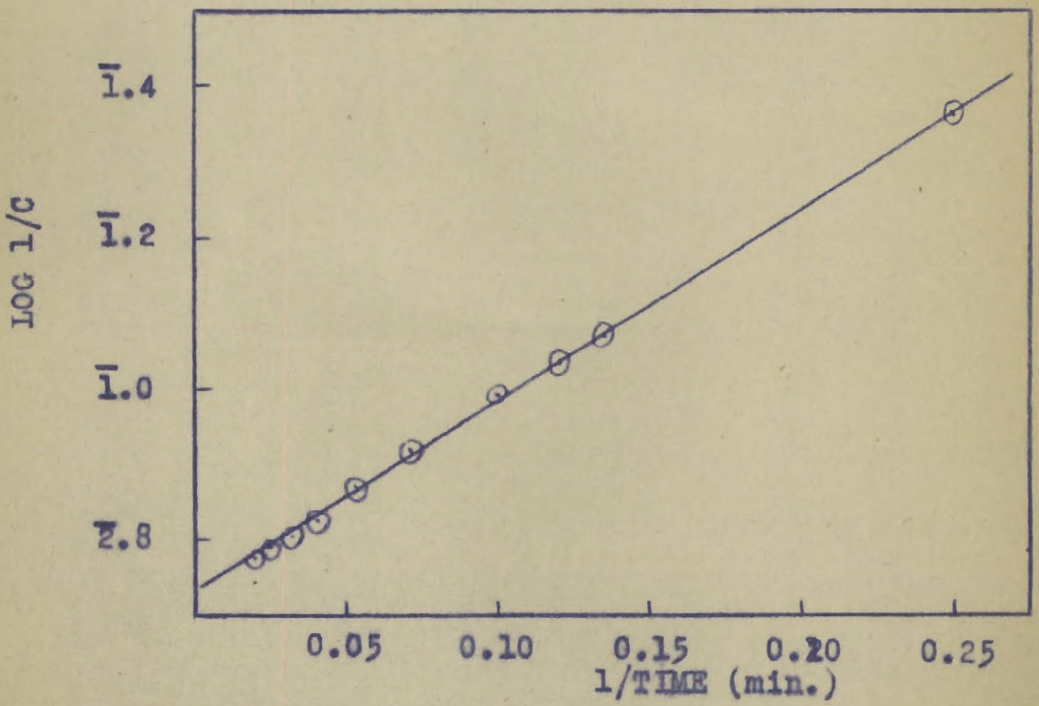

FIGURE 25.

3. Service Time Data

The service time was determined in these investigations as the time when the charcoal ceased to be 100% efficient in removing the ammonia from the air stream. This was the time at which the weight-time curves first deviated from the linear relation. Service times calculated on this basis agreed within 2% of those determined using a phenolphthalein test paper in the effluent gas line. The deviation between the weight and the analytical results would have no effect on the service time since, if the true weight of ammonia sorbed were plotted against time, the amount of ammonia taken up by the charcoal when the graph deviates from the linear relation would be greater, but the time at which this occurs would be unchanged.

The service times at various column lengths and rates of air and ammonia flow are given in tables IX and X and are shown graphically as a function of these variables in figures 26 - 31. A straight line is obtained when service time is plotted against column length, (figures 26 and 27) which if extrapolated cuts the column length axis at a positive length. This intercept is the "critical" or "dead" length mentioned in the introduction. It was not possible to test the behavior at very short bed lengths since ammonia is not appreciably sorbed, so that it cannot be stated whether or not the graph curves in toward the origin at short column lengths, as found by Dubinin et al

TABLE IX

Service Times at Various Air Rates and Column Lengths

(ammonia rate = 60 cc/min.)

Air Rate (cc/min.)	Column Length (cm.) 5	4	3
0	45	-	2.8
100	22.5	17.5	12.5
200	16	12	8.5
300	14	11	8

TABLE X

Service Times at Various Ammonia Rates and Column Lengths

(air rate = 200 cc/min.)

NH_3 Rate (cc/min.)	Column Length (cm) 5	4	3
15	30	23	17
42	20.5	16	11.5
60	16	12	8.5
100	8	6	4

SERVICE TIME AGAINST COLUMN LENGTH

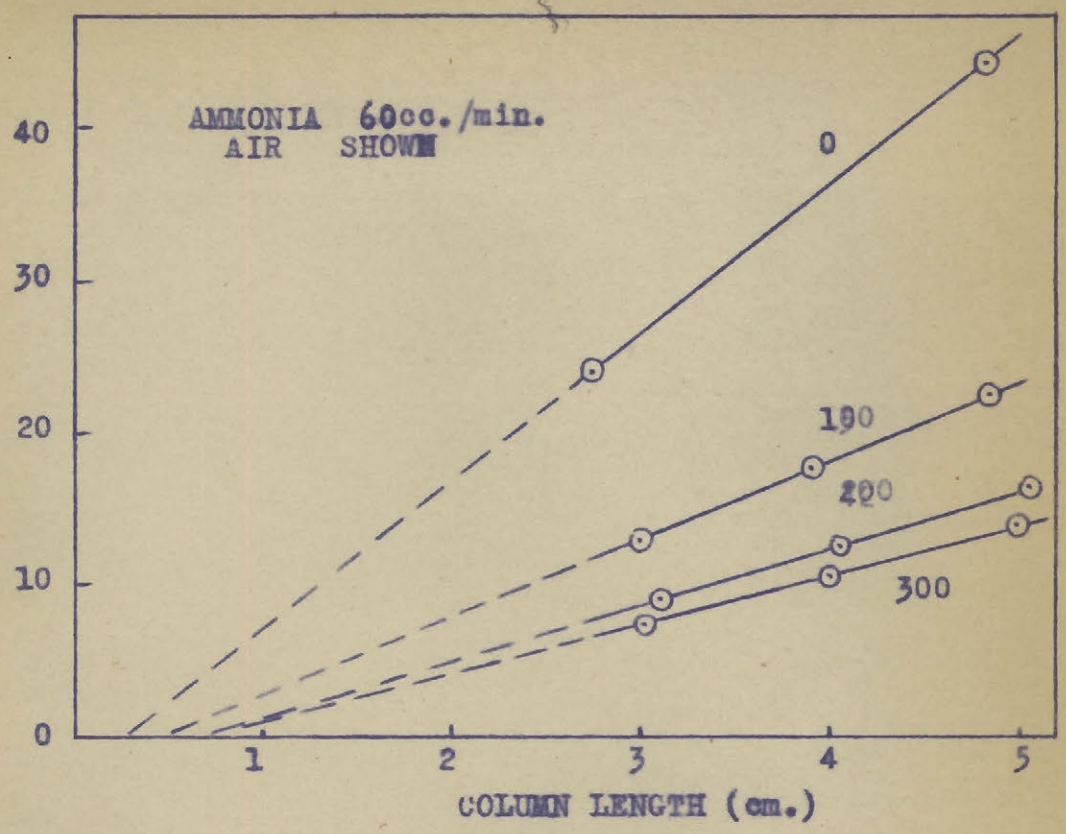

FIGURE 26.

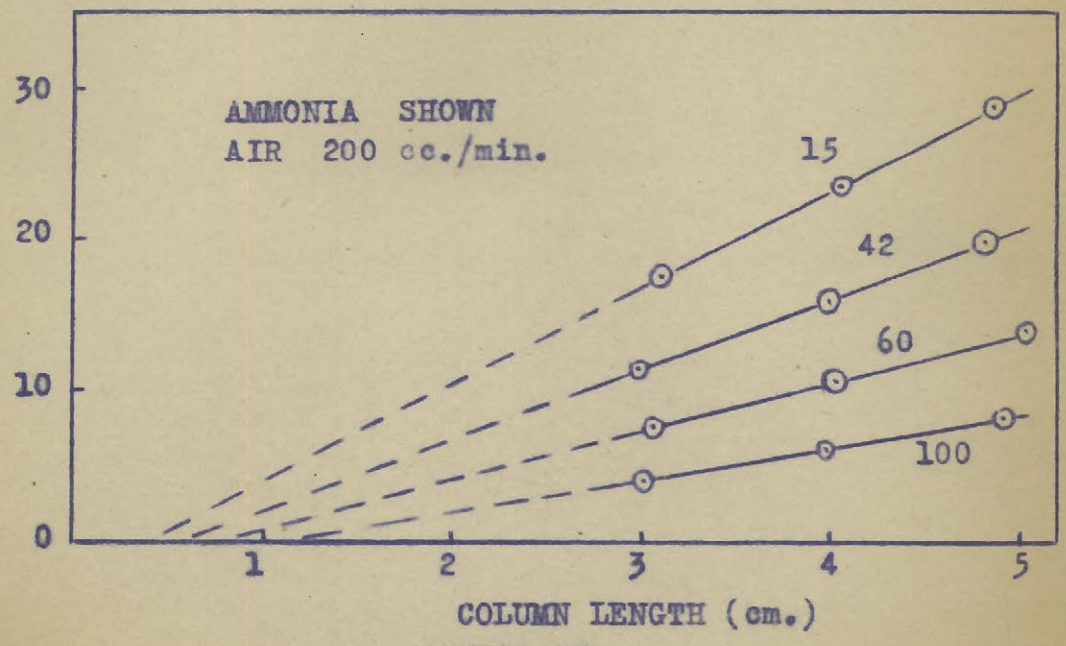

FIGURE 27.

(17) and Mecklenberg (14). At various concentrations these extrapolated straight lines appear to converge to a point below the origin. No theoretical significance is attached to this fact however. The linear relation which was found to hold agrees with the theories of Danby et al and Mecklenberg which give the equations:

$$T' = \frac{N_o}{C_o L}\left[\lambda - \lambda_c\right]$$

$$T' = \frac{kQ}{VC_o}\left(L - h\right)$$

respectively. The slope of these curves is the coefficient of protective action used by Shilow (16) and Dubinin (21) in their equations for the dead length and service time (equations ix and xiv).

Since the service time thus varies with column length it is important in discussing its variation with flow-rate, concentration etc., that comparable runs be done at exactly equal column lengths. This is impractical so that a method of calculating "corrected" service times was devised. It consisted of linear interpolation of the service time-column length graphs to the nearest integral column length i.e. to 3, 4 or 5 cm. $\pm$ 0.01 cm. It is these corrected service times which have been plotted in figures 26 - 31 and recorded in tables IX and X.

Figure 28 shows the effect on the service time of varying the rate of air flow at constant butane flowrate.

The service time using 60 cc. per minute of pure ammonia is quite high but decreases rapidly as an air stream is added and increased but reaches an almost constant value as the air flowrate is increased above 300 cc. per minute. When the logarithm of the service time is plotted against the logarithm of the air flowrate as in figure (29) a straight line results. The service time decreases also as the ammonia flowrate is increased at constant air rate as in figure (30), but the logarithm of the service time decreases linearly with the ammonia flowrate (figure 31). From the slopes of the logarithmic curves it may be noted that the service time is much more dependent on the ammonia flowrate than on the air flowrate since the service time decreases exponentially with the ammonia rate but only with the 0.4 power of the air flowrate.

At constant concentration of ammonia in the entering gas, the service time depends upon the reciprocal of the flowrate as shown in table XI and figure 32. Extrapolation of the straight line so obtained intercepts the flowrate axis, corresponding to a "critical" flowrate above which there would presumably be immediate breakdown of the charcoal bed, at this particular concentration. Experimental proof of the existence of this critical flowrate is, however, lacking.

At constant flowrate the dependence of the service time on the initial concentration of the ammonia in the entering stream was studied. The data are given in table XII.

EFFECT OF AIR RATE ON SERVICE TIME

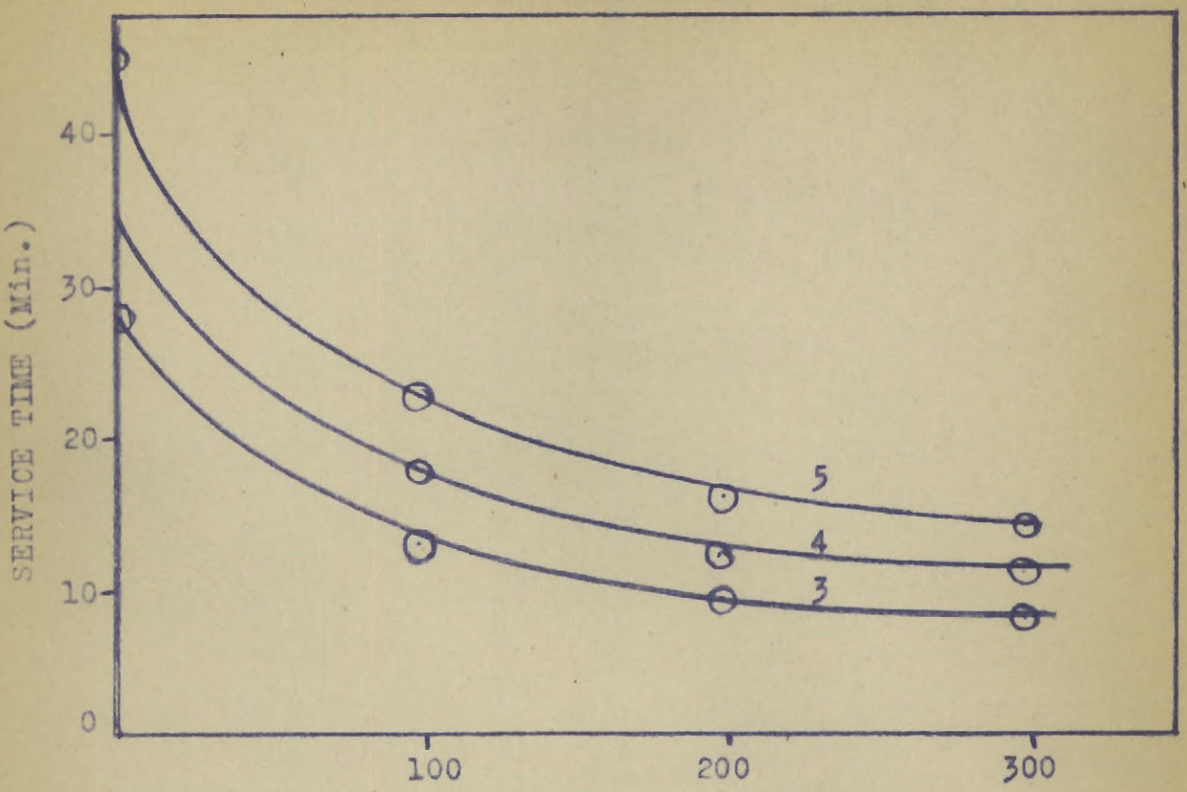

FIGURE 28.

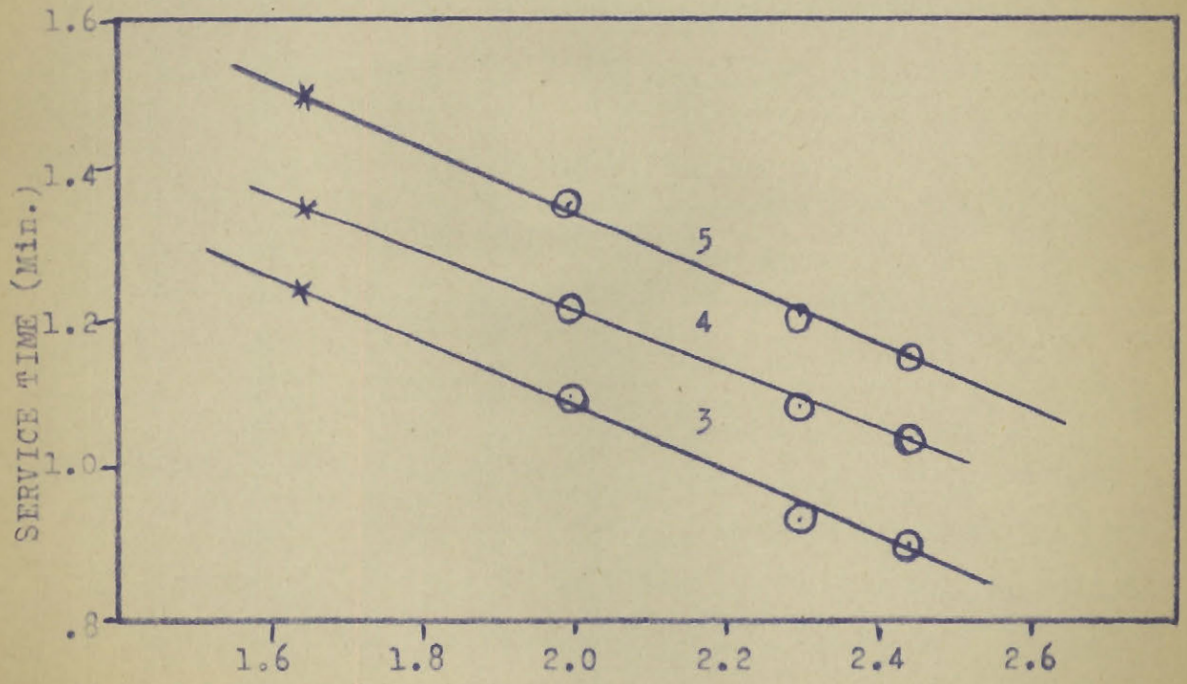

FIGURE 29

EFFECT OF AMMONIA RATE ON SERVICE TIME

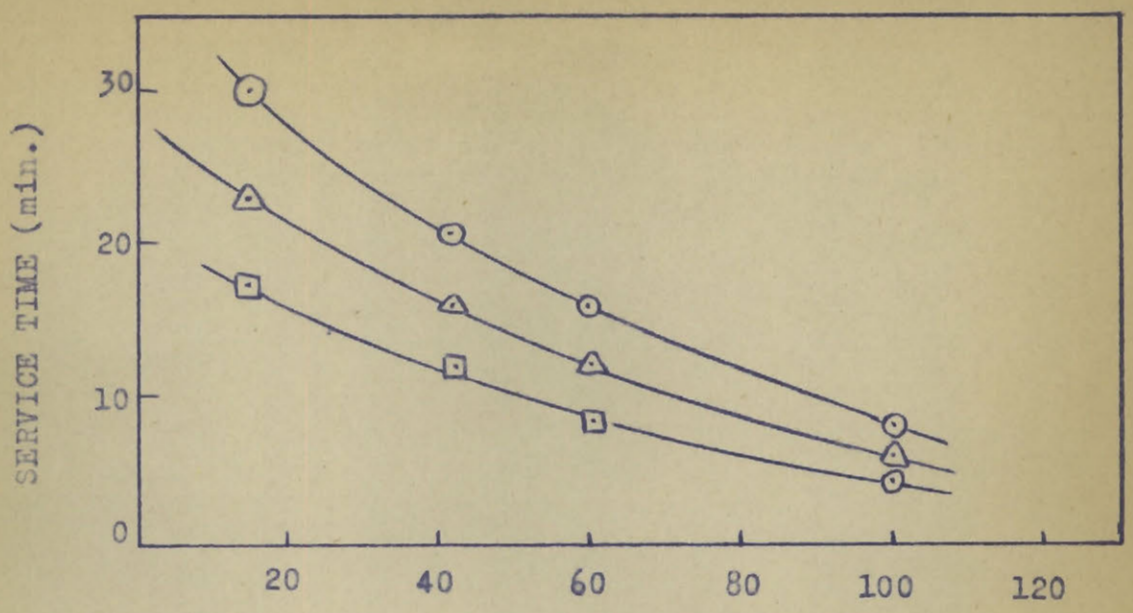

FIGURE 30

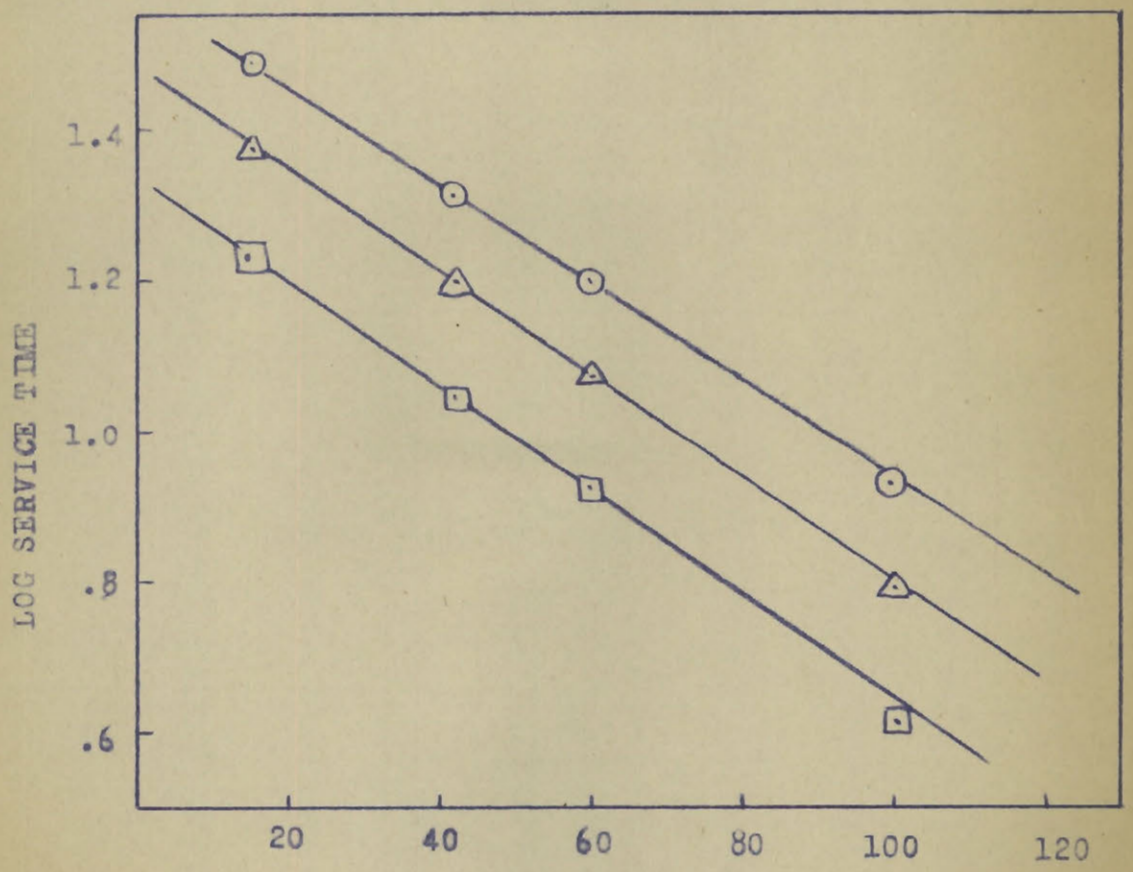

FIGURE 31

A linear relation was found to hold (figure 33) between the service time and the reciprocal of the initial concentration over the range of ammonia concentrations of 17 - 40%, but which fell off rapidly at lower concentrations. Danby et al predicted a linear relation should be obtained at low, but not at high concentrations from the formula:

$$T' = \frac{1}{kC_o}\left[\frac{kN_oX}{L} - \ln\frac{C_o}{C'}\right]$$

where $\ln C_o/C'$ was assumed negligible at low concentrations and N_o independent of C_o. These assumptions seem therefore not to be completely justified. Shilow et al have found a linear relation for chlorine over the concentration range 0.66 to 1.36%.

An illuminating way of showing this relation is to plot service time times initial concentration against the initial concentration (figure 34). It is readily seen over what range of concentration the relation:

$$C_o \times T = \text{constant}$$

holds. Arnell (2) has also noted the increase of the product $C_o \times T$ from zero until it reaches a constant value.

TABLE XI

Effect of Flowrate on Service Time at Constant Composition

(cross section of cell = 12.6 $cm.^2$)

Air Rate (cc/min.)	NH_3 Rate (cc/min.)	Flowrate (cc/min.)	Flowrate (cc/sec.)	Service time min.
100	20	120	0.16	42
200	42	242	0.32	20.5
300	60	360	0.48	14
500	100	600	0.79	6

TABLE XII

Effect of Concentration on Service Time

(flowrate = 250 cc/min.)

Air Rate (cc/min.)	NH_3 Rate (cc/min.)	C_o %	Service time min.	$1/C_o$
150	97	39.2	9	0.0254
200	54	21.2	17	0.0470
200	60	23.0	16	0.0435
200	42	17.4	20.5	0.0576
235	19.5	7.65	22	0.131

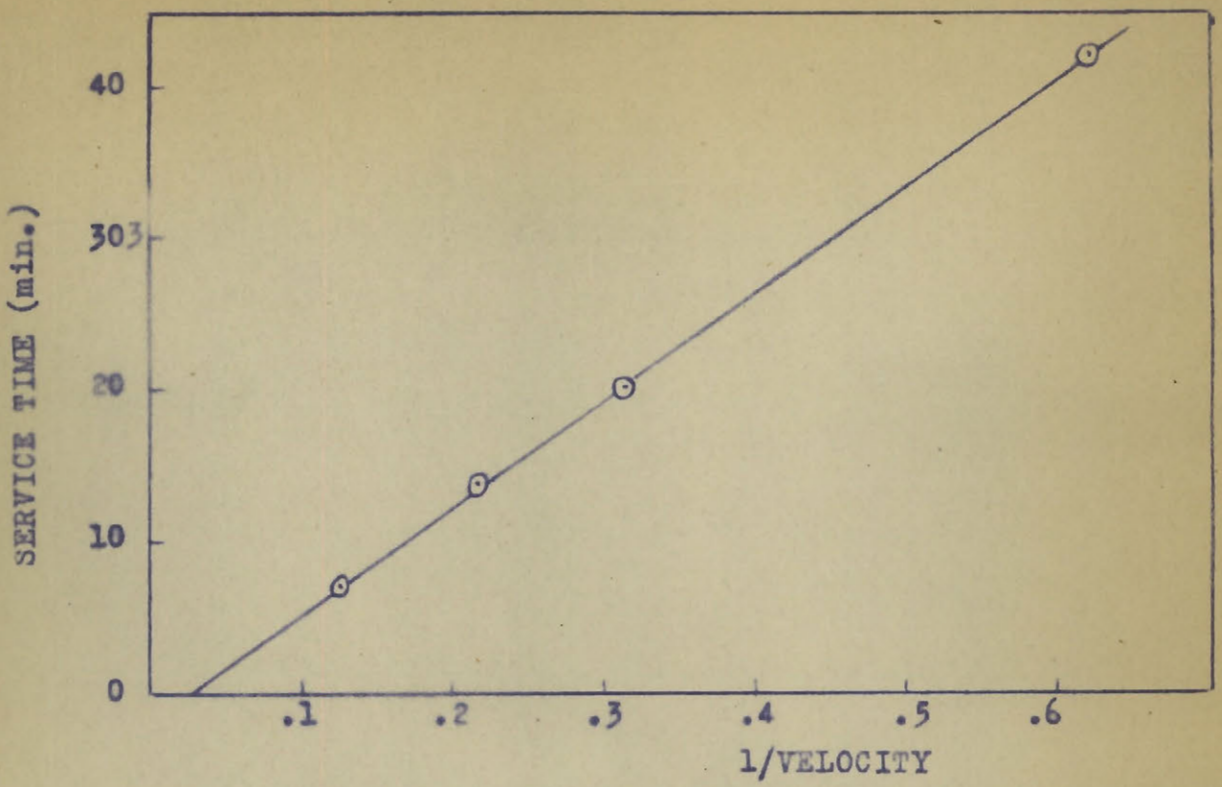

EFFECT OF FLOWRATE ON SERVICE TIME

FIGURE 32.

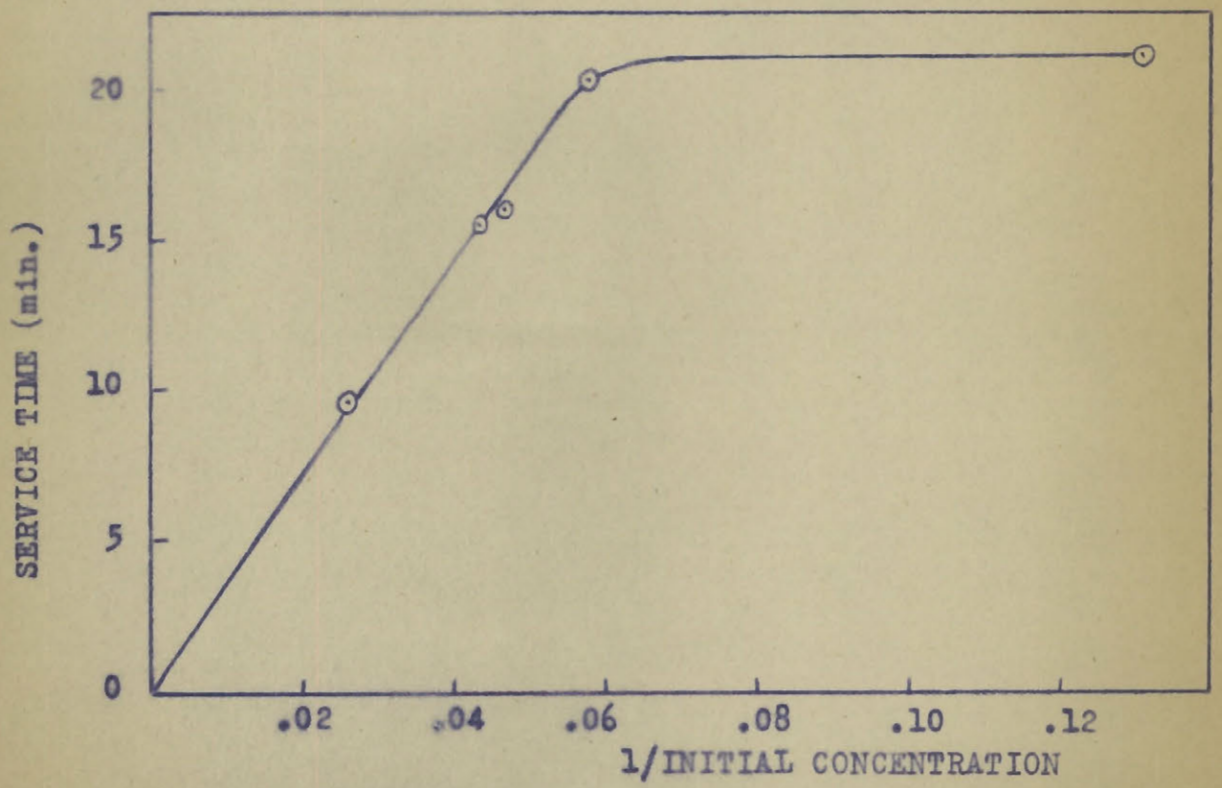

EFFECT OF INITIAL CONCENTRATION ON SERVICE TIME

FIGURE33.

4. Critical lengths

These are determined by the intercept of the extrapolated service time - column length curves. Roughly this "critical" or "dead" length increases with increase in the air flowrate at constant ammonia rate, and with increased ammonia rate at constant air rate similar to the decrease of the service time with these variables. The long extrapolation necessary in the curves shown in figures 26 and 27, makes calculation of numerical values for the critical length rather inaccurate.

EFFECT OF INITIAL CONCENTRATION
ON SERVICE TIME

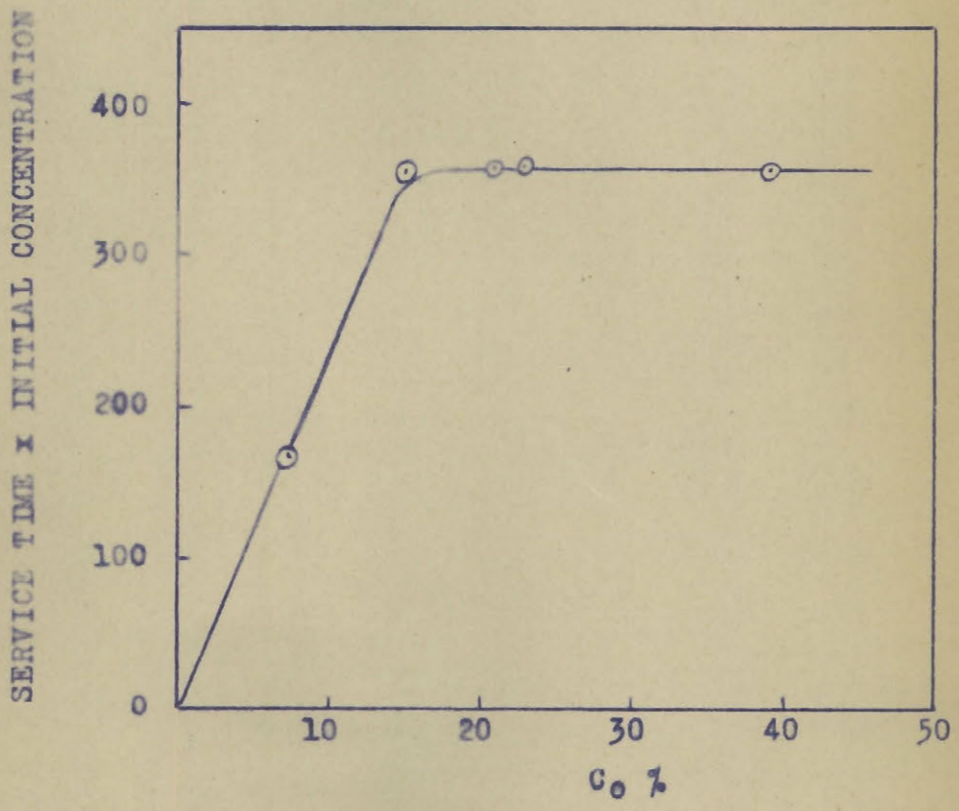

FIGURE 34.

5. Temperature Data

The temperature rise in the bottom (T_2) and third from the bottom (T_1) centimeter charcoal layers is shown as a function of time for a number of typical cases in figure 34. The temperature rises rapidly in both layers at first to a maximum value and falls more slowly as the charcoal bed cools to room temperature. The maximum temperature rise in the upper layer was found to be greater than that in the bottom layer, presumably due to heat losses by greater contact of the bottom layer with the surroundings. Table XIII and figure 36 show that the maximum temperature rise is a linear function of the ammonia flowrate at a constant air flowrate. An increase in the air flowrate at constant ammonia flow has a slight cooling effect as shown in figure 37. The relation between the maximum temperature rise and the linear flowrate is shown in table XIV and figure 38. The increase with increasing flow is due to the increased amount of ammonia passing through the bed in unit time. The cooling effect of the increased air flow is also obvious from the graph.

Since sorption is affected greatly by change in the temperature at which it takes place, it seems important to discuss the effect of the temperature rise on the shapes of the weight-time curves, the escaping concentration and the service time. The service time should be decreased where there is an appreciable temperature rise due to the sorption, since the length of the working layer would be increased due to the decreased sorption capacity of the charcoal, thus

TABLE XIII

Maximum Temperature Rise

NH_3 Rate	Air Rate (cc/min.)			
cc/min.	0	100	200	300
15	-	-	4.5	-
42	-	-	16.	-
60	25.5	24.5	21.	19.5
100	-	-	32.	-

TABLE XIV

Effect of Flowrate on Maximum Temperature Rise

Flowrate				
cc/min.	120	242	360	600
T_1	10.5	19	21	27
T_2	9	12.5	16	19

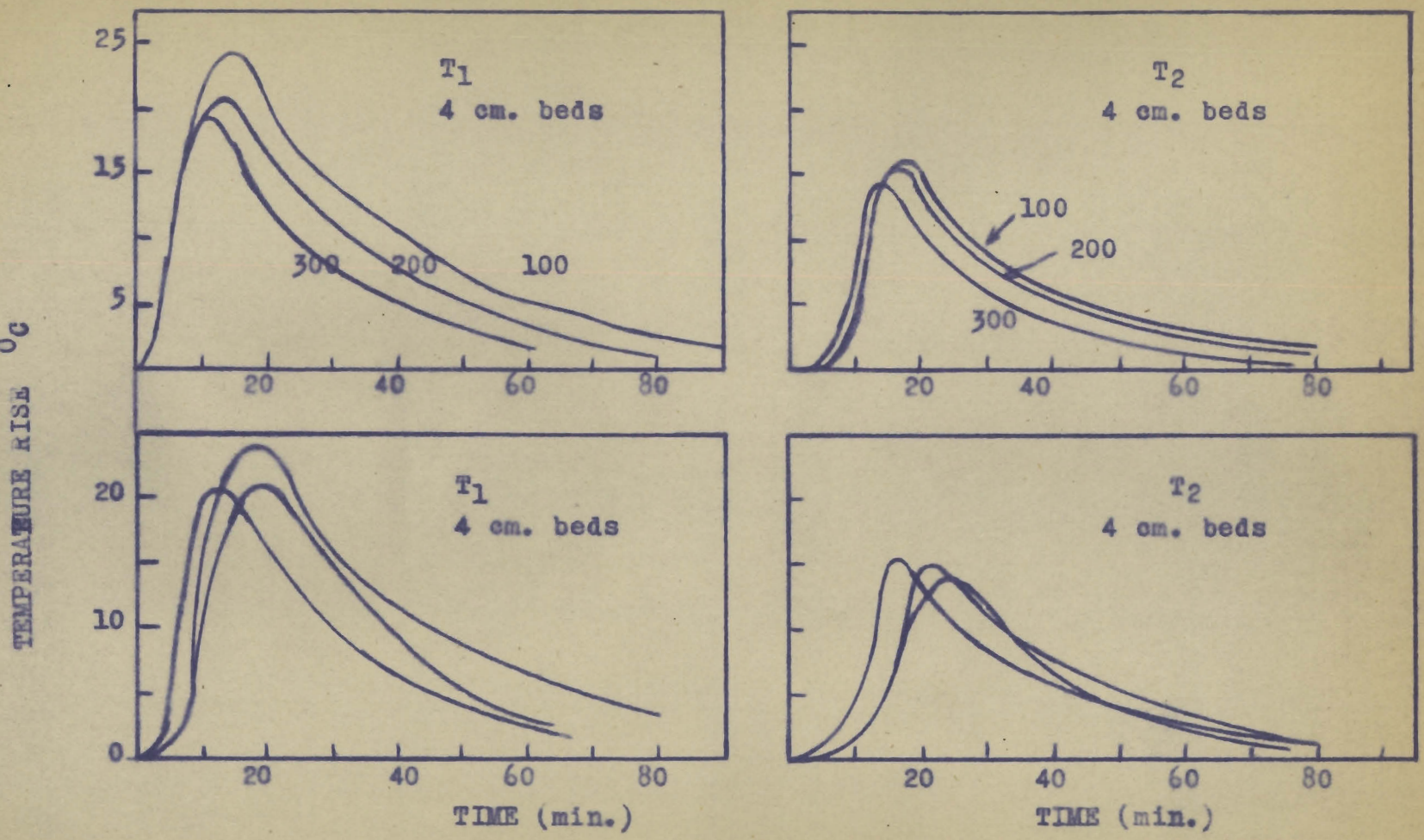

TYPICAL TEMPERATURE CURVES
AMMONIA 60 cc./min
AIR SHOWN

FIGURE35.

MAXIMUM TEMPERATURE RISE DATA

EFFECT OF AMMONIA RATE

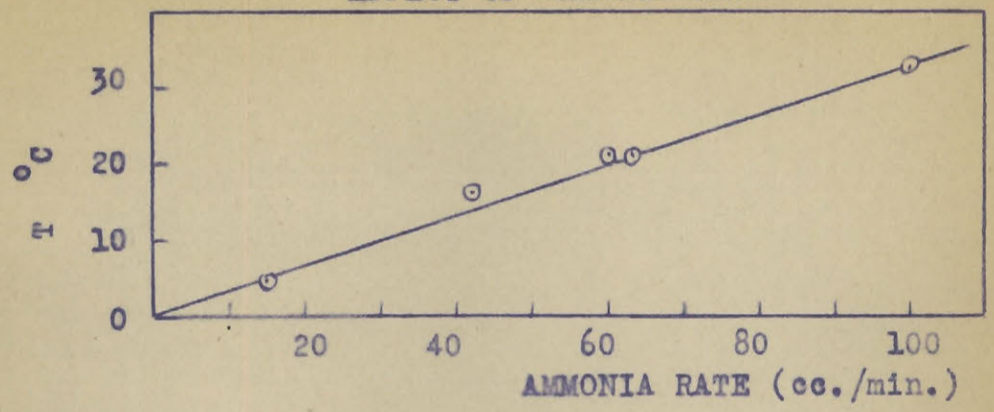

FIGURE 36.

EFFECT OF AIR RATE

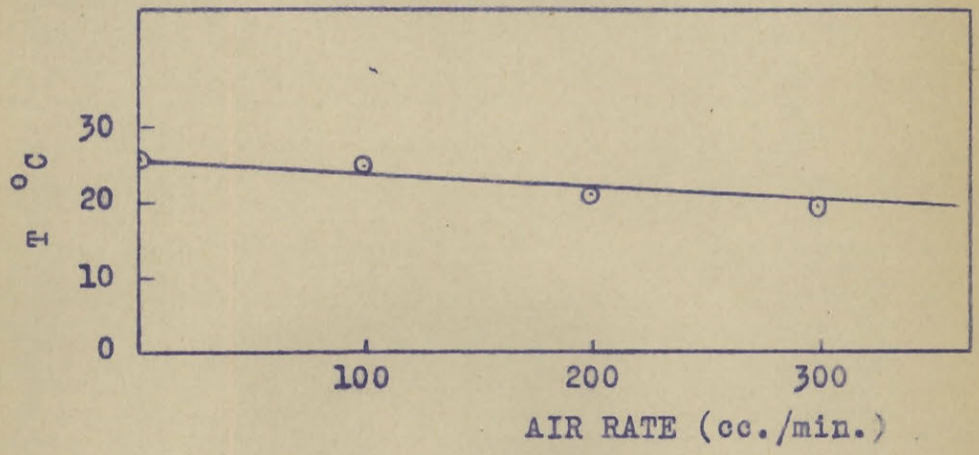

FIGURE 37.

EFFECT OF STREAM VELOCITY

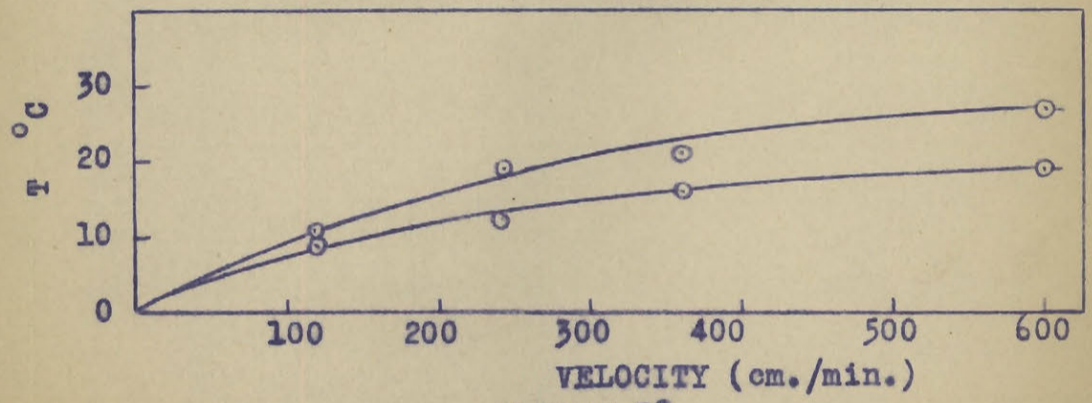

FIGURE 38.

increasing the residual activity, and hence also the dead length. The weight-time curves would slope off more gradually due to the decreased sorption when the bed is heating and the continuance of the sorption as the bed cools down to room temperature. This would increase the saturation time. Since the service time would be decreased and the saturation time increased, the escaping concentration would be lower at any given time (measured from the service time).

B. Butane

The sorption of butane was studied over the concentration range of 0.3 - 10% and at 100% butane, and at flowrates of 0.2 - 40 cm. per second, for column lengths of 1 to 5 centimetres.

1. Amount of Sorption

In table XV the weight sorbed and $x/_m$ data are presented. The height given in column one is the column length calculated from the weight of the charcoal bed. The data in the last column give the number of cc. of butane sorbed per minute as determined by the slope of the linear portion of the weight-time curves (some of which are shown in figures 39 and 40). This linear portion of the curve, since it depends solely on the rate of supply of the butane, should have a slope equal to the butane rate as given in column three. Here, as in the ammonia sorption, this difference is due to air displaced from the charcoal.

In figure 39, the weight-time curves as determined directly from the weight readings are presented. As in the case of ammonia sorption, the charcoal is 100% efficient until the service time when the curve ceases to be linear and butane is present in the effluent gas stream. The curve then bends to a horizontal straight line which is the saturation weight under those conditions. It will be noted that the sloping off of these curves is more rapid than those found for ammonia. This is partly due to the more rapid removal of the heat of sorption by the greater air flow used in the

TABLE XV

Weights Sorbed and $x/_m$ Data

Column Length cm.	Air Rate (cc/min.)	Butane Rate (cc/min.)	Partial Pressure mm.Hg.	Weight Sorbed gm.	$x/_m$ (cc/gm)	Slope (cc/min.)
4.08	3,130	53	12.7	4.32	62.0	51.6
1.94	3,020	53	13.2	2.07	63.0	51.5
5.01	1,590	53	24.5	5.80	68.0	51.5
4.09	1,530	53	24.5	4.73	68.0	51.5
2.96	1,520	53	24.5	3.43	68.0	51.5
2.13	1,530	53	24.5	2.47	68.0	51.5
1.19	1,520	53	24.5	1.38	68.0	51.5
3.96	500	53	72.8	5.26	78.1	51.4
3.95	0	71	760.	5.98	89.2	69.1
4.12	0	53	760.	6.26	89.2	51.5
4.00	3,020	71	17.4	4.42	65.0	69.0
3.70	3,020	30	7.5	3.60	57.2	29.0
2.18	3,020	30	7.5	2.12	57.2	29.0
4.23	3,045	24	5.7	3.96	54.9	22.6
4.16	3,040	9	2.3	3.13	44.3	8.7
2.12	3,000	9	2.3	1.66	45.1	8.8
1.27	3,020	9	2.3	0.96	44.5	8.7
4.01	1,500	30	15.0	4.34	63.7	29.0
2.09	1,500	30	15.0	2.27	63.7	29.0
3.99	1,403	30	15.9	4.26	62.6	29.0
3.88	151	2.7	13.7	4.20	63.7	2.5

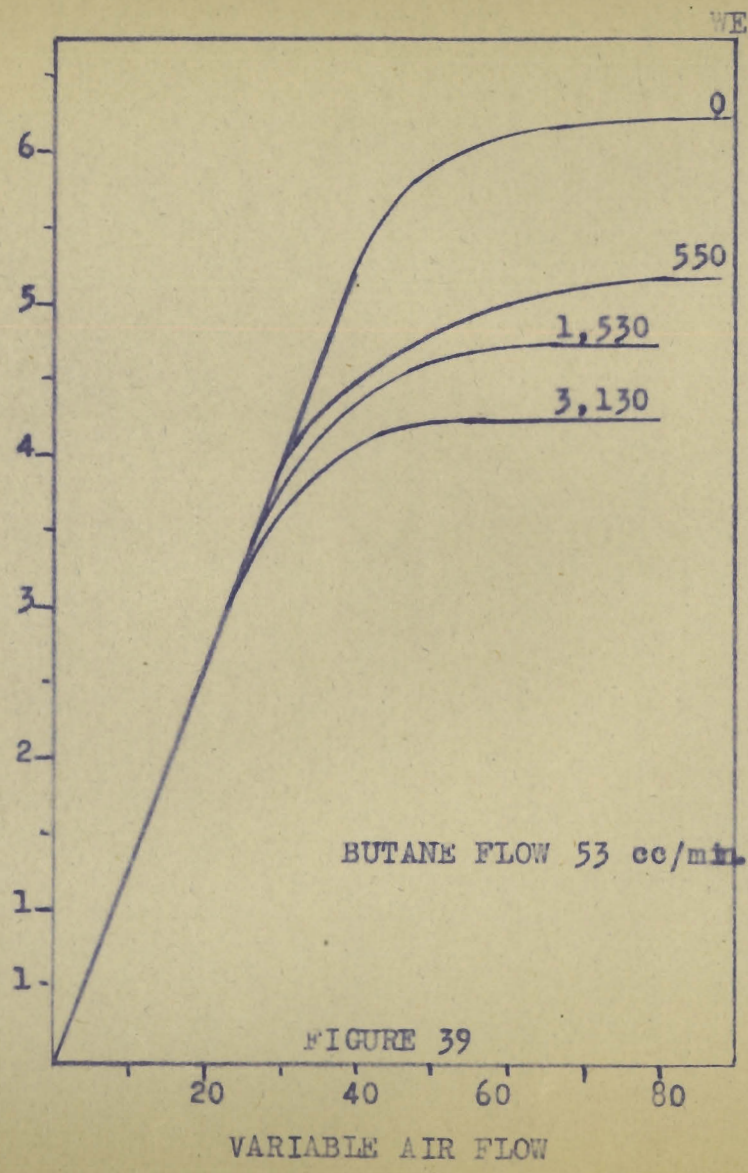

FIGURE 39

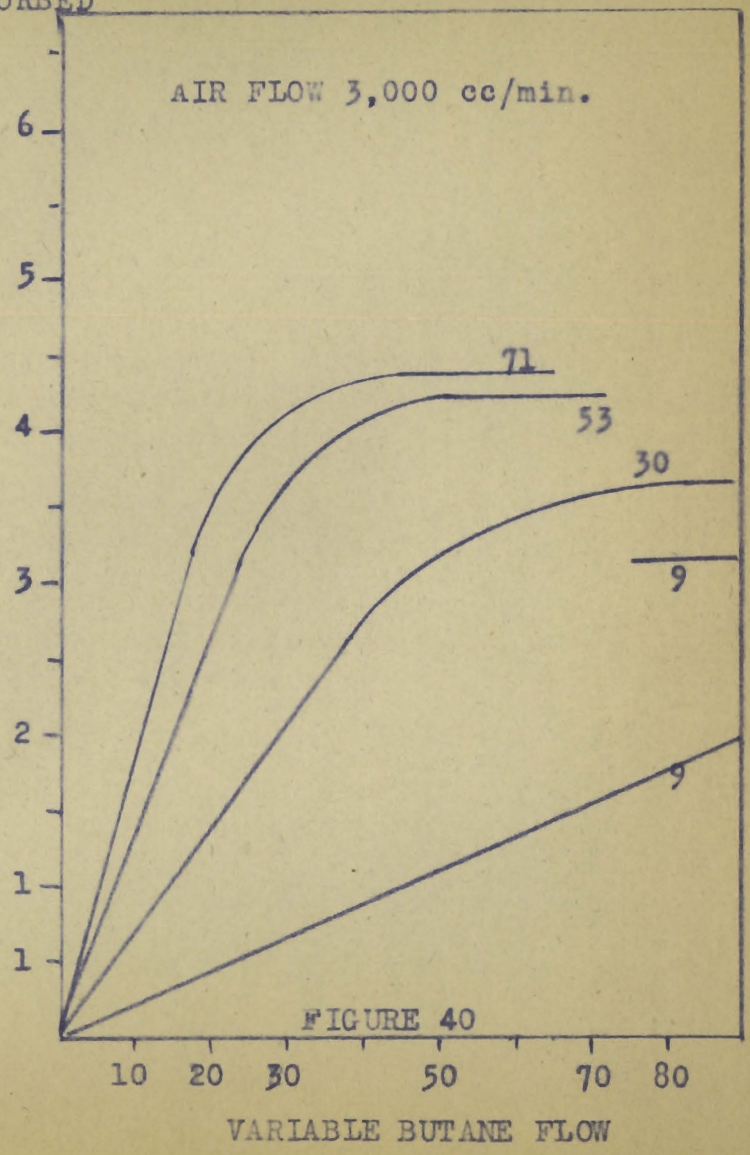

FIGURE 40

butane sorption.

It is seen from the curves that the air rate has no effect on the initial slope, but that the final value increases as the air flowrate is decreased.

In figure 40 a similar set of curves is shown with a constant air rate and variable butane rate. Here the slope of the straight line portion of the curve is different for different butane rates. The saturation value increases as the butane flow is increased.

Figure 41 shows the variation in $x/_m$ (cc. sorbed per gram of charcoal) due to the increased air rate. A curve results which decreases from a high value with zero air stream. The logarithm of $x/_m$ plotted against the logarithm of the air rate gives straight lines for different bed lengths which converge (figure 42).

The effect of butane concentration on the $x/_m$ is shown in figure 43. Since the total flowrate is approximately constant (varying from 3,030 to 3,090 cc/min.) the partial pressure could be plotted instead of the butane flowrate. The logarithmic relation is shown in figure 44. Here the relation is linear for high butane concentrations but falls off for the lower butane concentrations.

Figure 45 shows the complete curve of $x/_m$ against partial pressure up to 760 mm. of mercury. This curve does not follow a Langmuir or Freundlich isotherm over its whole range. A portion of the curve for partial pressures below 70 mm. of Hg is shown plotted on a larger scale in figure

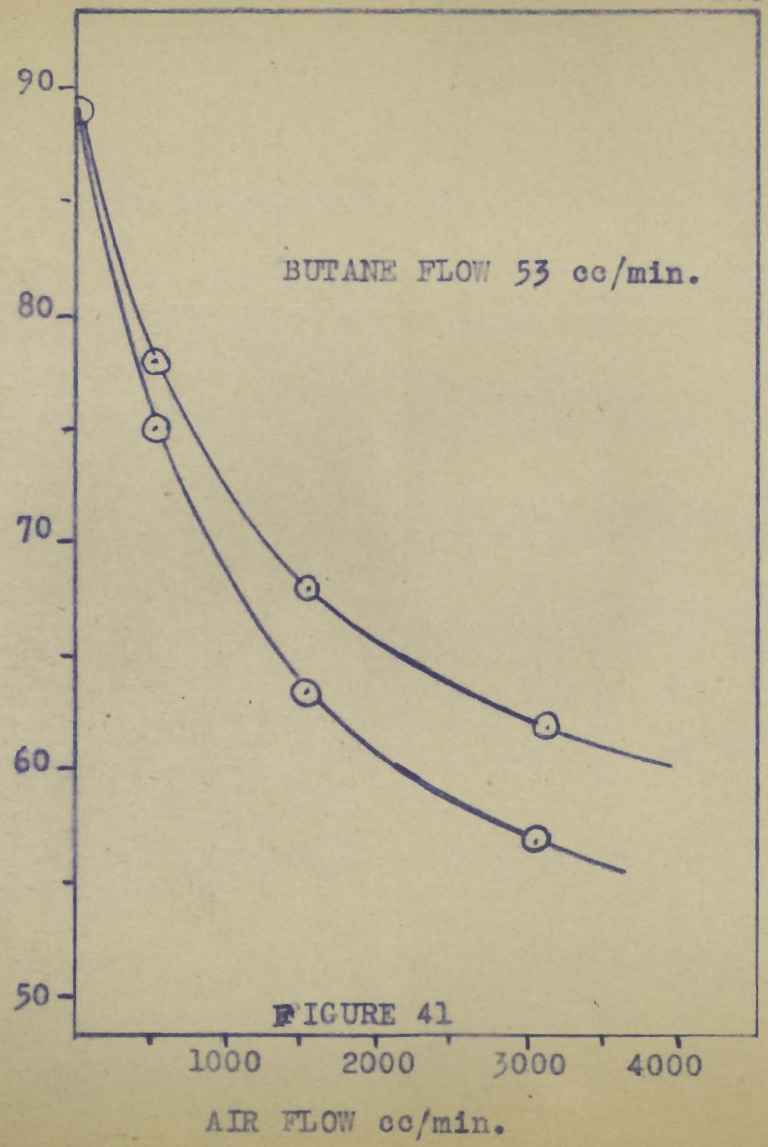

FIGURE 41

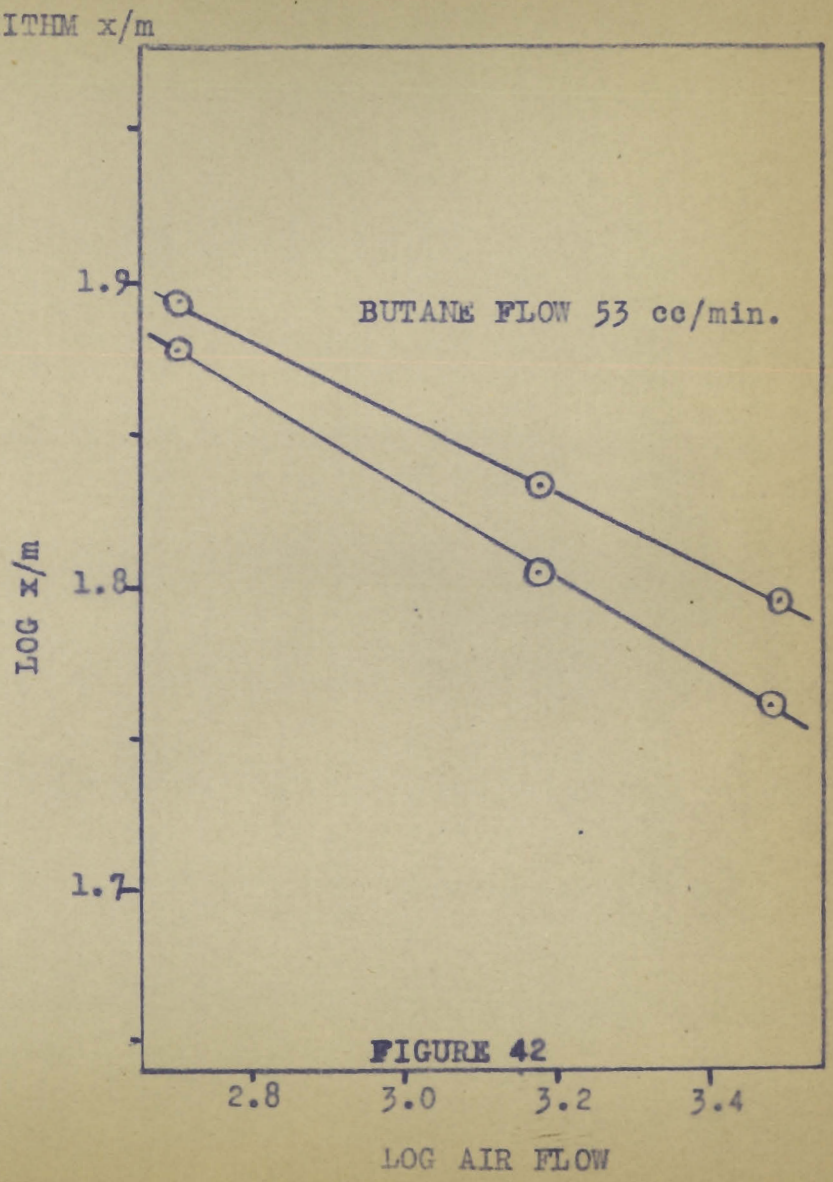

FIGURE 42

x/m AGAINST BUTANE FLOW

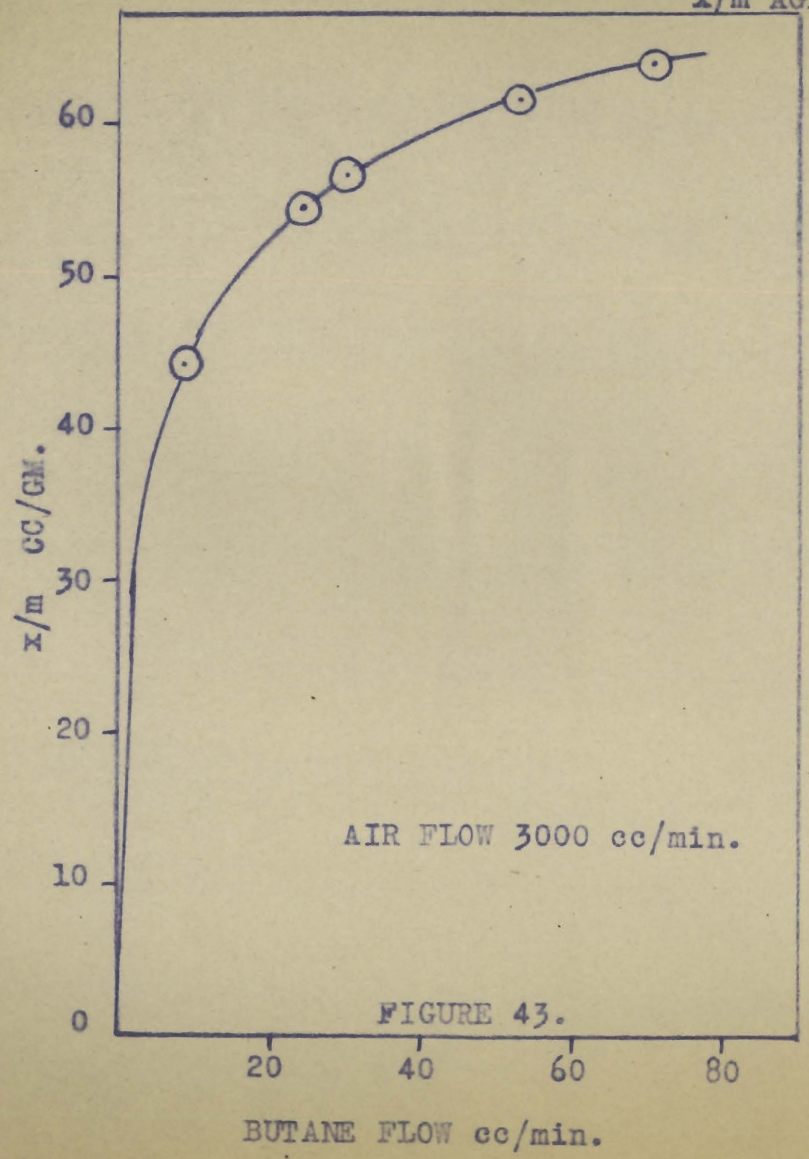

FIGURE 43.

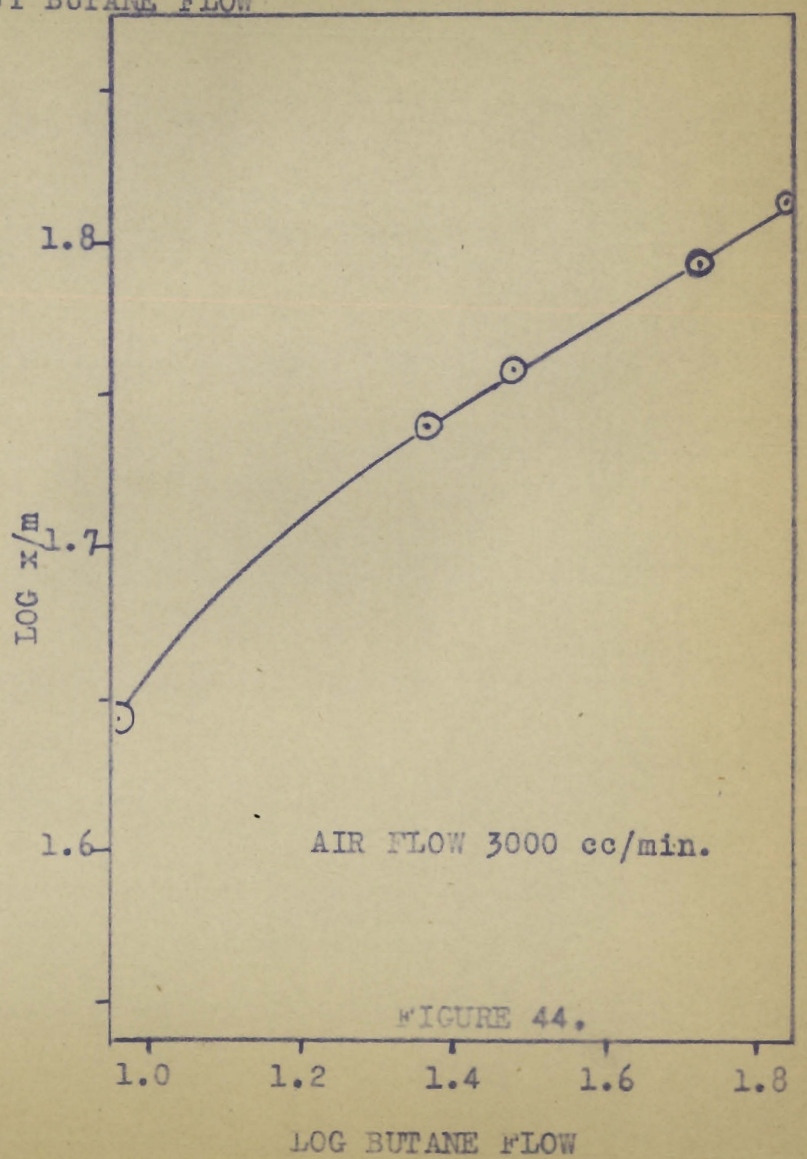

FIGURE 44.

46. The experimental points are not more than one division from the curve which indicates that, in this respect at least, the experimental error is about 1%.

The curve shown rises steeply at first and then flattens off quite rapidly to a constant value of x/m. This is in contrast with the behavior of ammonia, where the partial pressure curve was linear and did not reach a maximum value in the pressure range studied. This might possibly indicate a different type of sorption mechanism in the two cases.

This difference is also shown in figure 47 where the logarithm of x/m is plotted against the logarithm of the partial pressure. This does not give the straight line relation found for ammonia sorption.

As in the case with ammonia the magnitude of the total flowrate had no effect on the value of x/m over the range investigated from 153 to 3,180 cc. per minute.

In figure 48 the slope of the linear portion of the weight-time curves is plotted against the actual butane flow rate as determined by analysis of the escaping gases after the charcoal was saturated. A linear relation is obtained. The difference between the calculated and actual value is approximately the same on a weight basis; at 60 cc. per minute the difference for ammonia is 7.5 cc. = 0.0056 gm. and for butane 2 cc. = 0.0052 gm., but on a mole basis the discrepancy is much less for butane than for ammonia.

SORPTION ISOTHERM OF BUTANE

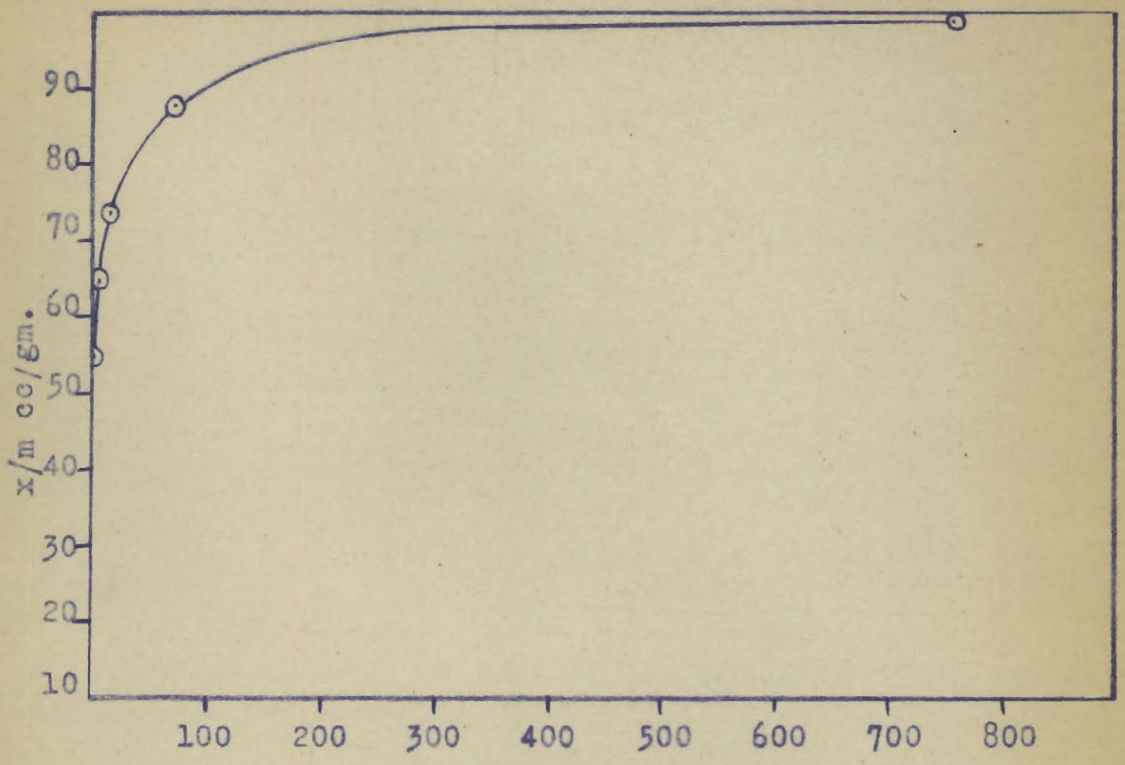

FIGURE 45.

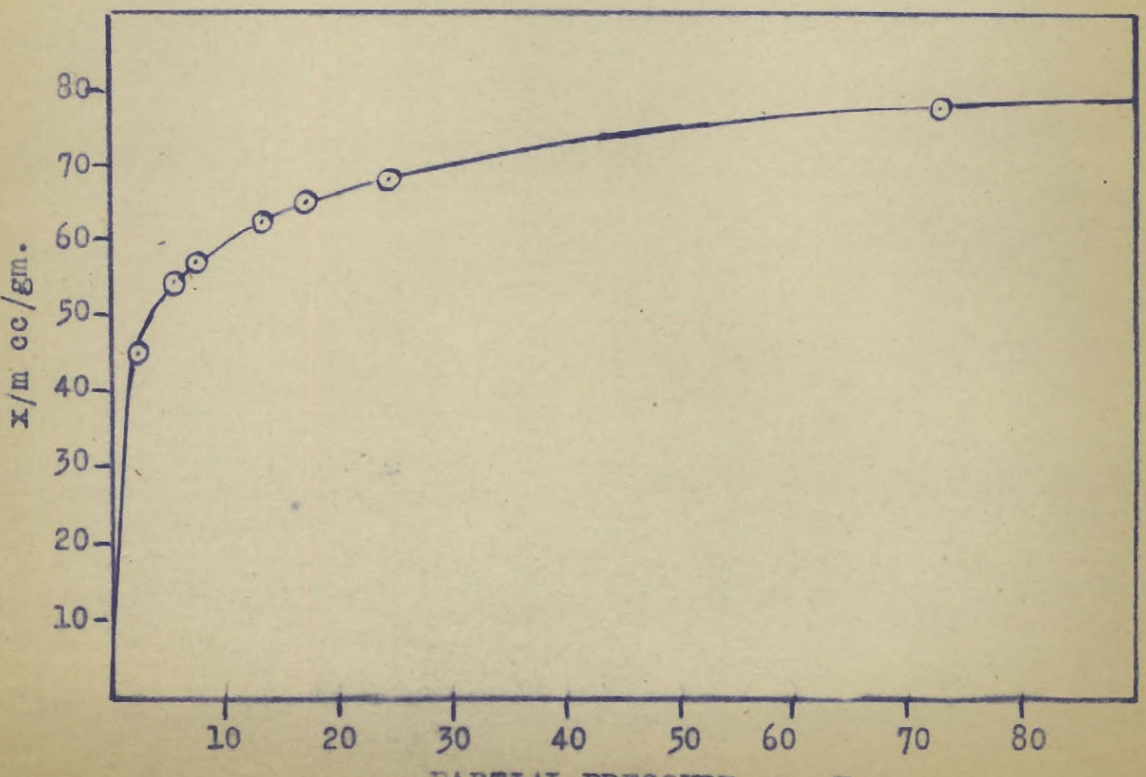

FIGURE 46

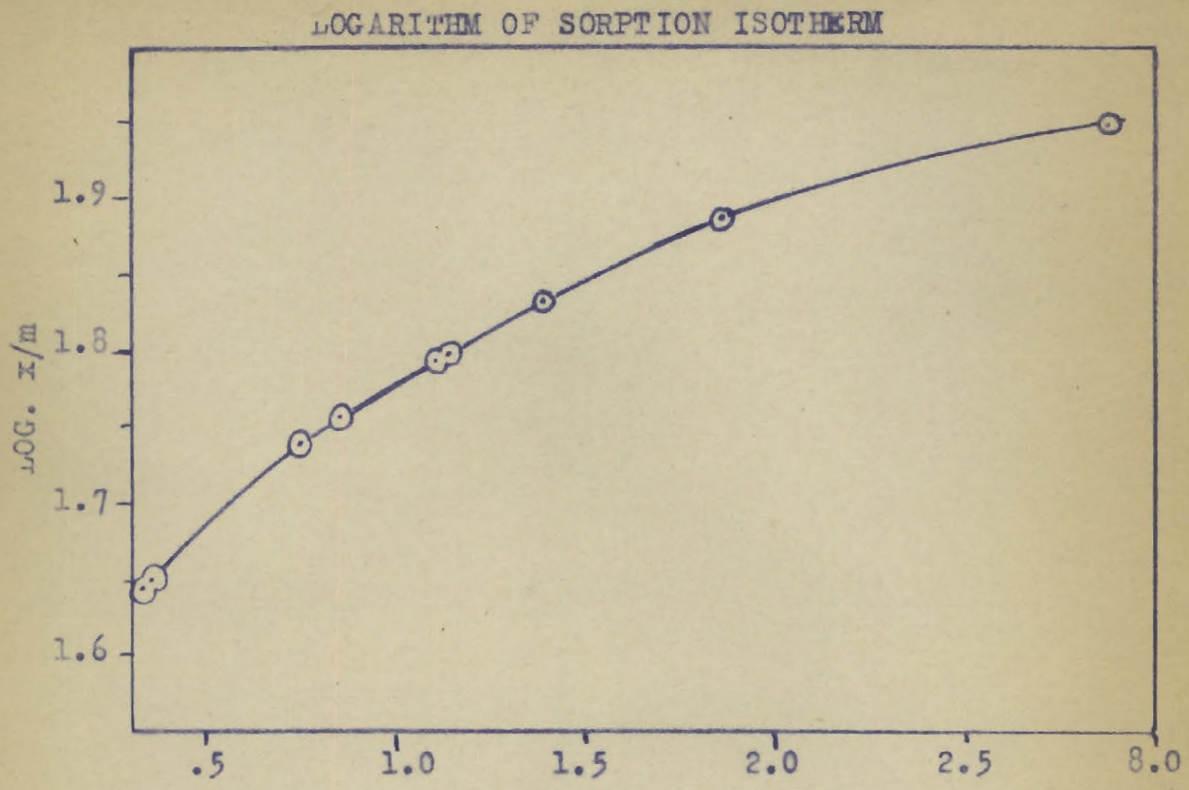

FIGURE 47.

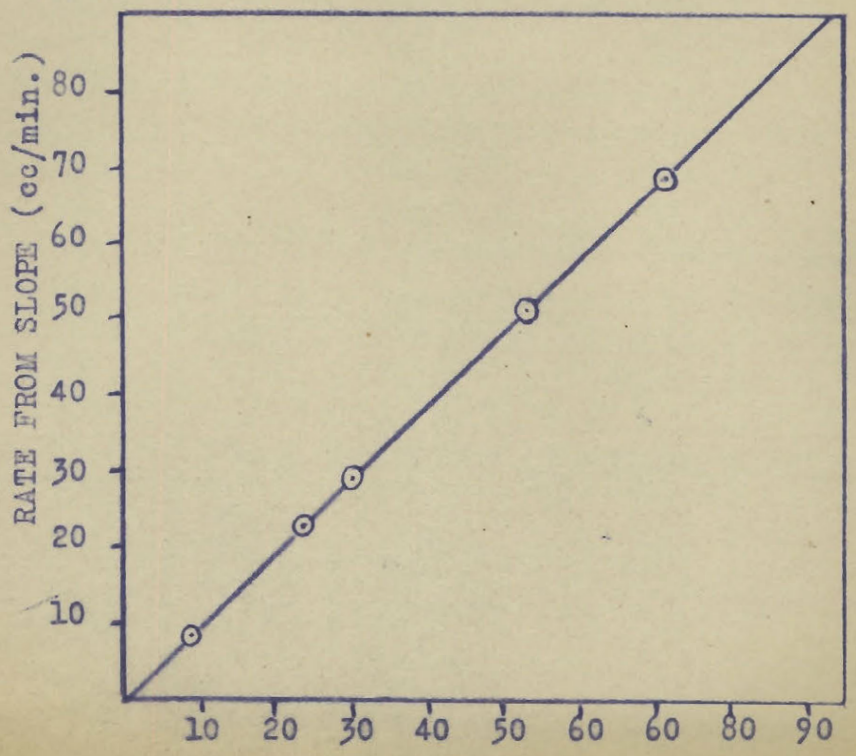

SLOPE AGAINST BUTANE FLOWRATE
FIGURE 48

2. Analytical Data

The data for the following sets of curves, figures 49 to 52 are not presented in tabular form since they are too extensive. The curves,however, indicate the data adequately.

These curves are plots of grams of sorbate per minute against time. The curves starting from zero are the analytical curves determined from the concentration of butane in the effluent gases. The curve starting from the top is obtained by graphical differentiation of the weight-time curves. The analytical curve reaches a higher value than the differential curve due to the air displaced from the charcoal.

In figure 49 the curves are obtained from the five column lengths of the 53 cc. butane - 1,520 cc. air runs. The curves are horizontal until the service times are reached, then break off rapidly and curve exponentially to a final horizontal straight line. The shapes of the curves are quite similar after the first centimetre bed. In the one centimetre bed the break is not so sharp but soon assumes a shape similar to the others.

The analytical curves, as will be shown later, can be used to determine the concentration gradients of the sorbate-air stream throughout a five centimetre bed since the exit gas for a one centimetre bed would be the same as that entering the second layer of a two centimetre bed, etc.

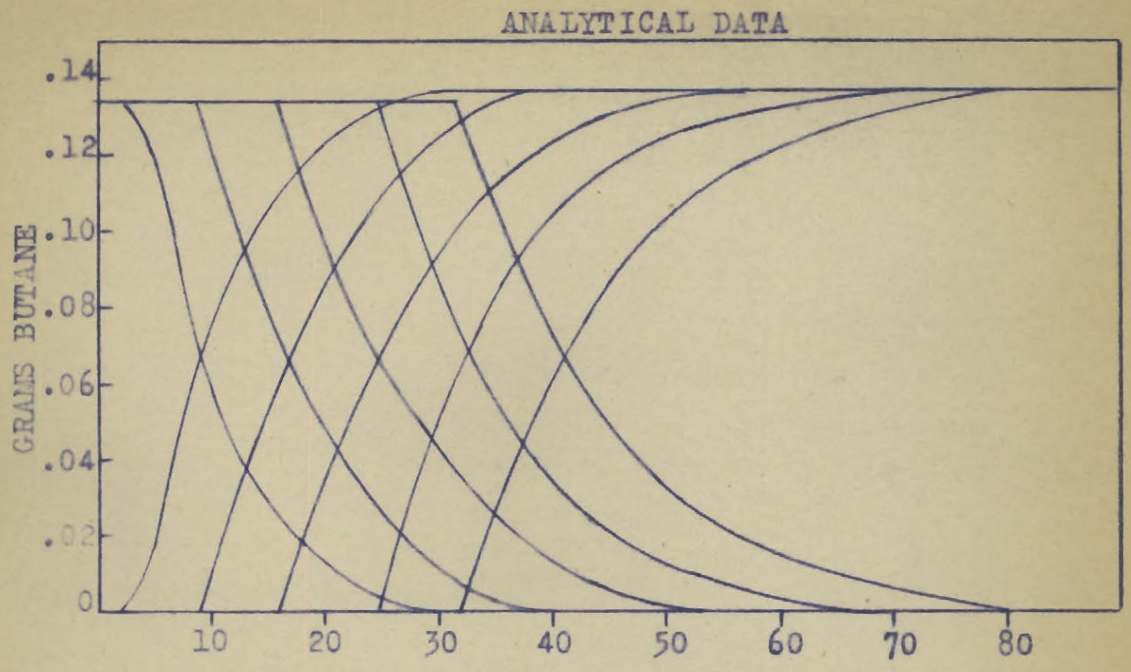

CONSTANT FLOW AND CONCENTRATION

FIGURE 49.

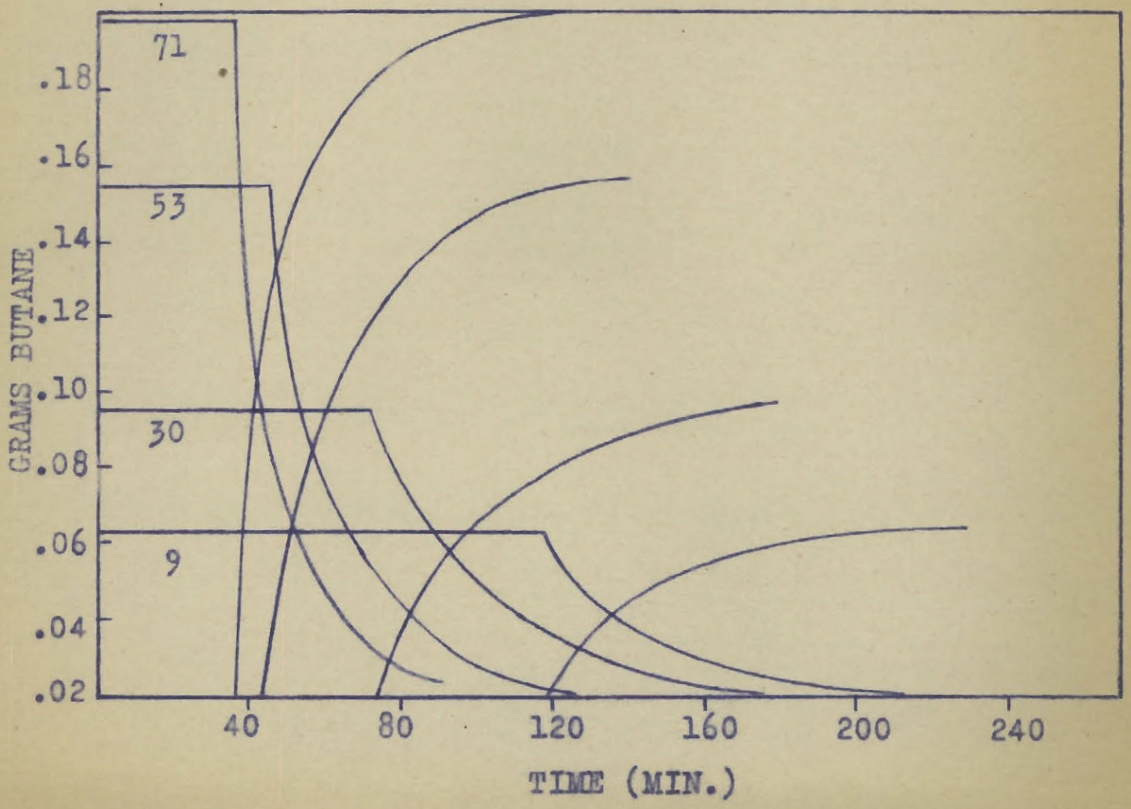

VARIABLE BUTANE CONSTANT AIR FLOW

FIGURE 50.

ANALYTICAL DATA

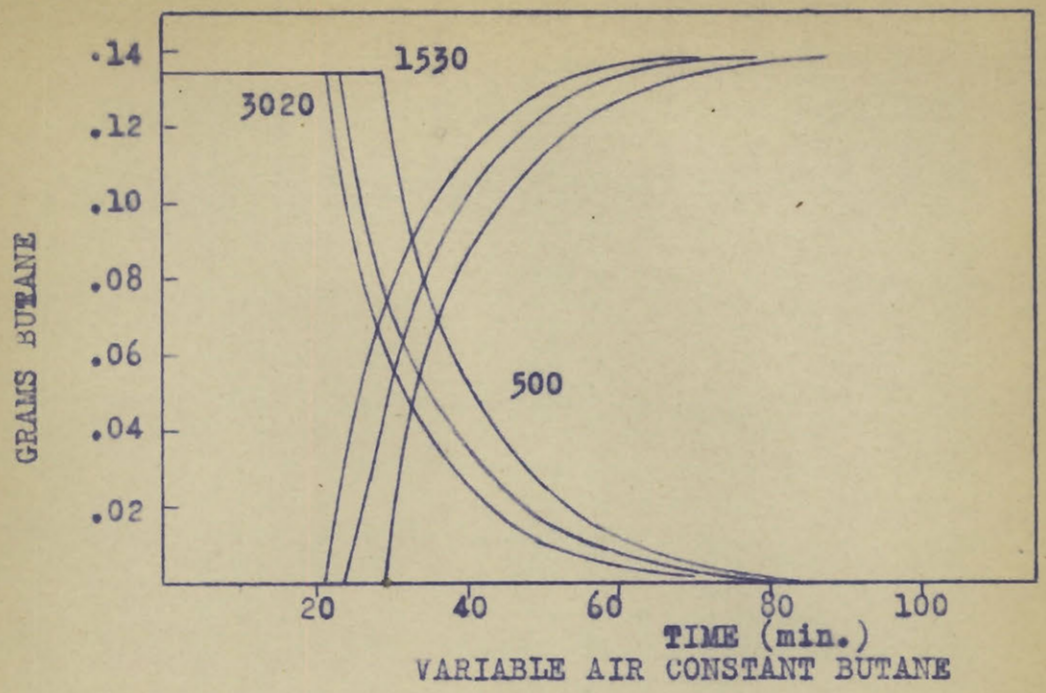

VARIABLE AIR CONSTANT BUTANE

FIGURE 51.

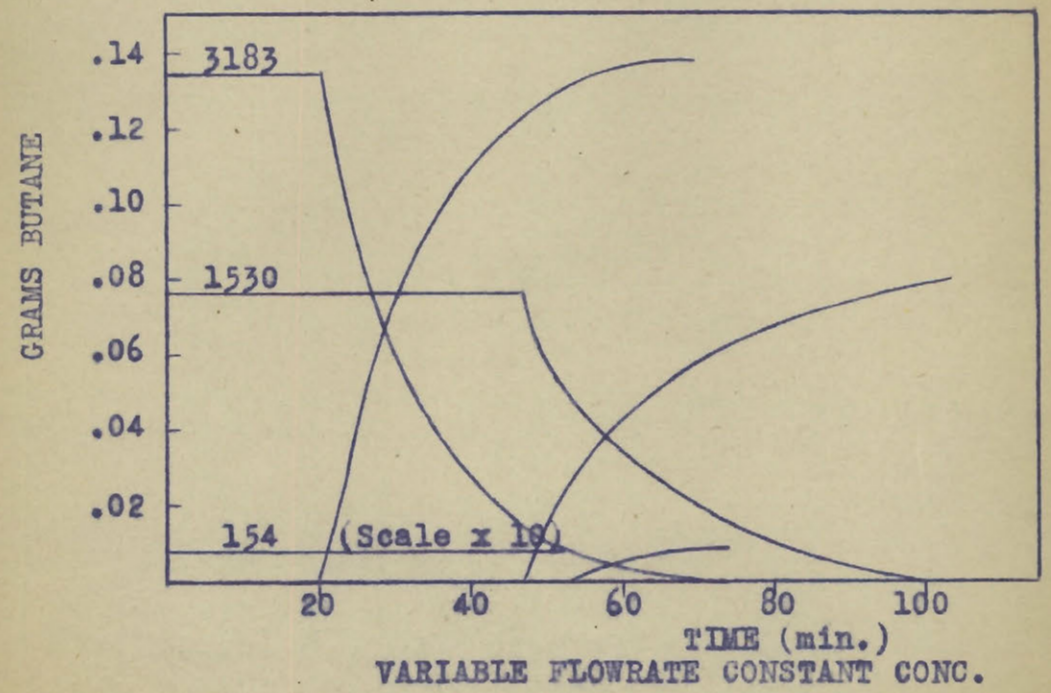

VARIABLE FLOWRATE CONSTANT CONC.

FIGURE 52.

Figure 50 shows the analytical and differential sorption curves for 3,000 cc. per minute air flow, four centimetre beds, and varying butane concentrations. It is seen that the initial slope of these curves is decreased as the butane concentration is decreased.

Figure 51 shows the effect of air flowrate on the curves. These are for a constant butane flow of 53 cc. per minute and for four centimetre beds. The shapes of the curves are not affected by the air rate except that the breaking point decreases with increased air flow.

The analytical and differential sorption curves for variable flowrate and constant butane concentration are shown in figure 52. The partial pressure of butane in the entering gases is 13.8 mm. of Hg, and the flowrate is varied from 154 to 3,183 cc. per minute. The rate of change of these curves is decreased with decreased stream velocity. Thus from the service time to the saturation time the 3,183 cc/min. curve extends over 50 minutes while the 154 cc/min. curve extends for over 200 minutes.

The data for the relation between the escaping concentration and time are shown in table XVI. These are the data obtained from one run; all other runs gave similar data. The time axis is started at the service time. The concentration of the escaping gases is expressed as grams of butane per minute.

In figure 53 the logarithm of the reciprocal of the escaping concentration is plotted against time. A

TABLE XVI

Escaping Concentration as a Function of Time

(Butane Rate = 53 cc/min; Air Rate = 1,500 cc/min; Bed depth = 5cm

Time after Service Time min.	Escaping Concentration gm/min.	Log C.	Log $1/C$	$1/T$
0	0			
3.5	0.031	$\bar{2}.491$	$\bar{1}.509$	0.286
8.5	0.062	$\bar{2}.792$	$\bar{1}.208$	0.118
13.5	0.085	$\bar{2}.929$	1.071	0.074
18.5	0.102	$\bar{1}.009$	0.991	0.054
23.5	0.116	$\bar{1}.065$	0.935	0.0425
28.5	0.122	$\bar{1}.086$	0.914	0.0349
33.5	0.129	$\bar{1}.110$	0.890	0.0298
38.5	0.133	$\bar{1}.124$	0.876	0.0260
43.5	0.136	$\bar{1}.134$	0.866	0.0230
48.5	0.137	$\bar{1}.137$	0.863	0.0205

ESCAPING CONCENTRATION

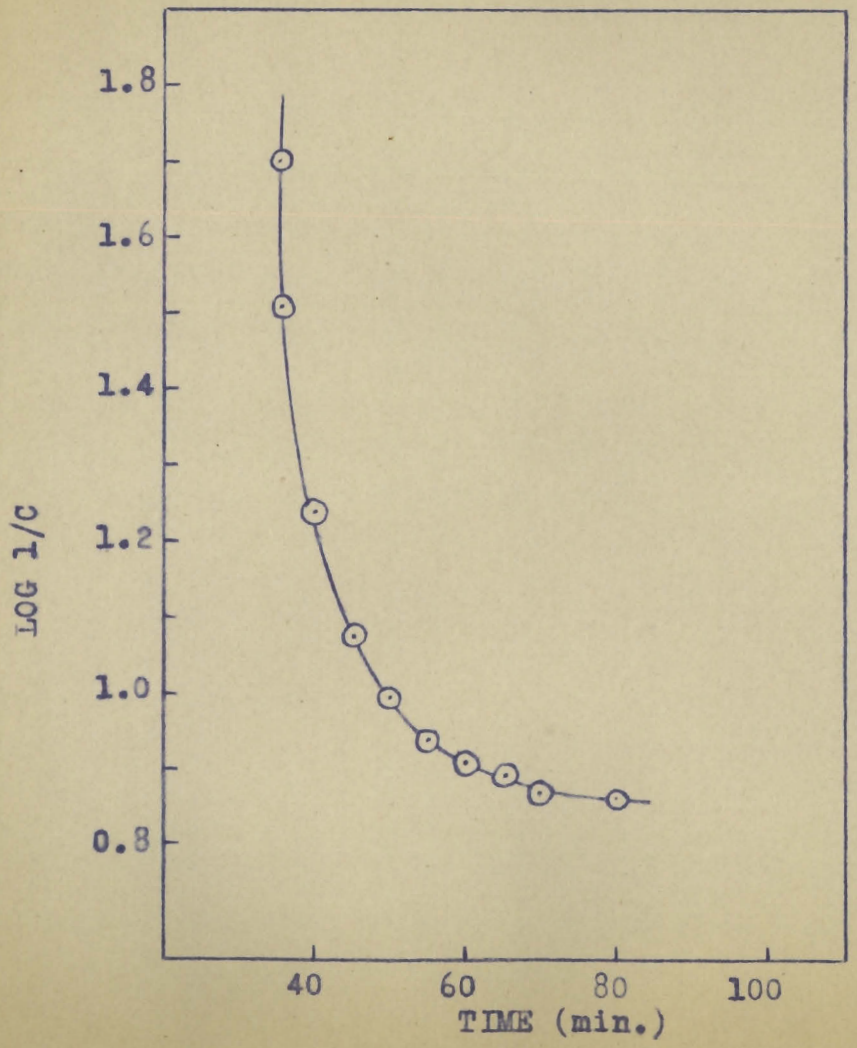

FIGURE53

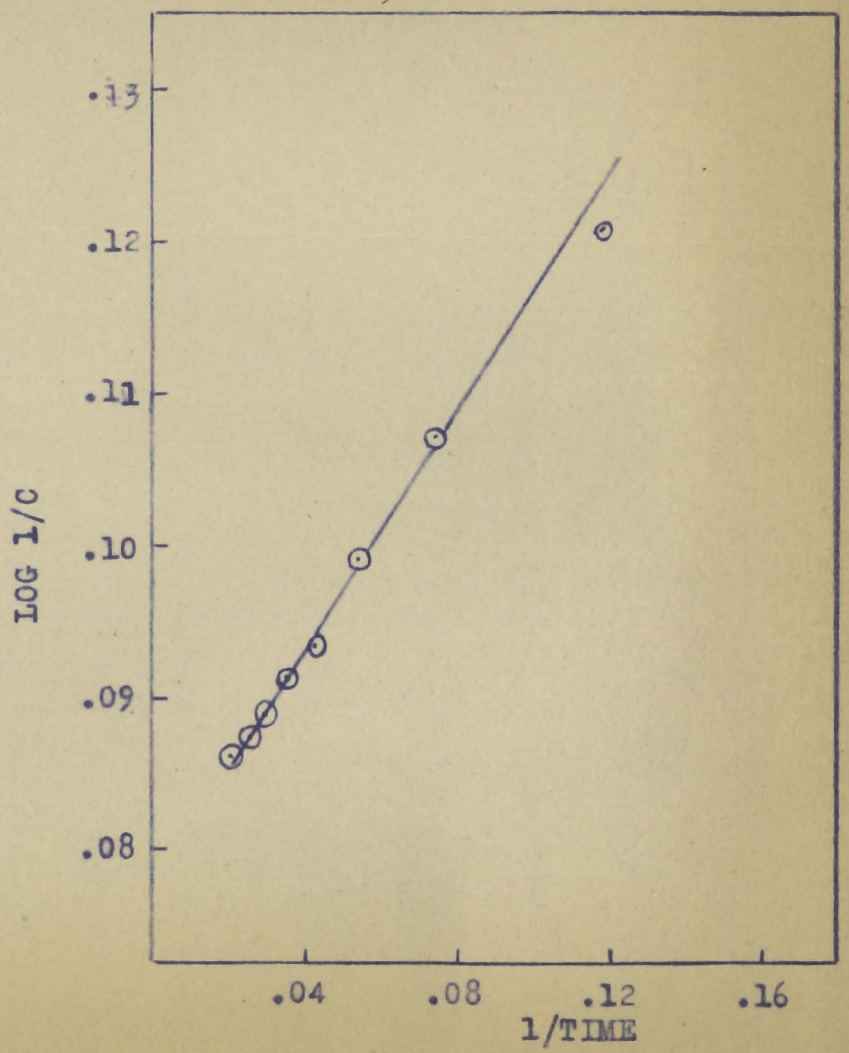

FIGURE 54.

curve is obtained in contrast to the prediction of a straight line by Danby et al. However, they state that the straight line relation only holds when C_o/C is large i.e. in the early stages of breakdown. It is seen that this is approximately true for the first few minutes. If the logarithm of the escaping concentration is plotted against the reciprocal of the time, a straight line relation is obtained as in figure 54.

3. Service Time Data

The service time was again taken as the break in the linear portion of the weight-time curves. The data for the service time relations are given in table XVII. Here the first four columns are the same as those in table XV. In column five the observed service time is given while in column 6 the "corrected" service time is recorded.

Figure 55 shows the service time-column length relation for constant butane flowrate and variable air flow-rate. Figure 56 shows similar curves for constant air and variable butane. The straight lines intersect at a common point below the origin, except for those at high air rates and low butane rates. The various critical lengths can be determined from the intercepts of these lines on the column length axis. Here again the column lengths used were too long to show the curvature of the lines toward the origin.

In figure 57 the service times for a four centi-metre bed and constant butane flow are plotted against air rate. The service time decreases from its maximum value at zero air rate but the rate of decrease becomes small at high air flowrates. The logarithm of the service time is plotted against the logarithm of the air rate in figure 58, and a linear relation is obtained.

The effect of varying the butane rate at constant air rate and constant bed length is shown in figure 59.

TABLE XVII

Service Time Data

Column Length cm.	Air Rate (cc/min.)	Butane Rate (cc/min.)	Partial Pressure mm. Hg.	Service Time min.	Corrected Service Time min.
4.08	3,130	53	12.7	22.0	21.5
1.94	3,020	53	13.2	7.0	7.5
5.01	1,590	53	24.5	31.5	31.0
4.09	1,530	53	24.5	24.5	24.0
2.96	1,520	53	24.5	16.5	16.0
2.13	1,530	53	24.5	9.0	8.0
1.19	1,520	53	24.5	2.0	0.2
3.96	500	53	72.8	29.0	29.5
3.95	0	71	760.0	25.0	25.5
4.12	0	53	760.0	40.0	38.5
4.00	3,020	71	17.4	17.5	17.5
3.70	3,020	30	7.5	37.0	39.0
2.18	3,020	30	7.5	19.0	16.0
4.23	3,045	24	5.7	53.0	49.5
4.16	3,040	9	2.3	129.	123.
2.12	3,000	9	2.3	62.0	61.0
1.27	3,020	9	2.3	34.0	30.5
4.01	1,500	30	15.0	47.0	47.0
2.09	1,500	30	15.0	21.5	20.5
3.99	1,403	30	15.9	48.0	48.0
3.88	151	2.7	13.7	540	558

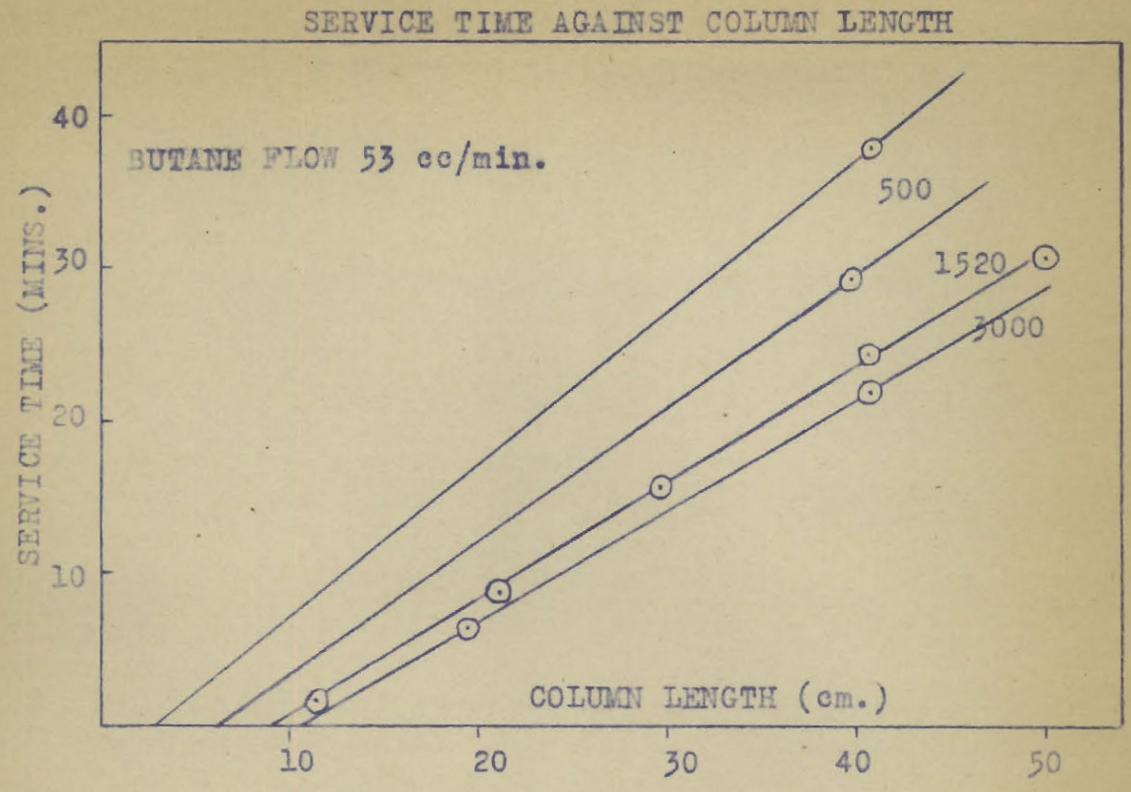

VARIABLE AIR CONSTANT BUTANE FLOW
FIGURE 55

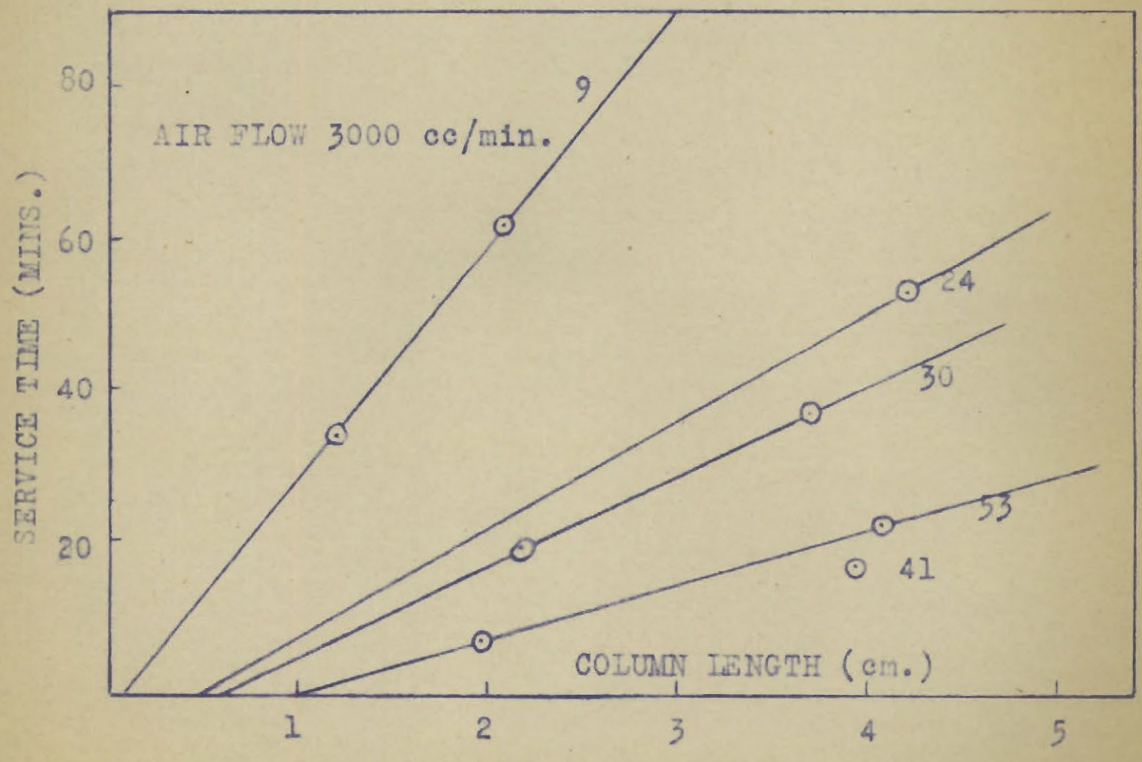

VARIABLE BUTANE CONSTANT AIR FLOW
FIGURE 56

The partial pressures corresponding to the butane flowrate are also shown. These determinations were made essentially at constant flowrate since the effect of the change in butane rate on the total flow is negligible. The relation between the logarithm of the service time and the logarithm of the butane rate is shown in figure 60, and is seen to be linear. This is in contrast with the ammonia results where the logarithm of the service time varied with the actual ammonia rate.

The theories of Danby et al and of Mecklenberg predict that the service time should vary as the reciprocal of the initial concentration. The data for the plot of service time against the reciprocal of the initial concentration are given in table XVIII. The plot of service time against $1/C_o$ is shown in figure 61. A straight line is obtained which is in agreement with the Danby et al and Mecklenberg predictions. The abrupt curve that was found in this plot for ammonia is not seen over the concentration range studied here. The value obtained by multiplying the concentration and the service time is approximately constant in agreement with the results of Shilow et al (16).

The data showing the effect of flowrate are given in table XIX. The concentration here is approximately constant and a four centimetre bed was used. The curve of service time against flowrate is plotted in figure 62. The service time decreases rapidly with increase in the

SERVICE TIME AGAINST AIR RATE

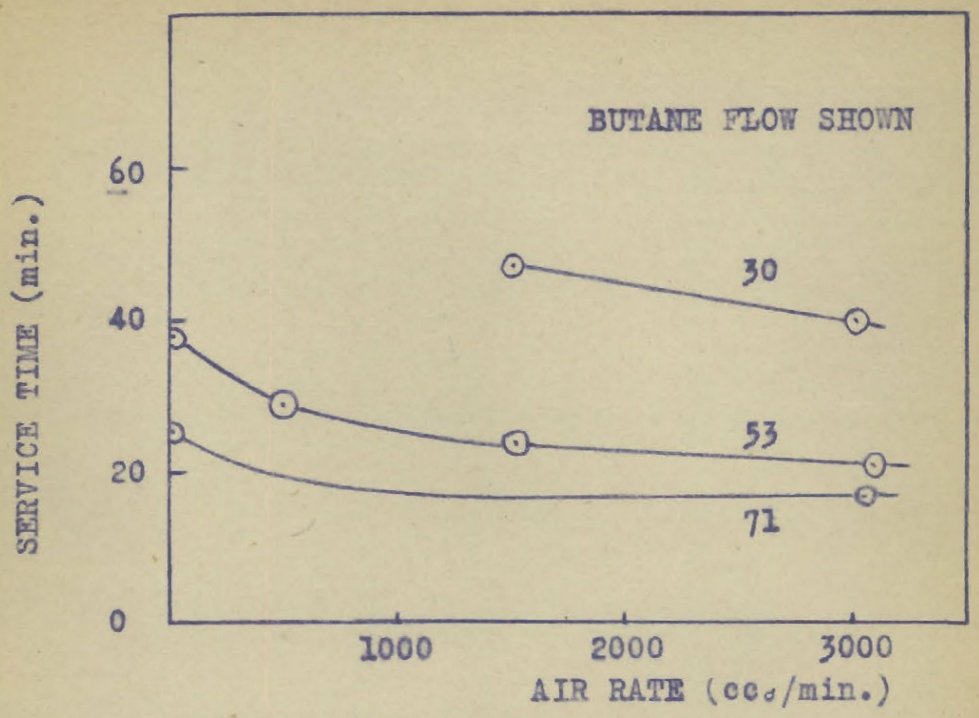

FIGURE 57.

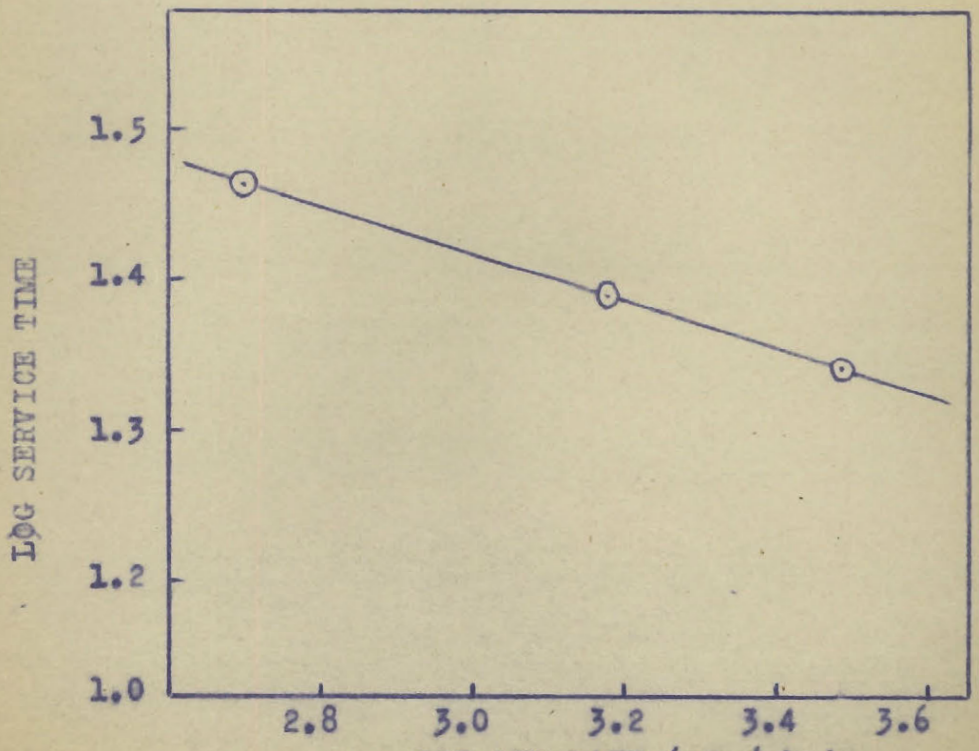

FIGURE 58.

SERVICE TIME AGAINST BUTANE RATE

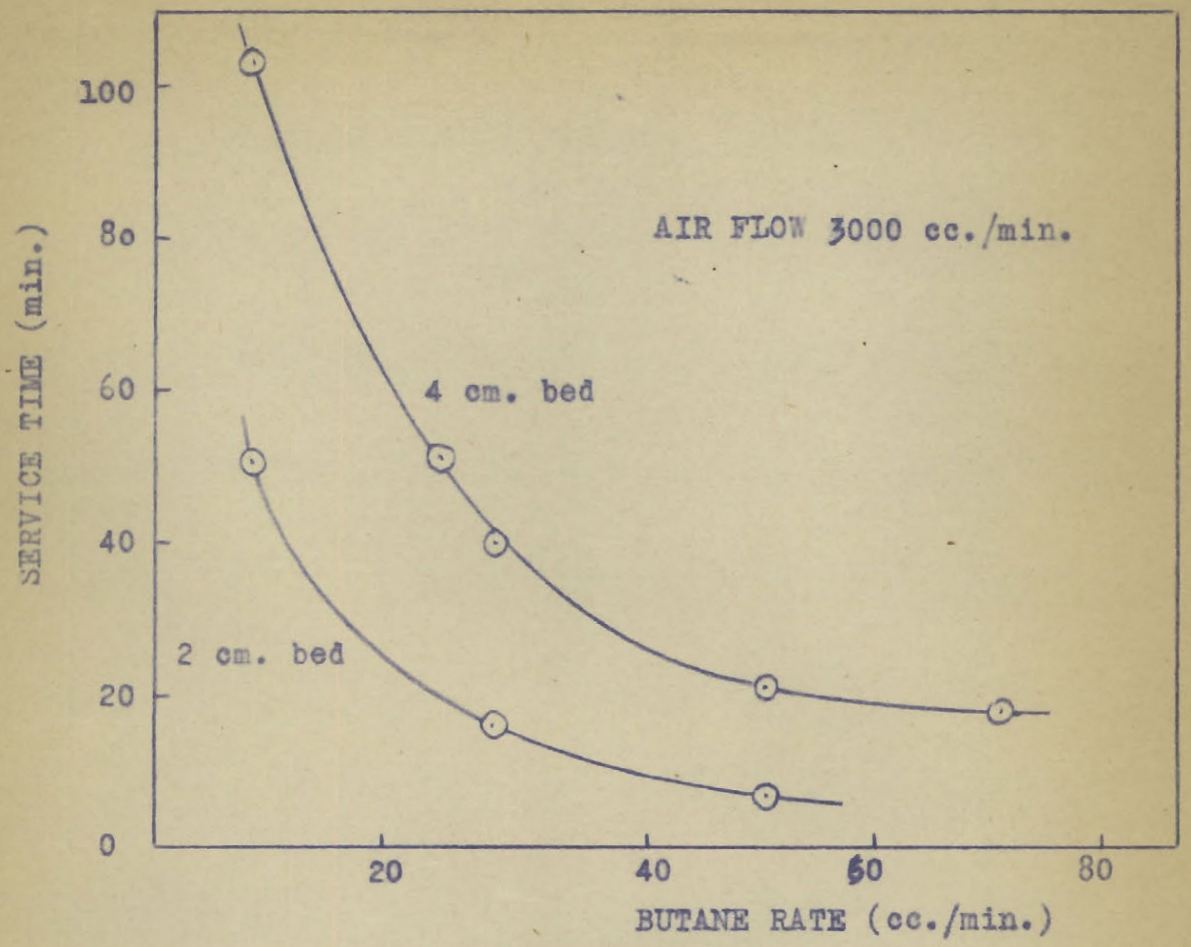

FIGURE 59.

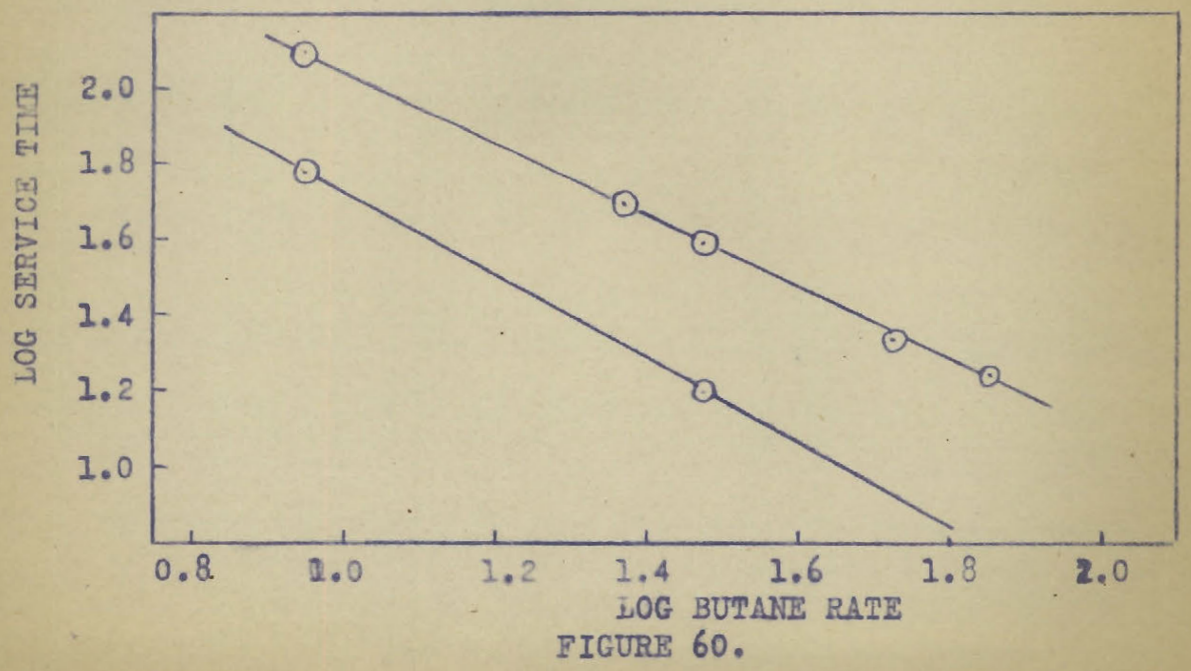

FIGURE 60.

TABLE XVIII

Service Time as a Function of Initial Concentration

Air Rate (cc/min)	Butane Rate (cc/min.)	Initial Conc. (C_o) %	$1/C_o$	Service Time min.
3,040	9	0.296	3.38	123
3,045	24	0.788	1.27	49.5
3,020	30	0.995	1.007	39.0
3,020	53	1.695	0.590	21.5
3,020	71	2.300	0.435	17.5

TABLE XIX

Air Rate (cc/min)	Butane Rate (cc/min.)	Total Flow (cc/min.)	Velocity L (cm/sec.)	Service Time min.	$1/L$
151	2.7	154	12.2	558	0.0818
1,500	30	1,530	121.4	47	0.00823
3,130	53	3,183	252.4	21.5	0.00396

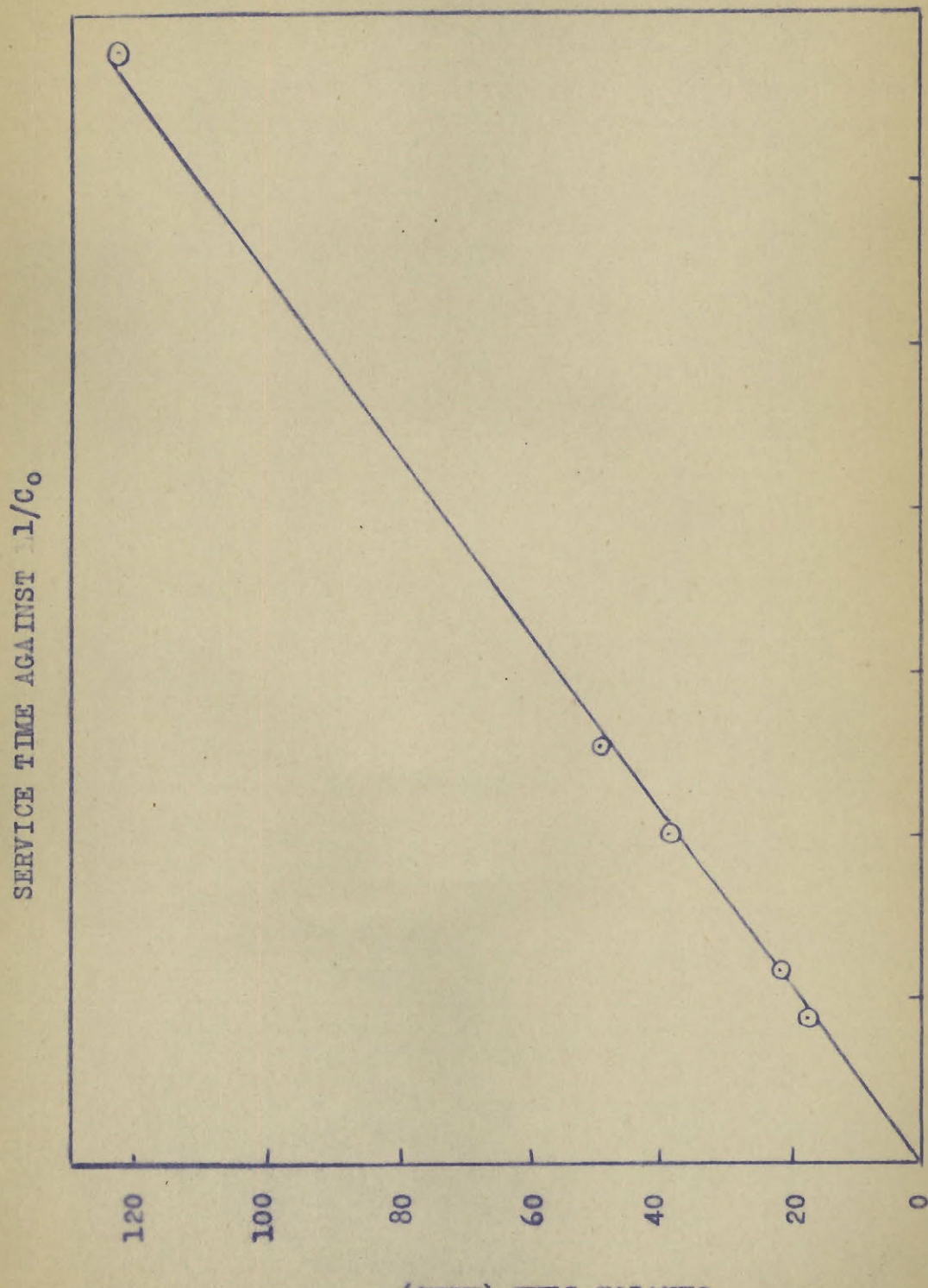
SERVICE TIME AGAINST $1/C_o$
SERVICE TIME (min.)
0
20
40
60
80
100
120
50
100
150
200
250
300
$1/C_o$ →

FIGURE 61.

flowrate at first but the effect is not so marked at flowrates greater than 1,500 cc. per minute.

The velocity of the gas stream through the cell is calculated from the rate in cc. per minute and the cross section of the cell. The service time was plotted against the reciprocal of the velocity in figure 63. A linear relation is obtained which is in agreement with the equation of Danby et al:

$$T' = \frac{N_o \lambda}{C_o} \left[\frac{1}{L} - \frac{1}{L_c} \right]$$

The critical flowrate L_c for the butane concentration used here, as found by extrapolation of the line to the flowrate axis is 10,000 cm. per second. This value was not checked experimentally.

EFFECT OF FLOWRATE ON SERVICE TIME

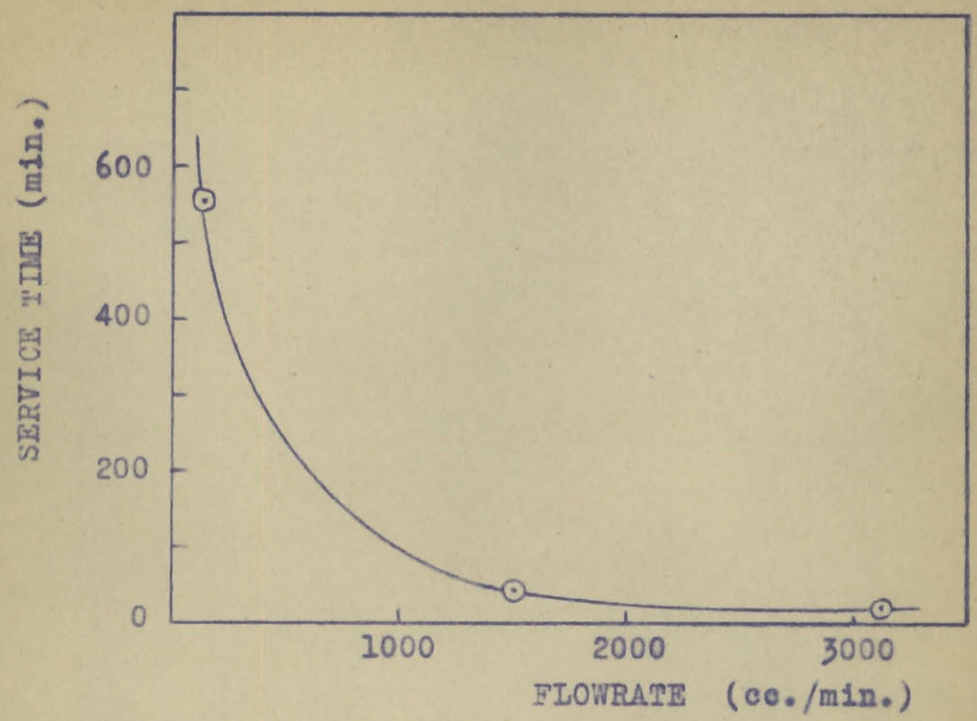

FIGURE 62.

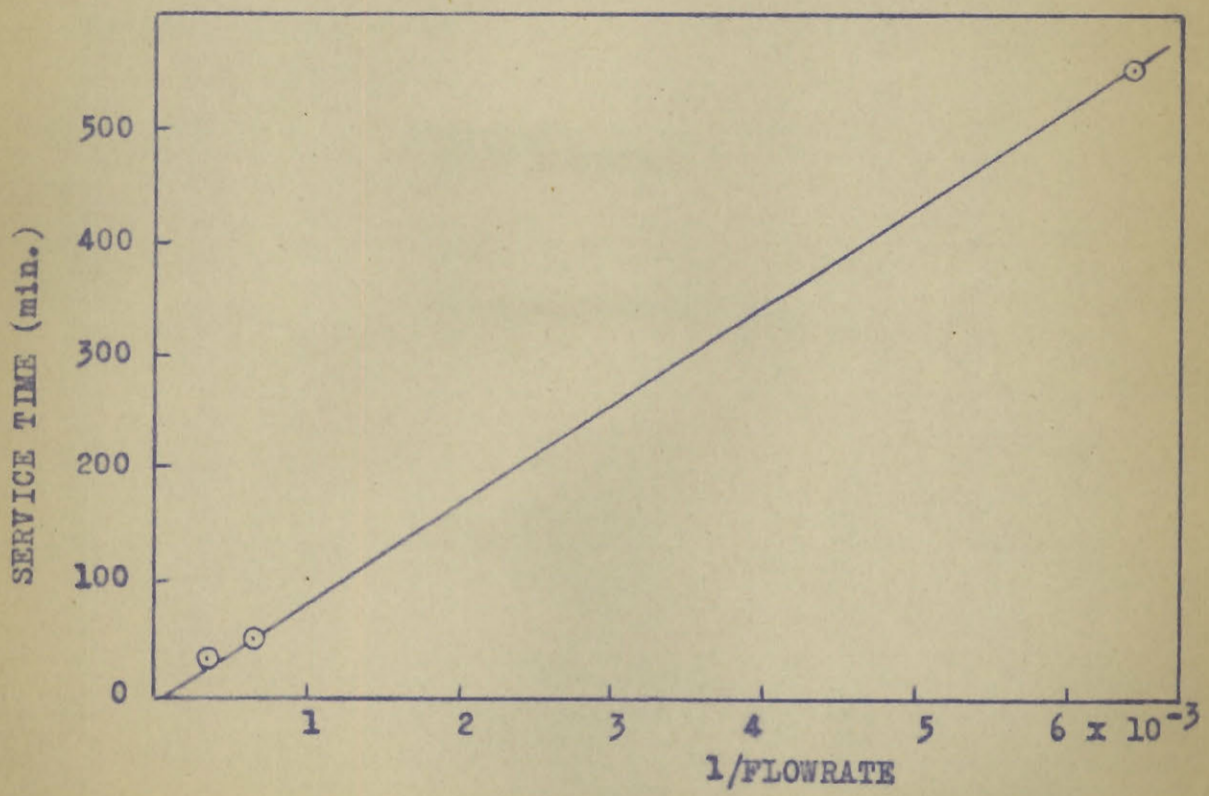

FIGURE 63.

4. Critical Lengths

The data for the variation of critical length with the air flowrate are given in table XX. The plot of critical length against air rate is shown in figure 64. The critical length is increased by increasing the air rate but the relative effect decreases at higher air rates. In figure 65, the critical length is plotted against the logarithm of the air rate and a straight line is obtained.

The theory of Danby et al predicts that the relation between critical length and concentration of the gas in the air stream follows the equation:

$$\lambda_c = \frac{L}{kN_o} \ln \left(C_o/C' - 1 \right)$$

where is the critical length. If L, k and N_o are constant the critical length should vary as the logarithm of the initial concentration C_o.

The equation of Mecklenberg for the dead length:

$$h = \frac{\delta_r}{D F} \left(\frac{K Q}{V} \right)^{n-1} \left[\ln \frac{C_o - C'}{C_x - C'} - \frac{C_o}{C_o - C'} \right]$$

also predicts that it should vary with the logarithm of the initial concentration, if as is assumed for his "mathematical" charcoal the vapor pressure in the capillaries C' is constant.

The data for the effect of concentration on critical length are given in table XXI. In figure 66 the critical

TABLE XX

Effect of Air Rate on Critical Length

Air Rate (cc/min.)	Critical Length cm.
0	0.57
500	0.75
1,530	0.95
3,130	1.03

TABLE XXI

Effect of Concentration on Critical Length

(constant flowrate = 3,050 cc/min.)

Partial Pressure of Butane mm. Hg.	Critical Length cm.
2.3	0.10
5.7	0.40
7.5	0.55
12.7	1.03
17.4	1.26

CRITICAL LENGTH AGAINST AIR RATE

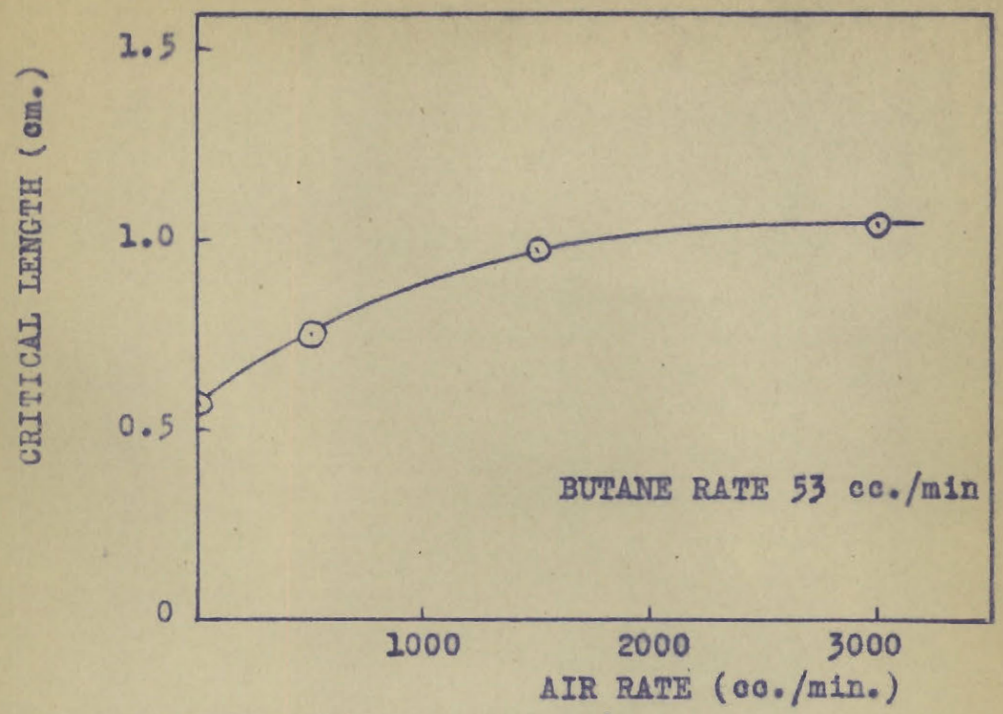

FIGURE 64.

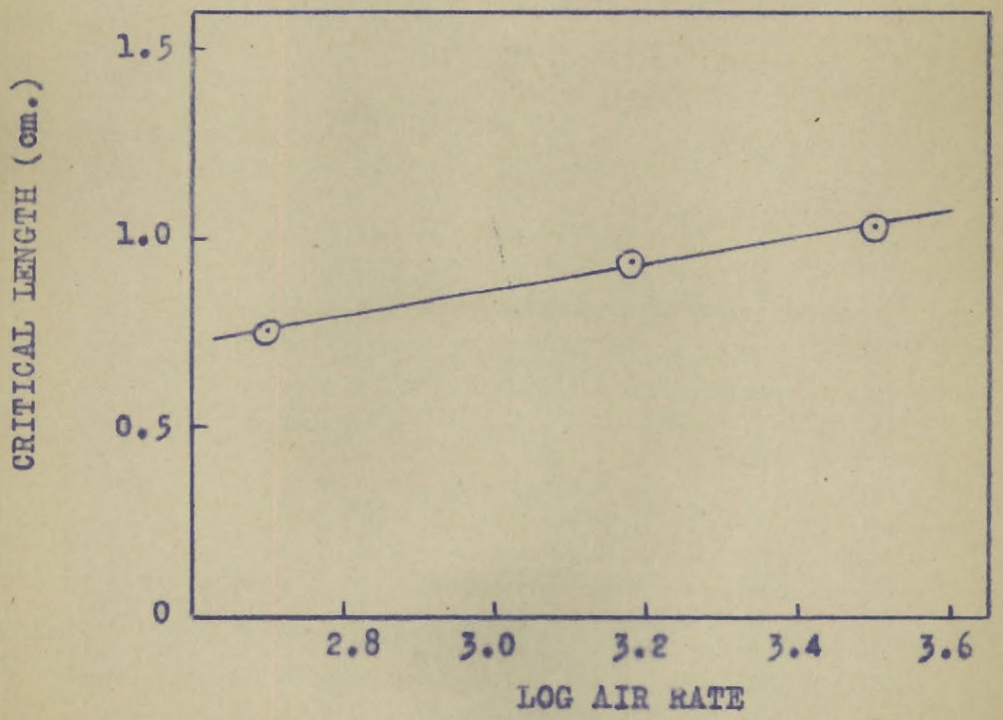

FIGURE 65.

length was plotted against the partial pressure of butane. The critical length is seen to increase with the partial pressure of butane but the curve seems to tend towards a maximum at higher partial pressures. The critical length is plotted against the logarithm of the partial pressure in figure 67, and a linear relation is found at higher partial pressures (above 7 mm. Hg.) but the graph curves toward the origin at partial pressures lower than this.

EFFECT OF CONCENTRATION ON CRITICAL LENGTH

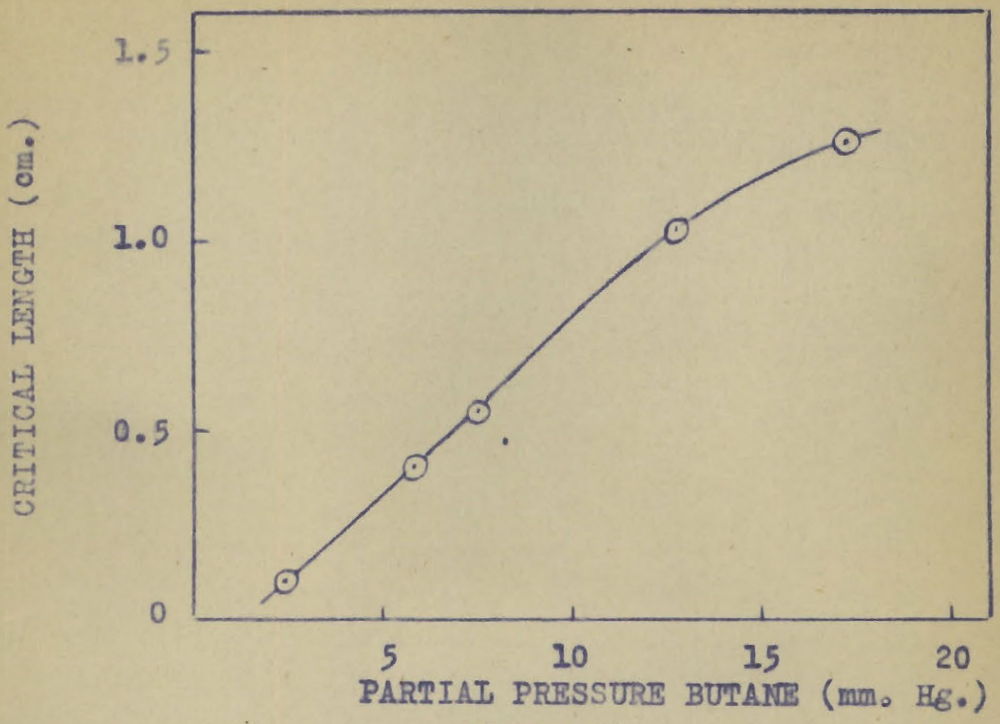

FIGURE 66.

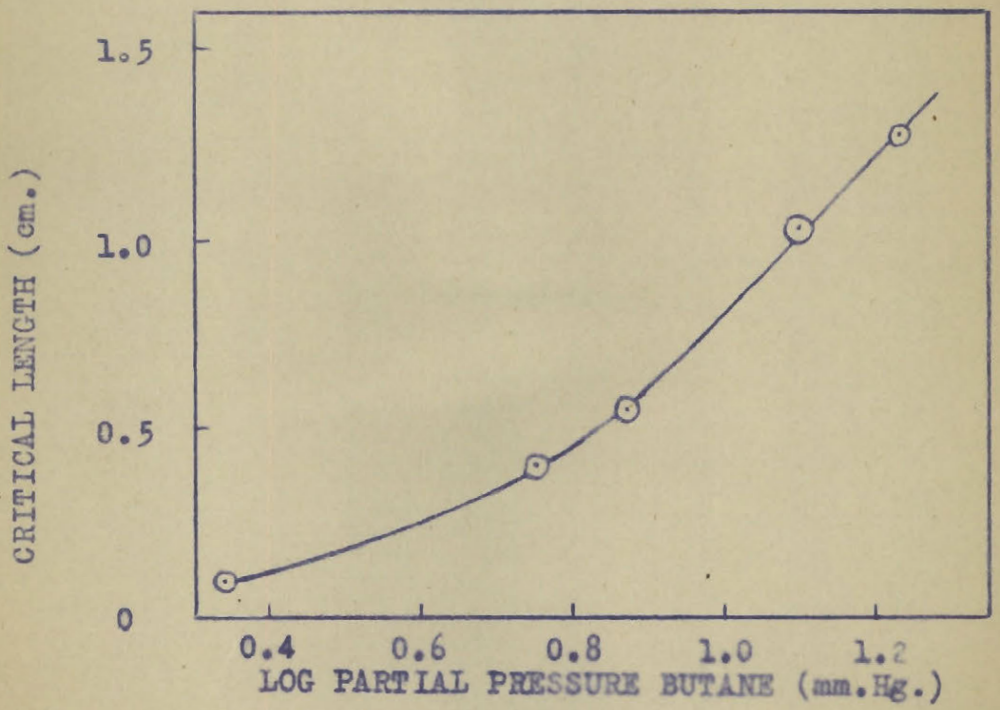

FIGURE 67.

5. Distribution of Butane in the Charcoal Cell

(a) Distribution of Sorbed Butane

From a consideration of the characteristics of sorption of 1, 2, 3, 4 and 5 centimetre beds, it is possible to determine both the distribution of the sorbate throughout a five centimetre bed and the concentration gradient in the air stream passing through the bed, at various times. The concentration gradients for a five centimetre bed, at various times and with a butane flowrate of 53 cc. per minute and an air flowrate of 1,520 cc. per minute are determined in these sections. Similar curves could be constructed for other flowrates reported in this investigation.

The data for the time of saturation of the 1, 2, 3, 4 and 5 cm. beds are found in table XXII. The curve of saturation time against bed depth is shown in figure 68. From this curve, the bed depth that is just saturated in times 2, 4, 10 min. etc. are determined and plotted on the horizontal line of figure 70 corresponding to 1.16 grams of butane sorbed per centimetre of charcoal, which is the saturation concentration for a one centimetre bed under these conditions.

The column lengths which have service times of 2, 4, 10 min. etc. as determined from figure 55 are plotted along the base line of figure 70.

The weight-time data for the 1, 2, 3, 4 and 5 centimetre beds are shown in table XXII. The curves showing these data graphically are given in figure 69. From these

TABLE XXII

Weight - Time Data

Time	Column Length (cm.)				
Min.	1.19	2.13	2.96	4.09	5.01
2	0.215	0.22			
4	0.45	0.46			
10	1.06	1.24	1.24		
15	1.29	1.83	1.92		
20	1.35	2.18	2.59	2.60	
30	1.38	2.42	3.17	3.79	3.95
40		2.47	3.35	4.34	4.94
50			3.39	4.62	5.44
60			3.42	4.72	5.64
70				4.73	5.75
80					5.80

TABLE XXIII

Weight Increments (Gm/cm.)

Time	Column Length (cm.)				
Min.	0.5	1.66	2.54	3.52	4.55
2	0.18	0.016			
4	0.38	0.053			
10	0.89	0.18	0.012		
15	1.08	0.575	0.108		
20	1.135	0.88	0.495	0.009	
30	1.16	1.105	0.904	0.55	.174
40		1.16	1.06	0.875	.65
50			1.11	1.09	.89
60			1.16	1.15	1.00
70				1.16	1.11
80					1.16

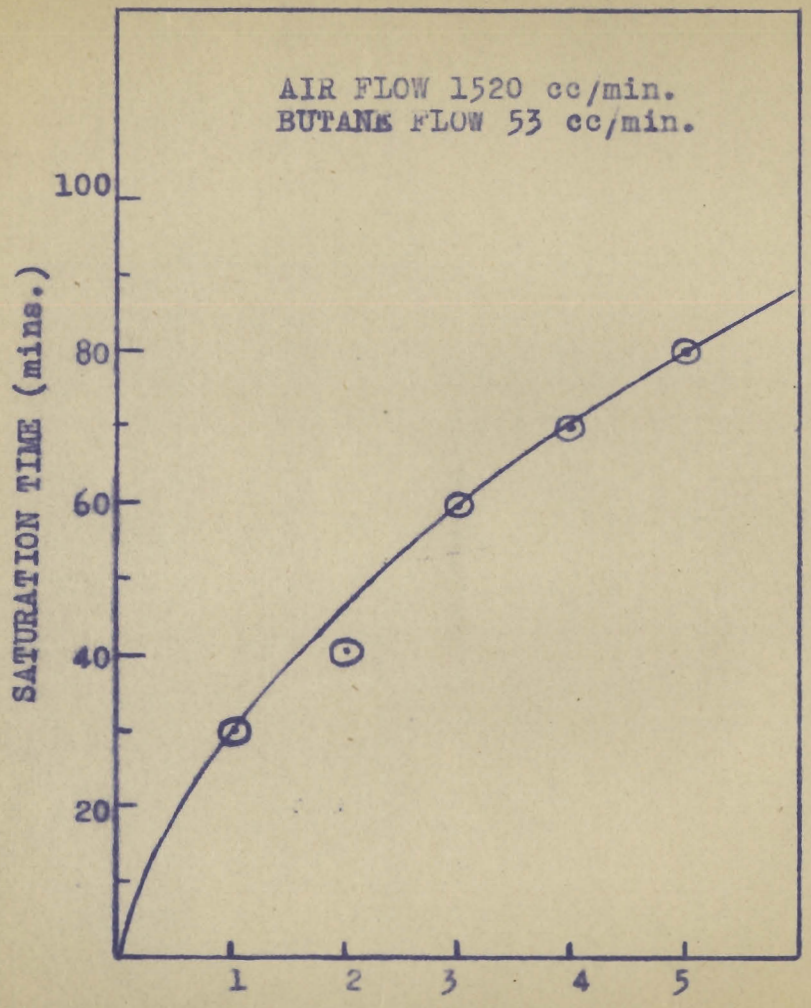

FIGURE 68

SATURATION TIME AGAINST COLUMN LENGTH

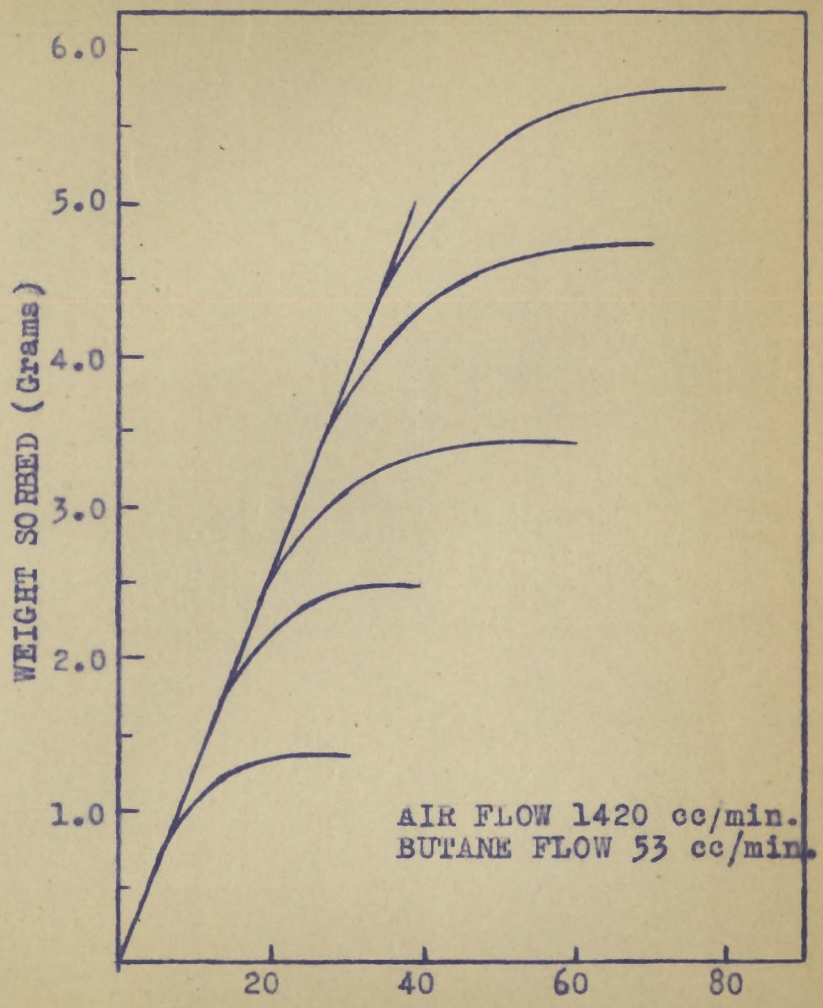

FIGURE 69

WEIGHT SORBED

data the number of grams of butane per centimetre sorbed at times 2, 4, 10 minutes etc. were determined as shown in table XXIII and this value assigned to the mid point of that centimetre layer. These values were then plotted on figure 70 at their respective mid points. The curves joining points of equal time were then drawn, giving the concentration gradients of the sorbed butane throughout the charcoal bed at various times.

From figure 70 it can be seen that the gradient is changing shape at times below 30 minutes until the final shape is established. It will be shown later that actually the 30 minute gradient is not the final shape, but that there is a slight change in shape until the 60 minute gradient is established. The first gradients appear to follow the exponential curves of the "mathematical" charcoal of Mecklenberg, or the curves postulated in the approximate theory of Danby et al, but they leave this form as Mecklenberg predicted. This behavior is in agreement with that predicted by the detailed theory of Danby et al.

Mecklenberg explains the falling off of the top part of the concentration gradient as due to larger capillaries of the charcoal, and due to the slow migration of the outer sorbed material into the inner capillaries. But it appears that another factor operating to increase the time required for saturation is the temperature change due to the heat of sorption. As will be seen in the following section, the temperature rise for butane (and also ammonia) is quite

CONCENTRATION GRADIENTS OF SORBED BUTANE

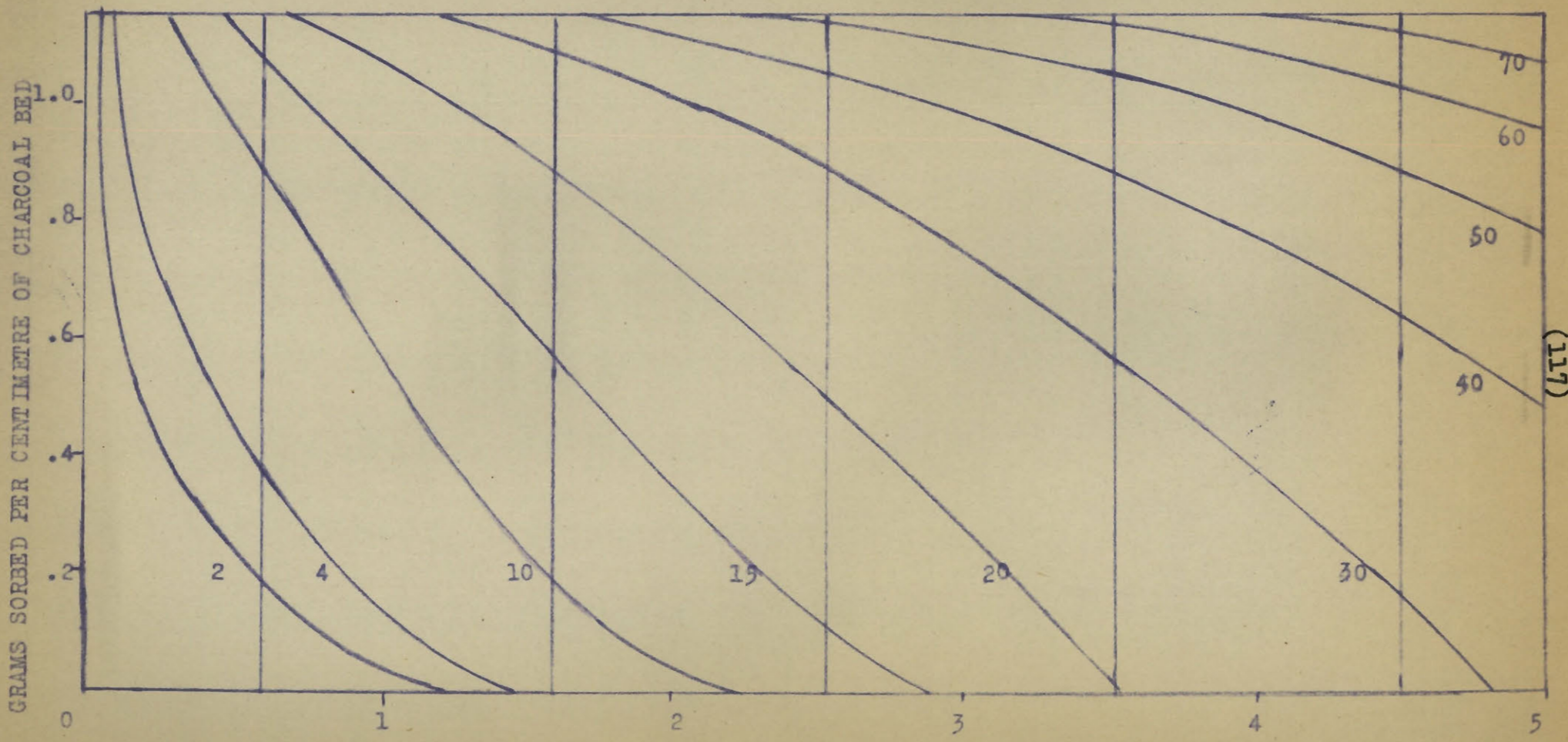

FIGURE 70.

high. Before the final saturation value can be attained this heat must be removed by the air stream and this delays the time of saturation. This, of course, would not be so marked at very low initial concentrations.

These concentration gradients could also be obtained by graphical differentiation of the integral sorption curves shown in figure 71. These integral sorption curves are drawn from the data in table XXII, and are a plot of the weight sorbed against the column length at constant times.

In figure 72, the differential weight of gas sorbed is plotted against time at different depths in the bed. The relation between the weight sorbed and time appeared to follow an exponential curve of the type

$$x = W_s \left(1 - e^{-bt}\right)$$

where x is the weight sorbed in time t and W_s is the equilibrium sorption weighed, and b is a constant. The relation is identical to that given by Syrkin and Kondrashow (18).

There is another relation between the weight of gas sorbed and time at constant bed depth. This is shown in figure 73 where the logarithm of the weight of gas sorbed is plotted against the reciprocal of the time of passage for different depths in the bed. The data give straight lines which intersect at a point. This point does not seem to have any particular significance. It is possible, however, to write an equation for these curves

$$x = W1^{-1/t}$$

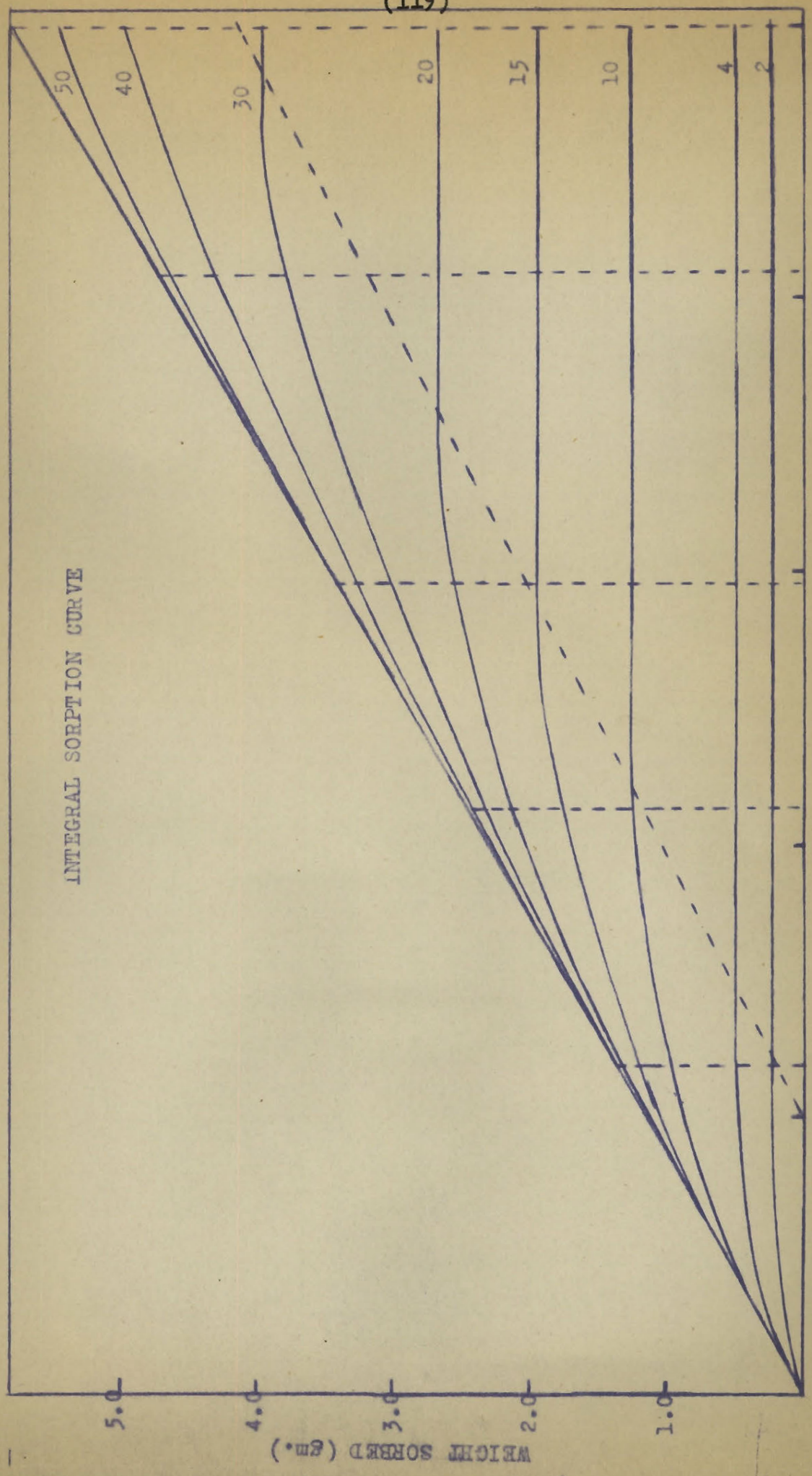
INTEGRAL SORPTION CURVE
WEIGHT SORBED (gm.)
5.0
4.0
3.0
2.0
1.0
50
40
30
20
15
10
4
2
1
2
3
4
5
BED DEPTH (cm.)

FIGURE 71

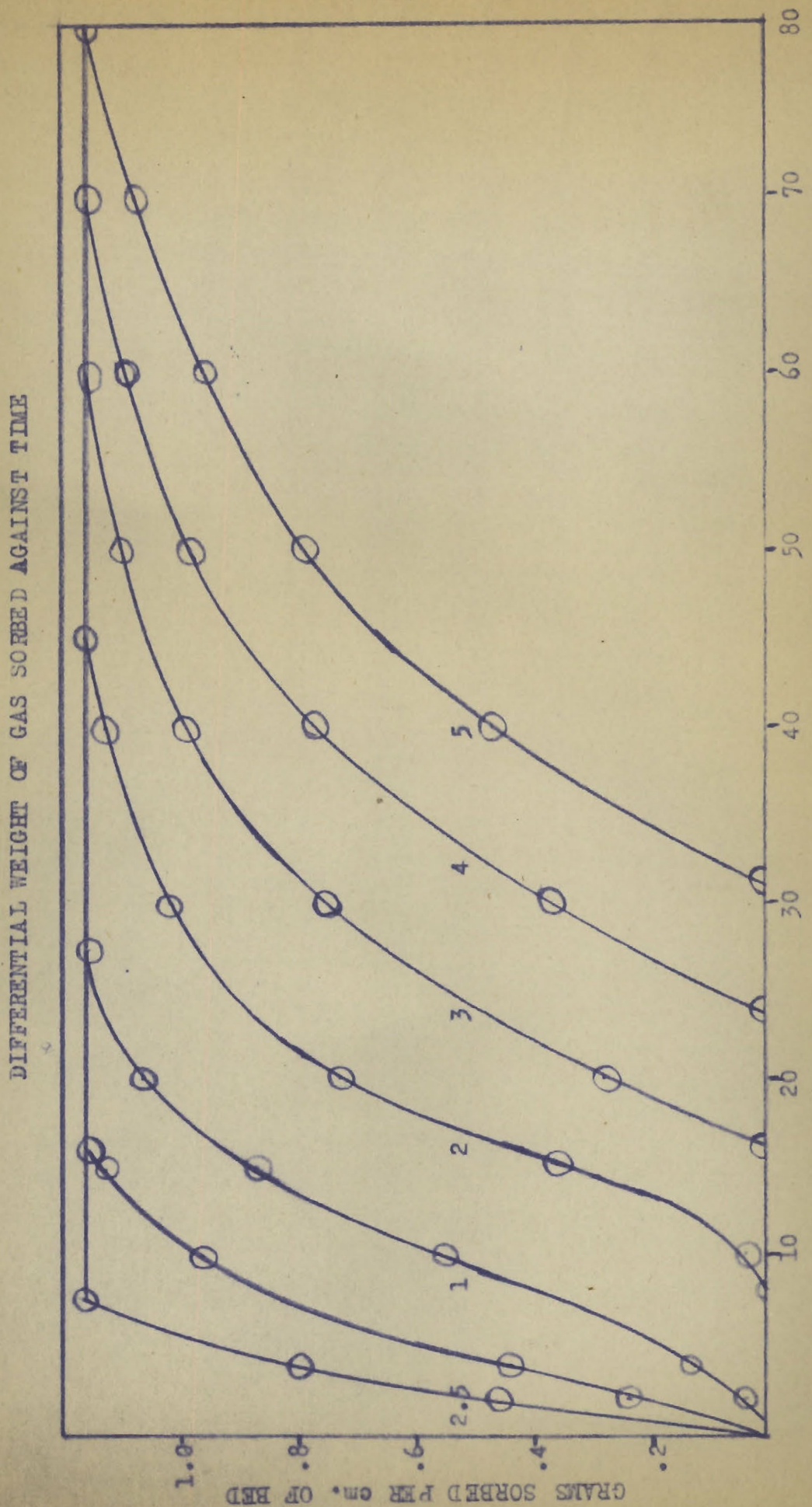
DIFFERENTIAL WEIGHT OF GAS SORBED AGAINST TIME
GRAMS SORBED PER gm. OF BED
1.0
.8
.6
.4
.2
2.5
1
2
3
4
5
10
20
30
40
50
60
70
80
TIME (Mins.)

FIGURE 72.

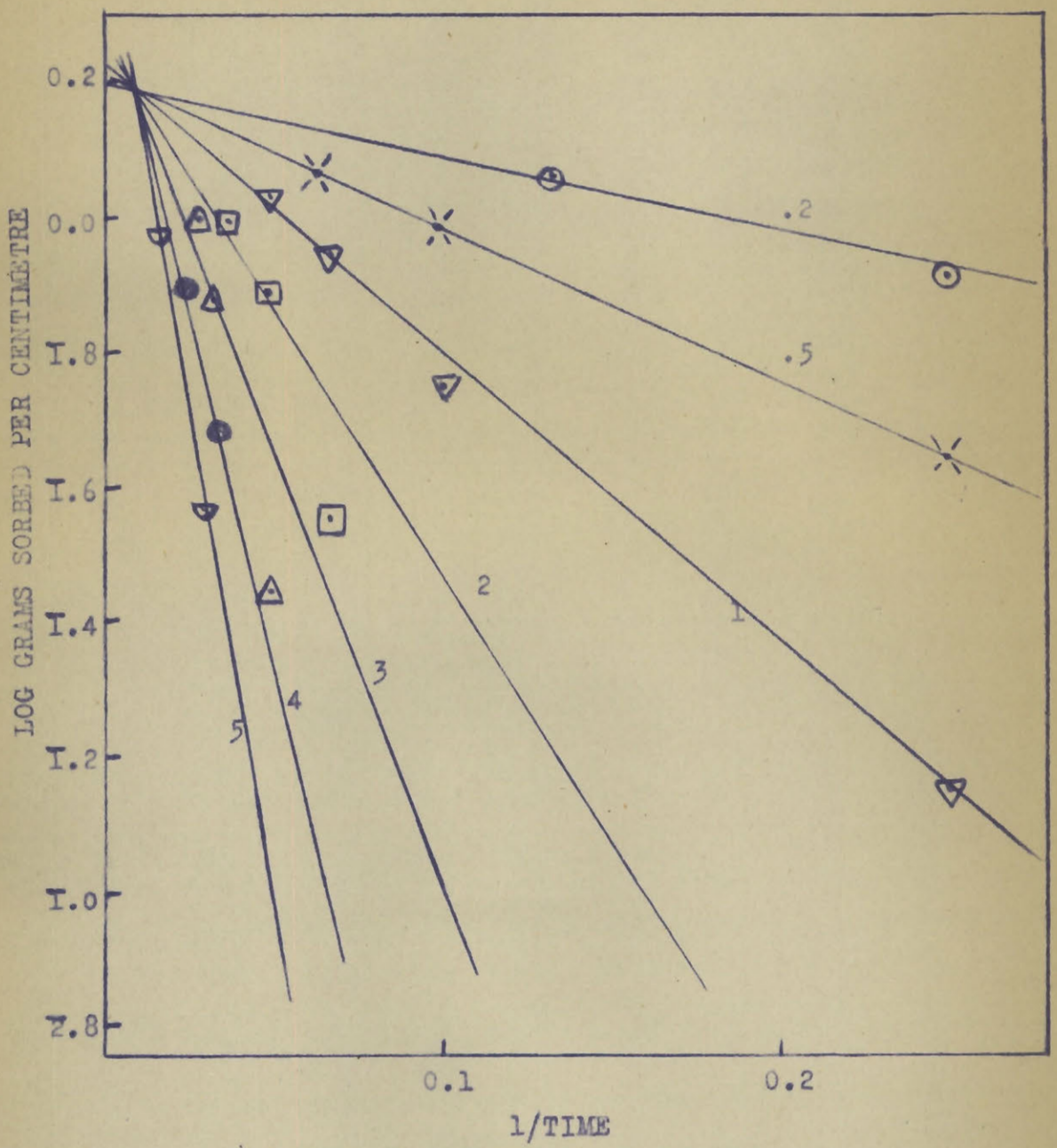
0.2
0.0
1.8
1.6
1.4
1.2
1.0
2.8
LOG GRAMS SORBED PER CENTIMETRE
.2
.5
1
2
3
4
5
0.1
0.2
1/TIME

FIGURE 73.

where W is a constant relating to the equilibrium weight of the gas sorbed and l a constant for any given bed length.

(b) Concentration Gradient in the Gas Stream Over the Charcoal.

From figure 49 the concentration gradients shown in figure 74 were drawn. Figure 49 gave the concentration of the gases leaving each centimetre layer and entering the next. The values obtained by erecting verticals at times 4, 10, 15 mm. etc. were plotted against the corresponding bed depth on figure 74. As before, in figure 70, the saturation lines were plotted along the maximum concentration and the service times along the zero axis.

The gradients obtained are very similar to those obtained for the amount of the gas sorbed on the charcoal. These gradients agree with those postulated by Danby et al as shown in figure 2 and verifies the application of their equations for the concentration of gases in equilibrium with the charcoal bed.

The initial exponential curves follow the relation predicted by Danby et al:

$$C - C_o \, e^{- k N_o \, l/L}$$

when very few of the active centres have been used up. The gradients then change gradually to their final shape which follows the equation:

$$C = \frac{C_o}{e^{-kC_oT\left(e^{kN_ol/L}-1\right)} \neq 1}$$

as given by the detailed theory.

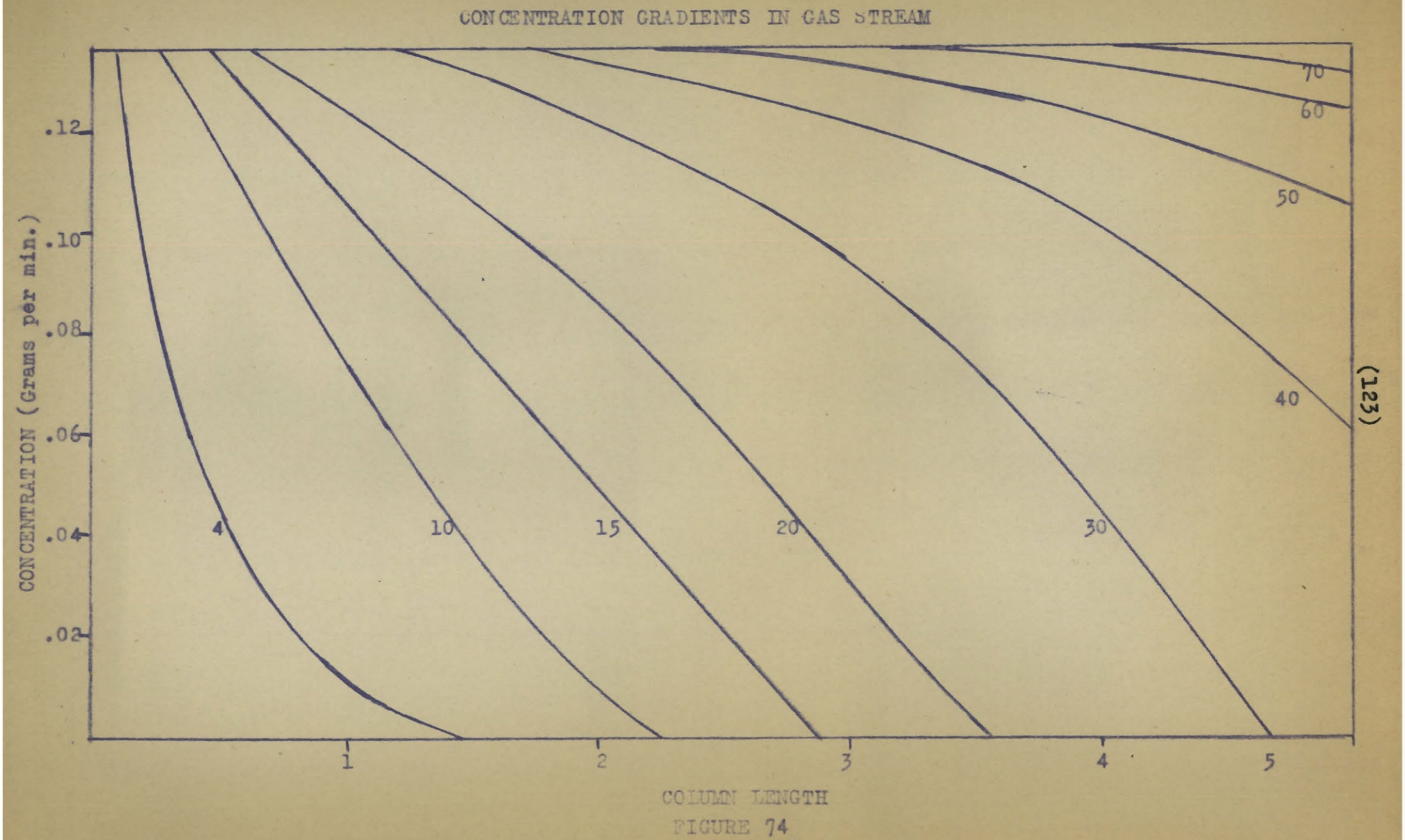
CONCENTRATION GRADIENTS IN GAS STREAM
CONCENTRATION (Grams per min.)
.12
.10
.08
.06
.04
.02
4
10
15
20
30
40
50
60
70
1
2
3
4
5
COLUMN LENGTH

FIGURE 74

The increase in length of the working layer with time is given in table XXIV. The values given are those measured from the curves in figures 70 and 74. The graph of this relation, shown in figure 75, indicates that in a five centimetre bed the gradient has not yet been completely established. The final length of the working layer would appear to be about 4.8 cm. and would be established at about 60 minutes. It would then move through the bed at constant velocity.

TABLE XXIV

Length of Working Layer

Time (min.)	Working Layer (cm.)
2	1.20
4	1.36
10	1.96
15	2.45
20	2.89
30	3.64

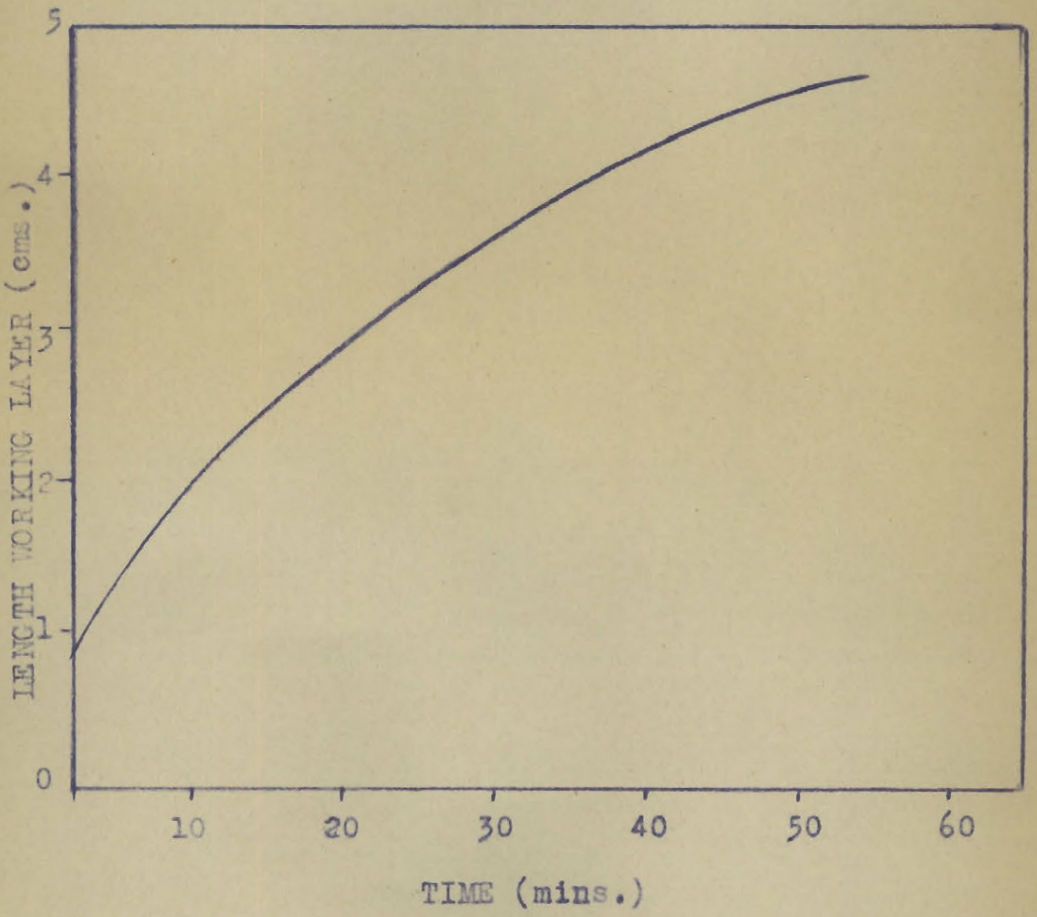

LENGTH OF WORKING LAYER AT VARIOUS TIMES

FIGURE 75

6. Temperature Data

The temperature rise in the centre of the second and fourth centimetre layers from the bottom of the charcoal bed were measured as a function of time (table XXV). The temperature rise-time curves are similar in shape to those for ammonia (figure 35). However, with these positions of the thermocouples both indicated approximately equal maximum temperature rise since they were both further than one centimetre from the top. The maximum temperature rise was found to be mainly dependent on the rate at which the butane was supplied. A linear relation was obtained between them (figure 76). Increase in the rate of air flow causes a linear decrease in the maximum temperature attained as shown in figure 77. By determining the temperature for various depths of charcoal beds the maximum temperature rise in any layer of a five centimetre bed may be determined. These are plotted in figure 78. The maximum temperature attained is constant down the bed except for the top centimetre layer the temperature of which is lower probably because of the cooling by greater contact of that particular layer with the cell.

The times at which these maximum temperatures were attained are plotted in figures 79 and 80. These were found to decrease with butane and air flowrates.

TABLE XXV

Temperature Data

Column Length (cm.)	Air Rate (cc/min.)	Butane Rate (cc/min.)	Maximum Temperature Rise T and Time t T_1 °C	t_1 min.	T_2 °C	t_2 min.
4.08	3,130	53	18	6	23	17
1.94	3,020	53			16	4
5.01	1,590	53	30	14	29	30
4.09	1,530	53	25	7	29	21
2.96	1,520	53			27.5	15
2.13	1,530	53			24	9
1.19	1,520	53				
3.96	500	53	29.5	13	33	27.5
3.95	0	71	36.5	13.5	39	24
4.12	0	53	32	20	36	37
4.00	3,020	71	23	5	28	12
3.70	3,020	30	10	11	12	27
2.18	3,020	30			10.5	8
4.23	3,045	24	9.5	18	10	34
4.16	3,040	9	1.7	25	3	90
2.12	3,000	9			4	24
1.27	3,020	9				
4.01	1,500	30.	16.5	12	16.5	33
2.09	1,500	30.			6	8
3.99	1,403	30	11.5	13.5	12	34
3.88	151	2.7	0		0	

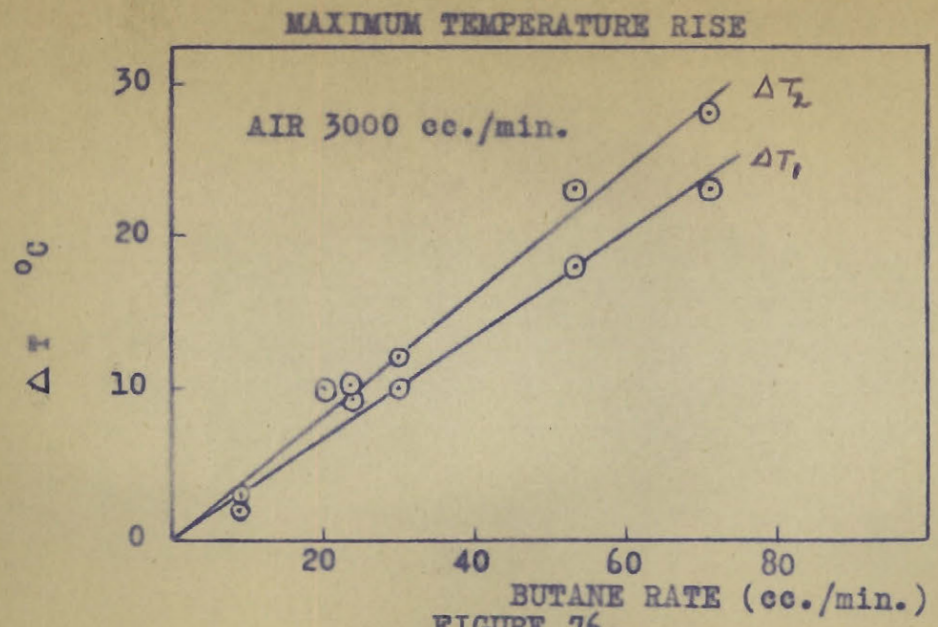

FIGURE 76.
EFFECT OF BUTANE RATE

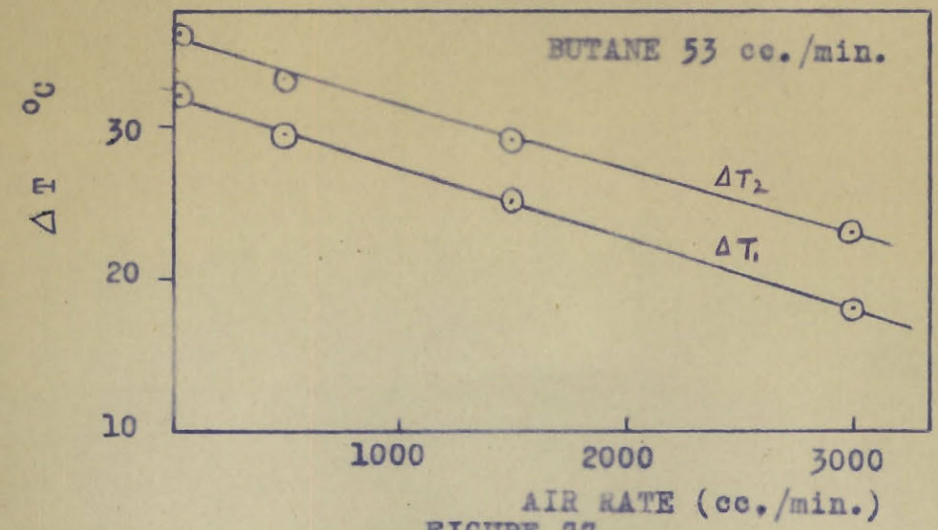

FIGURE 77.
EFFECT OF AIR RATE

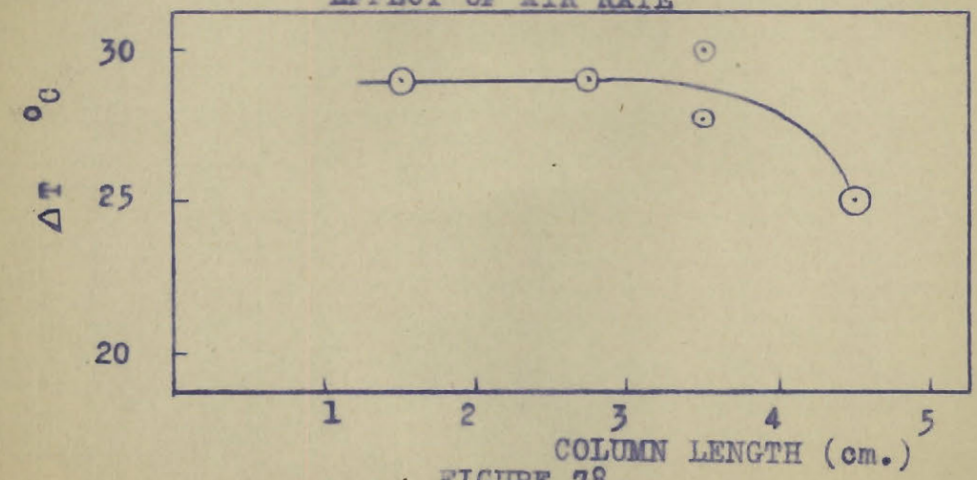

FIGURE 78.
TEMPERATURE ALONG THE BED

TIME OF
MAXIMUM TEMPERATURE RISE

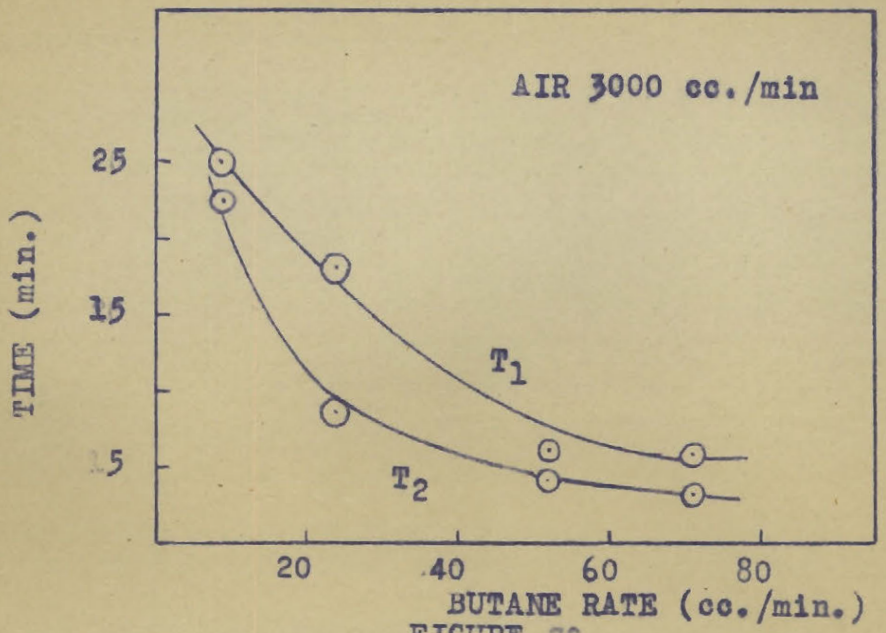

FIGURE 79
EFFECT OF BUTANE RATE

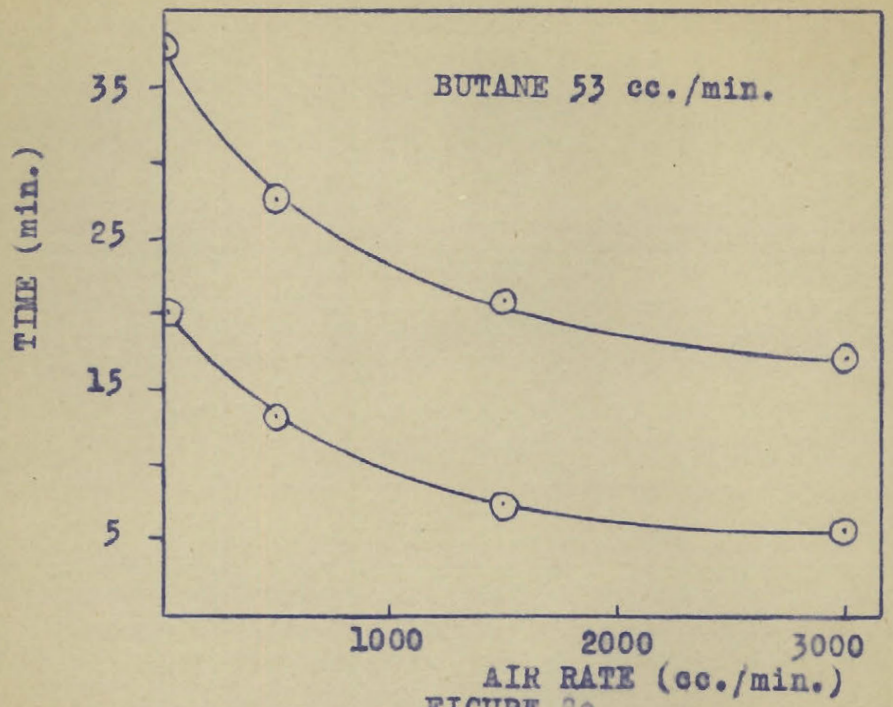

FIGURE 80.
EFFECT OF AIR RATE

C. Desorption Studies

As mentioned in the discussion of the analytical results for both ammonia and butane, the rate of increase in weight of the charcoal over the linear portion of the weight-time curve did not correspond to the total amount of gas admitted to the cell, yet no sorbate appeared in the effluent stream. It was thought that this might perhaps be due to competition for active centres between the sorbate and the air. The charcoal is saturated with oxygen and nitrogen before any sorbate is admitted. These molecules would be displaced, at least in part, from the charcoal surface by ammonia or butane molecules. This would result in a weight being recorded which would be less than actual amount of butane or ammonia taken up by the charcoal, by the amount of oxygen and nitrogen displaced.

To confirm this behavior and to investigate the reversibility of the sorption, studies on the desorption of both ammonia and butane were carried out as previously described. The data for these studies are given in table XXVI. For the first two runs, the charcoal was allowed to come to equilibrium with a stream of pure ammonia at a flow rate of 60 cc. per minute. It was then desorbed using air streams (no ammonia) of 100 cc. and 500 cc. per minute. The results are shown graphically in figure 81. As might be expected, the desorption occurs very rapidly at first, the rate gradually decreasing to zero. The desorption does not, however, follow a logarithmic relation with time. Further examination of

figure 81 shows that not all of the ammonia is desorbed at equilibrium, 0.2 gms. are left out of an initial sorbed weight of 2.16 gm. ammonia. Furthermore, this equilibrium amount is the same for desorption by both 100 and 500 cc. per minute of air. The rate of desorption is at first more rapid, the greater the velocity of the desorbing stream. Two runs were also carried out using charcoal saturated as above but this time were desorbed using ammonia-air streams of 200 cc. air and 60 cc/min. ammonia and 300 cc/min. air and 60 cc/min. of ammonia. The equilibrium weights for sorption, using these conditions, are 0.67 gm. and 0.59 gm. respectively. The equilibrium desorption weight was 0.79 in each of the above case. Here again sorption was more rapid initially with the faster air stream. Starting from charcoal which was in equilibrium with ammonia-air streams of 60-200 cc/min. and 60-300 cc/min. and desorbing by curring off the ammonia supply resulted in the desorption curves shown in figure 82. In these cases only 0.09 and 0.05 grams of ammonia respectively remained on the charcoal at equilibrium. Figure 83 shows a typical desorption of butane. The charcoal was saturated using a pure butane stream of 53 cc. per minute, and desorbed using an air stream of 3,000 cc. per minute, from 6.26 gm. butane to 0.40 gm. butane after 30 hours, but had not yet reached equilibrium, so it seems probable that the butane would be completely desorbed. These desorption results are summarized in table XXVI.

TABLE XXVI

Desorption Studies

A. Ammonia

Air (cc/min.)	NH_3 (cc/min.)	Equel'm Weight gms.	Air (cc/min.)	NH_3 (cc/min.)	Equel'm Weight gms.	Equel'm Sorption gms.
0	60	2.16	100	0	0.20	0
0	60	2.16	500	0	0.20	0
0	60	2.16	200	60	0.79	0.67
0	60	2.16	300	60	0.79	0.59
200	60	0.67	200	0	0.09	0
300	60	0.59	300	0	0.05	0

B. Butane

0	53	6.26	3,000	0	(0.40)	0

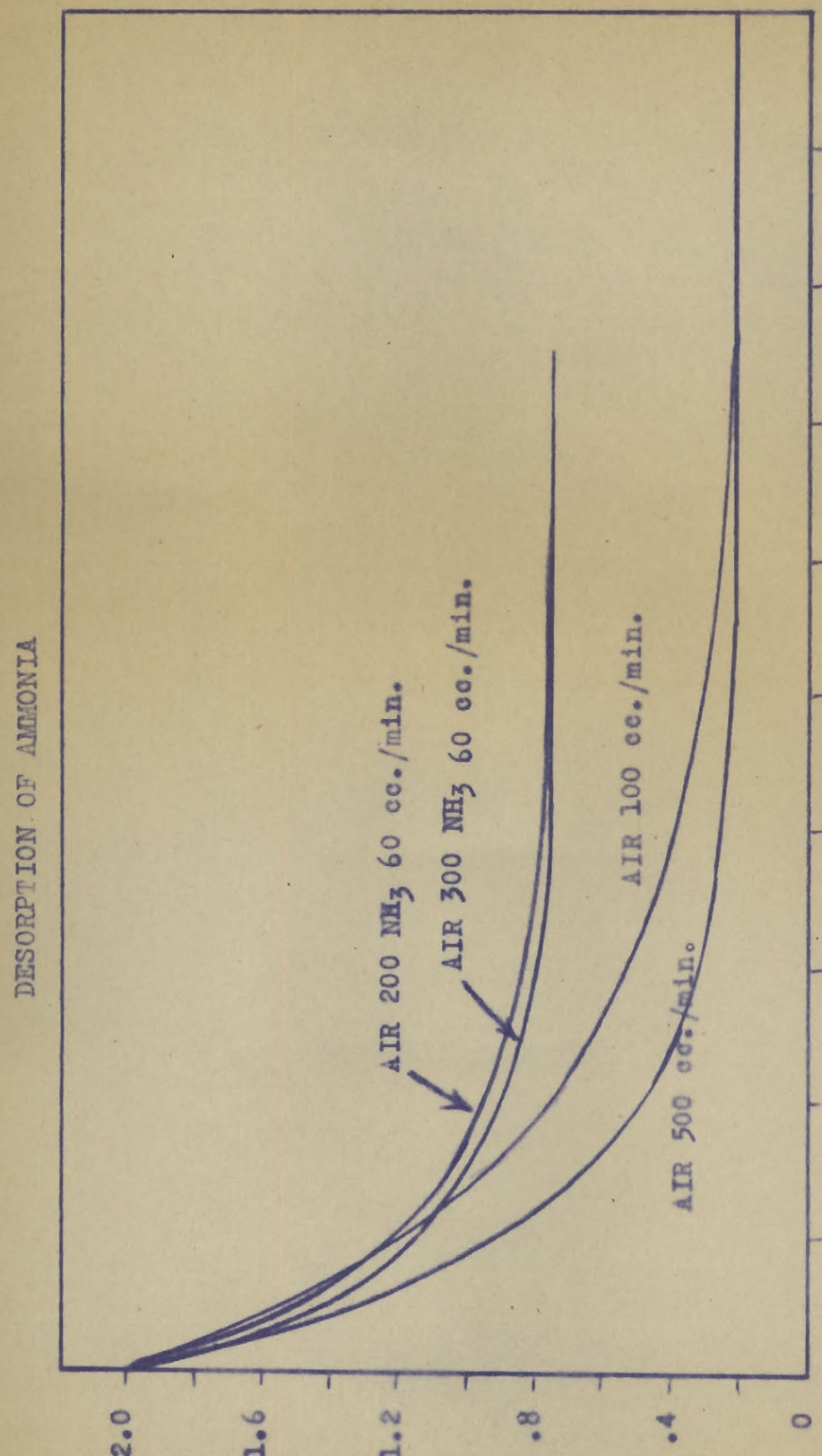
DESORPTION OF AMMONIA
AIR 200 NH3 60 cc./min.
AIR 300 NH3 60 cc./min.
AIR 100 cc./min.
AIR 500 cc./min.
WEIGHT SORBED (gm.)
TIME (min.)
0
.4
.8
1.2
1.6
2.0
20
40
60
80
100
120
140
160
180

FIGURE 81.

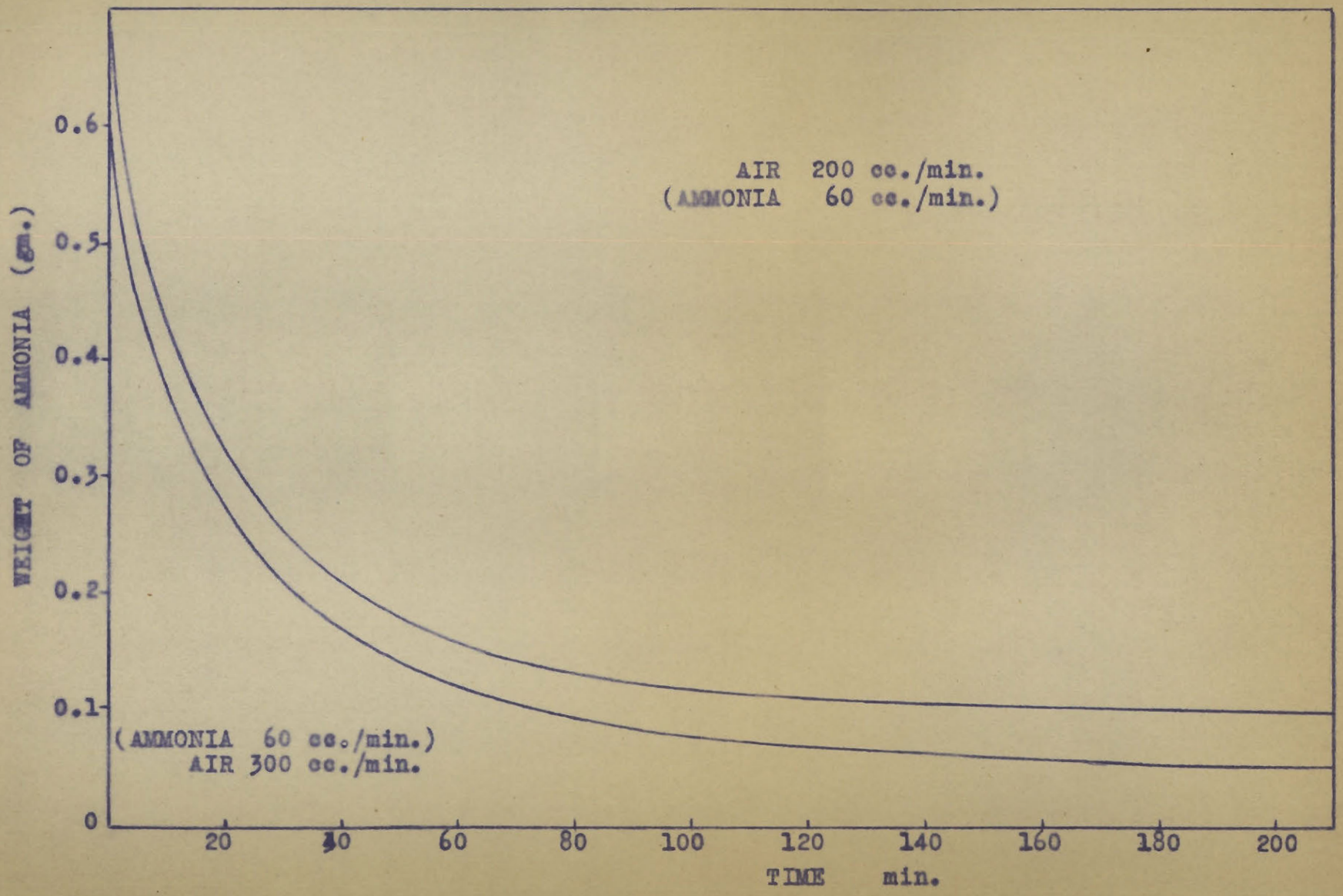

DESORPTION OF AMMONIA

FIGURE 82.

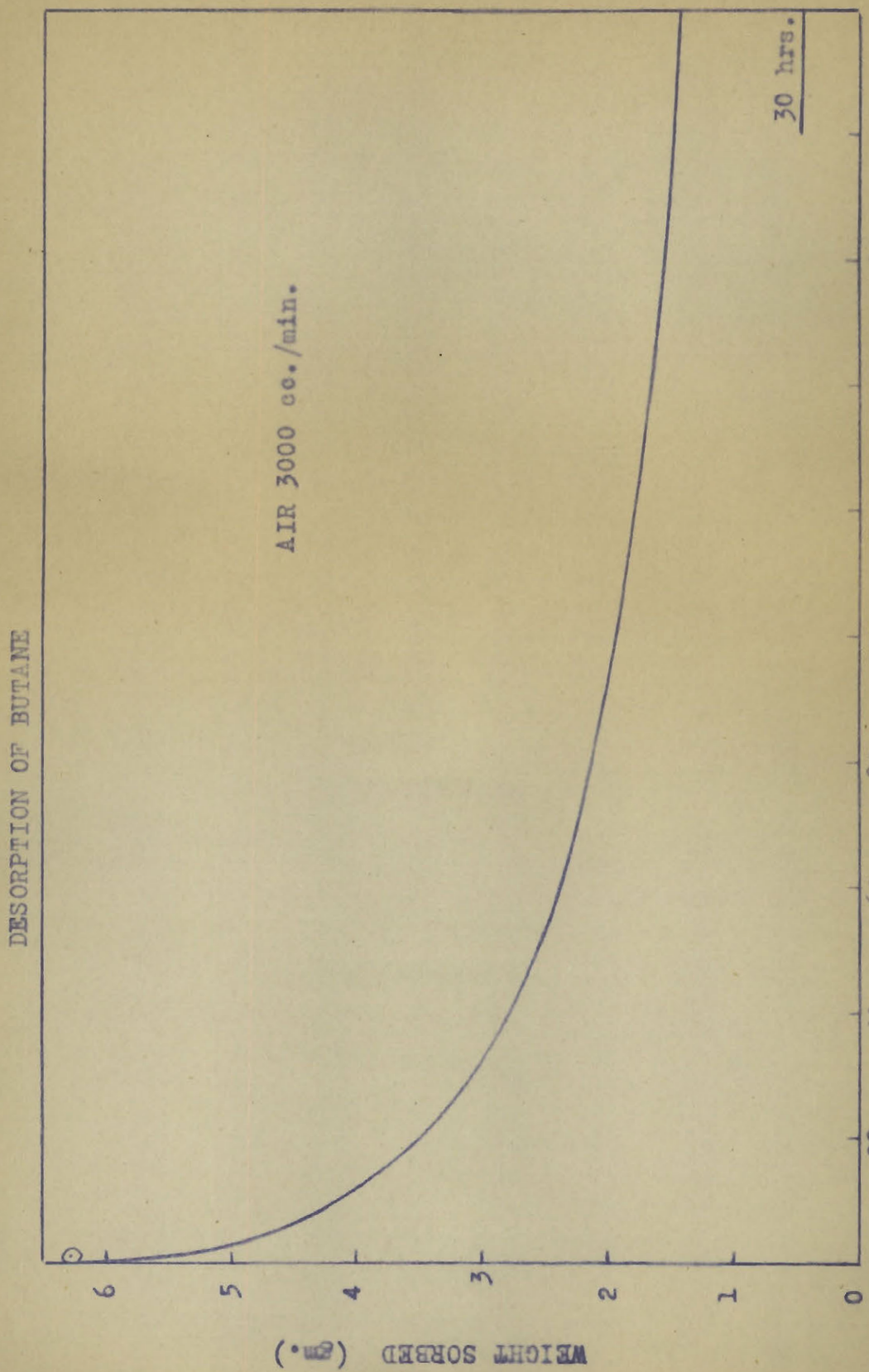
DESORPTION OF BUTANE
AIR 3000 cc./min.
30 hrs.
WEIGHT SORBED (gm.)
TIME (min.)
0
1
2
3
4
5
6
20
40
60
80
100
120
140
160
180

FIGURE 83.

Thus for ammonia the sorption does not appear to be completely reversible but does for butane. This would indicate that there is at least in part a different mechanism of sorption for butane and ammonia.

Figure 84 shows the differential desorption curves plotted against time as volume desorbed per minute. The lower curve was calculated from the loss in weight of the charcoal and the upper one from the analysis of the effluent gases. This means that more sorbate is detected in the gases passing out of the cell than appears to be desorbed from the charcoal from its loss in weight. The deviation between the two curves is very great at first but gradually decreases to zero as the curves approach one another. When the logarithm of this deviation is plotted against time as in figure 85 a straight line is obtained except during the very first and very last stages of the desorption. If it is assumed that during sorption air is displaced from the charcoal by sorbate molecules and during desorption sorbate is displaced from the charcoal to be replaced by molecules of oxygen and nitrogen, then these deviations between sorption weight and analytical data are readily explained. It may be noted that the analytical methods are sufficiently accurate to justify this explanation.

Berl and Andress (23) have noted this displacement of adsorbed air from charcoal by the vapors of several organic compounds and have determined the amount displaced.

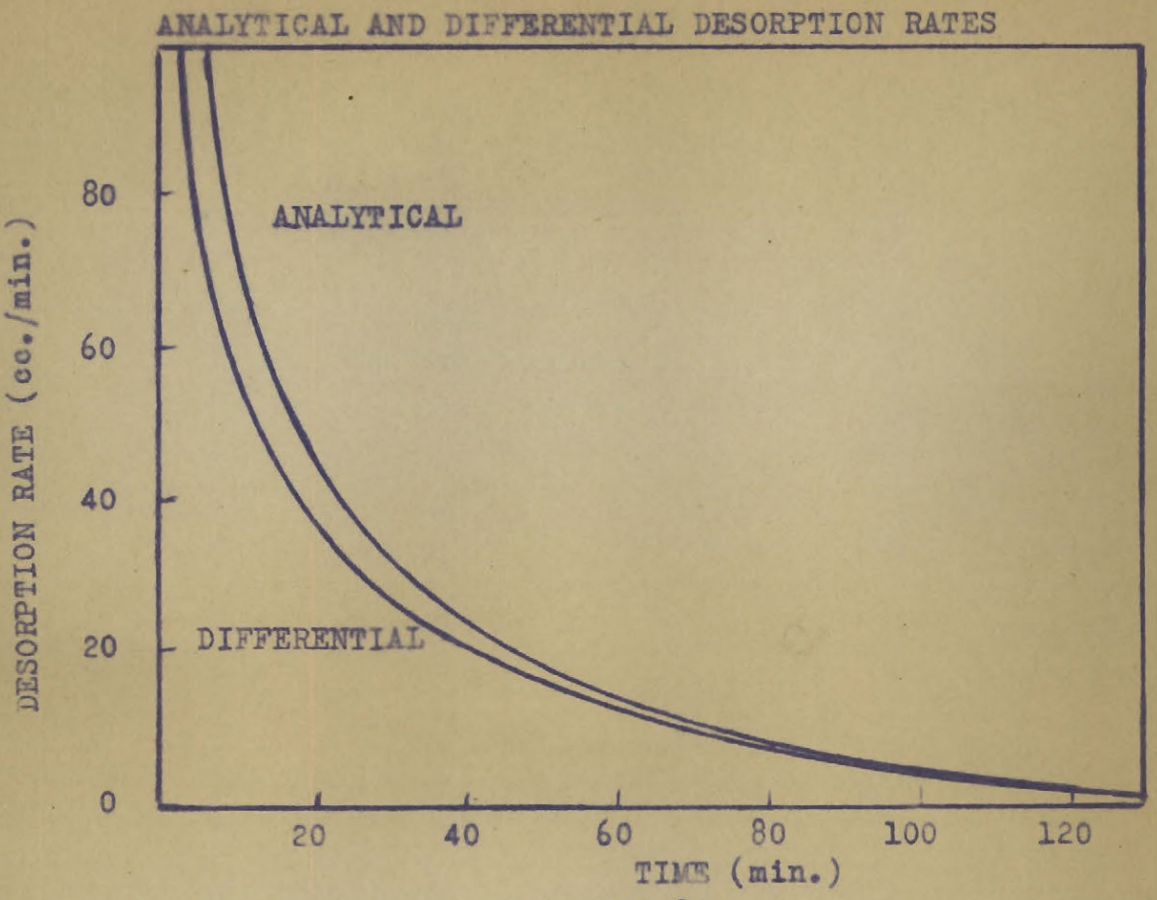

FIGURE 84.

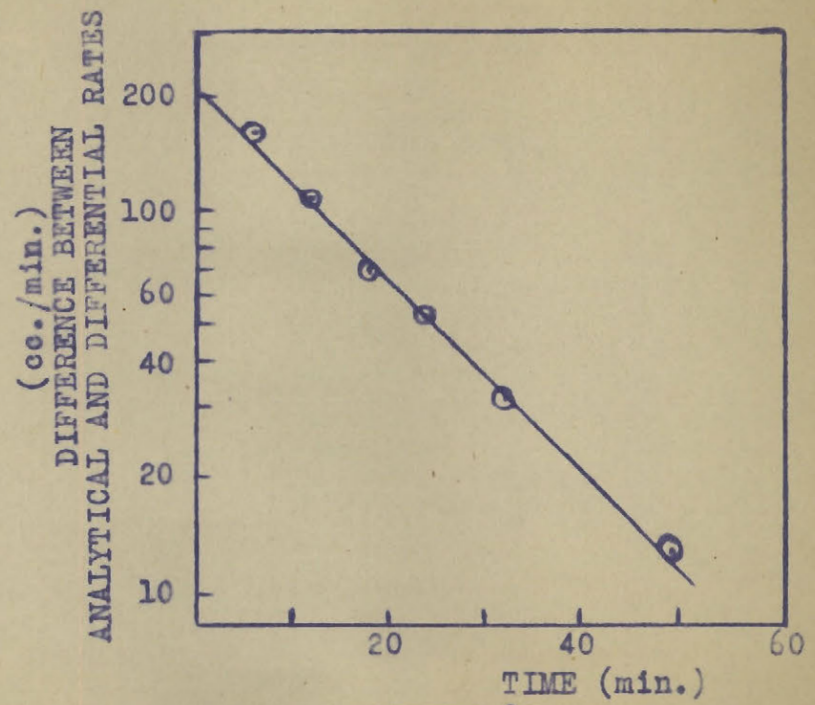

FIGURE 85.

DISCUSSION

A study of the dynamic sorption of ammonia and butane has been made using an apparatus which permitted the sorption to be followed as a function of time, in addition to temperature data and analysis of the effluent gas stream, over a wide range of conditions of sorbate concentration and flowrate.

The apparatus was found to be very convenient for accurate study of such sorption data as sorption capacity, service time, escaping concentrations, dead length, sorption gradients in both the charcoal and the gas stream, and temperature rise in various sections of the charcoal bed. This type of apparatus has the advantage of measuring the sorption as a function of time rather than of bed length as in a segmented cell. This results in a considerable saving of time as less runs are required for a complete study of any particular sorbate.

It seems advantageous to follow the sorption beyond the service time of any bed to the equilibrium value, for as pointed out by Mecklenberg (14) the escaping gases are in fact those in equilibrium with the working layer of the charcoal. From the analysis of the escaping gases the sorption gradients throughout the bed may be set up.

The method used herein for measurement of service times agreed closely with those indicated by the rise of test papers, at least for service times above five minutes, and could be used where suitable chemical tests are not available.

The accuracy of this apparatus may be increased by the use of a light cell of plastic material and a more sensitive balance.

The studies of the sorption of ammonia and butane appear to indicate some differences in their mechanism of sorption. On a weight basis butane is sorbed to a greater extent than ammonia but on a volume basis more ammonia is sorbed per gram of charcoal than is butane. For a four centimetre bed using a stream of pure sorbate approximately 66 cc. per minute 6.26 grams of butane are sorbed to 2.92 grams of ammonia. On a volume basis 146 cc. of ammonia and 89.2 cc. of butane are sorbed per gram of charcoal under these conditions.

The equilibrium sorption weights for ammonia were found to be expressed closely by the Langmuir and Freundlich isotherms over the range 50 - 760 mm. Hg. partial pressure of ammonia. The equations found were:

$$x = \frac{0.278\ P}{1 + 0.00055P}$$

$$x = 1.06\ P^{1/1.31}$$

The isotherm for ammonia still has not reached a constant value of the equilibrium sorption as the partial pressure increases. Below 50 mm. this isotherm fell off rather sharply to the origin. Butane, on the other hand, did not follow an isotherm of this type at all closely over the same partial pressure range. The sorption in this case increased rather rapidly at first then sloped off to a constant value more gradually than either isotherm would predict.

From a consideration of the desorption of both ammonia and butane using streams of pure air, ammonia was not found to be removed completely from the charcoal when equilibrium had been established between the desorbing stream and the charcoal, while butane was capable of complete removal. The ammonia sorption appears, then, not to be completely reversible while that of butane does.

The relation of the logarithm of the service time gives a straight line for ammonia when plotted against the actual ammonia flow whereas with butane a linear relation is obtained between the logarithm of the service time and the logarithm of the butane flowrate.

It seems possible that the ammonia is held to the charcoal in part by chemisorption forces, while the butane might possibly be held by a type of molecular sorption, either van der Waal's or capillary condensation. The covalent bonds between the ammonia molecules and the atoms in charcoal surface would thus be rather difficult to break so that the sorption would not be reversible.

The theories of sorption as developed by Danby et al and Mecklenberg were based on entirely different considerations. Mecklenberg assumed sorption to occur by capillary condensation while Danby et al postulated active centres each of which were capable of dealing with a certain number of molecules of sorbate. The Danby et al theory assumed that the sorption was the rate governing step while Mecklenberg assumed the process to be expressible by the Nernst formula for heterogeneous reactions which is dependent on the diffusion rate. Their predictions are, however, similar for the expressions of the sorption data in terms of the experimental variables.

From both theories the concentration of the gas decreases exponentially along the bed from the initial concentration of the entering gases, and increases exponentially with time, so that there is a working layer where the sorbate is being removed, which moves along the bed until sorbate appears in the effluent stream at the service time. The relations between the sorption data such as sorption capacity, service time, escaping concentration, dead length and sorption gradients has been discussed in the introduction in terms of the experimental variables.

In general, the results of the investigations presented herein are in good agreement with the theories of sorption and other data found by previous investigators.

The logarithm of the escaping concentration gives a linear relation with time during the early stages of breakdown, but deviates as the escaping concentration increases

which is as predicted by Danby et al.

The service time gives a linear relation with column length over the ranges investigated. The service time also varied with the reciprocal of the flowrate at constant concentration. There appears to be slight disagreement with theories as far as relation between service time and concentration is concerned at low concentrations. Theories predict $C_o \times T$ = a constant which was found to be true except at low ammonia concentrations where the product falls off as concentration is decreased. The partial pressure curve bends down sharply in this region.

Above 7 mm. partial pressure of butane the dead length varies as the logarithm of the initial concentration; below this it appears to vary directly with the concentration.

The sorption gradients obtained agree with those predicted by Danby et al in their detailed theory and with those found by Shilow and explained by Mecklenberg. The gradient differs in shape in the first sections of the bed from those later, but it gradually is built up to a constant shape and the gradient, once formed, moves along the bed at constant velocity. The length of the working layer thus increases to a constant value. Mecklenberg explained the change in shape by variation in capillary size and the slow migration from the outer to the inner layers. Another factor which is suggested by this work is that of temperature, which lengthens the working layer by reducing the sorption capacity

when the stream first passes through the bed, allowing the sorbate to penetrate further before being completely sorbed, and by the sorption continuing near the end of the gradient as the layers in this region cool back to room temperature.

REFERENCES

(1) Pearce, J.A. - Ph. D. Thesis, McGill University 1941.
- War Research Report CE 52 1941.

(2) Arnell, J.C. - War Research Reports, McGill University 1942.

(3) McBain, J.W. - The Sorption of Gases by Solids - Rutledge (1932).

(4) Gregg, S.J. - The Adsorption of Gases by Solids - Methuen (1934).

(5) Langmuir, I. - J.A.C.S. 40, p. 1,384 (1918).

(6) Titoff, A. - Z. Physik. Chem. 74, p. 652 (1910).

(7) Homfray, I.F.- Z. Physik. Chem. 74, p. 149 (1910).

(8) Hene, W. - Dissert. - Hamburg 1927, p. 21.

(9) Hempel, W.and Vater, W. - Z. Elektrochem 18, p. 724 (1912).

(10) Lamb, A.B. and Coolidge, A.S. - J.A.C.S. 42, p. 1,156 (1920).

(11) Gurwitsch, L.G. - J. Russ. Phys. Chem. Soc. 47, p. 805 (1915).

(12) Danby, C.J. Davoud, J.G. Everett, D.H., Hinshelwood, C.N., and Lodge, R.N. - Some Aspects of the Physical Chemistry of the Respirator (1940).

(13) Mecklenberg, W. - Z. Elektrochem 31, p. 485 (1925).

(14) Mecklenberg, W. - Kolloid Z. 56, p. 295 (1932).

(15) Engel, - Z. ges. Schiess und Spreng - Stoffwesen 24 p. 451, 495 (1929).

(16) Shilow, N., Lepin, L., and Wossnessensky, S. - Kolloid Z. 49, p. 288 (1929).

(17) Dubinin, Parshin and Pupuirev, J. Russ. Phys. Chem. Soc. 62, p. 1,947 (1930).

(18) Syrkin, J.K. and Kondraschow, A.J. - Kolloid Z. 56, p. 295 (1932).

(19) Izmailov and Sigalovskya - Traw.inst. chem. Charkow, 1, p. 133 (1935).

(20) Ruff, W. - Von Wasser 11, p. 251 (1936).

(21) Dubinin, - J. Russ. Phys. Chem. Soc. 62, p.683 (1930).

(22) Allmand - Final Summary Report from University of London (1941).

(23) Berl and Andress - Z. angew. chem. 34, p. 377, (1921).

SUMMARY AND CONTRIBUTION TO KNOWLEDGE

PART A

A Study of Pro Knock Activity

Quantitative data of the pro knock effectiveness of several compounds were obtained in an effort to determine whether such compounds might be used in military tactics to render automotive equipment inactive.

Techniques were developed for quantitative addition of gaseous, liquid and solid compounds to the air intake of an engine. The standard knock testing procedure was adapted for testing pro knocks on an Ethyl 30 B Knock Testing Engine. The relative pro knock activities of several elements and radicals were classified and the former related to their position in Mendeleef's periodic table. From these data compounds of the type

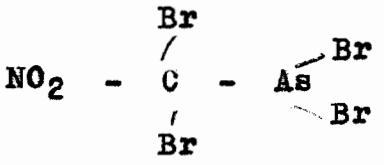

were predicted to have great pro knock activity. Arsenic tri-chloride was the best pro knock found in this work; it caused a ten octane drop in an 80 octane leaded aviation fuel

at 5.8 parts per million of air. It was also concluded that quantitative data on the octane drop required to seriously damage an aircraft engine is essential.

PART B

Dynamic Sorption of Ammonia and Butane on Charcoal

The dynamic sorption of butane and ammonia on charcoal was studied using an apparatus which followed the sorption by weight as a function of time and permitted measurement of temperature rise and analysis of the effluent gas stream over a wide range of sorbate concentrations and flowrates. The data were applied to the theories of Danby et al and of Mecklenberg and were found to be essentially in good agreement.